THE MINOR PLANET BULLETIN

BULLETIN OF THE MINOR PLANETS SECTION OF THE ASSOCIATION OF LUNAR AND PLANETARY OBSERVERS

VOLUME 49, NUMBER 3, A.D. 2022 JULY-SEPTEMBER 159.

LIGHTCURVE PHOTOMETRY OF ASTEROID 1637 SWINGS

Idris Abubakar Sani
NASRDA-Centre for Basic Space Science
Nsukka, Enugu State, NIGERIA
idrisabu4me@yahoo.com

Peter Offor, Nnaemeka Njoku-Achu
NASRDA-Centre for Basic Space Science

Matthew C. Nowinski
George Mason University
mnowinsk@gmu.edu

Chukwujekwu Ofodum, Bonaventure Okere
NASRDA-Centre for Basic Space Science

(Received: 2022 February 1)

Lightcurve photometry of the main-belt asteroid 1637 Swings yielded an estimated period of 10.226 ± 0.009 h and an amplitude of 0.25 ± 0.0075 mag.

CCD photometric observations of the main-belt asteroid 1637 Swings were carried out in October 2017 at the Stone Edge Observatory, Sonoma, CA, USA (G52). Data were obtained with a 0.5-m *f*/8.1 Ritchey-Chretien telescope and an FLI CG230 CCD camera using a clear filter. The pixel size was 1.55 arcseconds with binning set to 2×2. All exposures were 120 seconds.

Data processing and analysis were done with *MPO Canopus* (Warner, 2019). All images were calibrated with bias, dark, and flat field frames, and the instrumental magnitudes converted to R magnitudes using solar-colored field stars from the CMC-15 catalogue. Table I shows the observing circumstances and results.

1637 Swings was discovered in 1936 August by Joseph Hunaerts at the Royal Observatory of Belgium in Uccle, Belgium. It is a main-belt asteroid with an orbital period of 5.39 years, semi-major axis of 3.073 AU, eccentricity of 0.0459, and inclination of 14.070°. It has an absolute magnitude of 10.49. The WISE/NEOWISE survey (Masiero et al., 2011) reported a diameter of 52.994 ± 0.428 km and a visible albedo of 0.042 ± 0.004. Lazzaro et al. (2004) assigned a C-type taxonomic class. The asteroid dynamical family was identified as family 52 by Kozai (1979).

Observations for 1637 Swings were conducted over two nights and collected 362 data points. The lightcurve analysis shows a solution for the rotational period of P = 10.226 ± 0.009 h and with an amplitude A = 0.25 ± 0.0075 mag, suggested by the strongest peak in the period spectrum.

A search through the asteroid lightcurve database (LCDB; Warner et al., 2009) and ADS found a slightly longer period of 10.264 ± 0.004 h calculated by Brincat and Galdies (2018).

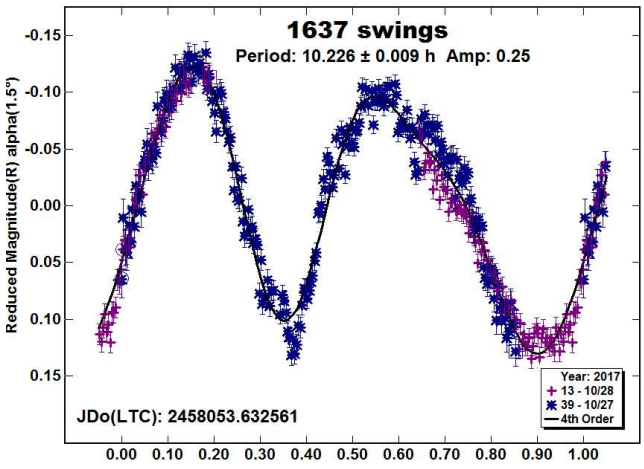

Number	Name	2017 mm/dd	Phase	L_{PAB}	B_{PAB}	Period(h)	P.E.	Amp	A.E.	Grp
1637	Swings	10/27-10/28	1.4	34	4	10.226	0.009	0.25	0.0075	MB

Table I. Observing circumstances and results. The phase angle is given for the first and last date. If preceded by an asterisk, the phase angle reached an extrema during the period. L_{PAB} and B_{PAB} are the approximate phase angle bisector longitude/latitude at mid-date range (see Harris et al., 1984). Grp is the asteroid family/group (Warner et al., 2009).

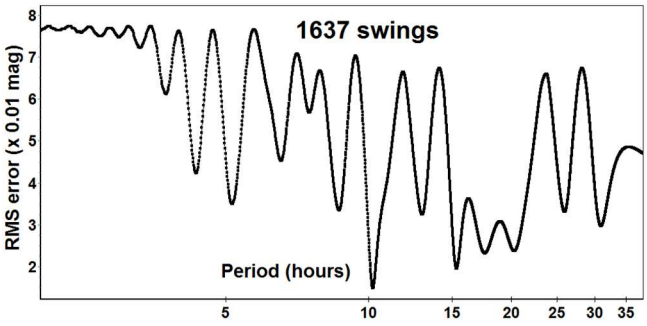

Acknowledgements

The authors would like to acknowledge the IAU ROAD offices, including NA-ROAD, WA-ROAD, and SA-ROAD; and Gena Lake Astrophysics and STEAM (GLAS) Education, in Lake Geneva, Wisconsin. We would like to specially thank Kate Meredith, Amanda Pagul, Adam McCulloch, and Katya Gozman. Our deepest appreciation is also extended to the McQuown Trust for financial support and access to the Stone Edge Observatory, Sonoma, CA, USA.

References

Brincat, M.; Galdies, C. (2018). "Photometric observations of main-belt asteroid 1637 swings, 10498 Bobgent and (25980) 2001 FK 53." *Minor Planet Bulletin* **45**, 115-116.

Harris, A.W.; Young, J.W.; Scaltriti, F.; Zappala, V. (1984). "Lightcurves and phase relations of the asteroids 82 Alkmene and 444 Gyptis." *Icarus* **57**, 251-258.

Kozai, Y. (1979). "Families of asteroids by a new criterion." *Annals of the Tokyo astronomical observatory* **17**, 194-220.

Lazzaro, D.; Angeli, C.A.; Carvano, J.M.; Mothe-Diniz, T.; Duffard, R; Florczak, M. (2004). "S3OS2: The visible spectroscopic survey of 820 asteroids." *Icarus* **172**, 179-220.

Masiero, J.R.; Mainzer, A.K.; Grav, T.; Bauer, J.M.; Cutri, R.M.; Dailey, J.; Eisenhardt, P.R.M.; McMillan, R.S.; Spahr, T.B.; Skrutskie, M.F.; Tholen, D.; Walker, R.G.; Wright, E.L.; DeBaun, E.; Elsbury, D.; Gautier IV, T.; Gomillion, S.; Wilkins, A. (2011). "Main Belt Asteroids with WISE/NEOWISE. I. Preliminary Albedos and Diameters." *Astrophys. J.* **741**, 68.

Warner, B.D.; Harris, A.W.; Pravec, P. (2009). "The Asteroid Lightcurve Database." *Icarus* **202**, 134-146. Updated 2016 Sep. *http://www.minorplanet.info/lightcurvedatabase.html*

Warner, B.D. (2019). MPO Canopus Software, version 10.8.1.1. BDW Publishing. *http://www.bdwpublishing.com*

1903 ADZHIMUSHKAJ: AN EXTREMELY SLOW ROTATOR

Tom Polakis
Command Module Observatory
121 W. Alameda Dr.
Tempe, AZ 85282
tpolakis@cox.net

(Received: 2022 March 16 Revised: 2022 May 28)

Photometric reductions from the first week of observations of 1903 Adzhimushkaj revealed that it would have a long period. Completing observations for one full rotation required a 75-night interval from November 2021 through February 2022. The phased lightcurve shows a period of 1793.8 ± 3.6 h. Recent analysis of survey images by other authors indicates that these "superslow" rotation rates are not uncommon.

CCD photometric observations of 1903 Adzhimushkaj were performed at Command Module Observatory (MPC V02) in Tempe, AZ. Images were taken using a 0.32-m f/6.7 Modified Dall-Kirkham telescope, SBIG STXL-6303 CCD camera, and a 'clear' glass filter. Exposure time for all the images was 2 minutes. The image scale after 2×2 binning was 1.76 arcsec/pixel. Table I shows the observing circumstances and results. All of the images for this asteroid were obtained between 2021 November and 2022 February.

Images were calibrated using a dozen bias, dark, and flat frames. Flat-field images were made using an electroluminescent panel. Image calibration and alignment was performed using *MaxIm DL* software.

The data reduction and period analysis were done using *MPO Canopus* (Warner, 2022). The 45′×30′ field of the CCD typically enables the use of the same field center for three consecutive nights. In these fields, the asteroid and three to five comparison stars were measured. Comparison stars were selected with colors within the range of 0.5 < B-V < 0.95 to correspond with color ranges of asteroids. In order to reduce the internal scatter in the data, the brightest stars of appropriate color that had peak ADU counts below the range where chip response becomes nonlinear were selected. *MPO Canopus* plots instrumental vs. catalog magnitudes for solar-colored stars, which is useful for selecting comp stars of suitable color and brightness.

Since the sensitivity of the KAF-6303 chip peaks in the red, the clear-filtered images were reduced to Sloan r′ to minimize error with respect to a color term. Comparison star magnitudes were obtained from the ATLAS catalog (Tonry et al., 2018), which is incorporated directly into *MPO Canopus*. The ATLAS catalog derives Sloan *griz* magnitudes using a number of available catalogs. The consistency of the ATLAS comp star magnitudes and color-indices allowed the separate nightly runs to be linked often with no zero-point offset required or shifts of only a few hundredths of a magnitude in a series.

A 9-pixel (16 arcsec) diameter measuring aperture was used for asteroids and comp stars. It was typically necessary to employ star subtraction to remove contamination by field stars. For the asteroid described here, I note the RMS scatter on the phased lightcurve, which gives an indication of the overall data quality including errors from the calibration of the frames, measurement of the comp stars,

Number	Name	yy/mm/dd	Phase	L_{PAB}	B_{PAB}	Period(h)	P.E.	Amp	A.E.	Grp
1903	Adzhimushkaj	21/11/22-22/02/04	7.8,19.5	47	-12	1793.8	3.6	1.17	0.06	EOS

Table I. Observing circumstances and results. The phase angle is given for the first and last date. If preceded by an asterisk, the phase angle reached an extrema during the period. L_{PAB} and B_{PAB} are the approximate phase angle bisector longitude/latitude at mid-date range (see Harris et al., 1984). Grp is the asteroid family/group (Warner et al., 2009).

the asteroid itself, and the period-fit. Period determination was done using the *MPO Canopus* Fourier-type FALC fitting method (cf. Harris et al., 1989). The phased lightcurve show the maximum at phase zero. Magnitudes in the plot are apparent and scaled by *MPO Canopus* to the first night.

1903 Adzhimushkaj is among the asteroids selected from the CALL website (Warner, 2011). The Asteroid Lightcurve Database (LCDB; Warner et al., 2009) was consulted to locate previously published results. All the new data for this asteroid can be found in the ALCDEF database.

1903 Adzhimushkaj was discovered by Tamara Smirnova at Nauchnyj in 1972. Two rotation periods appear in the LCDB. Loera-Gonzales et al. (2019) published a period of 4.622 ± 0.001 h, but cautioned that the scatter in the observations was high. Durech et al. (2020) computed a synodic period of 46.6585 ± 0.0006 h.

After the first five nights in November 2021, it became apparent from the slow upward ramp in brightness that this asteroid was a slow rotator. While 60 to 70 images were taken on each of those nights, all of the subsequent nights used two sets of 5 images, spaced by several hours. A total of 59 nights in the 75-night observing interval were useful enough to contribute to the lightcurve. Many of these nights were partly cloudy, and required changes on the fly from a scripted program to observe through gaps between clouds.

The asteroid was observed through one complete rotation, during which 877 images were acquired. The synodic period is 1793.8 ± 3.6 h, or roughly 75 days. The amplitude of the lightcurve is 1.17 mag, with an RMS error of 0.056 mag. The phase distance (H-G) correction in *MPO Canopus* proved particularly useful, since the changes in these values during the observing interval were 11.7° and 1.1 magnitudes, respectively.

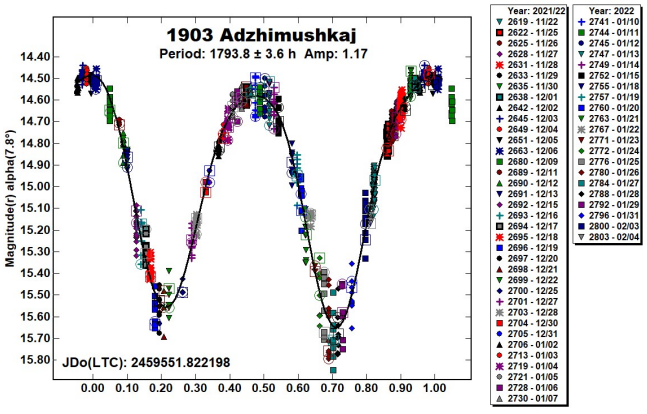

Based on data through 2021 August, the rotation period of this asteroid was the longest known. However, Erasmus et al. (2021) presented the discovery of 25 "superslow" rotating asteroids with periods that are longer than that of 1903 Adzhimushkaj. Minor planets that rotate this slowly have not been characterized until recently due to selection effects. The authors concluded that these slow rotators are common, with more than 0.4% of ordinary main-belt asteroids ranging between 2 and 20 km in diameter having rotation periods in excess of 1000 hours.

Acknowledgements

The author would like to express his gratitude to Brian Skiff for his indispensable mentoring in data acquisition and reduction. Thanks also go out to Brian Warner for support of his *MPO Canopus* software package.

References

Durech, J.; Tonry, J.; Erasmus, N.; Denneau, L.; Heinze, A.N.; Flewelling, H.; Vanco, R. (2020). "Asteroid models reconstructed from ATLAS photometry." *Astron. Astrophys*. **643**, A59.

Erasmus, N.; Kramer, D.; McNeill, A.; Trilling, D.E.; Janse van Rensburg, P.; van Belle, G.T.; Tonry, J.L.; Denneau, L.; Heinze, A.; Weiland, H.J. (2021). "Discovery of superslow rotating asteroids with ATLAS and ZTF photometry." *Monthly Notices of the Royal Astronomical Society* **506**, 3872-3881.

Harris, A.W.; Young, J.W.; Scaltriti, F.; Zappala, V. (1984). "Lightcurves and phase relations of the asteroids 82 Alkmene and 444 Gyptis." *Icarus* **57**, 251-258.

Harris, A.W.; Young, J.W.; Bowell, E.; Martin, L.J.; Millis, R.L.; Poutanen, M.; Scaltriti, F.; Zappala, V.; Schober, H.J.; Debehogne, H.; Zeigler, K.W. (1989). "Photoelectric Observations of Asteroids 3, 24, 60, 261, and 863." *Icarus* **77**, 171-186.

Loera-Gonzalez, P.; Olguin, L.; Saucedo, J.C.; Nunez-Lopez, R.; Yahia-Keith, N.A. (2019). "Lightcurve Based Rotational Period Determination for Asteroids at Unison Observatory: First Half of 2018." *Minor Planet Bull*. **46**, 97-98.

Tonry, J.L.; Denneau, L.; Flewelling, H.; Heinze, A.N.; Onken, C.A.; Smartt, S.J.; Stalder, B.; Weiland, H.J.; Wolf, C. (2018). "The ATLAS All-Sky Stellar Reference Catalog." *Ap. J.* **867**, A105.

Warner, B.D.; Harris, A.W.; Pravec, P. (2009). "The Asteroid Lightcurve Database." *Icarus* **202**, 134-146. Updated 2021 Dec. *http://www.minorplanet.info/lightcurvedatabase.html*

Warner, B.D. (2011). Collaborative Asteroid Lightcurve Link website. *http://www.minorplanet.info/call.html*

Warner, B.D. (2022). *MPO Canopus* software. *http://bdwpublishing.com*

THE ROTATION PERIOD OF 128 NEMESIS IS RE-EXAMINED

Frederick Pilcher
Organ Mesa Observatory (G50)
4438 Organ Mesa Loop
Las Cruces, NM 88011 USA
fpilcher35@gmail.com

(Received: 2022 April 6)

A synthesis of all published rotation periods of 128 Nemesis shows that the period is ambiguous and may be either 38.91 hours or 77.81 hours. The author explains why he prefers the 38.91-hour period.

The first published lightcurve of 128 Nemesis was by Scaltriti et al. (1979), who found a period of 39 ± 0.5 hours, amplitude 0.10 magnitudes, based on a dense somewhat unsymmetric bimodal lightcurve from 5 consecutive nights of observations 1977 Dec. 16-20.

This author (Pilcher, 2015) was unable to fit his observations from 2015 Jan. 5 - Apr 14 to a period near 39 hours and published a lightcurve, reprinted in this paper, that had a good fit to an unsymmetic bimodal lightcurve with twice the period of Scaltriti et al., 77.81 ± 0.01 hours, and smaller amplitude 0.08 magnitudes. The reader should note that the data at phases 0.5 to 1.0 are systematically about 0.03 magnitudes below those at phases 0.0 to 0.5. The corresponding segments of the descending branches, denoted by A and B, respectively, have different shapes. The incompatibility of the shapes of these segments prompted the author to adopt twice the period by Scaltriti et al.

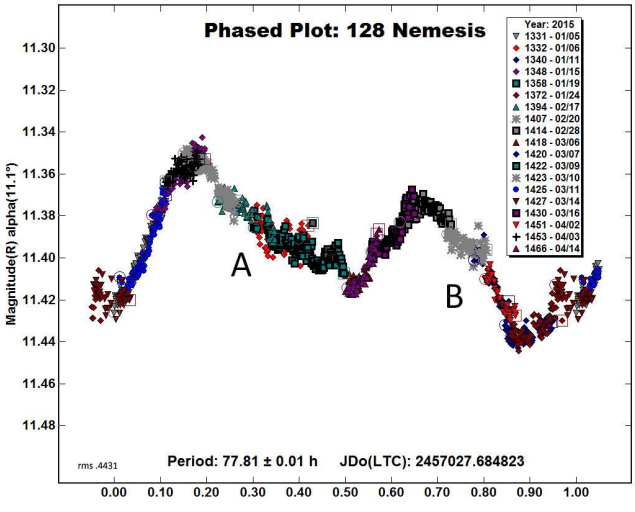

Colazo et al. (2022) published the next photometric observations of 128 Nemesis, based on data obtained 2021 June 2 - July 2. Their data provided a good fit to an unsymmetric bimodal lightcurve with period 38.907 ± 0.006 hours, amplitude 0.14 ± 0.01 magnitudes, and fully compatible with the 39 hours by Scaltriti et al.

Vernazza et al. (2021) obtained disk resolved images of 128 Nemesis in 2018 along with 41 other asteroids with the SPHERE (Spectro-Polarimetric High contrast Exoplanet Research) instrument on the 8-meter VLT at the European Southern Observatory. They claim for 128 Nemesis a sidereal rotation period of 38.9325 ± 0.0001 hours and a rotational pole located at celestial longitude 313º, celestial latitude -19º. For each of the three data sets the angle between the phase angle bisector and Vernazza's equator has been computed, that is, the asterocentric latitude of the photometric data set. It is shown in the column Ast. Lat. in Table I below.

All of these results are compatible with a rotation period near 38.9 hours except for Pilcher (2015) who obtained exactly the double amount. In this paper I show, with *MPO Canopus* software, that my data from 2015 are also compatible with a period near 38.9 hours.

MPO Canopus software uses the FALC algorithm written by Alan Harris to find the rotation period within the range specified by the user that best fits the data. This algorithm finds the coefficients of each order of the Fourier series up to a user specified maximum number, 10 in the calculations performed here, for a specified range of periods and computes the for each period within that range the rms residual, in units of 0.01 magnitudes, of all the individual data points from the graph specified by the Fourier components. It then plots the lightcurve for that period within the specified range for which the rms is a minimum and writes the both the period and rms residual of the individual data points.

It has been this author's standard practice to adjust the zero points of the individual lightcurves plotted in the phased lightcurve up or down until minimum rms is found. This practice was adopted here. Given that the CMC15 catalog magnitudes of the calibration stars have errors of an order of a few times 0.01 magnitudes, zero-point adjustments of these magnitudes are allowed. First the period from the 2015 data was forced to 38.91 hours and the zero points of individual sessions were adjusted. The largest adjustment was that most of the sessions between phases 0.5 and 1.0 were lifted about 0.03 magnitudes. Nearly all the sessions had additional smaller adjustments. When a close fit to 38.91 hours had been achieved, a period range from 38.4 to 39.4 hours was allowed to find the period in this range which best fit the original data from year 2015. This period was 38.91 ± 0.01 hours with one maximum and minimum per cycle (monomodal) and amplitude reduced to 0.05 ± 0.01 magnitudes.

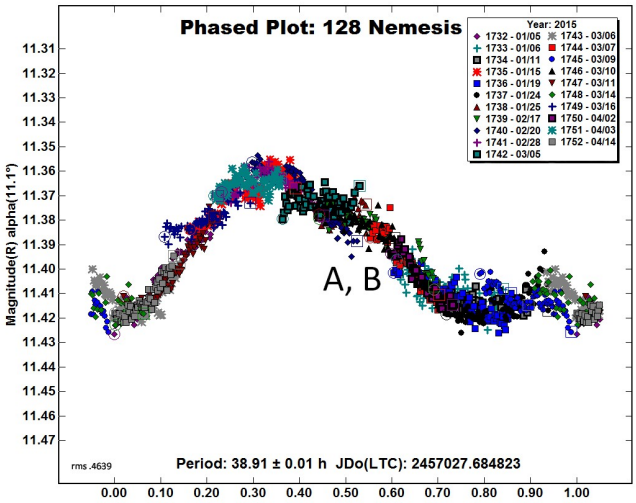

Before any zero-point adjustments were made, the 77.81-hour lightcurve published in Pilcher (2015) was plotted again. The rms was noted and written onto the lightcurve: 0.4431 × 0.01 magnitudes. After the best fit to 38.91 hours was achieved, the rms was 0.4639 × 0.01 magnitudes and again written onto the lightcurve. The fits to 77.81 hours and 38.91 hours are almost equally good. The discordances between A and B in the descending segments of the 77.81-hour lightcurve are hardly visible when phased to 38.91 hours and the segments are superposed. A split halves plot of the double period for the 38.91 hour best fit data set shows no recognizable differences between the descending segments.

It is commonly assumed that when the split halves plot of the double period shows both halves of the lightcurve to be the same, then the double period is unlikely if not rejected. By this assumption, the 38.91-hour period found from the year 2015 data is the correct one. All photometric data sets and the direct imaging are now compatible with a period close to 38.91 hours.

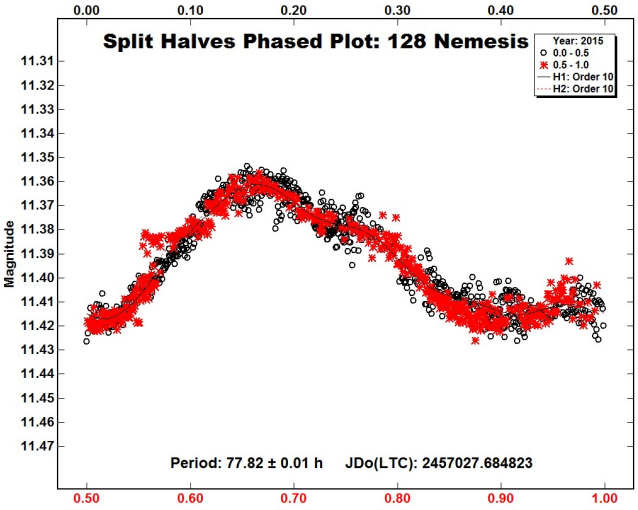

I suggest the follow scenario to explain all the observations of 128 Nemesis with a 38.91-hour rotation period. The amplitude of the lightcurve becomes smaller as viewing aspect is farther from the equator. Quite commonly an asteroid with a small amplitude bimodal lightcurve at near equatorial viewing aspect, as is the case for 128 Nemesis, has near polar aspect a lightcurve with only one maximum and minimum per cycle. The angle between the rotational equator, 90º from the pole by Vernazza et al., and the phase angle bisector (the asterocentric latitude) is included in Table I below of the observational circumstances and results. It shows the largest amplitude, 0.14 magnitudes for the Colazo et al. (2022) data set, also occurring for the smallest asterocentric latitude 22º.

The Scaltriti et al. (1979) data set, at intermediate asterocentric latitude 35º has an intermediate amplitude 0.10 magnitudes. Both of these low latitude lightcurves are bimodal. The smallest amplitude, and a monomodal lightcurve, is found for the Pilcher (2015) data set at a high asterocentric latitude -77º, where the - sign indicates the viewing aspect is toward the southern hemisphere.

I conclude that all available data considered together favor the 38.91-hour period over the 77.81-hour period. My data from year 2015 are on file in the web source ALCDEF.org with sharing allowed. I invite any interested reader to download these data and make an independent investigation.

References

Colazo, M.; Morales, M.; Chapman, C.; Garcia, A.; Santos, F.; Melia, R.; Suarez, N.; Stechina, A.; Scotta, D.; Martini, M.; Santucho, M.; Moreschi, A.; Wilberger, A.; Mottino, A.; Bellocchio, E.; Quinones, C.; Speranza, T.; Llanos, R.; Altuna, L; Caballero, M.; Romero, F.; Galarza, C.; Colazo, C. (2022). "Photometry and light curve analysis of eight asteroids by GORA's observatories." *Minor Planet Bull.* **49**, 48-50.

Harris, A.W.; Young, J.W.; Scaltriti, F.; Zappala, V. (1984). "Lightcurves and phase relations of the asteroids 82 Alkmene and 444 Gyptis." *Icarus* **57**, 251-258.

Pilcher, F. (2015). "New photometric observations of 128 Nemesis, 249 Ilse, and 279 Thule." *Minor Planet Bull.* **42**, 190-192.

Scaltriti, F.; Zappala, V.; Schober, H.J. (1979). "The rotations of 128 Nemesis and 393 Lampetia: The longest known periods to date." *Icarus* **37**, 133-141.

Vernazza, P.; and 66 co-authors (2021). "VLT/SPHERE imaging survey of the largest main-belt asteroids: Final results and synthesis." *Astron. Astrophys.* **A56**.

Author	yyyy/mm/dd	Phase	Ast. Lat.	L_{PAB}	B_{PAB}	Period(h)	P.E	Amp	A.E.
		All data refer to 128 Nemesis							
Scaltriti et al.	1977/12/16-12/20	2.9, 4.8	35	78	0	39.	0.5	0.10	0.01
Pilcher	2015/01/05-04/14	*11.1, 19.5	-77	131	1	38.91	0.01	0.05	0.01
						77.81	0.01	0.08	0.01
Colazo et al.	2021/06/02-07/02	2.6, 13.2	22	245	1	38.907	0.006	0.14	0.01

Table I. Observing circumstances and results. The phase angle is given for the first and last date, unless a minimum (second value) was reached. L_{PAB} and B_{PAB} are the approximate phase angle bisector longitude and latitude at mid-date range (see Harris *et al.*, 1984). Data for Colazo et al. (2022) are compiled from their reference. All other data are computed by the author.

748 SIMEISA – AN ASTEROID WITH AN EARTH-COMMENSURATE ROTATION PERIOD IS SOLVED

Frederick Pilcher
Organ Mesa Observatory (G50)
4438 Organ Mesa Loop
Las Cruces, NM 88011 USA
fpilcher35@gmail.com

Lorenzo Franco
Balzaretto Observatory (A81), Rome, ITALY

Alessandro Marchini, Riccardo Papini
Astronomical Observatory, DSFTA – University of Siena (K54)
Via Roma 56, 53100 – Siena, ITALY

Julian Oey
Blue Mountains Observatory (Q68)
94 Rawson Pde. Leura, NSW, AUSTRALIA

(Received: 2022 Mar 13)

A global collaboration of observers from Australia, Europe, and North America finds for 748 Simeisa a synodic rotation period 11.905 ± 0.001 h, amplitude 0.28 ± 0.02 magnitudes, V-R = 0.45 magnitudes, in the V band H = 9.224 ± 0.050, G = 0.316 ± 0.087.

Observations to produce the results reported in this paper have been contributed by Frederick Pilcher in the USA, Lorenzo Franco, Alessandro Marchini, and Riccardo Papini in Italy, and Julian Oey in Australia. Equipment details are on Table II. Image photometric measurement and lightcurve construction were done by *MPO Canopus* software. To reduce the number of data points on the lightcurves and make them easier to read, data points have been binned in sets of 3 with maximum time difference 5 minutes.

Minor planet 748 Simeisa is a Hilda-type asteroid with orbit in the 3:2 resonance with Jupiter. Previously published rotation periods, amplitudes, and celestial longitudes of observation for 748 Simeisa are by Behrend (2011web), 2011 Oct. 4-14, 11.919 h, 0.36 mag, celestial longitude 345º; and Dahlgren et al. (1998), 1995 Aug 31-Sept. 2, 11.88 h, >0.22 mag, celestial longitude 327º. Both observations sets were from a single observatory and show only about 8 hours, or 2/3 phase coverage. Being obtained at similar celestial longitudes, both published lightcurves show a single double-humped maximum rising about 0.2 magnitudes above nearly equal minima about 6 hours apart and a rise toward a second maximum in the missing segment of the lightcurve. Warner and Stephens (2021); and the authors of this paper (Pilcher et al., 2021) with data obtained at the same opposition, late 2020, near celestial longitude 63º, obtained discordant rotation periods, 23.633 hours and 11.903 hours, respectively, both with amplitude near 0.10 magnitudes. The contrast of amplitudes at the celestial longitudes of the previous observations suggested that the rotational pole is much closer to 63º than to 327º and 345º. At the following opposition in early 2022 the amplitude was expected to be much larger and the period ambiguity could be resolved.

The authors of this paper obtained twelve sessions of new observations 2021 Dec. 27 – 2022 Feb. 10 from their respective widely separated longitudes, with target celestial longitude of mid-date 143º. The data from these sessions provide an excellent fit to a phased lightcurve with a period of 11.905 ± 0.001 hours, two unequal maxima and minima per rotational cycle, and amplitude decreasing from 0.28 mag to 0.24 mag as the phase angle decreased from 13.3º on the first date to 0.9º. Observations from Europe, North America, and Australia cover the entire double period of 23.809 hours. The split-halves plot of the double period shows that the two halves are identical except for the decrease in depth of the minimum near phases 0.12 and 0.62. This change is caused by the commonly encountered decrease of amplitude with decreasing phase angle, and is not an indication that the double period is correct. This new result is compatible with all previously published periods except 23.633 hours by Warner and Stephens (2021). A period nearly twice 11.9 hours can now be safely rejected, and our period of 11.905 hours can be considered secure.

On 2022 Jan. 30, first author Pilcher alternately obtained 20 images each through the R and V filters. The same solar-colored calibration stars were used for both image sets with their respective R and V magnitudes stated in the *MPO Canopus* comparison star selector. Plotted together on a single raw lightcurve, they show that V-R = 0.45. The *MPO Canopus* H-G calculator routine was applied to our data at mid-light for each session in the V filter band, adding the derived color index V-R. Applied to the data of the early 2022 opposition, H = 9.224 ± 0.050, G = 0.316 ± 0.087. For the 2020 opposition, we find H = 9.098 ± 0.032, G = 0.396 ± 0.062.

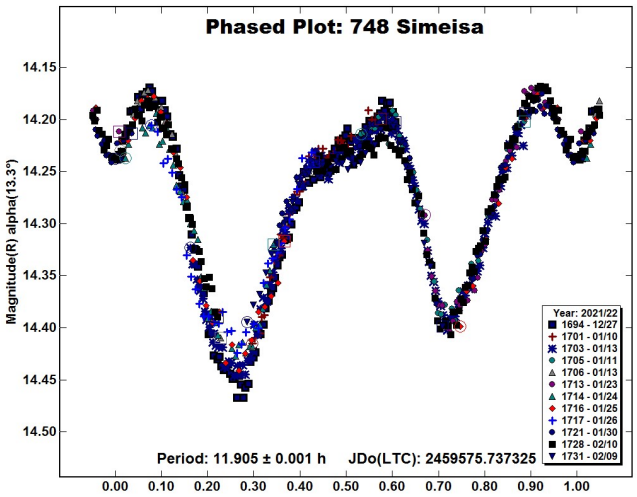

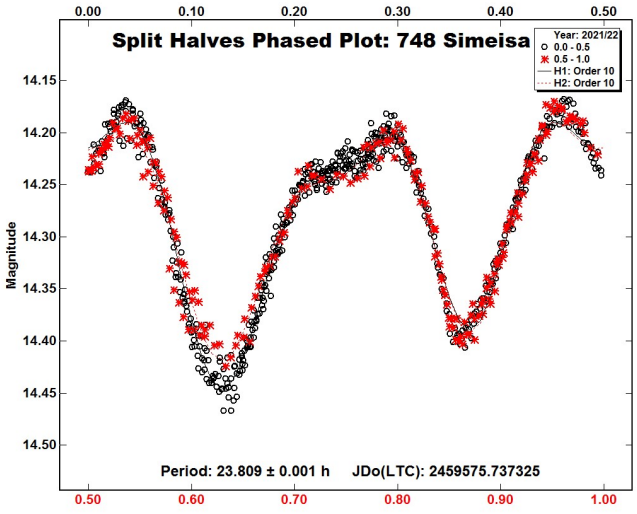

Number	Name	yyyy/mm/dd	Phase	L_{PAB}	B_{PAB}	Period (h)	P.E.	Amp	A.E.
748	Simeisa	2021/12/27-2022/02/10	13.3,0.9	143	-2	11.905	0.001	0.28	0.02

Table I. Observing circumstances and results. The phase angle is given for the first and last date. L_{PAB} and B_{PAB} are the approximate phase angle bisector longitude and latitude at mid-date range (see Harris *et al.*, 1984).

Observer Observatory (MPC code)	Telescope	CCD	Session Filter
Frederick Pilcher Organ Mesa Observatory (G50)	0.35-m SCT f/10.0	SBIG STL-1001E	1694, 1701, 1703, 1721, 1728 all C
Lorenzo Franco Balzaretto Observatory (A81)	0.20-m SCT f/5.0	SBIG ST7-XME	1716 R
Alessandro Marchini, Riccardo Papini Astronomical Observatory of the University of Siena (K54)	0.30-m MCT f/5.6	SBIG STL-6303e (bin 2x2)	1705 C, 1706 C, 1713 R, 1714 R
Julian Oey Blue Mountains Observatory (Q68)	0.61-m CDK f/6.8 0.35-m SCT f/5.9	SBIG STL 11000 SBIG ST-8XME	1717 C 1731 C

Table II. Observing equipment. CDK: Corrected Dall-Kirkham, MCT: Maksutov-Cassegrain, SCT: Schmidt-Cassegrain.

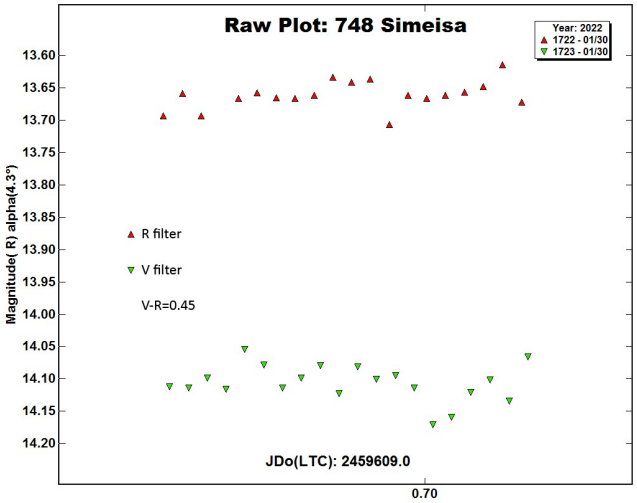

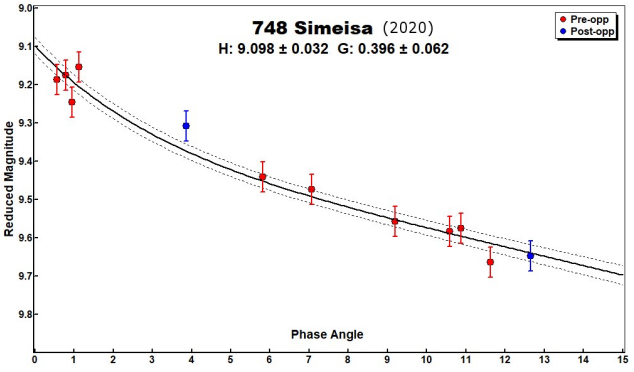

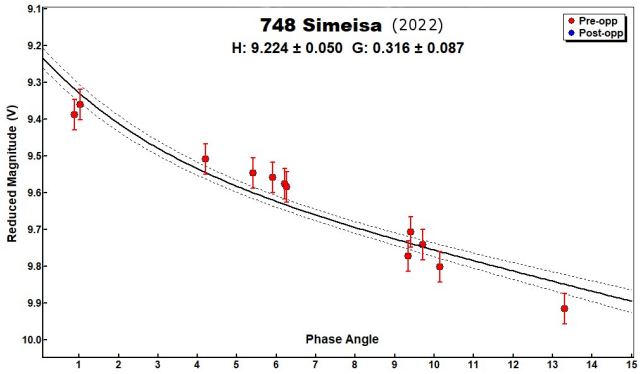

References

Behrend, R. (2011web). Observatoire de Geneve web site. *http://obswww.unige.ch/~behrend/page_cou.html*.

Dahlgren, M.; Lahulla, J.F.; Lagerkvist, C.-I.; Lagerros, J.; Mottola, S.; Erikson, A.; Gonano-Beurer, M.; Di Martino, M. (1998). "A Study of Hilda Asteroids. V. Lightcurves of 47 Hilda Asteroids." *Icarus* **133**, 247-285.

Harris, A.W.; Young, J.W.; Scaltriti, F.; Zappala, V. (1984). "Lightcurves and phase relations of the asteroids 82 Alkmene and 444 Gyptis." *Icarus* **57**, 251-258.

Pilcher, F.; Franco, L.; Marchini, A.; Oey, J. (2021). "357 Ninina and 748 Simeisa – two asteroids with Earth commensurate rotation periods." *Minor Planet Bull.* **48**, 233-235.

Warner, B.D.; Stephens, R.D. (2021). "Lightcurve analysis of Hilda asteroids at the center for Solar System Studies, 2020 October - December." *Minor Planet Bull.* **48**, 164-165.

ROTATIONAL PERIOD DETERMINATION OF 2282 ANDRÉS BELLO

Jack Smith
Institute for Astronomy, Royal Observatory, Edinburgh
jackleesmith100@gmail.com

(Received: 2022 Apr 15)

The asteroid 2282 Andrés Bello was observed over the course of one night using the PIRATE telescope at Teide Observatory, Las Palmas. The rotation period and lightcurve amplitude observed were P = 3.394 h and A = 0.64 mag. These values are consistent with those previously reported by D. Klinglesmith et al. (2016). The diameter and mass of 2282 Andrés Bello are found to be 7.1 km and 6×10^14 kg.

The aim of these observations was to obtain an updated value of the rotational period of 2282 Andrés Bello and compare it to the most recent previous literature value of 3.425 h (Klinglesmith et al., 2016). By assigning the asteroid a spectral type, its diameter and mass were also found.

The PIRATE (Physics Innovations Robotic Astronomical Telescope Explorer) telescope consists of a 0.6-m PlaneWave CDK24 telescope at f/6.5. It is mounted on a 10Micron GM4000 mount and uses a FLI ProLine KAF-16803 CCD camera which was binned at 2×2. Images were taken with exposures of 180 s.

Ephemerides were obtained from NASA's Horizons System (JPL, 2022). The 74 images captured were reduced through use of flat field and bias images; dark-current images were not used as the PIRATE telescope is actively cooled. In subsequent lightcurve analysis and orbit fitting (Gauss' Method), the light travel time to the asteroid was taken into account.

2282 Andrés Bello (1974 FE; 1979 YL; 1974 HO; 1962 QC; 1951 EH2; 1931 AC1) was discovered on 1974 March 22 at the Cerro El Roble observatory in Chile by Carlos Torres and later named after the Venezuelan Andrés Bello in 1981. It is a main-belt asteroid of semi-major axis 2.20 AU, eccentricity 0.079, inclination 4.985°, and orbital period 3.22 years. As found in this analysis, its spectral type in the Bus-DeMeo system is L and it has a diameter of 7.1 km.

Analysis of the lightcurve gave a rotational period of P = 3.394 ± 0.043 h and an accompanying amplitude of A = 0.64 ± 0.08 mag. These values agree very closely to prior literature. The L spectral type classification was obtained from photometry performed in the Johnson-Cousins BVRI filters and led to an approximation for the density, albedo, and phase coefficient of 2282 Andrés Bello (DeMeo and Carry, 2013; Belskaya and Shevchenko, 2000). These values were in turn used to estimate the mass and diameter of the asteroid: M = 6 ± 2 × 10^14 kg, D = 7.1 ± 0.3 km.

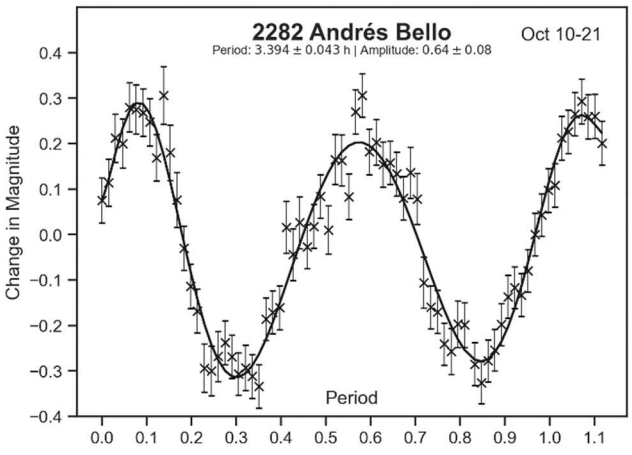

Acknowledgements

My thanks to Dr. Colin Snodgrass (Institute for Astronomy, Royal Observatory Edinburgh) for his support in this research. Thanks also to Freya Shepherd, Katherine Schofield, Sian Robertson, and Claire Jameson at the University of Edinburgh.

References

Belskaya, I.; Shevchenko, V. (2000). "Opposition effect of asteroids." *Icarus* **147**, 94-105.

DeMeo, F.; Carry, B. (2013). "The taxonomic distribution of asteroids from multi-filter all-sky photometric surveys." *Icarus* **226**, 723-741.

Harris, A.W.; Young, J.W.; Scaltriti, F.; Zappala, V. (1984). "Lightcurves and phase relations of the asteroids 82 Alkmene and 444 Gyptis." *Icarus* **57**, 251-258.

JPL (2022). "NASA Horizons System." *https://ssd.jpl.nasa.gov/horizons/app.html#/*

Klinglesmith, D.A., III; Hendrickx, S.; Madden, K.; Montgomery, S. (2016). "Asteroid Lightcurves from Estcorn Observatory." *Minor Planet Bulletin* **43**, 234-239.

Number	Name	yyyy mm/dd	Phase	L_{PAB}	B_{PAB}	Period(h)	P.E.	Amp	A.E.	D
2282	Andrés Bello	2021 10/10-10/10	10.9	2	0	3.394	0.043	0.64	0.08	7.1

Table I. Observing circumstances and results. The phase angle is given for the first and last date. If preceded by an asterisk, the phase angle reached an extremum during the period. L_{PAB} and B_{PAB} are the approximate phase angle bisector longitude/latitude at mid-date range (see Harris *et al.*, 1984). D is the diameter (km; derived from albedo).

ROTATION PERIOD DETERMINATION FOR (9659) 1996 EJ

Alessandro Marchini
Astronomical Observatory, DSFTA - University of Siena (K54)
Via Roma 56, 53100 - Siena, ITALY
marchini@unisi.it

Riccardo Papini, Fabio Salvaggio
Wild Boar Remote Observatory (K49)
San Casciano in Val di Pesa (FI), ITALY

(Received: 2022 April 14 Revised: 2022 June 1)

Photometric observations of the main-belt asteroid (9659) 1996 EJ were conducted in order to determine its synodic rotation period. We found P = 6.527 ± 0.001 h, A = 0.09 ± 0.03 mag.

CCD photometric observations of the main-belt asteroid (9659) 1996 EJ were carried out in March 2022 at the Astronomical Observatory of the University of Siena (K54), a facility inside the Department of Physical Sciences, Earth and Environment (DSFTA, 2022). We used a 0.30-m *f*/5.6 Maksutov-Cassegrain telescope, SBIG STL-6303E NABG CCD camera, and clear filter; the pixel scale was 2.30 arcsec when binned at 2×2 pixels and all exposures were 300 seconds.

Data processing and analysis were done with *MPO Canopus* (Warner, 2018). All images were calibrated with dark and flat-field frames and the instrumental magnitudes converted to R magnitudes using solar-colored field stars from a version of the CMC-15 catalogue distributed with *MPO Canopus*. Table I shows the observing circumstances and results.

A search through the asteroid lightcurve database (LCDB; Warner et al., 2009) indicates that our result may be the first reported lightcurve observations and results for this asteroid.

(9659) 1996 EJ was discovered on 1996 March 10 at Kushiro by S. Ueda and H. Kaneda. It is a main-belt asteroid with a semi-major axis of 2.660 AU, eccentricity 0.090, inclination 13.461°, and an orbital period of 4.34 years. Its absolute magnitude is H = 12.36 (JPL, 2022). The NEOWISE satellite infrared radiometry survey (Masiero et al., 2011) found a diameter D = 8.883 ± 0.141 km using an absolute magnitude H = 12.1.

Observations were conducted over four nights and collected 223 data points. The period analysis shows two possible solutions for the rotational period of this asteroid: P = 3.243 h and P = 6.527 h (Fig. 1). As noted by Harris et al. (2014), given the low amplitude, either solution was plausible and so we used a split-halves plot to see which period to favor. The "split-halves" test (Fig. 2) shows a significant mismatch between the two halves of the half-period lightcurve, well beyond the data scatter level. This favors the longer period of P = 6.527 ± 0.001 h (Fig. 3) with an amplitude A = 0.09 ± 0.03 mag that is formally adopted as a solution in this paper (Fig. 4), but further observations are highly recommended in future apparitions to verify the result.

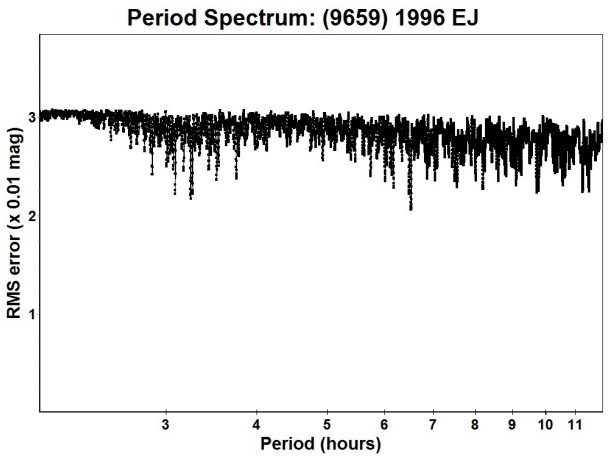

Figure 1: Period spectrum with two possible solutions at 3.243 h and 6.527 h.

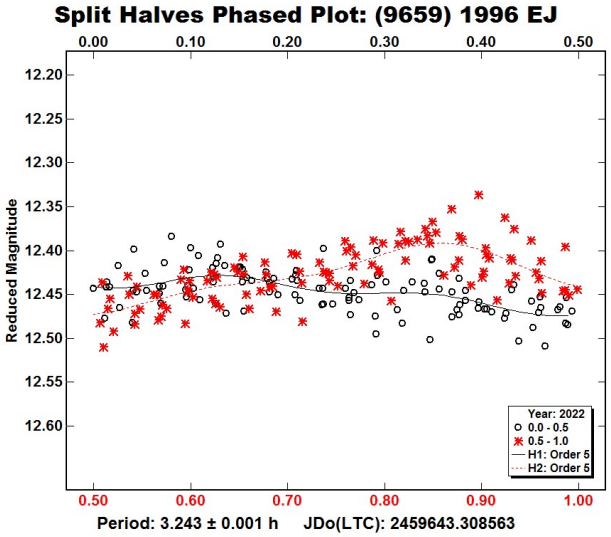

Figure 2: Split halves plot for the period of 3.243 h.

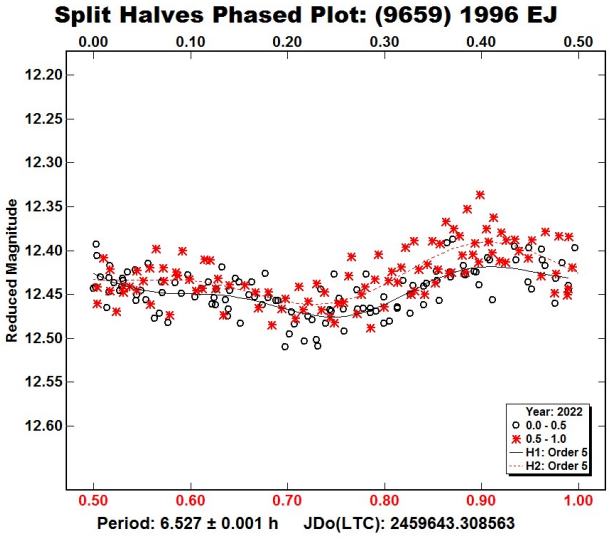

Figure 3: Split halves plot for the period of 6.527 h.

Number	Name	2022/mm/dd	Phase	L_{PAB}	B_{PAB}	Period(h)	P.E.	Amp	A.E.	Grp
9659	1996 EJ	03/04-03/29	*3.6,10.2	168	6	6.527	0.001	0.09	0.03	MB

Table I. Observing circumstances and results. The phase angle is given for the first and last date. If preceded by an asterisk, the phase angle reached an extrema during the period. L_{PAB} and B_{PAB} are the approximate phase angle bisector longitude/latitude at mid-date range (see Harris et al., 1984). Grp is the asteroid family/group (Warner et al., 2009).

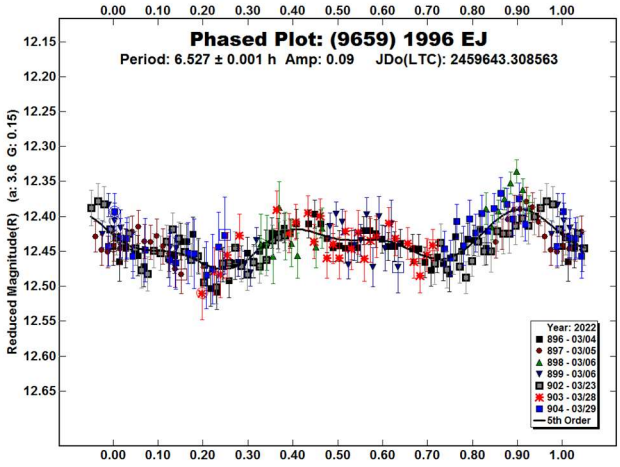

Figure 4: Lightcurve for (9659) 1996 EJ with the preferred period of 6.527 h.

Acknowledgements

The authors want to thank a group of high school students involved in an interesting vocational guidance project about astrophysics; they attended some observing sessions and participated in data analysis. From Liceo "Poliziano" (Montepulciano): G. Accursi, B. Belelli, F. Casanova, S. Corazza, M. Di Bernardini, C. Di Renzone, G. Fascetti, F. Gavagni, S. Lionelli, F. Materazzi, S. Mazzetti, A. Meacci, G. Meocci, S. Nicorescu, F. Pepi, C. Rachini, M. Rosignoli, F. Sabatino, B. Socea; from Liceo "Alessandro Volta (Colle Val d'Elsa): M. Calabrò, G. Cortonesi, M. Fedele, A. Giurleo, A. Guidi, A. Lazemataj, P. Lupini, A. Sciarrotta, F. Vanni.

References

DSFTA (2022). Dipartimento di Scienze Fisiche, della Terra e dell'Ambiente – Astronomical Observatory. *https://www.dsfta.unisi.it/en/research/labs/astronomical-observatory*

Harris, A.W.; Young, J.W.; Scaltriti, F.; Zappala, V. (1984). "Lightcurves and phase relations of the asteroids 82 Alkmene and 444 Gyptis." *Icarus* **57**, 251-258.

Harris, A.W.; Pravec, P.; Galad, A.; Skiff, B.A.; Warner, B.D.; Vilagi, J.; Gajdos, S.; Carbognani, A.; Hornoch, K.; Kusnirak, P.; Cooney, W.R.; Gross, J.; Terrell, D.; Higgins, D.; Bowell, E.; Koehn, B.W. (2014). "On the maximum amplitude of harmonics on an asteroid lightcurve." *Icarus* **235**, 55-59.

JPL (2022). Small Body Database Search Engine. *https://ssd.jpl.nasa.gov*

Masiero, J.R.; Mainzer, A.K.; Grav, T.; Bauer, J.M.; Cutri, R.M.; Dailey, J.; Eisenhardt, P.R.M.; McMillan, R.S.; Spahr, T.B.; Skrutskie, M.F.; Tholen, D.; Walker, R.G.; Wright, E.L.; DeBaun, E.; Elsbury, D.; Gautier, T. IV; Gomillion, S.; Wilkins, A. (2011). "Main Belt Asteroids with WISE/NEOWISE. I. Preliminary Albedos and Diameters." *Astrophys. J.* **741**, A68.

Warner, B.D.; Harris, A.W.; Pravec, P. (2009). "The Asteroid Lightcurve Database." *Icarus* **202**, 134-146. Updated 2020 Oct. *http://www.minorplanet.info/lightcurvedatabase.html*

Warner, B.D. (2018). MPO Software, MPO Canopus v10.7.7.0. Bdw Publishing. *http://minorplanetobserver.com*

LIGHTCURVE ANALYSIS FOR NINE NEAR-EARTH ASTEROIDS

Peter Birtwhistle
Great Shefford Observatory
Phlox Cottage, Wantage Road
Great Shefford, Berkshire, RG17 7DA
United Kingdom
peter@birtwhistle.org.uk

(Received: 2022 April 9)

Lightcurves and amplitudes for nine small near-Earth asteroids observed from Great Shefford Observatory during close approaches between January and March 2022 are reported. Seven are superfast rotators with periods < 8 minutes and include two tumblers. Another shows indications of tumbling with likely periods > 1 h and one shows no discernable rotation.

Photometric observations of near-Earth asteroids during close approaches to Earth between January and March 2022 were made at Great Shefford Observatory using a 0.40-m Schmidt-Cassegrain and Apogee Alta U47+ CCD camera. All observations were made unfiltered and with the telescope operating with a focal reducer at f/6. The 1K×1K, 13-micron CCD was binned 2×2 resulting in an image scale of 2.16 arc seconds/pixel. All the images were calibrated with dark and flat frames and *Astrometrica* (Raab, 2018) was used to measure photometry using APASS Johnson V band data from the UCAC4 catalogue (Zacharias et al., 2013). *MPO Canopus* (Warner, 2022), incorporating the Fourier algorithm developed by Harris (Harris et al., 1989) was used for lightcurve analysis.

No previously reported results for any of the objects reported here have been found in the Asteroid Lightcurve Database (LCDB) (Warner et al., 2009), from searches via the Astrophysics Data System (ADS, 2022) or from wider searches unless otherwise noted. All size estimates are calculated using H values from the Small-Body Database Lookup (JPL 2022b), using an assumed albedo for NEAs of 0.2 (LCDB readme.pdf file) and are therefore uncertain and offered for relative comparison only.

2022 AO6. This Apollo passed Earth at 1.1 Lunar Distances (LD) 16 hours before discovery by the ATLAS team on 2022 Jan 13.5 UTC (Ikari et al., 2022a). It was observed for 3 hours later that day when it was at mag +16, at 2.2 LD and moving at 50 arcsec/min. The telescope was repositioned 15 times during image capture and exposures ranged from 4 to 7.6 seconds. The resulting analysis reveals an asymmetric bimodal lightcurve of 2.2-minute period and, with H = 25.26 an approximate size of 26 m is inferred.

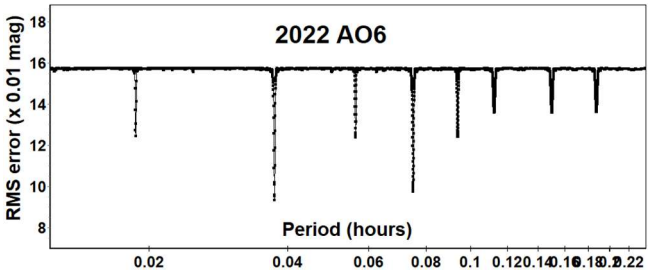

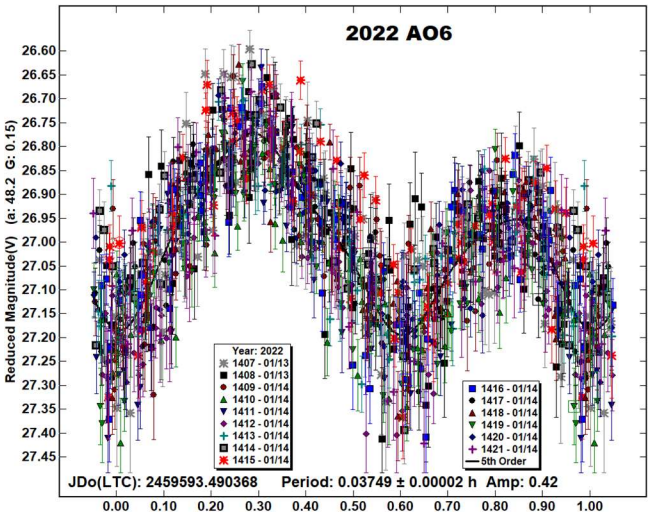

2022 CV5. The Mt. Lemmon Survey discovered this 9-m dia. Apollo 1.5 days before an approach to 1.6 LD (Ikari et al., 2022b). It was followed for 4 h starting at 2022 Feb 10.94 UTC when it was at 1.7 LD and moving at 64 arcsec/min. Exposures were varied between 3 and 6.3 seconds and the telescope was repositioned 19 times, with a total of 1680 images being obtained. 2022 CV5 was relatively faint at 17th mag but variation was readily apparent, with maxima visible approximately every 90 s. To strengthen the signal the images were then stacked using *Astrometrica*, combining between 4 and 7 images in each stack, arranged so that the longest effective exposure (Δt) from start of the first to the end of the last exposure in each stack was 30 seconds or less. This was chosen using the assumed period P = ~180 s, so that Δt / P was no greater than ~0.185 to ensure the amount of lightcurve smearing would not be excessive (Pravec et al., 2000). 401 measurements were obtained from the stacked images and then analysed, the resulting period spectrum indicating a bimodal fit at 3.3 minutes being a slightly better fit than a quadrimodal solution at double that period. The bimodal lightcurve with amplitude 0.72 is given here, labelled "PAR assumed", together with the period spectrum.

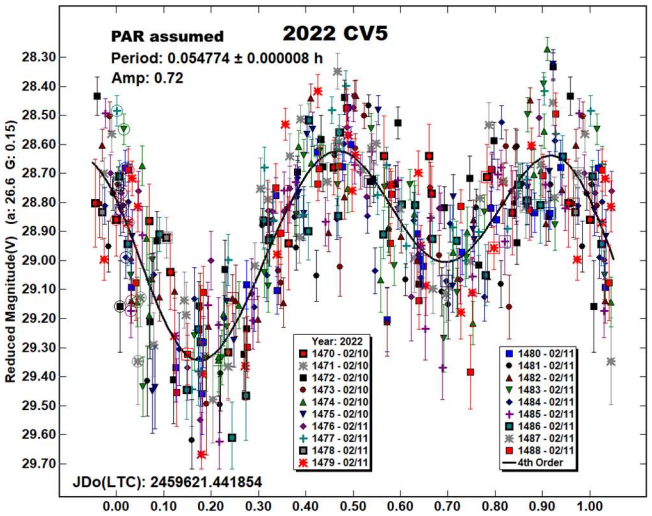

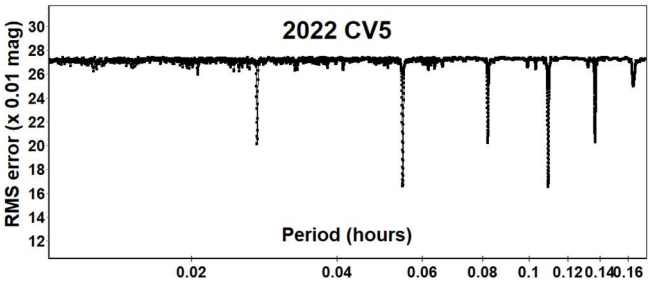

However, there is a larger than expected degree of scatter in the points, especially noticeable around the maxima and therefore non-principal axis (NPA) rotation was suspected. Although not designed for analysing NPA rotation, the Dual-Period search functionality in Canopus was used and resulted in a second period being resolved. The two lightcurves are labelled here as P1 and P2:

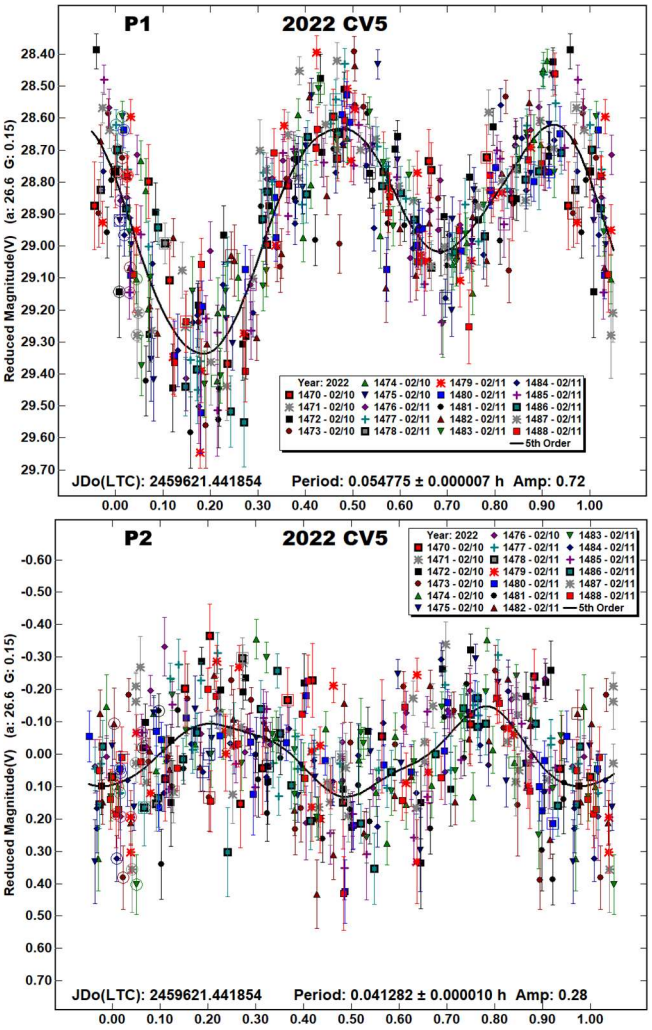

The shorter of the two periods, P2 is 148.6 s and therefore $\Delta t / P = 30 / 148.6 = 0.202$, large enough to reduce the amplitude of the normally dominant 2nd harmonic to 75% of its likely true value (see Table I) but not severe enough to alter the overall interpretation of the P2 lightcurve (Birtwhistle, 2021).

Without a full physical model available it is possible that one or both of the frequencies of the derived periods may be linear combinations of the real frequencies of rotation and precession of the object. But with periods P1 and P2 being well defined it is expected that this may be rated as PAR = -3, NPA rotation reliably detected with the two periods resolved. (Petr Pravec, personal communication).

	Period (h)	Δt/P	*f*1	*f*2	*f*3	*f*4
P1	0.0548	0.152	0.96	0.86	0.69	0.49
P2	0.0413	0.202	0.93	0.75	0.50	0.22

Table I. Factors f_n reducing the strength of the first four harmonics in the lightcurve of 2022 CV5 for NPA rotation periods P1 and P2 (see Pravec et al., 2000).

2022 CO6. An amateur discovery by the MAP team in Chile on 2022 Feb 10.0 UTC, this small Aten (dia. ~18 m) passed Earth at 0.6 LD on 2022 Feb 15.4 UTC (Bressi et al., 2022). It was observed on its approach for 3.4 h starting at 2022 Feb 14.90 UTC, at mag +14. Its apparent speed increased from 135 to 221 arcsec/min. and the telescope needed to be repositioned 22 times. Exposures were limited to 3.4 seconds or less and a total of 1339 usable images were obtained. The analysis indicates that a bimodal solution at 0.047287 h is the strongest of a number of similar solutions identified in the period spectrum. 2022 CO6 was at low altitude throughout, rising from 17° to 32°. Small adjustments to the zero-points of the 22 sessions reduced the lightcurve RMS residual from 0.12 to 0.08 magnitudes and are incorporated in the phased lightcurve.

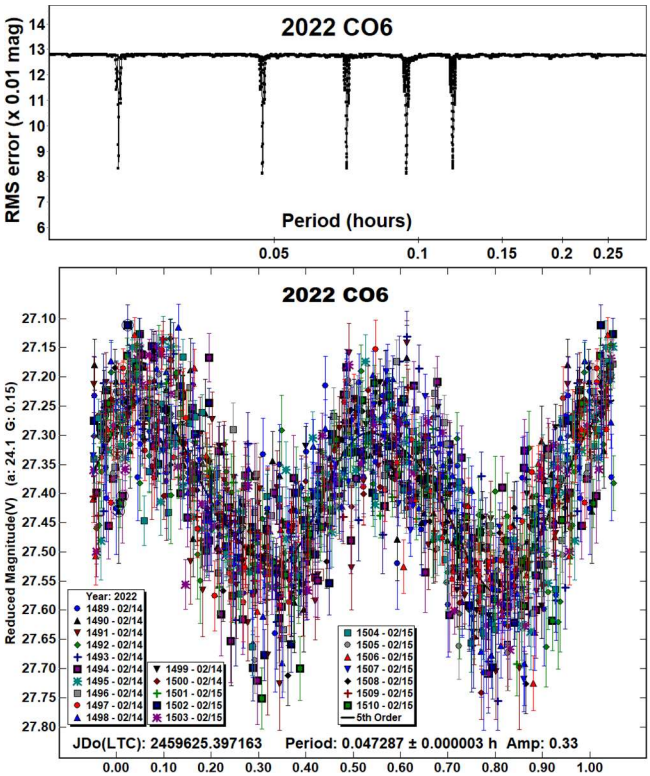

2022 DA. With H = 25.1 this is a ~28 m sized Apollo, discovered from the ATLAS site in Sutherland, South Africa on 2022 Feb 18.84 UTC (Urbanik et al., 2022). It was observed 3 h later for 1.7 h when it was 15th mag, at 2.3 LD and was moving at 114 arcsec/min. 659 measurements were made, 21 from exposures of 4.6 s and the remainder from exposures of 3.4 s. The period spectrum shows the overall RMS scatter of the data points is 0.102 mag. and remarkably, no periodicity is revealed within the range of periods from 11 s - 2 h. The raw plot also shows no significant slope across the 1.7 h span of observations. With 97% of the integration times, Δt being 3.4 s, even though not optimal, it would be expected that a detectable signal would result from a rotation period P as short

as ~11 s, where $\Delta t / P = 0.3$ and the strength of the second harmonic would be reduced by about 50% (Pravec et al., 2000). The conclusion is that 2022 DA has P < 2h with an amplitude < 0.10, or P >> 2h, or P < 11 s. Presumably the most likely scenario is P < 2h with very small amplitude, possibly due to a pole-on orientation.

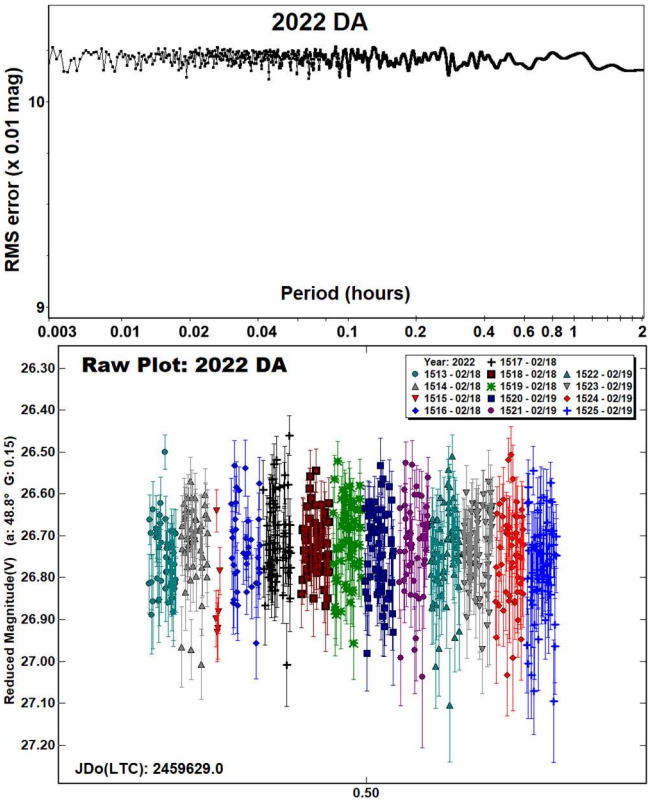

2022 ER5. The Pan-STARRS 2 telescope on Haleakala discovered this Apollo 9 days before an approach to 2 LD on 2022 Mar 20.2 UTC (Evans et al., 2022). It was followed for 2.4 h starting on 2022 Mar 19.82 UTC when it was 16th mag and accelerated from 155 to 169 arcsec/min, requiring the telescope be repositioned 28 times. 1325 usable images were obtained with exposure lengths between 2.5 and 3.3 s. The analysis showed that a bimodal solution with period 0.11581 h provides a slightly better fit to the data points than a quadrimodal one at double that period and is given here. With H = 25.7 it has an estimated diameter of 21 m.

Radar echoes from 2022 ER5 were detected from Goldstone on 2022 Mar 20 and their result includes the statement: "*The bandwidth of about 10 Hz and the absolute magnitude of 25.5, which suggests a diameter of 20-30 meters, strongly imply that this asteroid is a rapid rotator with a period of less than about 0.5 hours.*" (Benner, 2022). This is in good agreement with the period determined in this paper. The lightcurve was subsequently shared with Dr. Lance Benner and he has revised the Goldstone results page, stating the reported period and amplitude "*suggests an elongated shape. This period combined with the maximum bandwidth of 14 Hz place a lower bound on the maximum pole-on breadth of about 16 meters.*"

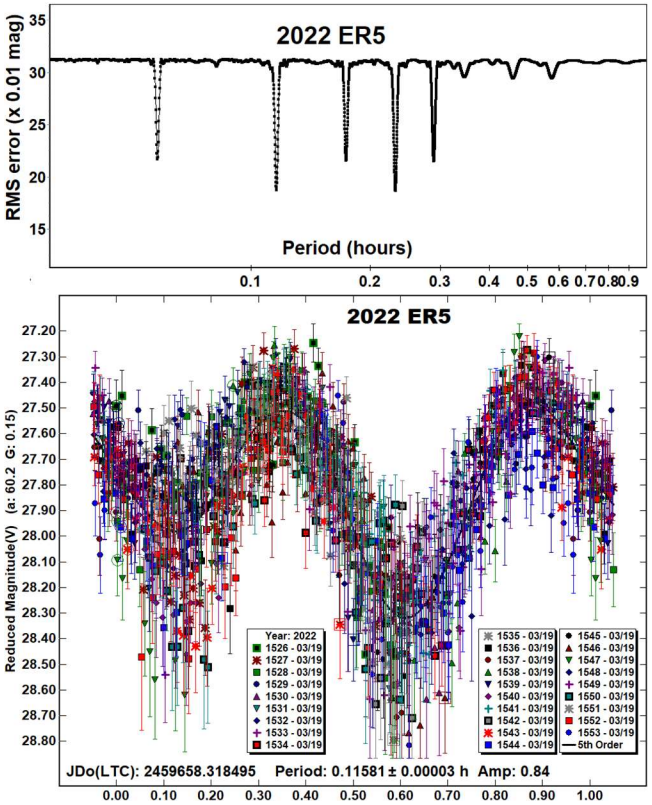

2022 FC. Another small, ~18 m diameter Apollo discovered by the Catalina Sky Survey team some 33 hours before passing Earth at 1.8 LD on 2022 Mar 23.7 UTC (Bacci et al., 2022a). It was observed for 3.5 h starting at 2022 Mar 23.0 UTC and with apparent sky motion increasing from 92 to 124 arcsec/min. exposure lengths were kept between 4.2 and 5.7 s with the telescope being repositioned 24 times and 1575 measurable images were obtained. An initial reduction again indicated a bimodal solution at 0.03 h gave a slightly better fit than a quadrimodal fit at double the period, the bimodal lightcurve is labelled here as "PAR assumed".

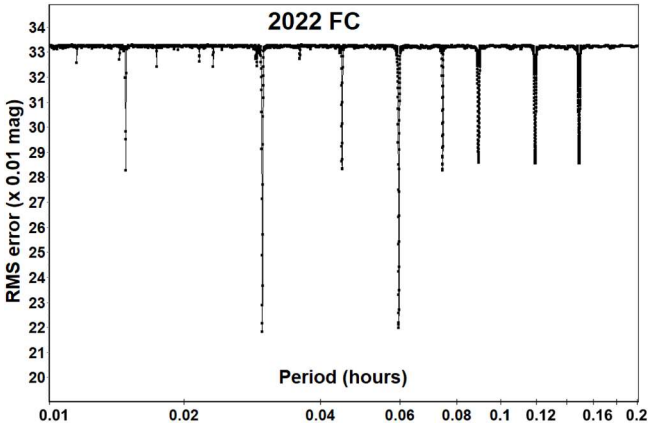

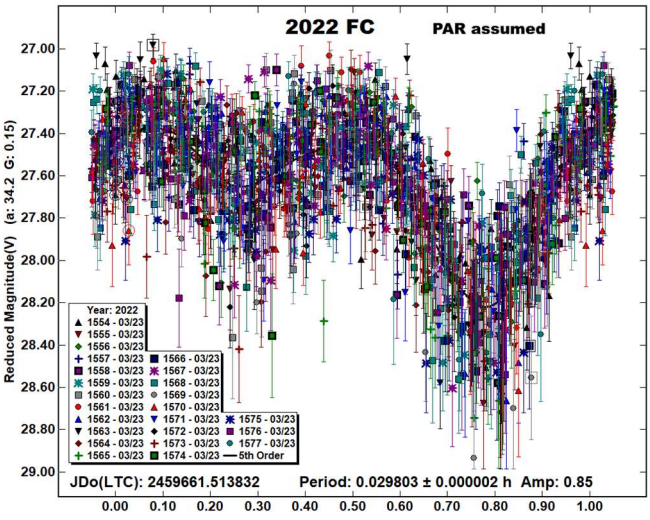

However, like 2022 CV5, there was apparently more scatter at the maxima of the lightcurve than might be expected from the SNr's of individual measurements, as well as a number of secondary RMS minima being present in the period spectrum. A Dual-Period search was again run in Canopus to see whether non-principal axis (NPA) rotation could be detected within the noise of the dominant large amplitude 0.0298 h period. This was successful and resulted in two lightcurves being resolved, labelled here as P1 and P2.

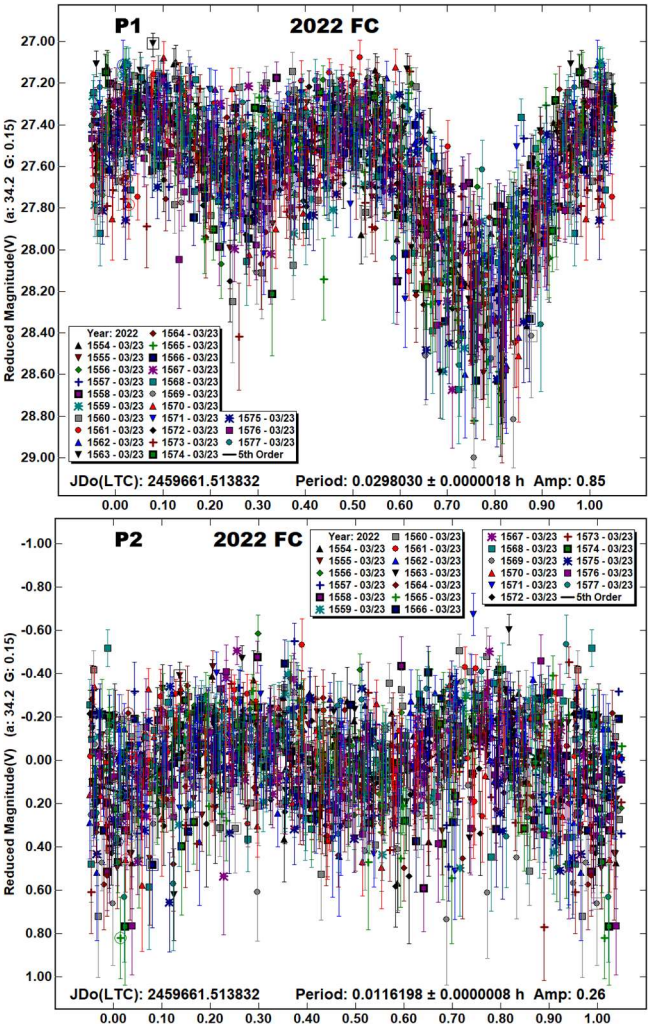

Even though the RMS of the NPA rotation fit is still 0.2 mag, both curves are reasonably well defined, indicating that during the 1.7 h of observation, 117 P1 and 300 P2 periods were completed. So, again, with the ambiguity that one or both of the frequencies of the derived periods may be linear combinations of the real frequencies, it is expected that this may be rated as PAR = -3, NPA rotation reliably detected with the two periods resolved. (Petr Pravec, personal communication).

2022 FD. The Mauna Loa ATLAS telescope discovered this Apollo on images taken on 2022 Mar 22.5 UTC, 3 days after an approach to 1.4 LD (Bacci et al., 2022b). Another small object with estimated diameter ~18 m it was observed on three nights, 2022 Mar 23.0, 24.1 and 25.1 UTC, primarily to obtain astrometry. Since the second date it has been listed as a Virtual Impactor by Sentry (JPL, 2022a), with over 100 low probability impacts predicted, the first in 2072. The images were subsequently reviewed for suitability to extract photometry. Over the three dates 2022 FD was fading and its sky motion slowing down as it receded from Earth. Exposures of 10 s were used on the first date, 12 s on the second and 14 and 18 s on the last date. On all three dates it was faint, at 18th mag but exhibited similar fast magnitude variations, with short, < 20 s duration bright maxima, repeated approximately every two minutes. All images were measured but those with SNr < 3 were rejected. The remainder were used to analyse the three dates separately and each result in similar lightcurves, here labelled Mar 23.0, Mar 24.1 and Mar 25.1.

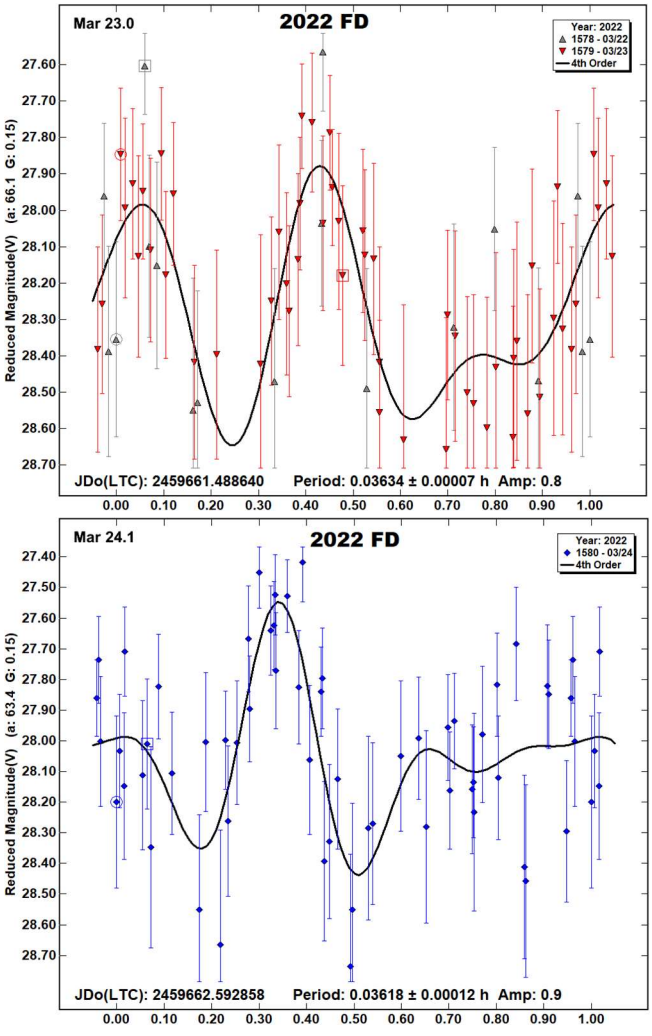

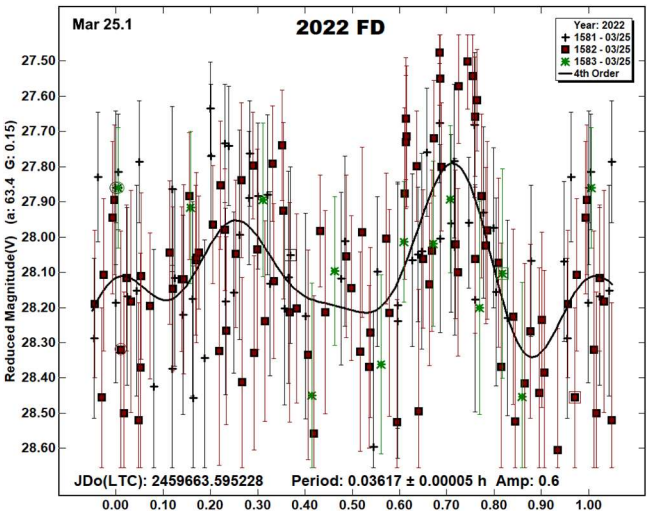

It is likely that the amplitude may be underestimated, as a number of the fainter points in the lightcurve were too weak to measure reliably. Combining all three dates in the reduction results the following period spectrum and lightcurve.

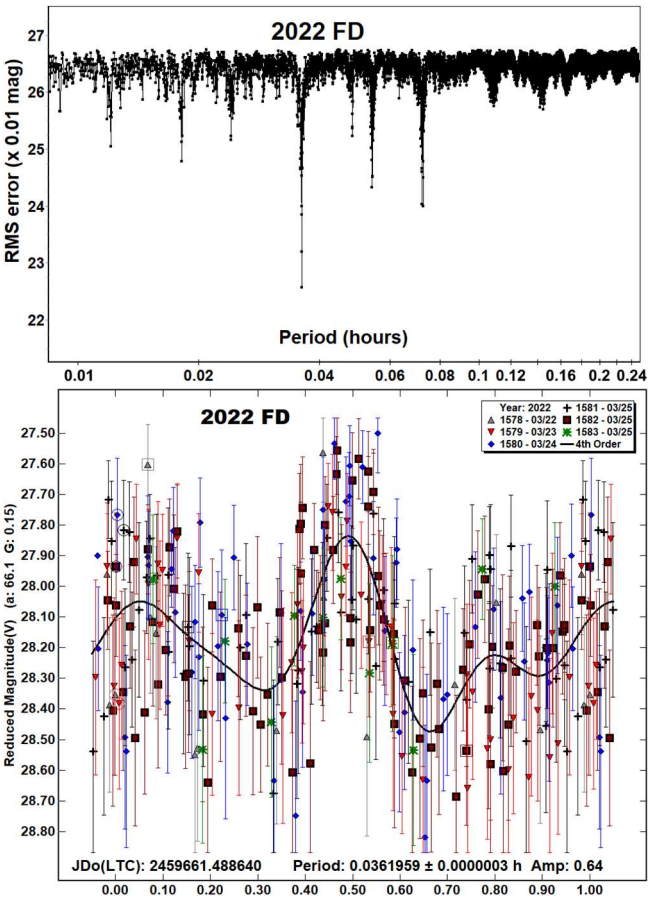

The best-fit periods from the three separate dates and also from combining measurements from all dates are:

Mar 23.0	0.03634	± 0.00007 h
Mar 24.1	0.03618	± 0.00012 h
Mar 25.1	0.03617	± 0.00005 h
All dates	0.0361959	± 0.0000003 h

Although a fast rotator, with period P = 130 s, the longest exposure of 18 s is 0.138 P and therefore lightcurve smoothing is not expected to be significant (Pravec et al., 2000).

2022 FB2. This ~13-m diameter Apollo was discovered 2 days before an approach to within 0.4 LD on 2022 Mar 28.67 UTC (Foglia et al., 2022). It was observed on its inbound leg for 4.4 h starting at 2022 Mar 27.93 UTC when it was at 2 LD and brightened due to changing geometry from 17th to 15th mag. Speed was not excessive, rising from 35 to 62 arcsec/min. A range of short exposure times did not reveal any obvious fast brightness changes during image capture and subsequent analysis shows large amplitude variations in time scales of ~0.5 h, with a period spectrum indicating a solution at 2.646 h.

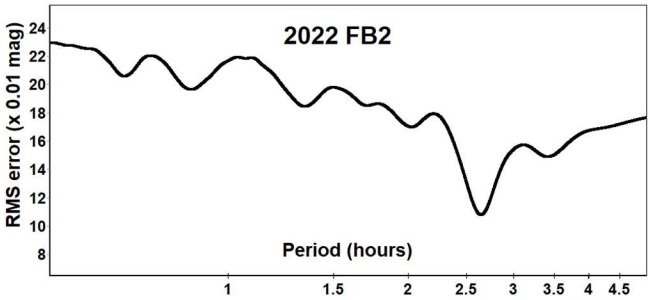

However, a raw plot of the measurements shows the lightcurve is irregular, with uneven maxima and minima, indicating the possibility of non-principal axis (tumbling) rotation.

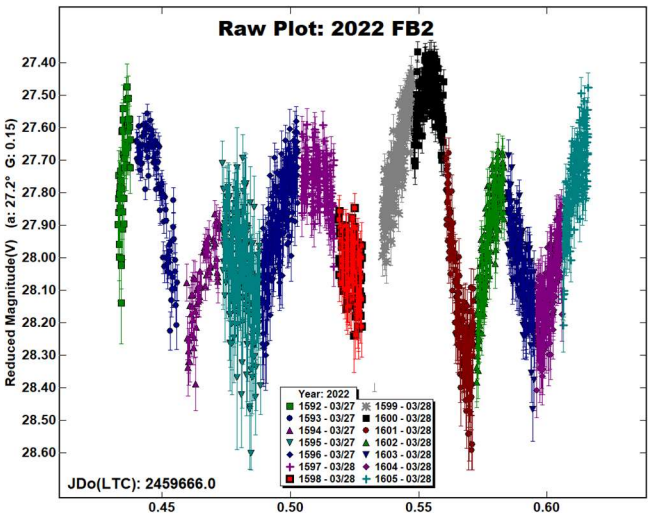

The 2.646 h phased solution is also given here but is a poor fit to the observations in places, especially in the first rise to maximum.

Number	Name	Integration times	Max intg/Pd	Min a/b	Pts	Flds	NPA
	2022 AO6	4-7.6	0.056	1.2	1107	15	
	2022 CV5	30Σ	0.152	1.6	401	19	P1
	2022 CV5		0.202				P2
	2022 CO6	2.1-3.4	0.020	1.2	1339	22	
	2022 DA	3.4,4.6	n/a	n/a	659	13	
	2022 ER5	2.5-3.3	0.008	1.3	1325	28	
	2022 FC	4.2-5.7	0.053	1.7	1575	24	P1
	2022 FC		0.136				P2
	2022 FD	10-18	0.138	1.2	274	6	
	2022 FB2	3.2-14.3	0.002	1.5	2020	14	
	2022 FL4	9	0.147	1.4	615	8	

Table II. Ancillary information, listing the integration times used (seconds), the fraction of the period represented by the longest integration time (Pravec et al., 2000), the calculated minimum elongation of the asteroid (Kwiatkowski et al., 2010), the number of data points used in the analysis, the number of times the telescope was repositioned to different fields and for NPA rotation the respective period. Note: Σ = Longest elapsed integration time for stacked images (start of first to end of last exposure used).

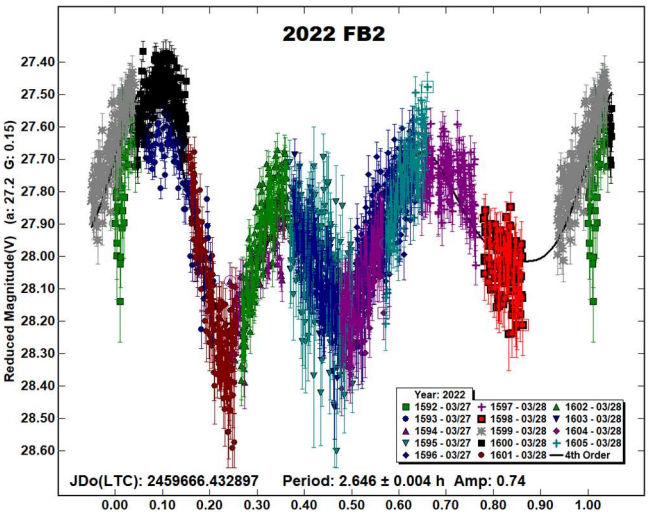

The coverage is too short to reliably identify the periods of any non-principal axis rotation that may be present, but the curve is suggestive of solutions in the range of 1 – 2 h. It is expected that this object may be rated as PAR = -1, NPA rotation possible, i.e., deviations from a single period are seen, but not conclusively. Entries for 2022 FB2 in Tables II and III are included on the basis of the 2.646 h period but those values may therefore be somewhat in error.

2022 FL4. Another very small ~14-m diameter Apollo, discovered by the ATLAS Haleakala telescope almost two days after an approach to 2 LD from Earth (Dupouy et al., 2022). It was observed for 2.5 h starting at 2022 Mar 31.96 UTC to obtain photometry after rapid variation had been evident in a set of 4 s exposures obtained 3 h earlier to measure astrometry. Maxima were evident approximately every 30 s in those images and assuming simple, principal axis rotation, a period P of ~60 s was implied. For the photometric run, exposure length was set at 9 s, balancing the trailing of the NEO which was moving at 40 arcsec/min against the effects of lightcurve smoothing that could be expected to be become appreciable with exposures much beyond 0.185 P, i.e., > ~11 s. The best fit solution from 615 measurements results in a bimodal lightcurve of period of 61.1 s, confirming the initial assumption and indicating that 148 rotations occurred during the period of observation.

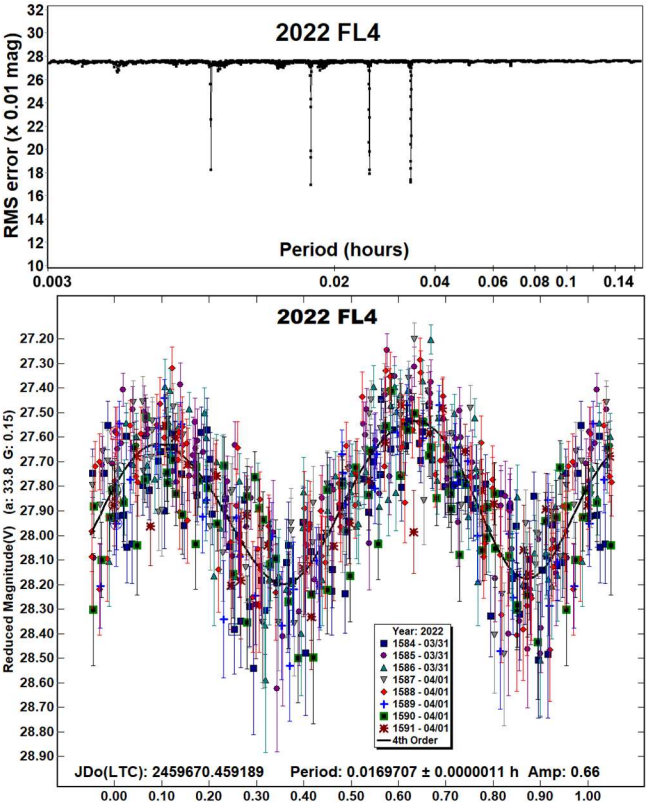

Number	Name	yyyy mm/ dd	Phase	L_{PAB}	B_{PAB}	Period(h)	P.E.	Amp	A.E	PAR	H
	2022 AO6	2022 01/13-01/14	48.7,50.6	135	-14	0.03749	0.00002	0.42	0.12		25.26
	2022 CV5	2022 02/10-02/11	27.1,25.5	149	-11	0.054775	0.000007	0.72	0.20	-3	27.70
						0.041282	0.000010	0.28	0.20		
	2022 CO6	2022 02/14-02/15	24.8,19.1	148	-11	0.047287	0.000003	0.33	0.11		26.03
	2022 DA	2022 02/18-02/19	49.0,46.4	126	-4	n/a		n/a			25.15
	2022 ER5	2022 03/19-03/19	60.0,64.6	152	17	0.11581	0.00003	0.84	0.26		25.71
	2022 FC	2022 03/23-03/23	34.2,28.1	187	15	0.0298030	0.000018	0.85	0.29	-3	26.13
						0.0116198	0.000008	0.26	0.29		
	2022 FD	2022 03/22-03/25	66.2,61.7	201	28	0.0361959	0.0000003	0.64	0.32		26.11
	2022 FB2	2022 03/27-03/28	27.1,23.7	188	13	2.646	0.004	0.74	0.15	-1	26.78
	2022 FL4	2022 03/31-04/01	33.8,32.8	194	17	0.0169707	0.0000011	0.66	0.24		26.63

Table III. Observing circumstances and results. Where more than one line is given, these include periods determined for NPA rotation. The phase angle is given for the first and last date. If preceded by an asterisk, the phase angle reached an extrema during the period. LPAB and BPAB are the approximate phase angle bisector longitude/latitude at mid-date range (see Harris et al., 1984). Amplitude error (A.E.) is calculated as √2 * (lightcurve RMS residual). PAR is the expected Principal Axis Rotation quality detection code (Pravec et al., 2005) and H is the absolute magnitude at 1 au from Sun and Earth taken from the Small-Body Database Lookup (JPL, 2022b).

Acknowledgements

The author is indebted to Petr Pravec for his continued help on the analysis of tumbling asteroids. The author also gratefully acknowledges a Gene Shoemaker NEO Grant from the Planetary Society (2005) and a Ridley Grant from the British Astronomical Association (2005), both of which facilitated upgrades to observatory equipment used in this study.

References

ADS (2022). Astrophysics Data System. *https://ui.adsabs.harvard.edu/*

Bacci, P.; Maestripieri, M.; Tesi, L.; Fagioli, G.; Foglia, S.; Galli, G.; Tichy, M.; Ticha, J.; Honkova, M.; Pettarin, E.; Hogan, J.K.; Kowalski, R.A.; Christensen, E.J.; Farneth, G.A.; Fazekas, J.B. and 33 colleagues (2022a). "2022 FC." MPEC 2022-F16. *https://minorplanetcenter.net/mpec/K22/K22F16.html*

Bacci, P.; Maestripieri, M.; Tesi, L.; Fagioli, G.; Foglia, S.; Galli, G.; Tichy, M.; Ticha, J.; Honkova, M.; Losse, F.; Birtwhistle, P.; Scarfi, G.; Sannino, L.; Korlevic, K.; Denneau, L. and 8 colleagues (2022b). "2022 FD." MPEC 2022-F17. *https://minorplanetcenter.net/mpec/K22/K22F17.html*

Benner, L.A.M. (2022). "Goldstone Radar Observations Planning: (137170) 1999 HF1, 2022 ER5, 2022 DP3, and 2022 EO4." *https://echo.jpl.nasa.gov/asteroids/1999HF1/1999HF1.2022.planning.html*

Birtwhistle, P. (2021). "Ultra-Fast Rotators: Results and Recommendations for Observing Strategies." *Minor Planet Bull.* **48**, 346-352.

Bressi, T.H.; Linder, T.; Holmes, R.; Horn, L.; Armstrong, J.D.; Jacques, C.; Durig, D.T.; Maury, A.; Attard, G.; Parrott, D.; Fabrega, J. (2022). "2022 CO6." MPEC 2022-C216. *https://minorplanetcenter.net/mpec/K22/K22CL6.html*

Dupouy, P.; Jahn, J.; Kelley, T.; Rankin, D.; Christensen, E.J.; Farneth, G.A.; Fazekas, J.B.; Fuls, D.C.; Gibbs, A.R.; Grauer, A.D.; Groeller, H.; Hogan, J.K.; Kowalski, R.A.; Larson, S.M.; Leonard, G.J. and 20 colleagues (2022). "2022 FL4." MPEC 2022-G02. *https://minorplanetcenter.net/mpec/K22/K22G02.html*

Evans, N.; Choi, P.; Saini, N.; Zhai, C.; Trahan, R.; Shao, M.; Linder, T.; Holmes, R.; Horn, L.; Bulger, J.; Lowe, T.; Schultz, A.; Smith, I.; Chambers, K.; Dukes, T. and 26 colleagues (2022). "2022 ER5." MPEC 2022-E197. *https://minorplanetcenter.net/mpec/K22/K22EJ7.html*

Foglia, S.; Galli, G.; Tichy, M.; Ticha, J.; Honkova, M.; Fazekas, J.B.; Christensen, E.J.; Farneth, G.A.; Fuls, D.C.; Gibbs, A.R.; Grauer, A.D.; Groeller, H.; Hogan, J.K.; Kowalski, R.A.; Larson, S.M. and 16 colleagues (2022). "2022 FB2." MPEC 2022-F81. *https://minorplanetcenter.net/mpec/K22/K22F81.html*

Harris, A.W.; Young, J.W.; Scaltriti, F.; Zappala, V. (1984). "Lightcurves and phase relations of the asteroids 82 Alkmene and 444 Gyptis." *Icarus* **57**, 251-258.

Harris, A.W.; Young, J.W.; Bowell, E.; Martin, L.J.; Millis, R.L.; Poutanen, M.; Scaltriti, F.; Zappala, V.; Schober, H.J.; Debehogne, H.; Zeigler, K. (1989). "Photoelectric Observations of Asteroids 3, 24, 60, 261, and 863." *Icarus* **77**, 171-186.

Ikari, Y.; Bulger, J.; Chambers, K.; Dukes, T.; Lowe, T.; Schultz, A.; Smith, I.; Chastel, S.; Huber, M.; Ramanjooloo, Y.; Wainscoat, R.; Weryk, R.; Wierzchos, K.W.; Christensen, E.J.; Farneth, G.A. and 22 colleagues (2022a). "2022 AO6." MPEC 2022-A176. *https://minorplanetcenter.net/mpec/K22/K22AH6.html*

Ikari, Y.; Dupouy, P.; Jahn, J.; Grazzini, L.; Gibbs, A.R.; Christensen, E.J.; Farneth, G.A.; Fazekas, J.B.; Fuls, D.C.; Grauer, A.D.; Groeller, H.; Kowalski, R.A.; Larson, S.M.; Leonard, G.J.; Rankin, D. and 23 colleagues (2022b). "2022 CV5." MPEC 2022-C201. *https://minorplanetcenter.net/mpec/K22/K22CK1.html*

JPL (2022a). Sentry: Earth Impact Monitoring. *https://cneos.jpl.nasa.gov/sentry/*

JPL (2022b). Small-Body Database Lookup. *https://ssd.jpl.nasa.gov/tools/sbdb_lookup.html*

Kwiatkowski, T.; Buckley, D.A.H.; O'Donoghue, D.; Crause, L.; Crawford, S.; Hashimoto, Y.; Kniazev, A.; Loaring, N.; Romero Colmenero, E.; Sefako, R.; Still, M.; Vaisanen, P. (2010). "Photometric survey of the very small near-Earth asteroids with the SALT telescope - I. Lightcurves and periods for 14 objects.", *Astronomy & Astrophysics* **509**, A94.

Pravec, P.; Hergenrother, C.; Whiteley, R.; Sarounova, L.; Kusnirak, P.; Wolf, M. (2000). "Fast Rotating Asteroids 1999 TY2, 1999 SF10, and 1998 WB2." *Icarus* **147**, 477-486.

Pravec, P.; Harris, A.W.; Scheirich, P.; Kušnirák, P.; Šarounová, L.; Hergenrother, C.W.; Mottola, S.; Hicks, M.D.; Masi, G.; Krugly, Yu.N.; Shevchenko, V.G.; Nolan, M.C.; Howell, E.S.; Kaasalainen, M.; Galád, A. and 5 colleagues. (2005). "Tumbling Asteroids." *Icarus* **173**, 108-131.

Raab, H. (2018). Astrometrica software, version 4.12.0.448. *http://www.astrometrica.at/*

Urbanik, M.; Holmes, R.; Linder, T.; Horn, L.; Kowalski, R.A.; Christensen, E.J.; Farneth, G.A.; Fazekas, J.B.; Fuls, D.C.; Gibbs, A.R.; Grauer, A.D.; Groeller, H.; Larson, S.M.; Leonard, G.J.; Rankin, D. and 16 colleagues (2022). "2022 DA." MPEC 2022-D11. *https://minorplanetcenter.net/mpec/K22/K22D11.html*

Warner, B.D.; Harris, A.W.; Pravec, P. (2009). "The Asteroid Lightcurve Database." *Icarus* **202**, 134-146. Updated 2021 Dec. *https://minplanobs.org/mpinfo/php/lcdb.php*

Warner, B.D. (2022). MPO Software, Canopus version 10.8.6.9. Bdw Publishing, Colorado Springs, CO.

Zacharias, N.; Finch, C.T.; Girard, T.M.; Henden, A.; Bartlett, J.L.; Monet, D.G.; Zacharias, M.I. (2013). "The Fourth US Naval Observatory CCD Astrograph Catalog (UCAC4)." *The Astronomical Journal* **145**, 44-57.

NEAR-EARTH ASTEROID LIGHTCURVE ANALYSIS AT THE CENTER FOR SOLAR SYSTEM STUDIES: 2022 FEBRUARY-MARCH

Brian D. Warner
Center for Solar System Studies (CS3)
446 Sycamore Ave.
Eaton, CO 80615 USA
brian@MinorPlanetObserver.com

Robert D. Stephens
Center for Solar System Studies (CS3)
Rancho Cucamonga, CA

(Received: 2022 April 10)

Lightcurves of six near-Earth asteroids (NEAs) obtained at the Center for Solar System Studies (CS3) in 2022 February and March were analyzed for rotation period, peak-to-peak amplitude, and signs of satellites or tumbling. There are good indications that (138971) is in a low-level tumbling state.

CCD photometric observations of six near-Earth asteroids (NEAs) were made at the Center for Solar System Studies (CS3) in 2022 February and March. Table I lists the telescopes and CCD cameras that were available to make observations.

Up to nine telescopes can be used but seven is more common. All the cameras use CCD chips from the KAF blue-enhanced family and so have essentially the same response. The pixel scales ranged from 1.24-1.60 arcsec/pixel.

Telescopes	Cameras
0.30-m *f*/10 Schmidt-Cass	FLI Microline 1001E
0.35-m *f*/9.1 Schmidt-Cass	FLI Proline 1001E
0.40-m *f*/10 Schmidt-Cass	SBIG STL-1001E
0.40-m *f*/10 Schmidt-Cass	
0.50-m *f*/8.1 Ritchey-Chrétien	

Table I. List of available telescopes and CCD cameras at CS3. The exact combination for each telescope/camera pair can vary due to maintenance or specific needs.

All lightcurve observations were unfiltered since a clear filter can cause a 0.1-0.3 mag loss. The exposure duration varied depending on the asteroid's brightness and sky motion. Guiding on a field star sometimes resulted in a trailed image for the asteroid.

Measurements were made using *MPO Canopus*. The Comp Star Selector utility in *MPO Canopus* found up to five comparison stars of near solar-color for differential photometry. To reduce the number of times and amounts of adjusting nightly zero points, we use the ATLAS catalog r´ (SR) magnitudes (Tonry et al., 2018). Those adjustments are usually $|\Delta| \leq 0.03$ mag. The larger corrections, which are rare, may have been related in part to using unfiltered observations, poor centroiding of the reference stars, and not correcting for second-order extinction. Another cause may be selecting what appears to be a single star but is actually an unresolved pair.

The Y-axis values are ATLAS SR "sky" (catalog) magnitudes. The two values in the parentheses are the phase angle (a) and the value of *G* used to normalize the data to the comparison stars used in the earliest session. This, in effect, corrected all the observations to seem to have been made at a single fixed date/time and phase angle, leaving any variations due only to the asteroid's rotation and/or albedo changes. The X-axis shows rotational phase from –0.05 to 1.05. If the plot includes the amplitude, e.g., "Amp: 0.65", this is the amplitude of the Fourier model curve and *not necessarily the adopted amplitude for the lightcurve*.

"LCDB" substitutes for "Warner et al. (2009)" from here on.

3103 Eger. The earliest reported period in the LCDB is from Wisniewski (1987). We observed the asteroid on four previous occasions (Warner, 2014; 2016; 2017; Warner and Stephens, 2019). All previous results put the rotation period close to 5.71 h. Our 2022 result using the full data set is in good agreement.

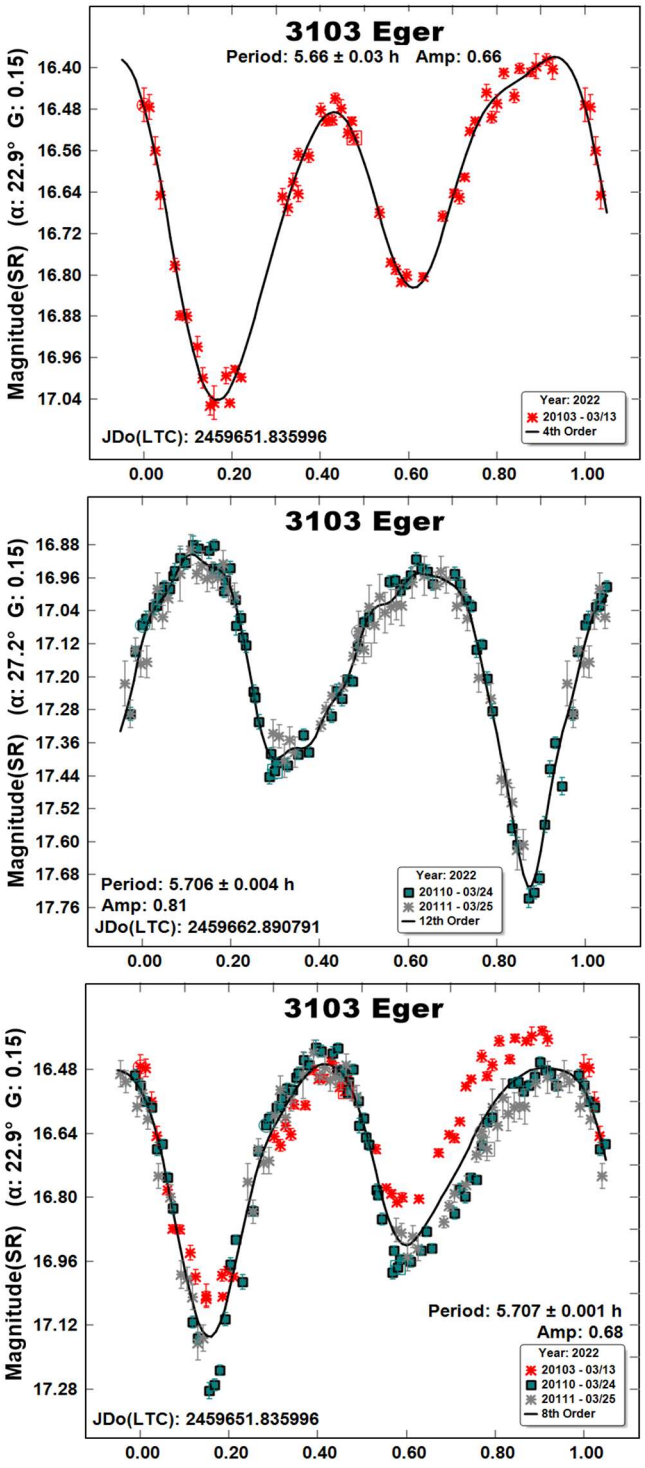

Over the fortnight of our 2022 observations, the shape and amplitude of the lightcurve changed noticeably. In mid-March, the amplitude was 0.61 mag at phase angle 22.7°. Towards the end of the month, the phase angle increased to about 27.4° and the amplitude to 0.81 mag. This is expected behavior (Zappala et al. 1990) but the amount of amplitude change is larger than expected for a relatively small change in phase angle. The phase angle bisector longitude and latitude (Harris et al, 1984) were almost constant, adding no insight for the large amplitude change.

5332 Davidaguilar. Binzel (1990) first reported a period of 5.82 h for this 3-km NEA, which has shown a large range of amplitudes over the years: 0.20-1.2 mag. The period from our latest data set of 5.80 h is in good agreement with earlier results, including ours (Warner and Stephens, 2019).

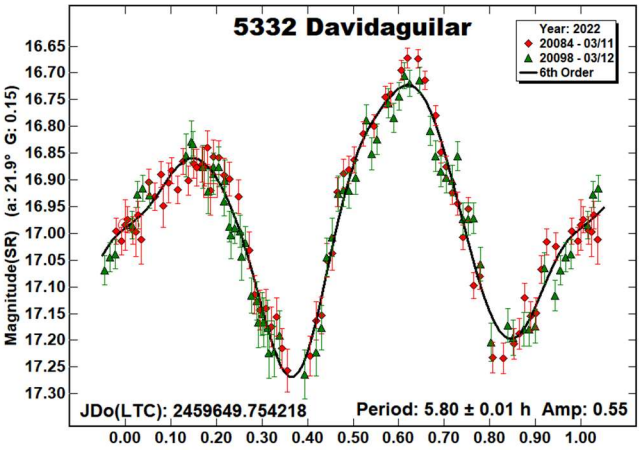

(22099) 2000 EX106. Pravec et al. (2000web) found a period of 6.334 h and we (Warner, 2015) reported 6.31 h. The 2022 data set gives similar results. The amplitude of 0.45 mag is within the small range of 0.40-0.45 mag reported so far.

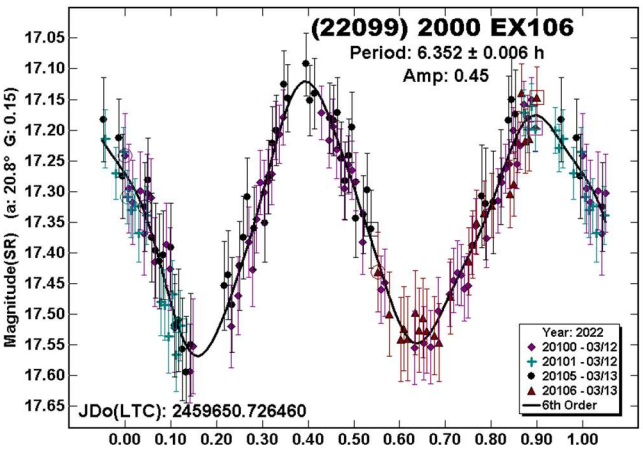

(138971) 2001 CB21. There are good indications that this asteroid is in a state of non-principal axis rotation (NPAR; see Pravec et al., 2005; 2014). It was not possible to find a single period to get a good fit to the data set. We tried a dual-period search in *MPO Canopus*, but to no avail. We considered the alternate period of 4.953 h found by Galad et al. (2005), also with unsatisfactory results.

The "No ZPA" and "w/ZPA" plots ("Zero-point Adjustment") show that the mismatch in the data was not strictly due to catalog errors for the comparison stars and other systematics.

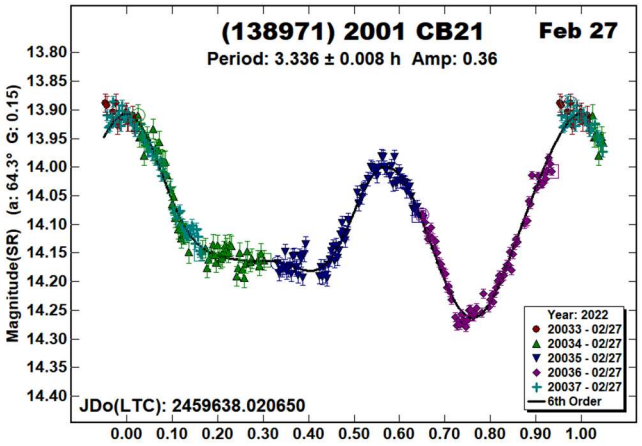

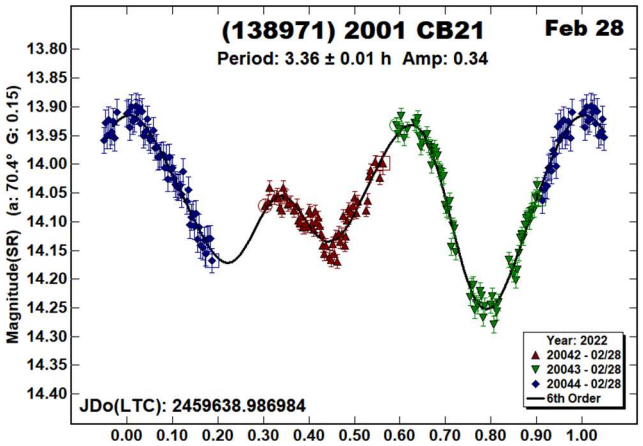

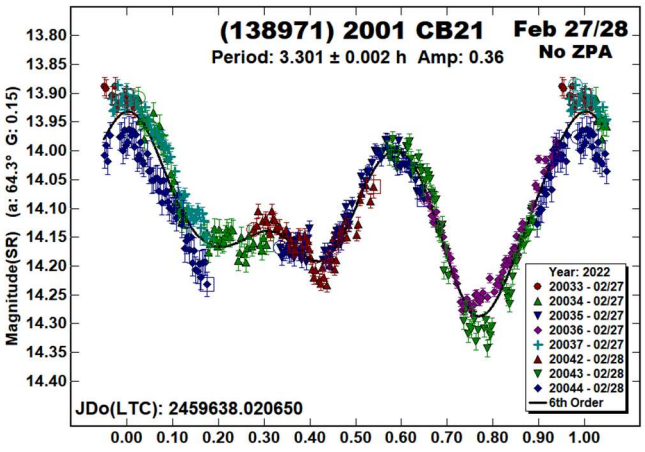

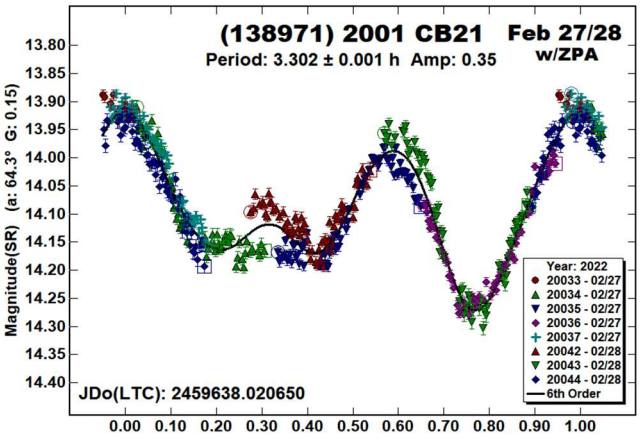

We should note, however, that the phase angle was very large, $\alpha > 65°$, which can lead to strong shadowing effects. This may be why we could not find a single-period, even with zero-point offsets.

(170891) 2004 TY16. The only previous report of a period in the LCDB is from Carbognani (2008), who found 2.795 h and amplitude of 0.18 mag at L_{PAB} 105°. Our observations, at L_{PAB} 168°, showed a similar period but much lower amplitude. This might suggest that the 2022 observations were more pole-on and, therefore, the asteroid's north pole has an ecliptic longitude in the vicinity of 170° or 350°.

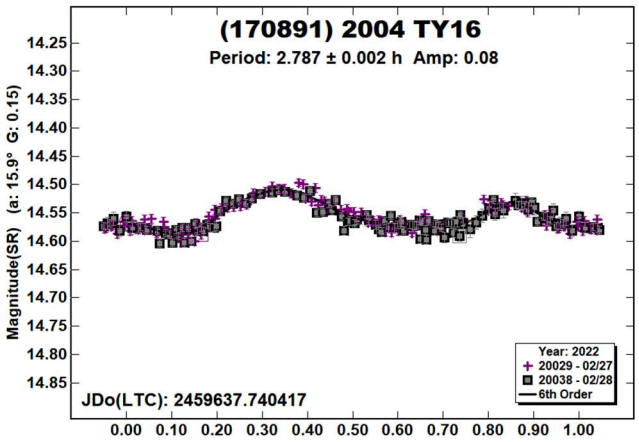

2010 VG1. Circumstances did not allow finding a complete lightcurve for 2010 VG1, mostly because the period is nearly commensurate with an Earth-day and the observations were from a single location.

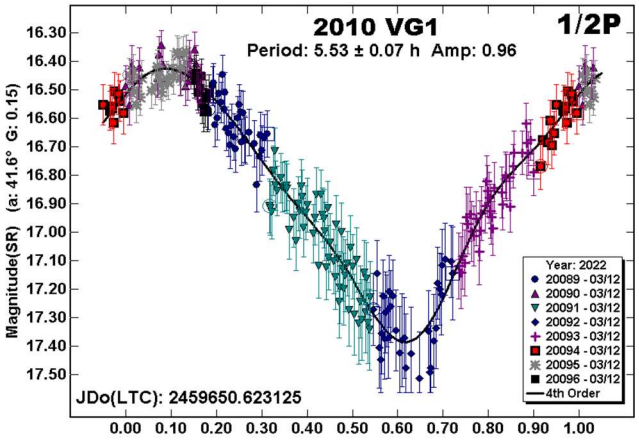

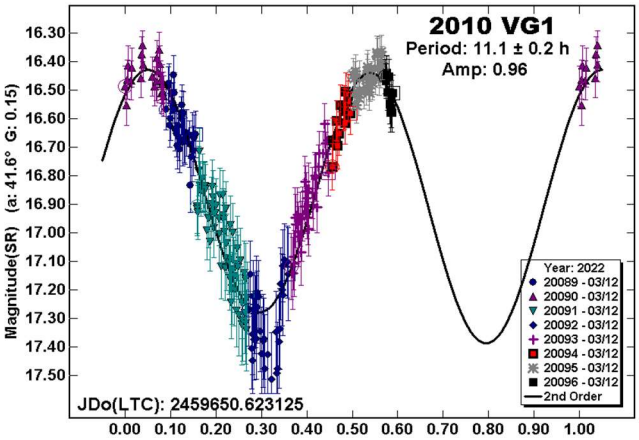

We found the half-period, which did provide full lightcurve coverage, to estimate the full period. Given the large amplitude, the large phase angle notwithstanding, a bimodal solution near 11 h is highly likely (Harris et al., 2014).

Acknowledgements

The authors gratefully acknowledge Shoemaker NEO Grants from the Planetary Society (2007, 2013). These were used to purchase some of the telescopes and CCD cameras used in this research. This work includes data from the Asteroid Terrestrial-impact Last Alert System (ATLAS) project. ATLAS is primarily funded to search for near earth asteroids through NASA grants NN12AR55G, 80NSSC18K0284, and 80NSSC18K1575; byproducts of the NEO search include images and catalogs from the survey area. The ATLAS science products have been made possible through the contributions of the University of Hawaii Institute for Astronomy, the Queen's University Belfast, the Space Telescope Science Institute, and the South African Astronomical Observatory. This paper made use of the services provided by the SAO/NASA Astrophysics Data System, which is operated by the Smithsonian Astrophysical Observatory under NASA Cooperative Agreement 80NSSC211M0056.

References

References from web sites should be considered transitory, unless from an agency with a long lifetime expectancy. Sites run by private individuals, even if on an institutional web site, do not necessarily fall into this category.

Binzel, R.P. (1990). "1990 DA." *IAUC* **4969**.

Carbognani, A. (2008). "Lightcurve Photometry of NEAs 4450 Pan, (170891) 2004 TY16, 2002 RC118, and 2007 VD12." *Minor Planet Bull.* **35**, 109-110.

Number	Name	2022 mm/dd	Phase	L_{PAB}	B_{PAB}	Period(h)	P.E.	Amp	A.E.
3103	Eger	03/13-03/25	*28.7,27.6	137	6	5.707	0.001	0.80	0.03
5332	Davidaguilar	03/11-03/12	22.0,21.6	191	26	5.80	0.01	0.55	0.03
22099	2000 EX106	03/12-03/13	20.8,20.6	182	15	6.352	0.006	0.45	0.03
138971	2001 CB21	02/27-02/28	64.0,69.9	184	26	3.301	0.002	0.36	0.03
170891	2004 TY16	02/27-02/28	16.0,15.7	169	-6	2.787	0.002	0.08	0.01
	2010 VG1	03/12-03/12	41.1	149	8	11.1	0.1	0.96	0.03

Table II. Observing circumstances and analysis results. The phase angle (α) is given at the start and end of each date range. If there is an asterisk before the first phase value, the phase angle reached a maximum or minimum during the period. L_{PAB} and B_{PAB} are, respectively the average phase angle bisector longitude and latitude (see Harris et al.,1984).

Galad, A.; Pravec, P.; Kusnirak, P.; Gajdos, S.; Kornos, L.; Vilagi, J. (2005). "Joint Lightcurve Observations of 10 Near-Earth Asteroids from Modra and ONDREJOV." *Earth, Moon, and Planets* **97**, 147-163.

Harris, A.W.; Young, J.W.; Scaltriti, F.; Zappala, V. (1984). "Lightcurves and phase relations of the asteroids 82 Alkmene and 444 Gyptis." *Icarus* **57**, 251-258.

Harris, A.W.; Pravec, P.; Galad, A.; Skiff, B.A.; Warner, B.D.; Vilagi, J.; Gajdos, S.; Carbognani, A.; Hornoch, K.; Kusnirak, P.; Cooney, W.R.; Gross, J.; Terrell, D.; Higgins, D.; Bowell, E.; Koehn, B.W. (2014). "On the maximum amplitude of harmonics on an asteroid lightcurve." *Icarus* **235**, 55-59.

Pravec, P.; Wolf, M.; Sarounova, L. (2000web). *http://www.asu.cas.cz/~ppravec/neo.htm*

Pravec, P.; Harris, A.W.; Scheirich, P.; Kušnirák, P.; Šarounová, L.; Hergenrother, C.W.; Mottola, S.; Hicks, M.D.; Masi, G.; Krugly, Yu.N.; Shevchenko, V.G.; Nolan, M.C.; Howell, E.S.; Kaasalainen, M.; Galád, A.; Brown, P.; Degraff, D.R.; Lambert, J.V.; Cooney, W.R.; Foglia, S. (2005). "Tumbling asteroids." *Icarus* **173**, 108-131.

Pravec, P.; Scheirich, P.; Durech, J.; Pollock, J.; Kusnirak, P.; Hornoch, K.; Galad, A.; Vokrouhlicky, D.; Harris, A.W.; Jehin, E.; Manfroid, J.; Opitom, C.; Gillon, M.; Colas, F.; Oey, J.; Vrastil, J.; Reichart, D.; Ivarsen, K.; Haislip, J.; LaCluyze, A. (2014). "The tumbling state of (99942) Apophis." *Icarus* **233**, 48-60.

Tonry, J.L.; Denneau, L.; Flewelling, H.; Heinze, A.N.; Onken, C.A.; Smartt, S.J.; Stalder, B.; Weiland, H.J.; Wolf, C. (2018). "The ATLAS All-Sky Stellar Reference Catalog." *Ap. J.* **867**, A105.

Warner, B.D. (2014). "Near-Earth Asteroid Lightcurve Analysis at CS3-Palmer Divide Station: 2014 March - June." *Minor Planet Bull*. **41**, 213-224.

Warner, B.D. (2015). "Near-Earth Asteroid Lightcurve Analysis at CS3-Palmer Divide Station: 2015 January - March." *Minor Planet Bull*. **42**, 172-183.

Warner, B.D. (2016). "Near-Earth Asteroid Lightcurve Analysis at CS3-Palmer Divide Station: 2016 April - July." *Minor Planet Bull*. **43**, 311-319.

Warner, B.D. (2017). "Near-Earth Asteroid Lightcurve Analysis at CS3-Palmer Divide Station: 2016 December thru 2017 April." *Minor Planet Bull*. **44**, 223-237.

Warner, B.D.; Stephens, R.D. (2019). "Near-Earth Asteroid Lightcurve Analysis at the Center for Solar System Studies." *Minor Planet Bull*. **46**, 423-438.

Warner, B.D.; Harris, A.W.; Pravec, P. (2009). "The Asteroid Lightcurve Database." *Icarus* **202**, 134-146. Updated 2021 June. *http://www.minorplanet.info/lightcurvedatabase.html*

Wisniewski, W.Z. (1987). "Photometry of six radar targets." *Icarus* **70**, 566-572.

Zappala, V.; Cellini, A.; Barucci, A.M.; Fulchignoni, M.; Lupishko, D.E. (1990). "An anlaysis of the amplitude-phase relationship among asteroids." *Astron. Astrophys*. **231**, 548-560.

LIGHTCURVES FOR FIFTEEN MINOR PLANETS

Tom Polakis
Command Module Observatory
121 W. Alameda Dr.
Tempe, AZ 85282
tpolakis@cox.net

(Received: 2022 March 9)

Photometric measurements were made for 15 main-belt asteroids, based on CCD observations made from 2022 January through 2022 March. Phased lightcurves were created for 14 asteroids, while one did not yield a period solution. All the data have been submitted to the ALCDEF database.

CCD photometric observations of 15 main-belt asteroids were performed at Command Module Observatory (MPC V02) in Tempe, AZ. Images were taken using a 0.32-m f/6.7 Modified Dall-Kirkham telescope, SBIG STXL-6303 CCD camera, and a 'clear' glass filter. Exposure time for all the images was 2 minutes. The image scale after 2×2 binning was 1.76 arcsec/pixel. Table I shows the observing circumstances and results. All of the images for these asteroids were obtained between 2022 January and 2022 March.

Images were calibrated using a dozen bias, dark, and flat frames. Flat-field images were made using an electroluminescent panel. Image calibration and alignment was performed using *MaxIm DL* software.

The data reduction and period analysis were done using *MPO Canopus* (Warner, 2022). The 45′×30′ field of the CCD typically enables the use of the same field center for three consecutive nights. In these fields, the asteroid and three to five comparison stars were measured. Comparison stars were selected with colors within the range of $0.5 < B\text{-}V < 0.95$ to correspond with color ranges of asteroids. In order to reduce the internal scatter in the data, the brightest stars of appropriate color that had peak ADU counts below the range where chip response becomes nonlinear were selected. *MPO Canopus* plots instrumental vs. catalog magnitudes for solar-colored stars, which is useful for selecting comp stars of suitable color and brightness.

Since the sensitivity of the KAF-6303 chip peaks in the red, the clear-filtered images were reduced to Sloan r′ to minimize error with respect to a color term. Comparison star magnitudes were obtained from the ATLAS catalog (Tonry et al., 2018), which is incorporated directly into *MPO Canopus*. The ATLAS catalog derives Sloan *griz* magnitudes using a number of available catalogs. The consistency of the ATLAS comp star magnitudes and color-indices allowed the separate nightly runs to be linked often with no zero-point offset required or shifts of only a few hundredths of a magnitude in a series.

A 9-pixel (16 arcsec) diameter measuring aperture was used for asteroids and comp stars. It was typically necessary to employ star subtraction to remove contamination by field stars. For the asteroids described here, I note the RMS scatter on the phased lightcurves, which gives an indication of the overall data quality including errors from the calibration of the frames, measurement of the comp stars, the asteroid itself, and the period-fit. Period determination was done using the *MPO Canopus* Fourier-type FALC fitting method (cf. Harris et al., 1989). Phased lightcurves show the maximum at phase

zero. Magnitudes in these plots are apparent and scaled by *MPO Canopus* to the first night. In cases where rotation periods could not be determined, raw lightcurves are presented, with "Raw" appearing in the upper right-hand corner of the plots.

Asteroids were selected from the CALL website (Warner, 2011). In this set of observations, 2 of the 15 asteroids had no previous period analysis, 1 had U = 1, and 12 had U=2. The Asteroid Lightcurve Database (LCDB; Warner et al. (2009) was consulted to locate previously published results. All the new data for these asteroids can be found in the ALCDEF database.

570 Kythera was discovered by Max Wolf at Heidelberg in 1905. Several papers show similar rotational periods: Aznar et al. (2016), 8.074 ± 0.016 h; Dose (2021a), 8.123 ± 0.004 h; and Pilcher (2021), 8.117 ± 0.001 h. During three nights, 249 images were taken to determine a period of 8.129 ± 0.010 h, agreeing with previous values. The amplitude of the lightcurve is 0.10 ± 0.001 mag.

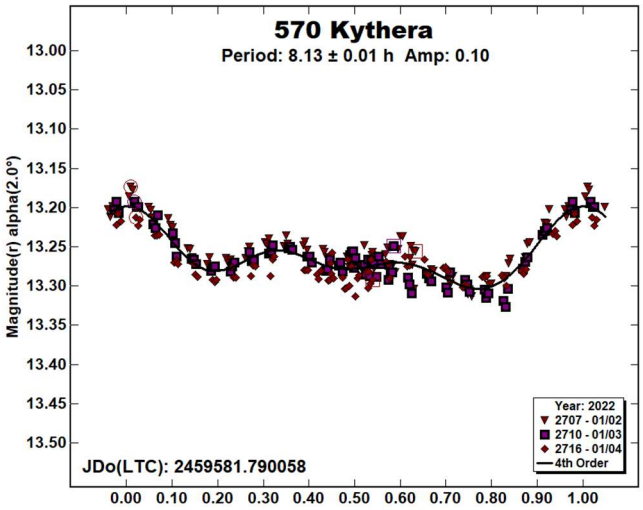

705 Erminia. Emil Ernst discovered this outer-belt asteroid at Heidelberg in 1910. Koff et al. (2006) computed a period of 53.96 ± 0.01 h and Behrend (2020web) calculated 53.96 ± 0.05 h. Its high inclination of 25° brought it to a very northerly declination throughout the 2022 opposition. Over the course of seven nights, 550 images were gathered, yielding a synodic period of 54.74 ± 0.10 h, and an amplitude of 0.06 ± 0.007 mag.

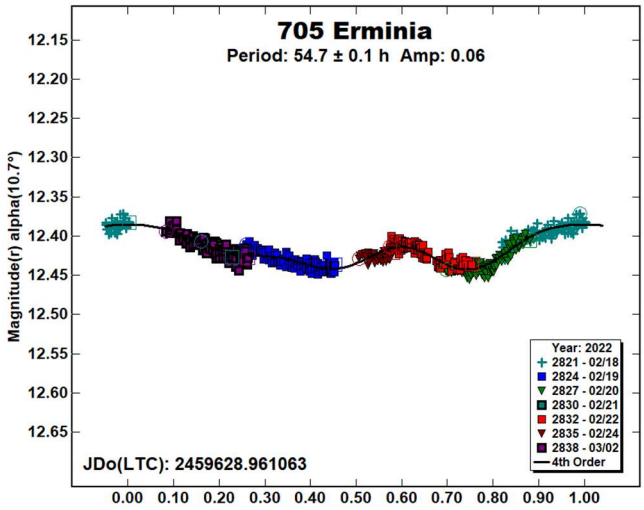

866 Fatme was discovered in 1917 at Heidelberg by Max Wolf. Polakis (2018) shows a period of 5.800 ± 0.002 h, but Dose (2021b) computed double that value: 11.800 ± 0.001 h. A total of 334 data points were collected in four nights, resulting in a period of 11.49 ± 0.05 h, and lending credence to Dose's value as the correct one. The amplitude of the lightcurve is 0.05 mag, with a large RMS error on the fit of 0.016 mag.

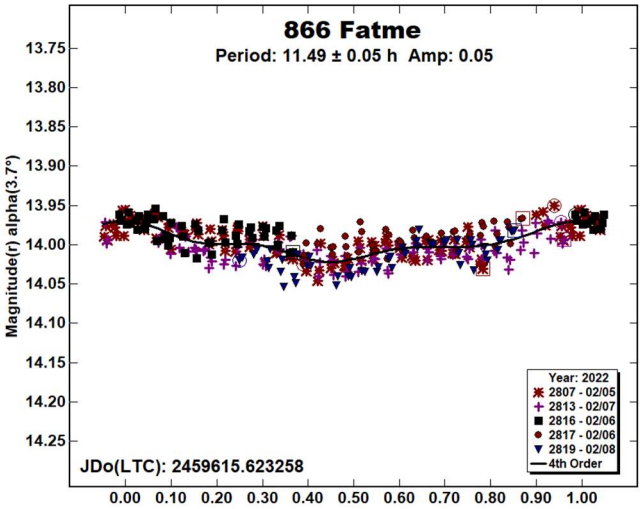

923 Herluga was discovered at Heidelberg by Karl Reinmuth in 1919. Marciniak et al. (2018) shows a period of 29.71 ± 0.04 h, and Durech et al. (2020) computed 29.7282 ± 0.0007 h. In four nights, 296 images were sufficient to compute a rotation period of 30.61 ± 0.08 h, using a 7th order fit. The lightcurve has an amplitude of 0.23 ± 0.031 mag.

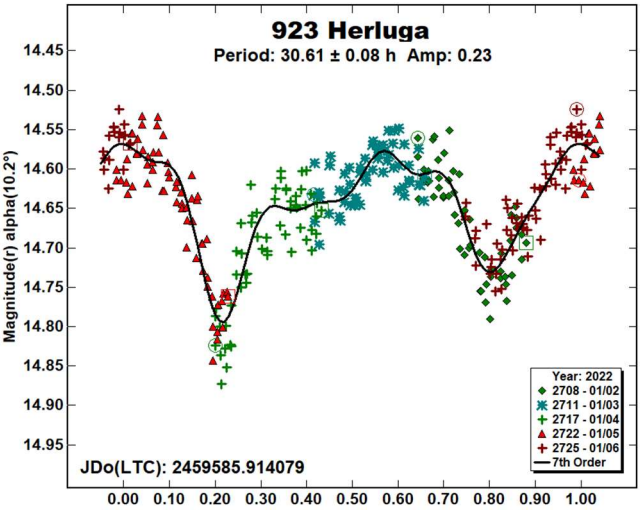

1030 Vijta. This outer-belt asteroid was discovered by Vladimir Albitsky at Semeis in 1924. Among the period solutions are those by Ferrero (2014), who published 6.332 ± 0.001h, and Durech et al. (2019), 6.336378 ± 0.000002 h. A three-night run yielded a synodic period solution of 6.346 ± 0.008 h, and an amplitude of 0.20 ± 0.063 mag.

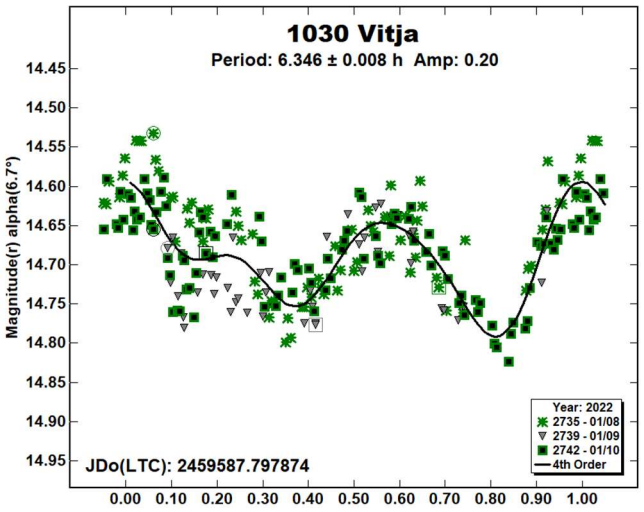

1122 Neith. Eugene Delporte found this minor planet in 1928 at Uccle. Two periods appear in the LCDB: Oey (2009), 12.599 ± 0.006 h, and Durech et al. (2020), 25.0304 ± 0.0004. During seven nights, 484 data points were acquired to produce a period solution of 25.11 ± 0.01 h, in agreement with Durech. The lightcurve has an amplitude of 0.36 ± 0.034 mag.

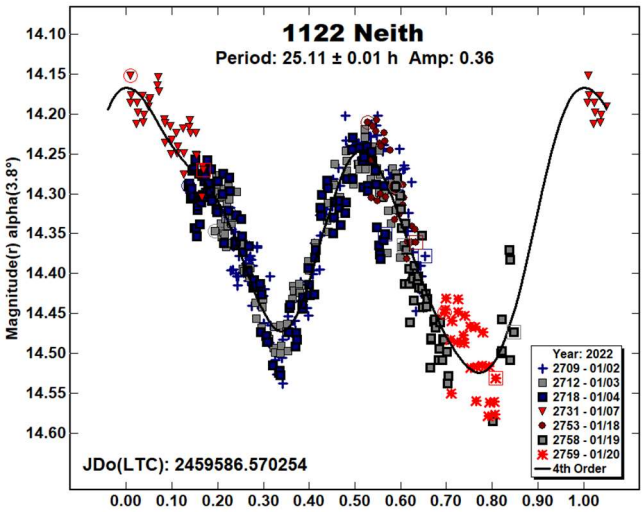

1351 Uzbekistania. This outer-belt asteroid was discovered at Semeis in in 1934 by Grigory Neujmin. Warner (2004) shows a period of 73.9 ± 0.2 h, and Durech et al. (2019) computed 73.976 ± 0.003 h. During 11 nights, 750 images were gathered. These produced a synodic period of 74.07 ± 0.03 h, and an amplitude of 0.46 ± 0.028 mag.

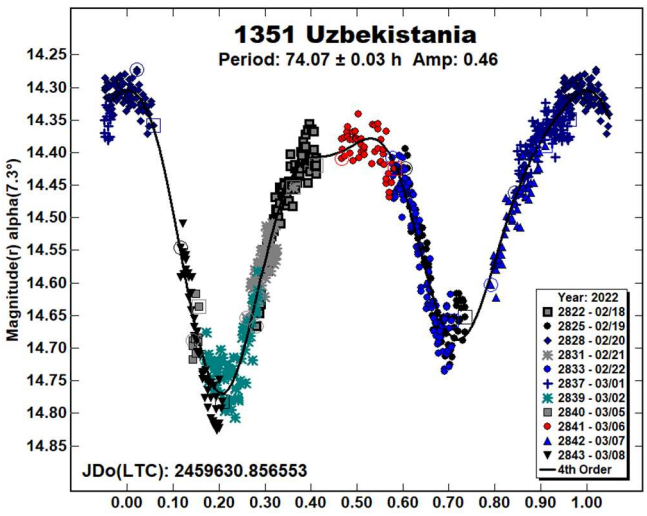

1450 Raimonda is one of Yrjö Väisälä's 128 asteroid discoveries, made at Turku in 1938. Two period solutions appear in the LCDB: LeCrone et al. (2005), 12.66 h and Hanus et al. (2013), 12.6344 ± 0.0002 h. A total of 209 images were taken during four nights to arrive at a similar synodic period of 12.67 ± 0.02 h, and an amplitude of 0.53 ± 0.043 mag.

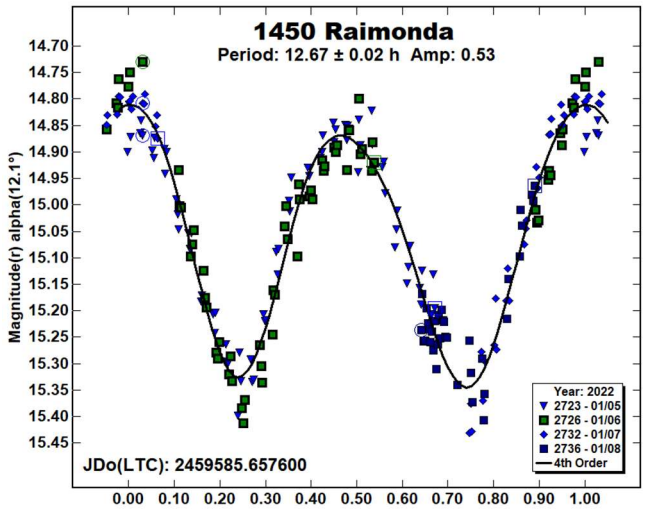

1657 Roemera was discovered by Paul Wild in 1951 at Zimmerwald. Wisniewski et al. (1997) shows a period of 4.5 ± 1 h, and Warner (2009) published a value of 34.0 ± 0.1 h. This slow rotator required 11 nights of observation, during which 610 images were taken. The synodic period is 301.7 ± 1.4 h. The solution is unambiguous due to its large amplitude of 0.63 ± 0.033 mag.

Number	Name	yy/mm/dd	Phase	L_{PAB}	B_{PAB}	Period(h)	P.E.	Amp	A.E.	Grp
570	Kythera	22/01/02-01/04	2.0,1.4	107	-2	8.129	0.010	0.10	0.01	MB-O
705	Erminia	22/02/18-03/02	10.6,12.9	136	22	54.74	0.10	0.06	0.01	MB-O
866	Fatme	22/02/05-02/08	3.7,3.2	143	8	11.49	0.05	0.05	0.02	MB-O
923	Herluga	22/01/02-01/06	10.2,10.5	100	-19	30.61	0.08	0.23	0.03	MB-M
1030	Vitja	22/01/08-01/10	6.7,6.8	108	-18	6.346	0.008	0.20	0.06	MB-O
1122	Neith	22/01/02-01/20	3.8,12.3	97	4	25.11	0.01	0.36	0.03	MB-M
1351	Uzbekistania	22/02/18-03/08	7.3,12.4	132	9	74.07	0.03	0.46	0.03	MB-O
1450	Raimonda	22/01/05-01/08	12.1,13.5	83	2	12.67	0.02	0.53	0.04	MB-M
1657	Roemera	22/01/06-01/16	*2.7,5.3	109	3	301.7	1.4	0.63	0.03	PHO
1815	Beethoven	22/02/04-02/08	6.7,4.9	149	2	8.181	0.008	0.10	0.03	MB-O
2068	Dangreen	22/02/04-02/07	5.1,5.0	138	11	--	--	--	--	MB-O
2069	Hubble	22/01/20-01/28	*5.5,6.1	122	12	44.62	0.09	0.34	0.03	MB-O
4512	Sinuhe	22/02/18-02/25	6.6,9.9	138	6	22.12	0.02	0.57	0.03	MB-O
5392	Parker	22/01/21-02/03	25.9,30.2	106	31	88.66	0.11	0.62	0.05	MARS
13249	Marcallen	22/01/20-02/03	3.2,9.6	115	-5	90.07	0.22	0.38	0.06	MB-M

Table I. Observing circumstances and results. The phase angle is given for the first and last date. If preceded by an asterisk, the phase angle reached an extrema during the period. L_{PAB} and B_{PAB} are the approximate phase angle bisector longitude/latitude at mid-date range (see Harris et al., 1984). Grp is the asteroid family/group (Warner et al., 2009).

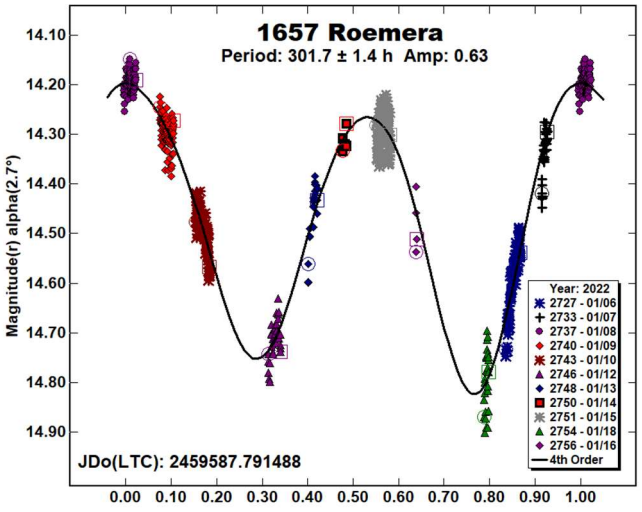

1815 Beethoven. This outer-belt asteroid was discovered by Karl Reinmuth at Heidelberg in 1932. The only period solution in the LCDB is that of Stephens (2005), who computed 54 ± 1 h. After five nights, 347 images were used to calculate a synodic period of 8.181 ± 0.008 h. The amplitude of the lightcurve is 0.10 mag, with a rather large RMS error of 0.029 mag.

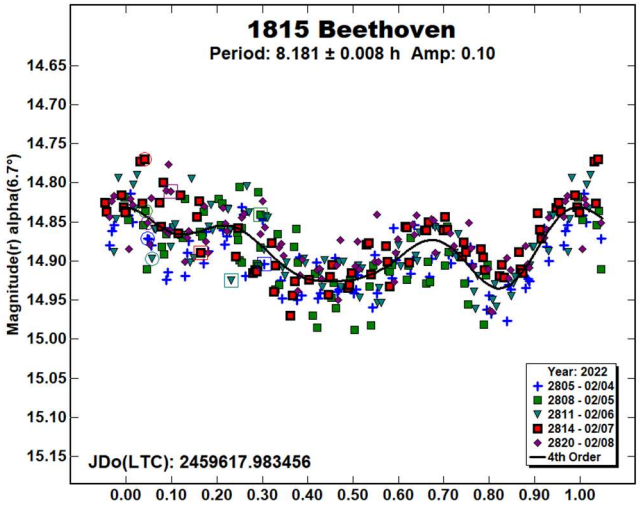

2068 Dangreen was identified by Marguerite Laugier at Nice in 1948. There are no period solutions in the LCDB. For four nights near the 2022 opposition, 370 images were taken, and no rotational period could be disentangled from the noisy data. The lightcurve below is raw.

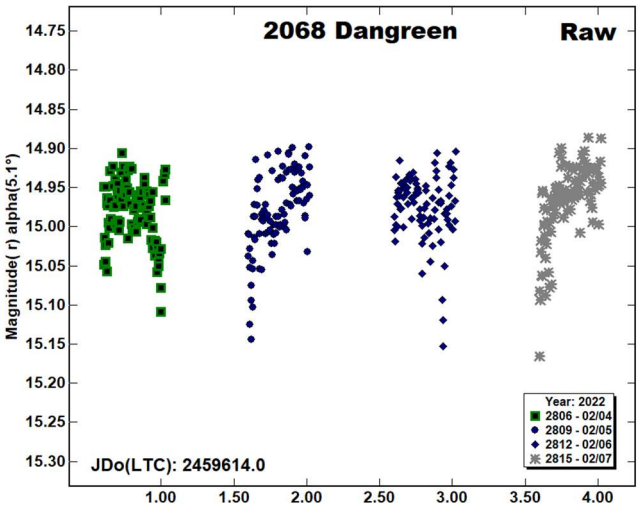

2069 Hubble. This minor planet's discovery was made at Goethe Link Observatory in 1955. The only period solution is that of Warner (2005), who published a value of 32.52 ± 0.02 h. A total of 712 data points from eight nights produced a synodic period of 44.62 ± 0.09 h. The amplitude of the lightcurve is 0.34 ± 0.033 mag.

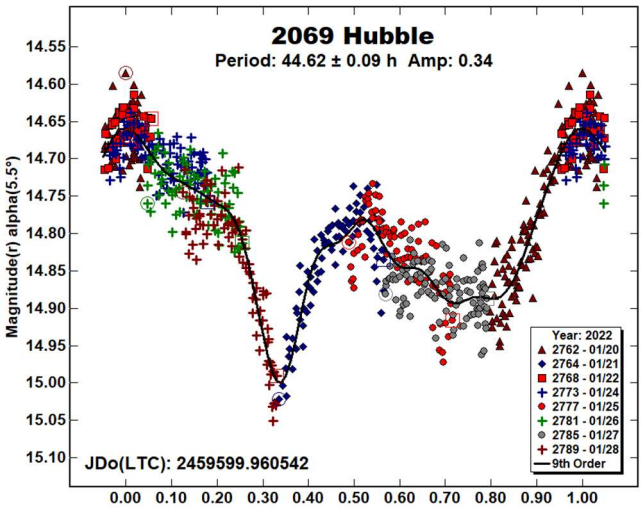

4512 Sinuhe is an outer-belt minor planet, discovered in 1939 at Turku by Yrjö Väisälä. Bennefeld et al. (2009) reported a period of 18.00 ± 0.01 h, and Behrend (2016web) computed 21.5 ± 0.7 h. In five nights, 332 images were gathered. The calculated period is 22.12 ± 0.02 h, with an amplitude of 0.57 ± 0.030 mag.

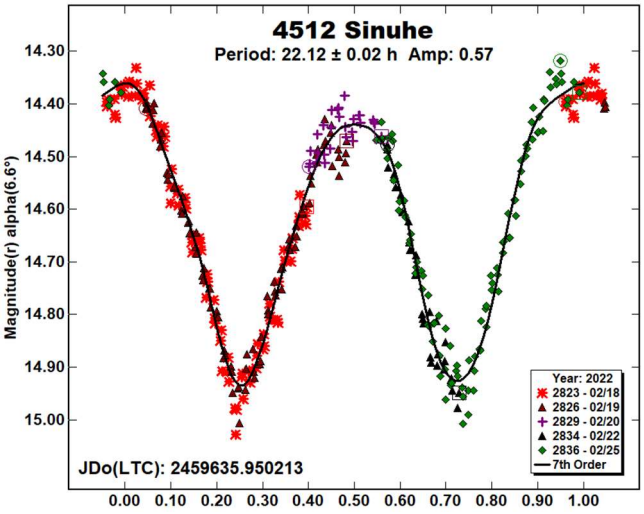

5392 Parker. This Mars-crosser was discovered in 1986 by Carolyn Shoemaker at Palomar. Its highly inclined and eccentric orbit brought it to a favorable, northerly opposition in 2022. The only period in the LCDB is that of Stephens (2018), who calculated 87.15 ± 0.03 h. Over the course of 10 nights, 735 images were used to compute a synodic period of 88.66 ± 0.11 h, in line with Stephens's value. However, the period spectrum shows a better fit with a trimodal lightcurve solution of 132.4 ± 0.3 h. The bimodal lightcurve amplitude is 0.62 ± 0.054 mag. There is evidence of tumbling in the curve morphology.

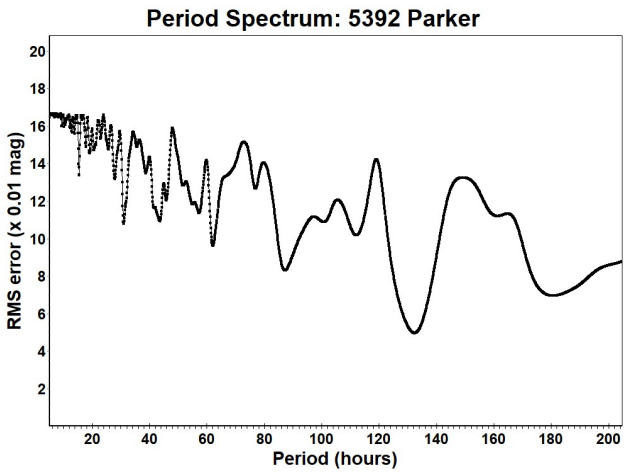

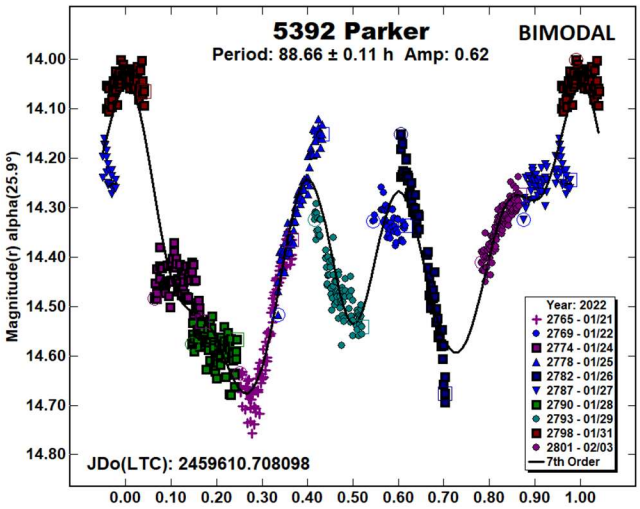

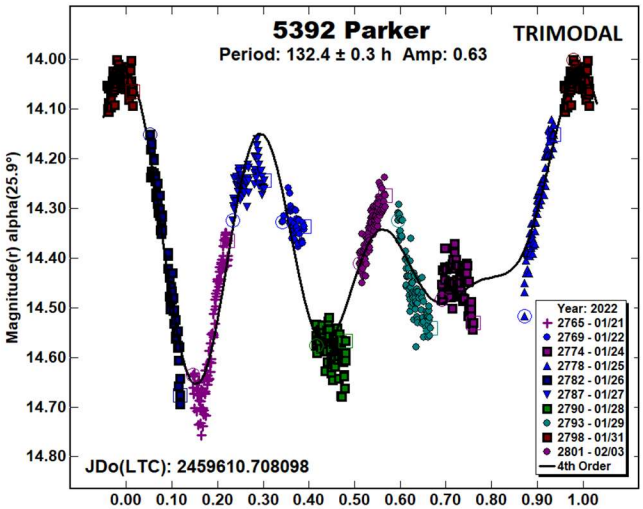

13249 Marcallen was discovered by the LONEOS survey near Flagtaff in 1998. There are no period solutions in the LCDB. After 11 nights, 767 data points had been acquired, and the period solution is 90.07 ± 0.22 h, with an amplitude of 0.38 ± 0.060 mag.

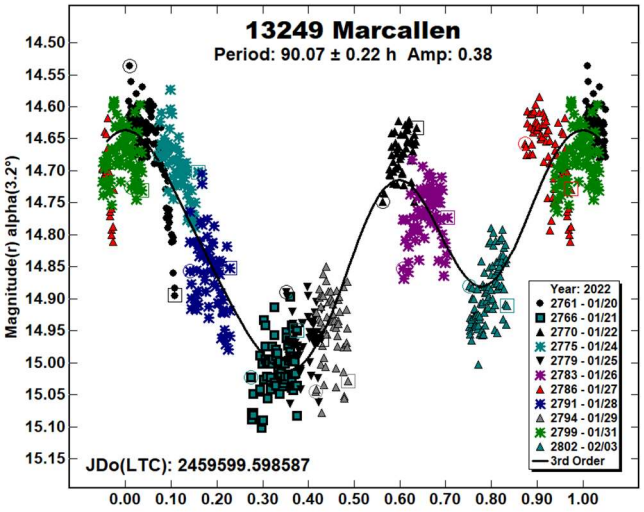

Acknowledgements

The author would like to express his gratitude to Brian Skiff for his indispensable mentoring in data acquisition and reduction. Thanks also go out to Brian Warner for support of his *MPO Canopus* software package.

References

Aznar, A.M.; Carreno Garcerain, A.; Arce Masego, E.; Brines Rodriques, P.; Lozano de Haro, J.; Fornas Silva, A.; Fornas Silva, G.; Mas Martinez, V.; Rodrigo Chiner, O.; Herrero Porta, D. (2016). "Twenty-one Asteroid Lightcurves at Group Observadores de Asteroides (OBAS): Late 2015 to Early 2016." *Minor Planet Bull*. **43**, 257-263.

Behrend, R. (2016web, 2020web). Observatoire de Geneve web site. *http://obswww.unige.ch/~behrend/page_cou.html*

Bennefeld, C.; Cantue, J.; Holly, V.; Jordon, L.; Martin, T.; Soar, E.; Swinney, T. (2009). "Asteroid Lightcurve Analysis at Ricky Observatory." *Minor Planet Bull*. **36**, 45-48.

Dose, E. (2021a) "Lightcurves of Nineteen Asteroids." *Minor Planet Bull*. **48**, 69-76.

Dose, E. (2021b). "Lightcurves of Eighteen Asteroids." *Minor Planet Bull*. **48**, 125-132.

Durech, J.; Hanus, J.; Vanco, R. (2019). "Inversion of asteroid photometry from Gaia DR2 and the Lowell Observatory photometric database." *Astron. Astrophys* **631**, A2.

Durech, J.; Tonry, J.; Erasmus, N.; Denneau, L.; Heinze, A.N.; Flewelling, H.; Vanco, R. (2020). "Asteroid models reconstructed from ATLAS photometry." *Astron. Astrophys*. **643**, A59.

Ferrero, A. (2014). "Period Determination of Four Main-belt Asteroids in Mid-2013." *Minor Planet Bull*. **41**, 24-25.

Hanus, J.; Durech, J.; Broz, M.; Marciniak, A.; Warner, B.D. and 115 colleagues (2013). "Asteroids' physical models from combined dense and sparse photometry and scaling of the YORP effect by the observed obliquity distribution." *Astron. Astrophys*. **551**, A67.

Harris, A.W.; Young, J.W.; Scaltriti, F.; Zappala, V. (1984). "Lightcurves and phase relations of the asteroids 82 Alkmene and 444 Gyptis." *Icarus* **57**, 251-258.

Harris, A.W.; Young, J.W.; Bowell, E.; Martin, L.J.; Millis, R.L.; Poutanen, M.; Scaltriti, F.; Zappala, V.; Schober, H.J.; Debehogne, H.; Zeigler, K.W. (1989). "Photoelectric Observations of Asteroids 3, 24, 60, 261, and 863." *Icarus* **77**, 171-186.

Koff, R.A.; Pravec, P.; Goncalves, R.; Antonini, P.; Behrend, R.; Pray, D.P. (2006). "Lightcurve photometry of asteroid 705 Erminia." *Minor Planet Bull*. **33**, 44.

LeCrone, C.; Addleman, D.; Butler, T.; Hudson, E.; Mulvihill, A.; Reichert, C.; Ross, I.; Starnes, H.; Ditteon, R. (2005). "2004-2005 winter observing campaign at Rose-Hulman Institute: results for 1098 Hakone, 1182 Ilona, 1294 Antwerpia, 1450 Raimonda, 2251 Tikhov, and 2365 Interkosmos." *Minor Planet Bull*. **32**, 46-48.

Marciniak, A.; Bartczak, P.; Müller, T.; Sanabria, J.J.; Alí-Lagoa, V. and 38 colleagues. (2018). "Photometric survey, modelling, and scaling of long-period and low-amplitude asteroids." *Astron. Astrophys*. **610**, A7.

Oey, J. (2009). "Lightcurve Analysis of Asteroids from Leura and Kingsgrove Observatory in the Second Half of 2008." *Minor Planet Bull*. **36**, 162-165.

Pilcher, F. (2021) "Lightcurves and Rotation Periods of 67 Asia, 74 Galatea, 356 Liguria, 570 Kythera, 581 Tauntonia, 589 Croatia, and 605 Juvisia." *Minor Planet Bull*. **48**, 132-135.

Polakis, T. (2018). "Lightcurve Analysis for Fourteen Main-belt Minor Planets." *Minor Planet Bull*. **45,** 347-352.

Stephens, R.D. (2005). "Asteroid lightcurve photometry from Santana Observatory - winter 2005." *Minor Planet Bull*. **32**, 66-68.

Stephens, R.D. (2018). "Asteroids Observed from CS3: 2017 October - December." *Minor Planet Bull*. **45**, 135-137.

Tonry, J.L.; Denneau, L.; Flewelling, H.; Heinze, A.N.; Onken, C.A.; Smartt, S.J.; Stalder, B.; Weiland, H.J.; Wolf, C. (2018). "The ATLAS All-Sky Stellar Reference Catalog." *Ap. J.* **867**, A105.

Warner, B.D. (2004). "Lightcurve analysis for numbered asteroids 1351, 1589, 2778, 5076, 5892, and 6386." *Minor Planet Bull*. **31**, 36-39.

Warner, B.D. (2005). "Asteroid lightcurve analysis at the Palmer Divide Observatory - winter 2004-2005." *Minor Planet Bull*. **32**, 54-58.

Warner, B.D. (2009). "Asteroid Lightcurve Analysis at the Palmer Divide Observatory: 2008 May - September." *Minor Planet Bull*. **36**, 7-13.

Warner, B.D.; Harris, A.W.; Pravec, P. (2009). "The Asteroid Lightcurve Database." *Icarus* **202**, 134-146. Updated 2021 Dec. *http://www.minorplanet.info/lightcurvedatabase.html*

Warner, B.D. (2011). Collaborative Asteroid Lightcurve Link website. *http://www.minorplanet.info/call.html*

Warner, B.D. (2022). *MPO Canopus* software. *http://bdwpublishing.com*

Wisniewski, W.Z.; Michalowski, T.M.; Harris, A.W.; McMillan, R.S. (1997). "Photometric Observations of 125 Asteroids." *Icarus* **126**, 395-449.

LIGHTCURVES AND ROTATION PERIODS OF 49 PALES, 424 GRATIA, 705 ERMINIA, 736 HARVARD, 1261 LEGIA, 1541 ESTONIA, AND 6371 HEINLEIN

Frederick Pilcher
Organ Mesa Observatory (G50)
4438 Organ Mesa Loop
Las Cruces, NM 88011 USA
fpilcher35@gmail.com

(Received: 2022 April 7)

Synodic rotation periods and amplitudes are found for 49 Pales, 20.702 ± 0.001 hours, 0.18 ± 0.01 magnitudes with 4 unequal maxima and minima per cycle; 424 Gratia, 20.063 ± 0.002 hours with one asymmetric maximum and minimum per cycle, 0.15 ± 0.01 magnitudes; 705 Erminia, 53.68 ± 0.01 hours, 0.09 ± 0.01 magnitudes with an irregular monomodal lightcurve; 736 Harvard, 6.742 ± 0.001 hours, 0.09 ± 0.01 magnitudes; 1261 Legia, 25.71 ± 0.01 hours, 0.12 ± 0.01 magnitudes; 1541 Estonia, 12.890 ± 0.001 hours, 0.16 ± 0.01 magnitudes; 6371 Heinlein, 4.962 ± 0.003 hours, 0.55 ± 0.05 magnitudes. For 49 Pales V-R = 0.36, H=7.69 in the V band, G=0.10.

Observations to obtain the data used in this paper were made at the Organ Mesa Observatory with a 0.35-meter Meade LX200 GPS Schmidt-Cassegrain (SCT) and SBIG STL-1001E CCD. Exposures were 60 seconds for 49 Pales, 424 Gratia, 705 Erminia, and 6371 Heinlein; 120 seconds for 736 Harvard, 1261 Legia, and 1541 Estonia, unguided, with a clear filter. Photometric measurement and lightcurve construction are with *MPO Canopus* software. To reduce the number of points on the lightcurves and make them easier to read, data points have been binned in sets of 3 with a maximum time difference of 5 minutes.

49 Pales. Two early published rotation periods were by Schober et al. (1979), 10.42 hours; and by Tedesco (1979), 10.3 hours, and for many years the period was believed to be near 10.4 hours. Behrend (2013web) published a very sparse lightcurve which suggested a period <10 hours. Pilcher et al. (2016) made a much more comprehensive investigation that found a period 20.704 hours with an unsymmetric quadrimodal lightcurve. Behrend (2016web) complemented this study with a period 20.7057 hours. Four subsequent studies confirm both the longer period and the unsymmetric quadrimodal lightcurve: Pilcher (2017), 20.705 hours; Pilcher (2018), 20.709 hours; Pilcher (2021), 20.702 hours; and Behrend (2020web), 2.7102 hours. New observations on 6 nights 2021 Dec 24 -2022 Jan 26 provide a fit to a period 20.702 ± 0.001 hours, again with an unsymmetric quadrimodal lightcurve, and amplitude 0.18 ± 0.01 magnitudes (Fig. 1). It is noteworthy that all the lightcurves published from 2016 onward have very nearly the same amplitudes and shapes despite being from very different positions in the sky. This indicates that the orbital plane and equatorial rotational plane are nearly parallel. Whether the rotation is prograde or retrograde is undetermined.

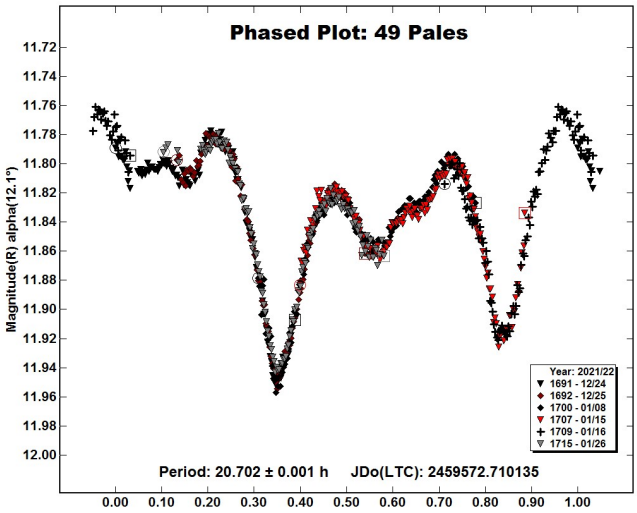

Fig. 1: Lightcurve of 49 Pales phased to 20.702 hours.

On 2022 Jan 30 twenty images were obtained alternately with the R and V filters and measured with the same calibration stars in R and V magnitudes, respectively, as obtained from the *MPO Canopus* comp star selector subroutine. The raw plot of these data shows that V-R = 0.36 (Fig. 2). The H-G plot in the V band shows that H=7.686 ± 0.034; G = 0.104 ± 0.052 (Fig. 3). Pilcher et al. (2016) also measured for the 2015 opposition V-R = 0.35; in the V band H=7.61 ± 0.06, G = 0.019 ± 0.30. The values of G in these two studies are not compatible.

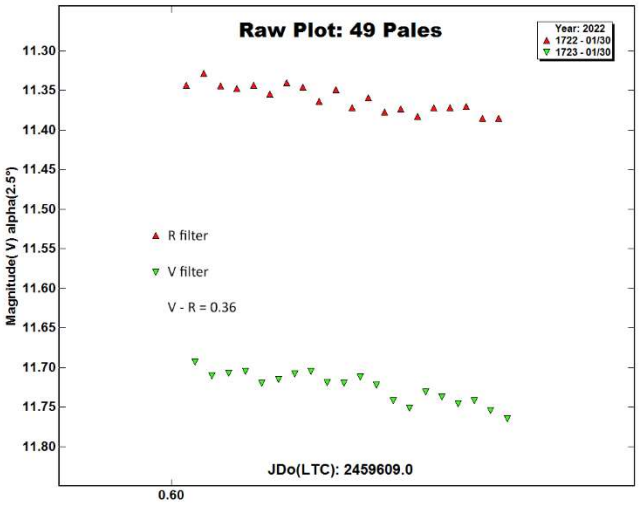

Fig. 2: Raw lightcurve of 49 Pales with R and V filters.

Number	Name	yyyy/mm/dd	Phase	LPAB	BPAB	Period (h)	P.E	Amp	A.E.
49	Pales	2021/12/24-2022/01/26	12.4, 1.0	124	-1	20.702	0.001	0.18	0.01
424	Gratia	2022/01/27-2022/03/02	*8.0, 8.5	144	7	20.063	0.002	0.15	0.01
705	Erminia	2021/12/26-2022/02/06	16.7, 9.7	156	25	53.68	0.01	0.09	0.01
736	Harvard	2022/03/12-2022/04/07	11.6, 2.8	196	5	6.742	0.001	0.09	0.01
1261	Legia	2022/02/26-2022/04/02	2.3 15.8	154	3	25.71	0.01	0.12	0.01
1541	Estonia	2022/02/25-2022/04/03	*6.6, 10.2	171	1	12.890	0.001	0.16	0.01
6371	Heinlein	2022/01/15-2022/01/16	4.0, 3.6	124	-1	4.962	0.003	0.55	0.05

Table I. Observing circumstances and results. Pts is the number of data points. The phase angle is given for the first and last date, unless a minimum (second value) was reached. LPAB and BPAB are the approximate phase angle bisector longitude and latitude at mid-date range (see Harris et al., 1984).

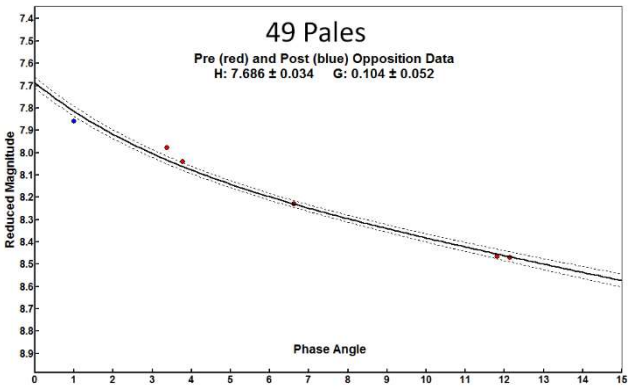

Fig. 3.: H-G plot for 49 Pales in the V magnitude band.

424 Gratia. Previously published rotation periods are by Florczak et al. (1997), 19.47 hours; Polakis (2018), 20.075 hours. Colazo et al. (2021), 40.106 hours, and Dose (2021), 40.118 hours. Colazo et al. and Dose published nearly symmetric bimodal lightcurves at the same opposition. Each lightcurve showed bumps near the middle of both rising segments that were slightly different from each other, but the shapes of the bumps in the two publications differed from each other by a greater amount.

New observations on eight nights 2022 Jan 27 - Mar 2 provide an excellent fit to a lightcurve with period 20.063 ± 0.002 hours with one aymmetric maximum and minimum per cycle, amplitude 0.15 ± 0.01 magnitudes (Fig. 4). The two halves of the split halves lightcurve. covering the entire double period of 40.124 hours, are almost identical (Fig. 5). The double period may be ruled out. If the nearly symmetric lightcurves plotted by Colazo et al. (2021) and by Dose (2021) represent twice the real period, then all reported results are compatible.

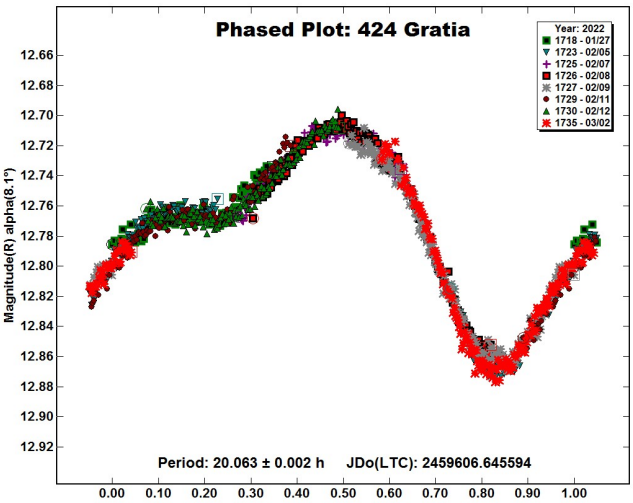

Fig. 4: Lightcurve of 424 Gratia phased to 20.063 hours.

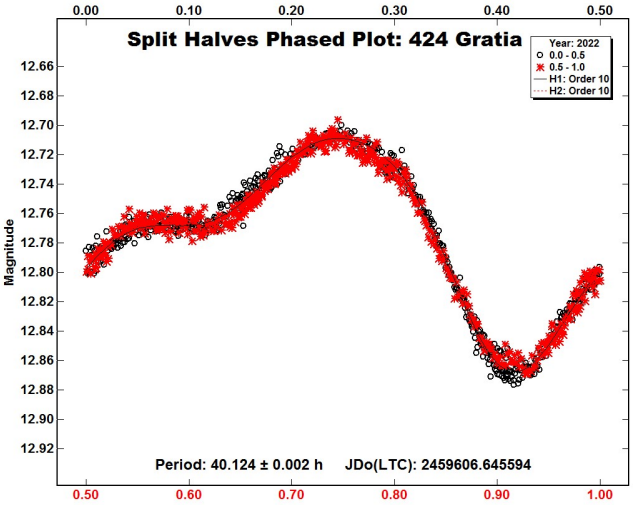

Fig. 5: Split halves phased plot of 424 Gratia.

705 Erminia. There have been several previously published lightcurves of greatly varying density and reliability. Koff et al. (2006) published a dense irregular bimodal lightcurve with full phase coverage that has an excellent fit to period of 53.95 hours, amplitude 0.12 mgnitudes, near celestial longitude 39º, celestial latitude 14º. Behrend (2005web) published a very similar lightcurve with some gaps based on data at the same opposition phased to period 53.864 hours. Rotation periods and amplitudes based on much sparser and much less reliable lightcurves have been published by Behrend (2020web), 53.96 hours, 0.16 magnitudes; and Di Martino et al. (1995), 7.22 hours, 0.07 magnitudes.

New observations near celestial longitude 156º, celestial latitude 25º were obtained on 11 nights 2021 Dec 26 - 2022 Feb 6. With a target at declination +42º, sessions of more than ten hours were possible, although some sessions were shortened by clouds that appeared late in the night. The data provide an excellent fit with full phase coverage to an irregular monomodal lightcurve with synodic period 53.68 ± 0.01 hours, amplitude 0.09 ± 0.01 magnitudes (Fig. 6). A split halves plot of the double period 107.30 hours shows a near perfect fit between the two halves but with several very small missing segments in each half (Fig. 7). The double period is ruled out.

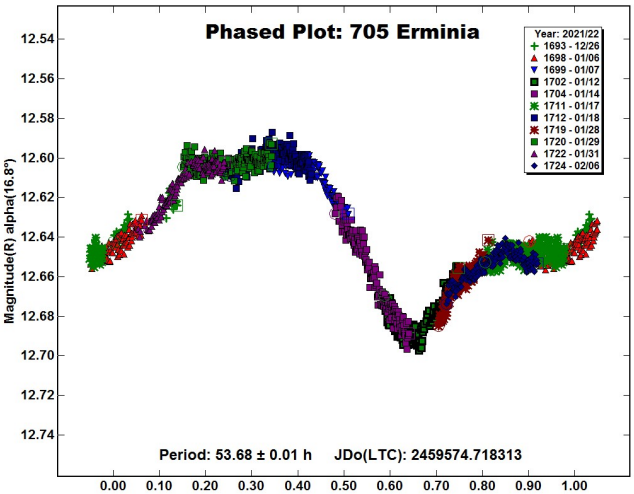

Fig. 6: Lightcurve of 705 Erminia phased to 52.68 hours.

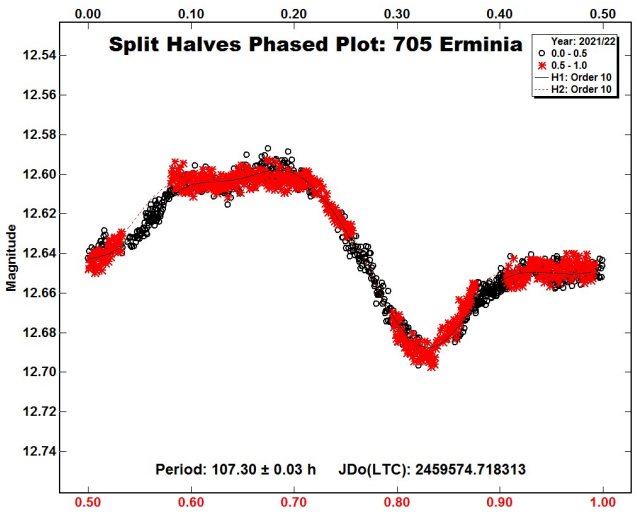

Fig. 7: Split halves phased plot of 705 Erminia.

As the amplitude of 0.12 magnitudes of the other high quality dense lightcuve by Koff et al. (2006) at celestial longitude 39º is larger than 0.09 magnitudes in the current study near celestial longitude 156º, it is inferred that the rotational pole lies closer to celestial longitude 156º. The synodic period of 53.68 hours in the current study is about 0.5% smaller than the 53.95 hours in Koff et al. The considerable discordance in the two values can be reasonably explained by the different aspect angles of the two data sets. These values are also compatible with Behrend (2005web), and Behrend (2020web). The 7.22-hour period by Di Martino et al. (1995) is now ruled out.

736 Harvard. The only previously published rotation period is by Tedesco (1979), 6.7 hours. New observations on 5 nights 2022 Mar 12 - Apr 7 provide a good fit to a lightcurve with period 6.742 ± 0.001 hours, amplitude 0.09 ± 0.01 magnitudes (Fig. 8). This value is consistent with and improves upon the accuracy of the value by Tedesco (1979).

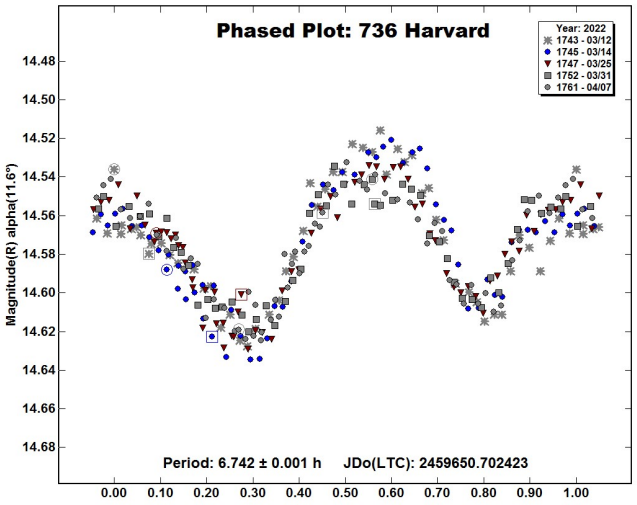

Fig. 8: Lightcurve of 736 Harvard phased to 6.742 hours.

1261 Legia. The only previously published lightcurve is by Behrend (2005web), 8.693 hours. New observations on eight nights 2022 Feb 26 - Apr 2 provide a good fit to an irregular bimodal lightcurve with period 25.71 ± 0.01 hours, amplitude 0.12 ± 0.01 magnitudes (Fig. 9). The new observations rule out a period near 8.693 hours as published by Behrend (2005web).

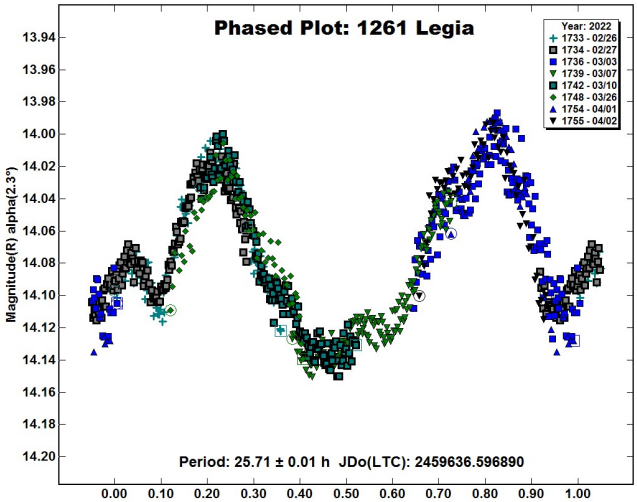

Fig. 9: Lightcurve of 1261 Legia phased to 25.71 hours.

1541 Estonia. Previously published rotation periods are by Behrend (2015web), 10.1 hours; and by Polakis (2021), 12.84 hours. Six new sessions were obtained from 2022 Feb 25 at phase angle -6.6º to a minimum phase angle 1.0º 2022 Mar 13 to 2022 Apr 3 at phase angle 10.2º. They provide a good fit to a lightcurve phased to 12.890 ± 0.001 hours with amplitude 0.16 ± 0.01 magnitudes (Fig. 10). The minimum near lightcurve phase 0.90 is deeper for the 02/25 session at phase angle -6.6º and the 04/03 session at phase angle 10.2º than for the four sessions from 03/08 at phase angle -1.6º through 03/24 at phase angle 6.0º. This increase in amplitude at increased phase angle is caused by shadowing by surface irregularities, a behavior observed for many asteroids. The new observations are consistent with Polakis (2021) and rule out the 10.1-hour period reported by Behrend (2015web).

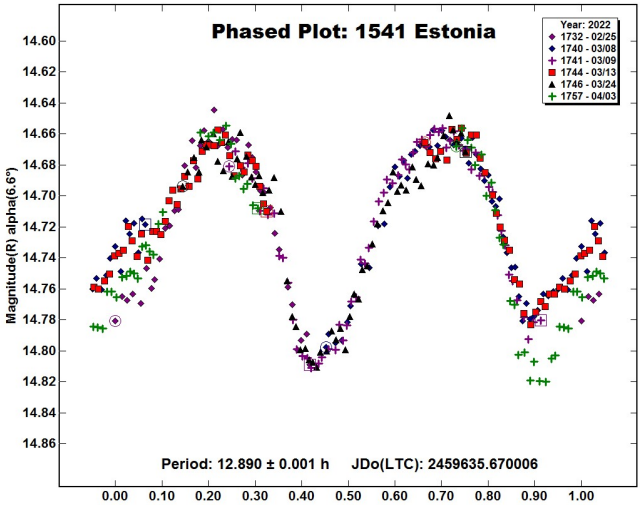

Fig. 10: Lightcurve of 1541 Estonia phased to 12.890 hours.

6371 Heinlein. Behrend (2017web) published a dense lightcurve with period 4.96328 hours, amplitude 0.53 magnitudes. On 2022 January 15 and 16, it was entirely fortuitous that 6371 Heinlein was on the same images as the primary target of the night, 49 Pales. At magnitude 15.5 and close to the nearly full moon, the error bars on the data points were of order 0.15 magnitudes. But the amplitude was much larger, 0.55 ± 0.05 magnitudes, and a good fit was obtained to a period of 4.962 ± 0.003 hours (Fig. 11). The period spectrum (Fig. 12) of 6371 Heinlein shows no other deep minima in the range from 4 to 6 hours. Considering that only seven rotational cycles were covered by the data, the consistency with Behrend (2017web) is very good.

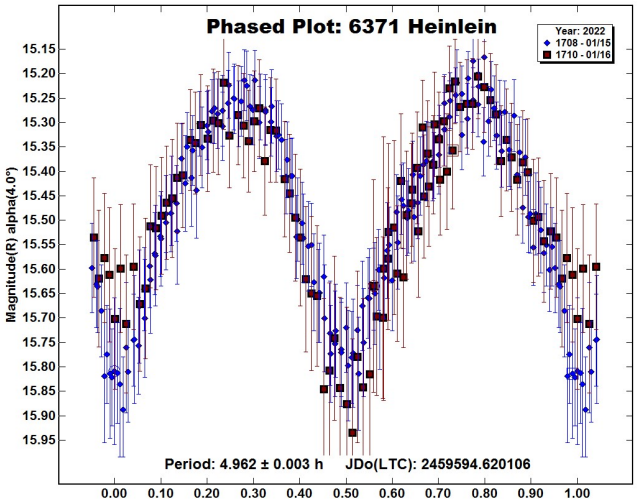

Fig. 11: Lightcurve of 6371 Heinlein phased to 4.962 hours.

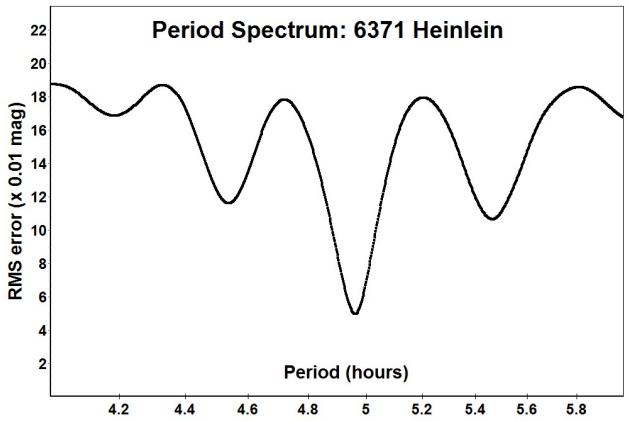

Fig. 12: Period spectrum of 6371 Heinlein.

References

Behrend, R. (2005web, 2013web, 2015web, 2016web, 2017web, 2020web). Observatoire de Geneve web site. *http://*obswww.unige.ch/*~behrend/page_cou.html*

Colazo, M.; Stechina, A.; Fornari, C.; Suárez, N.; Melia, R.; Morales, M.; Bellocchio, E.; Pulver, E.; Speranza, T.; Scotta, D.; Wilberger, A.; Mottino, A.; Meza, E.; Romero, F.; Tourne Passarino, P.; Suligoy, M.; Llanos, R.; Chapman, A.; Martini, M.; Colazo, C. (2021). "Asteroid Photometry and Lightcurve Analysis at GORA's Observatories, Part IV." *Minor Planet Bull.* **48**, 140-143.

Di Martino, M.; Dotto, E.; Celino, A.; Barucci, M.A.; Fulchignoni, M. (1995). "Intermediate size asteroids: Photoelectric photometry of 8 objects." *Astron. Astrophys. Suppl. Ser.* **112**, 1-7.

Dose, E. (2021). "Lightcurves of nineteen asteroids." *Minor Planet Bull.* **48**, 69-76.

Florczak, M.; Dotto, E.; Barucci, M.A.; Birlan, M.; Erikson, A.; Fulchignoni, M.; Nathues, A.; Perret, L.; Thebault. P. (1997). "Rotational properties of main belt asteroids: photoelectric and CCD observations of 15 objects." *Planet. Space Sci.* **45**, 1423-1435.

Harris, A.W.; Young, J.W.; Scaltriti, F.; Zappala, V. (1984). "Lightcurves and phase relations of the asteroids 82 Alkmene and 444 Gyptis." *Icarus* **57**, 251-258.

Koff, R.A.; Pravec, P.; Gonclaves, R.; Antonini, P.; Behrend, R.; Pray, D.P. (2006). "Lightcurve photometry of asteroid 705 Erminia." *Minor Planet Bull.* **33**, 44.

Pilcher, F.; Benishek, V.; Klinglesmith, D.A. (2016). "Rotation Period, Color Indices, and H-G Parameters for 49 Pales." *Minor Planet Bull.* **43**, 182-183.

Pilcher, F. (2017). "Rotation Period Determinations for 49 Pales, 96 Aegle, 106 Dione, 375 Ursula, and 576 Emanuela." *Minor Planet Bull.* **44**, 249-251.

Pilcher, F. (2018). "New lightcurves of 33 Polyhymnia, 49 Pales, 289 Nenetta, 504 Cora, and 821 Fanny." *Minor Planet Bull.* **45**, 356-359.

Pilcher, F. (2021). "Lightcurves and rotation periods of 49 Pales, 383 Janina, and 764 Gedania." *Minor Planet Bull.* **48**, 5-6.

Polakis, T. (2018). "Lightcurve analysis for fourteen main-belt minor planets." *Minor Planet Bull.* **45**, 347-352.

Polakis, T. (2021). "Period determination for seventeen minor planets." *Minor Planet Bull.* **48**, 158-163.

Schober, H.-J., Scaltriti, F.; Zappala, V. (1979). "Photoelectric photometry and rotation periods of three large and dark asteroids - 49 Pales, 88 Thisbe, and 92 Undina." *Astron. Astrophys. Suppl. Ser.* **36**, 1-8.

Tedesco, E.F. (1979). PhD Dissertation, New Mexico State University.

ASTEROID PHOTOMETRY AND LIGHTCURVE RESULTS FOR SEVEN ASTEROIDS

Milagros Colazo
Instituto de Astronomía Teórica y Experimental
(IATE-CONICET), ARGENTINA
Facultad de Matemática, Astronomía y Física
Universidad Nacional de Córdoba, ARGENTINA
Grupo de Observadores de Rotaciones de Asteroides (GORA)
ARGENTINA
milirita.colazovinovo@gmail.com

Bruno Monteleone, Francisco Santos, Mario Morales,
Alberto García, Néstor Suárez, Leopoldo Altuna,
Macarena Caballero, Fabricio Romero, Tiago Speranza,
Ezequiel Bellocchio, Marcos Santucho, César Fornari, Raúl Melia,
Ariel Stechina, Damián Scotta, Nicolás Arias, Andrés Chapman,
Giuseppe Ciancia, Aldo Wilberger, Marcos Anzola,
Aldo Mottino, Carlos Colazo.

Grupo de Observadores de Rotaciones de Asteroides (GORA)
ARGENTINA

Observatorio Astronómico Giordano Bruno (MPC G05)
Piconcillo (Córdoba-ESPAÑA)

Observatorio Cruz del Sur (MPC I39)
San Justo (Buenos Aires-ARGENTINA)

Observatorio de Sencelles (MPC K14)
Sencelles (Mallorca-Islas Baleares-ESPAÑA)

Observatorio Los Cabezones (MPC X12)
Santa Rosa (La Pampa-ARGENTINA)

Observatorio Orbis Tertius (MPC X14)
Córdoba (Córdoba-ARGENTINA)

Observatorio Galileo Galilei (MPC X31)
Oro Verde (Entre Ríos-ARGENTINA)

Observatorio Antares (MPC X39)
Pilar (Buenos Aires-ARGENTINA)

Observatorio Río Cofio (MPC Z03)
Robledo de Chavela (Madrid-ESPAÑA)

Observatorio AstroPilar (GORA APB)
Pilar (Buenos Aires-ARGENTINA)

Osservatorio Astronomico "La Macchina del Tempo"
(GORA BM1)
Ardore Marina (Reggio Calabria-ITALIA)

Osservatorio Astronomico "La Macchina del Tempo 2"
(GORA BM2)
Ardore Marina (Reggio Calabria-ITALIA)

Specola "Giuseppe Pustorino" (GORA GC1)
Palizzi Marina (Reggio Calabria-ITALIA)

Observatorio de Ariel Stechina 1 (GORA OAS)
Reconquista (Santa Fe-ARGENTINA)

Observatorio de Ariel Stechina 2 (GORA OA2)
Reconquista (Santa Fe-ARGENTINA)

Observatorio Cielos de Banfield (GORA OCB)
Banfield (Buenos Aires-ARGENTINA)

Observatorio de Damián Scotta 1 (GORA ODS)
San Carlos Centro (Santa Fe-ARGENTINA)

Observatorio de Damián Scotta 2 (GORA OD2)
San Carlos Centro (Santa Fe-ARGENTINA)

Observatorio Astronómico Vuelta por el Universo (GORA OMA)
Córdoba (Córdoba-ARGENTINA)

Observatorio Astronómico Municipal Reconquista (GORA OMR)
Reconquista (Santa Fe-ARGENTINA)

Observatorio de Raúl Melia (GORA RMG)
Gálvez (Santa Fe-ARGENTINA)

(Received: 2022 Mar 14)

Synodic rotation periods and lightcurve amplitudes are reported for: 308 Polyxo, 488 Kreusa, 494 Virtus, 570 Kythera, 702 Alauda, 877 Walkure, and 995 Sternberga.

The periods and amplitudes of asteroid lightcurves presented here are the product of collaborative work by GORA (Grupo de Observadores de Rotaciones de Asteroides) group. In all the studies we have applied relative photometry assigning V magnitudes to the calibration stars.

The image acquisition was performed without filters and with exposure times of a few minutes. All images used were corrected using dark frames and, in some cases, bias and flat-fields were also used. Photometry measurements were performed using *FotoDif* software and for the analysis, we employed *Periodos* software (Mazzone, 2012).

Below, we present the results for each asteroid under study. The lightcurve figures contain the following information: the estimated period and period error and the estimated amplitude and amplitude error. In the reference boxes, the columns represent, respectively, the marker, observatory MPC code, or – failing that – the GORA internal code, session date, session offset, and several data points.

Target selection was based on the following criteria: 1) those asteroids with magnitudes accessible to the equipment of all participants, 2) those with favorable observation conditions from Argentina, Spain, and/or Italy, and 3) objects with few periods reported in the literature and/or in the Lightcurve Database (LCDB) (Warner et al., 2009) with quality codes (U) of less than 3.

308 Polyxo is a T-type asteroid discovered in 1891 by Alphonse Borrelly. Previous reports of the period include 12.032 ± 0.008 h (Debehogne and Zapalà, 1980), 12.01 ± 0.02 h (Higgins, 2011), and 12.029 ± 0.001 h (Pilcher et al., 2014). As other authors have commented, the period is very close to commensurability with the terrestrial diurnal period. In this work, we present full lightcurve coverage, taking advantage of the several observatories belonging to GORA that are distributed at different longitudes. The results, consistent with previous reports, are P = 12.031 ± 0.007 h and A = 0.13 ± 0.01 mag.

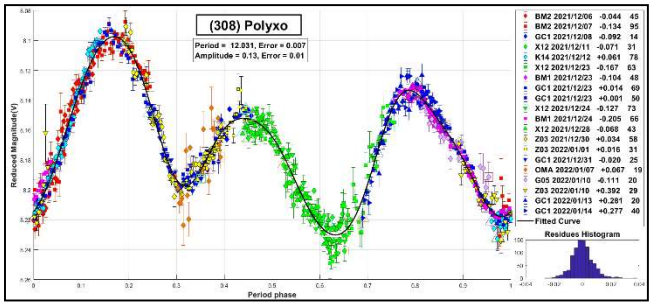

488 Kreusa is a C-type asteroid discovered in 1902 by Luigi Carnera and Max Wolf. Different authors have measured a variety of periods for this object. For example, 65.3 ± 0.1 h (Behrend, 2007web), 19.26 h (Robinson, 2011web), 32.666 ± 0.003 h (Stephens, 2014), and 32.645 ± 0.001 h (Pilcher, 2019). The coverage of these lightcurves was not completely reliable. In this work, we provide rather different results and propose this asteroid to be a slow rotator with a period of P = 639.319 ± 0.013 h and A = 0.21 ± 0.02 mag.

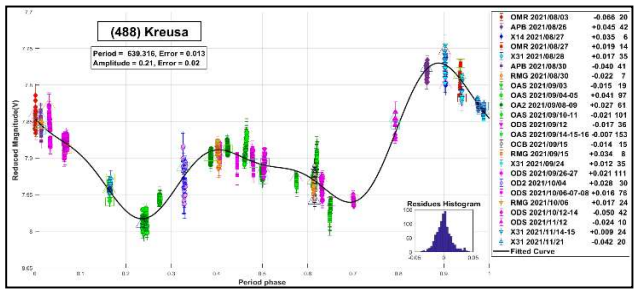

494 Virtus is a C-type asteroid discovered in 1902 by Max Wolf. Previous reported periods include 5.57 ± 0.01 h (Warner, 2006), 4.9903 ± 0.0004 h (Behrend, 2008web), and 5.570 ± 0.003 h (Hamanowa and Hamanowa, 2009). However, Tom Polakis (2018) reported a completely different period of 49.427 ± 0.022 h. In this paper we present a new, intermediate value of P = 20.000 ± 0.010 h and A = 0.19 ± 0.01 mag.

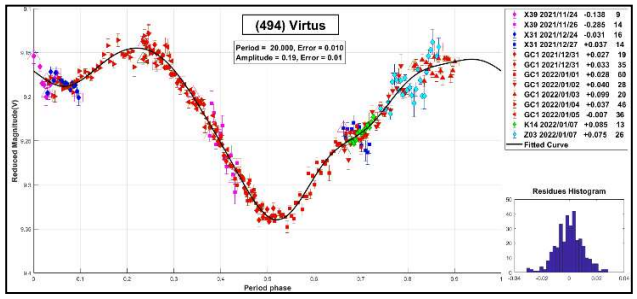

570 Kythera is classified as type ST. It was discovered by Max Wolf in 1905. Different periods have been reported before: 6.903 ± 0.002 h (Gil-Hutton, 2003), 8.120 ± 0.002 h (Behrend, 2004web), 10.5 ± 0.1 h (Chavez, 2014), 8.117 ± 0.001 h (Pilcher, 2021). In this paper, we present a result of P = 8.119 ± 0.013 h, which agrees with those from Behrend and Pilcher.

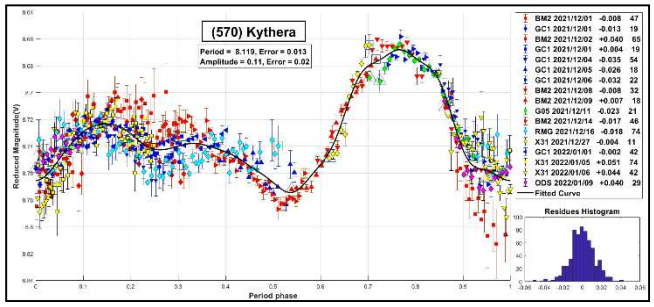

702 Alauda is a C-type asteroid discovered in 1910 by Joseph Helffrich. In 2007, it was proposed to be a binary system. We found previous works favored one of two periods, near 8 h or 16 h. Fauerbach and Bennett (2005) reported 8.348 ± 0.001 h while Benishek (2008) reported 8.3539 ± 0.0007 h and Alkema (2014) found 8.3531 ± 0.0004 h. On the other hand, Behrend (2014web) found a period of 16.7025 ± 0.0002 h. The results we obtained are P = 16.700 ± 0.004 h and A = 0.09 ± 0.01 mag. Our period well agrees with the one measured by Behrend.

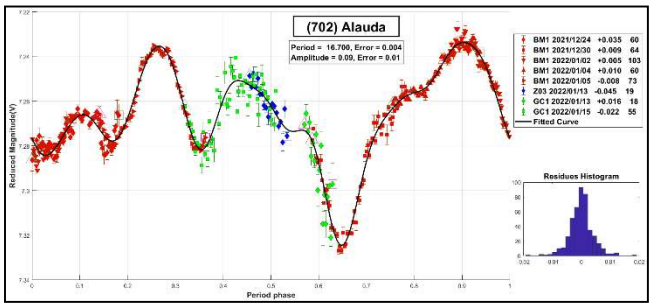

877 Walkure is an F-type asteroid discovered in 1915 by Grigori Neúimin. Binzel (1987) determined a synodic period of 17.49 h. In this work, we present a lightcurve with full coverage with a similar period, P = 17.437 ± 0.013 h with A = 0.42 ± 0.02mag.

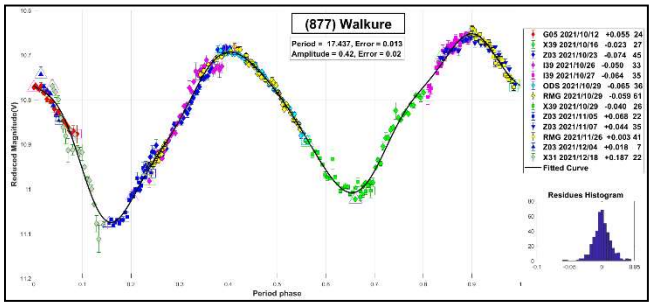

995 Sternberga was discovered in 1923 by Serguéi Beliavski. Several periods have been measured for this asteroid: 15.26 ± 0.01 h (Stephens, 2005), 14.612 ± 0.001 h (Stephens, 2013), and 22.404 ± 0.005 h (Marciniak et al., 2014). We have determined a period of 22.392 ± 0.006 h, which is consistent with the one proposed by Marciniak. Noticeably, we present a lightcurve with full coverage.

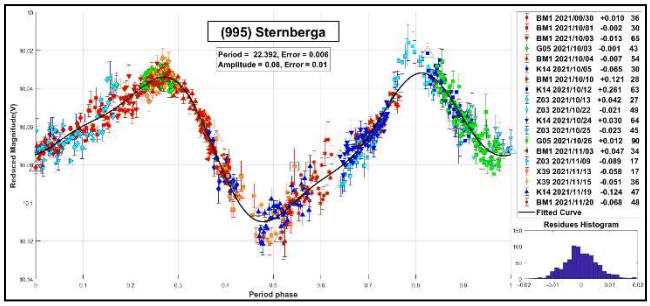

Number	Name	yy/ mm/dd- yy/ mm/dd	Phase	L_{PAB}	B_{PAB}	Period (h)	P.E.	Amp	A.E.	Grp
308	Polyxo	21/12/06-22/01/14	2.2,14.8	73	-5	12.031	0.007	0.13	0.01	MB-O
488	Kreusa	21/08/03-21/11/22	*4.6,15.2	319	-11	639.316	0.013	0.21	0.02	MB-O
494	Virtus	21/11/24-22/01/07	3.9,15.8	51	3	20.000	0.010	0.19	0.01	MB-O
570	Kythera	21/12/01-22/01/09	*12.0,9	107	-2	8.119	0.013	0.11	0.02	MB-O
702	Alauda	21/12/24-22/01/15	15.9,11.9	148	-13	16.700	0.004	0.09	0.01	MB-O
877	Walkure	21/10/12-21/12/18	4.6,26.8	18	-6	17.437	0.013	0.42	0.02	MB-O
995	Sternberga	21/09/30-21/11/20	*11.5,14.6	27	4	22.392	0.006	0.08	0.01	MB-O

Table I. Observing circumstances and results. The phase angle is given for the first and last date. If preceded by an asterisk, the phase angle reached an extremum during the period. L_{PAB} and B_{PAB} are the approximate phase angle bisector longitude/latitude at mid-date range (see Harris et al., 1984). Grp is the asteroid family/group (Warner et al., 2009). MB-O: main-belt outer.

Observatory	Telescope	Camera
G05 Obs.Astr.Giordano Bruno	SCT (D=203mm; f=6.0)	CCD Atik 420 m
I39 Obs.Astr.Cruz del Sur	Newtoniano (D=254mm; f=4.7)	CMOS QHY 174
K14 Obs.Astr.de Sencelles	Newtoniano (D=250mm; f=4.0)	CCD SBIG ST-7XME
X12 Obs.Astr.Los Cabezones	Newtoniano (D=200mm; f=5.0)	CMOS QHY 174M GPS
X14 Obs.Astr.Orbis Tertius	Newtoniano (D=200mm; f=5.0)	CMOS P1 Neptune M
X31 Obs.Astr.Galileo Galilei	RCT ap (D=405mm; f=8.0)	CCD SBIG STF8300M
X39 Obs.Astr.Antares	Newtoniano (D=250mm; f=4.7)	CCD QHY9 Mono
Z03 Obs.Astr.Río Cofio	SCT (D=254mm; f=6.3)	CCD SBIG ST8-XME
APB Obs.Astr.AstroPilar	Refractor (D=150mm; f=7.0)	CCD ZWO-ASI183
BM1 Oss.Astr.La Macchina del Tempo 1	Ritchey-Chretien (D250mm; f=8)	CMOS ZWO ASI 1600 MM
BM2 Oss.Astr.La Macchina del Tempo 2	Newtoniano (D=200mm; f=5.0)	CMOS ZWO ASI 294 MM
GC1 Specola Giuseppe Pustorino 1	Newtoniano (D=254mm; f=4.7)	CCD Atik 383l+Mono
OAS Obs.Astr.de Ariel Stechina 1	Newtoniano (D=254mm; f=4.7)	CCD SBIG STF402
OA2 Obs.Astr.de Ariel Stechina 2	Newtoniano (D=305mm; f=5.0)	CMOS QHY 174M
OCB Obs.Astr.Cielos de Banfield	Newtoniano (D=150mm; f=5.0)	CMOS QHY5L-II M
ODS Obs.Astr.de Damián Scotta 1	Newtoniano (D=300mm; f=4.0)	CMOS QHY 174M
OD2 Obs.Astr.de Damián Scotta 2	Newtoniano (D=250mm; f=4.0)	CCD Atik 314L+
OMA Obs.Astr.Vuelta por el Universo	Newtoniano (D=150mm; f=5.0)	CMOS Neptune-M
OMR Obs.Astr.Municipal Reconquista	Newtoniano (D=254mm; f=4.0)	CMOS QHY5 Mono
RMG Obs.Astr.de Raúl Melia	Newtoniano (D=254mm; f=4.7)	CMOS QHY 174M GPS

Table II. List of observatories and equipment.

Acknowledgments

We want to thank Julio Castellano as we use his *FotoDif* program for preliminary analyses, Fernando Mazzone for his *Periodos* program used in final analyses, and Matías Martini for his *CalculadorMDE_v0.2* used for generating ephemerides used in the planning stage of the observations. This research has made use of the Small Bodies Data Ferret (*http://sbn.psi.edu/ferret/*), supported by the NASA Planetary System. This research has made use of data and/or services provided by the International Astronomical Union's Minor Planet Center.

References

Alkema, M.S. (2014). "Asteroid Lightcurve Analysis at Elephant Head Observatory: 2013 October - November." *Minor Planet Bulletin* **41**, 186-187.

Behrend, R. (2004web, 2007web, 2008web, 2014web). Observatoire de Geneve website. *http://obswww.unige.ch/~behrend/page_cou.html*

Benishek, V. (2008). "CCD Photometry of Seven Asteroids at the Belgrade Astronomical Observatory." *Minor Planet Bulletin* **35**, 28-30.

Binzel, R.P. (1987). "A photoelectric survey of 130 asteroids." *Icarus* **72**, 135-208.

Chavez, C.F. (2014). "Photometric Observations of Asteroid 570 Kythera using the Virtual Telescope Project." *Minor Planet Bulletin* **41**, 60.

Debehogne, H.; Zappalà, V. (1980). "Photoelectric lightcurves and rotation period of 308 Polyxo, obtained at ESO-La Silla in May 1978." *Astron. Astrophys. Suppl. Series* **39**, 163-165.

Fauerbach, M.; Bennett, T. (2005). "Photometric lightcurve observations of 125 Liberatrix, 218 Bianca, 423 Diotima, 702 Alauda, 1963 Bezovec, and (5849) 1990 HF1." *Minor Planet Bulletin* **32**, 80-81.

Gil-Hutton, R. (2003). "Photometry of fourteen main belt asteroids." *Revista Mexicana de Astronomía y Astrofísica* **39**, 69-76.

Hamanowa, H.; Hamanowa, H. (2009). "Lightcurves of 494 Virtus, 556 Phyllis, 624 Hektor, 657 Gunlod, 111 Reinmuthia, 1188 Gothlandia, and 1376 Michelle." *Minor Planet Bulletin* **36**, 87-88.

Harris, A.W.; Young, J.W.; Scaltriti, F.; Zappala, V. (1984). "Lightcurves and phase relations of the asteroids 82 Alkmene and 444 Gyptis." *Icarus* **57**, 251-258.

Higgins, D. (2011). "Period Determination of Asteroid Targets Observed at Hunters Hill Observatory: May 2009 - September 2010." *Minor Planet Bulletin* **38**, 41-46.

Marciniak, A.; Pilcher, F.; Santana-Ros, T.; Oszkiewicz, D.; Kankiewicz, P. (2014). "Against the bias in physics of asteroids: Photometric survey of long-period and low-amplitude asteroids." *Proceedings of Asteroids, Comets, Meteors* **2014**, 333.

Mazzone, F.D. (2012). Periodos software, version 1.0. *http://www.astrosurf.com/salvador/Programas.html*

Pilcher, F.; Strabla, L.P.; Quadri, U.; Girelli, R. (2014). "Rotation Period Determination for 308 Polyxo." *Minor Planet Bulletin* **41**, 204.

Pilcher, F. (2019). "Rotation Period Determinations for 58 Concordia, 384 Burdigala, 464 Megaira, 488 Kreusa, and 491 Carina." *Minor Planet Bulletin* **46**, 360-363.

Pilcher, F. (2021). "Lightcurves and Rotation Periods of 67 Asia, 74 Galatea, 356 Liguria, 570 Kythera, 581 Tauntonia, 589 Croatia, and 605 Juvisia." *Minor Planet Bulletin* **48**, 132-135.

Polakis, T. (2018). "Lightcurve Analysis for Eleven Main-belt Asteroids." *Minor Planet Bulletin* **45**, 199-203.

Robinson, L. (2011web). Asteroid Lightcurves from Sunflower Observatory 739. *http://btboar.tripod.com/lightcurves/.*

Stephens, R.D. (2005). "Rotational periods of 743 Eugenisis, 995 Sternberga, 1185 Nikko, 2892 Filipenko, 3144 Brosche, and 3220 Murayama." *Minor Planet Bulletin* **32**, 27-28.

Stephens, R.D. (2013). "Asteroids Observed from Santana and CS3 Observatories: 2012 July - September." *Minor Planet Bulletin* **40**, 34-35.

Stephens, R.D. (2014). "Asteroids Observed from CS3: 2014 January - March." *Minor Planet Bulletin* **41**, 171-175.

Warner, B.D. (2006). "Asteroid lightcurve analysis at the Palmer Divide Observatory - late 2005 and early 2006." *Minor Planet Bulletin* **33**, 58-62.

Warner, B.D.; Harris, A.W.; Pravec, P. (2009). "The Asteroid Lightcurve Database." *Icarus* **202**, 134-146. Updated 2022 feb. *http://www.minorplanet.info/lightcurvedatabase.html*

ROTATION PERIOD DETERMINATION FOR ASTEROIDS (19469) 1998 HV45 AND (51442) 2001 FZ25

K. E. Ergashev, O. A. Burkhonov, Sh. A. Ehgamberdiev, S. M. Abduraimov
Ulugh Beg Astronomical Institute of the Uzbekistan Academy of Sciences,
33 Astronomicheskaya str., Tashkent, 100052 UZBEKISTAN
eke@astrin.uz

(Received: 2022 Feb 16)

We present the results of observations of the main-belt asteroids (19469) 1998 HV 45 and (51442) 2001 FZ25. Observations were carried out in 2020 September at the Maidanak Astronomical Observatory. We found a synodic period for (19469) 1998 HV 45 of P = 7.035 ± 0.002 h and for (51442) 2001 FZ25 we found P = 4.334 ± 0.001 h.

All observational data reported here were obtained in 2020 September using a 0.6-meter telescope at the Maidanak Astronomical Observatory (MPC 188) of the Ulugh Beg Astronomical Institute (UBAI), Uzbekistan Academy of Sciences. For the observations we used an FLI IMG1001E CCD camera (1K×1K) with a resolution of 0.67 arcsec/pixel, FOV of 10.7×10.7 arcmin, and Bessel R-filter. The temperature of the camera was set to -30°C. Image acquisition was done with *MaxIm DL* (2022). Calibration images were also obtained for each observational date.

All images were reduced with master bias, dark, and flat frames by using *IRAF* (Image Reduction and Analysis Facility; IRAF, 2022). Calibration frames were created also by using *IRAF*. Photometric measurements processing and analysis were done with *MPO Canopus* (Warner, 2021).

(19469) 1998 HV45. The asteroid (19469) 1998 HV45 was discovered by LINEAR (MPC 704) on 1998 April 20 (MPC, 2022; JPL, 2022). This asteroid orbits the Sun with a semi-major axis of 2.5806 AU, eccentricity 0.163, and orbital period of 4.15 years (MPC, 2022). The diameter and the geometric albedo of the asteroid were determined by the NEOWISE project, and are 7.242 km and 0.233, respectively (Mainzer et al., 2019). The synodic period was previously estimated at P = 8.16 ± 0.72 h (Behrend, 2022web), based on observations by René Roy on one night.

Asteroid (19469) 1998 HV45 was observed on August 25 and on four nights from September 21-27. As a result, 477 CCD images were obtained with an exposure of 90 seconds (Sept 25) and 120 seconds for all other nights.

The period analysis shows a synodic period of P = 7.035 ± 0.002 h with an amplitude A = 0.09 ± 0.02 mag. The perceptible difference between our and Behrend's periods is due to the amount of observation data and probably the shape of the asteroid. However, the amplitude of variability coincides within error scatter.

Number	Name	yyyy mm/dd	Phase	L_{PAB}	B_{PAB}	Period(h)	P.E.	Amp	A.E.	Grp
19469	1998 HV45	2020 09/21-09/27	9.1,10.6	351	13	7.035	0.002	0.09	0.02	MB-I
51442	2001 FZ25	2020 09/10-09/13	13.1,10.9	7	1	4.334	0.001	0.16	0.03	MB-O

Table I. Observing circumstances and results. The phase angle is given for the first and last date. If preceded by an asterisk, the phase angle reached an extrema during the period. L_{PAB} and B_{PAB} are the approximate phase angle bisector longitude/latitude at mid-date range (see Harris et al., 1984). Grp is the asteroid family/group (Warner et al., 2009).

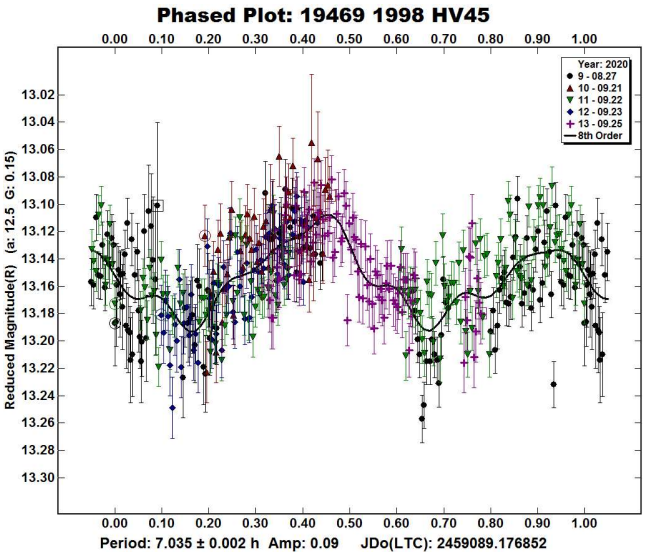

(51442) 2001 FZ25 was discovered by LINEAR (MPC 704) on 2001 March 18 (MPC, 2022; JPL, 2022). It orbits the Sun with a semi-major axis of 2.732 AU, eccentricity 0.346, and an orbital period of 4.51 years (MPC, 2022). The diameter and the geometric albedo of the asteroid were determined by the NEOWISE project, and are 4.533 km and 0.451, respectively (Mainzer et al., 2019). The Light Curve Database (LCDB; Warner et al., 2009) did not contain any references to the synodic period of this asteroid.

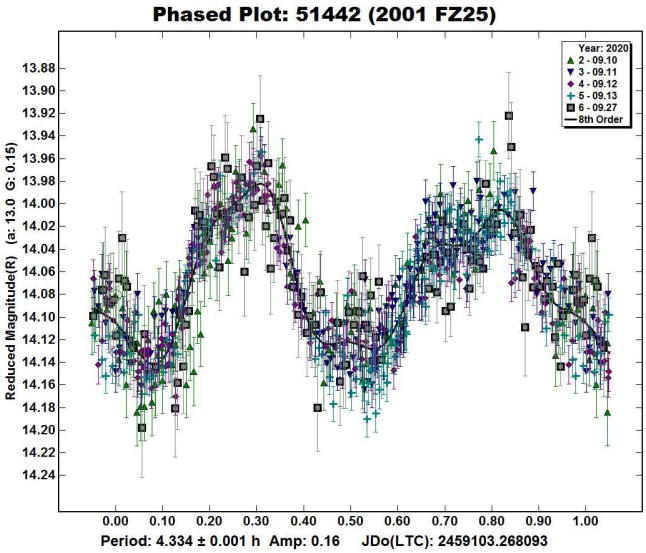

We observed 2001 FZ25 on five nights: Sept 10-13 and 27. A total of 743 CCD images were obtained. Exposures were 90 seconds on Sept 27 and 120 seconds for all other nights.

Analysis of the lightcurves found a synodic period of P = 4.334 ± 0.001 h. The average magnitude was R = 14.05 at phase angle of 13 deg and the amplitude was A = 0.16 ± 0.03 mag.

Acknowledgements

We acknowledge the efforts of Maidanak Astronomical Observatory staff to support our observation.

References

Behrend, R. (2022web). Observatoire de Geneve web site. *https://obswww.unige.ch/~behrend/page_cou.html*

Harris, A.W.; Young, J.W.; Scaltriti, F.; Zappala, V. (1984). "Lightcurves and phase relations of the asteroids 82 Alkmene and 444 Gyptis." *Icarus* **57**, 251-258.

IRAF (2022). IRAF Community Distribution *https://iraf-community.github.io/*

JPL (2022). Small-Body Database Browser. *https://ssd.jpl.nasa.gov/sb/orbits.html*

Mainzer, A.; Bauer, J.; Cutri, R.; Grav, T.; Kramer, E.; Masiero, J.; Sonnett, S.; Wright, E., Eds. (2019). NEOWISE Diameters and Albedos V2.0, NASA Planetary Data System.

Maxim DL (2022). *https://diffractionlimited.com/product/maxim-dl/*

MPC (2022). MPC Database. *http://www.minorplanetcenter.net/db_search/*

Warner, B.D.; Harris, A.W.; Pravec, P. (2009). "The Asteroid Lightcurve Database." *Icarus* **202**, 134-146. Updated 2022 Feb. *http://www.MinorPlanet.info/php/lcdb.php*

Warner, B.D. (2021). MPO Canopus v10.8.5.0. *http://www.minorplanetobserver.com/*

ASTEROID PHOTOMETRY FROM THE PRESTON GOTT OBSERVATORY

Dr. Maurice Clark
Department of Physics and Astronomy
Ball State University
Muncie, IN 47304
Maurice.clark@bsu.edu

(Received: 2022 March 24)

Asteroid period and amplitude results for six objects are reported for data obtained at the Preston Gott Observatory during June 2021.

Preston Gott Observatory of the Texas Tech University is located about 20km north of Lubbock. The main instrument is a 20" f/6.8 Dall-Kirkam Cassegrain with an SBIG STL-1001E CCD. Also available are several 12" Schmidt-Cassegrain telescopes, with SBIG ST9XE CCDs. All images reported here were unfiltered and were reduced with dark frames and twilight sky flats. Image analysis was accomplished using differential aperture photometry with *MPO Canopus*. Period analysis was also done in Canopus. Differential magnitudes were calculated using reference stars from the UCAC4 catalog.

Considerable cloudiness severely interfered with the observations, and reasonable results were only obtained for a couple of asteroids. Some other rather uncertain results are also presented in the hope they could be useful to other observers. These results are summarized in the table below, and the lightcurve plots are presented at the end of the paper. The data and curves are presented without additional comment except were circumstances warrant.

3934 Tove. A period of 9.49408h was published by Pál et al. (2020). The data presented here agree with that result.

5001 EMP. No reliable period could be derived from the data reported and composited here. However, a period of 26.3919h was published by Pál et al. (2020).

5838 Hamsun. A search of the Asteroid Lightcurve Database did not reveal any previously reported period for asteroid 5838 Hamsun. A period of 5.664 ± 0.003 hours is fit to the data.

18801 Noelleoas. A period of 12.7612h was published by Pál et al. (2020). The data reported here support that result although the full lightcurve was not observed.

29905 Kunitaka. A low amplitude lightcurve was exhibited and the 12.44 ± 0.02 hour period presented here is the best that could be derived from the data obtained. However, it is extremely uncertain and probably not correct. A search of the Asteroid Lightcurve Database did not reveal any previously reported period for asteroid 29905 Kunitaka.

(47786) 2000 EQ20. A simple bimodal lightcurve could not be fit to the low amplitude lighrcurve data obtained. The result 3.76 ± 0.09 hour period presented here is the best that could be derived and is extremely uncertain. A search of the Asteroid Lightcurve Database did not reveal any previously reported period for asteroid (47786) 2000 EQ20.

Acknowledgments

I would like to thank Dr Vallia Antoniou for allowing the use of the Preston Gott Observatory for this work, and Brian Warner for all of his work with the program *MPO Canopus* and for his efforts in maintaining the "CALL" website.

References

Harris, A.W.; Young, J.W.; Scaltriti, F.; Zappala, V. (1984). "Lightcurves and phase relations of the asteroids 82 Alkmene and 444 Gyptis." *Icarus* **57**, 251-258.

Pál, A.; Szakáts, R.; Kiss, C.; Bódi, A.; Bognár, Z.; Kalup, C.; Kiss, L.L.; Marton, G.; Molnár, L.; Plachy, E.; Sárneczky, K.; Szabó, G.M.; Szabó, R. (2020). "Solar System Objects Observed with TESS - First Data Release: Bright Main-belt and Trojan Asteroids from the Southern Survey." *Ap. J.* **247**, A26.

Warner, B.D.; Harris, A.W.; Pravec, P. (2009). "The Asteroid Lightcurve Database." *Icarus* **202**, 134-146. Updated 2022 Jan. *http://www.minorplanet.info/lightcurvedatabase.html*

Number	Name	2021 mm/dd	Phase	L_{PAB}	B_{PAB}	Period(h)	P.E.	Amp	A.E.	Grp
3934	Tove	06/06-06/16	12.0	248.1	18.3	9.495	0.001	0.29	0.02	MBA
5001	EMP	06/10-06/15	12.3	239.1	17.2	-----	-----	0.08	0.02	MBA
5838	Hamsun	06/10-06/14	12.6	246.7	18.1	5.664	0.003	0.28	0.03	MBA
18801	Noelleoas	06/06-06/15	8.3	247.8	8.1	12.730	0.003	0.73	0.05	MBA
29905	Kunitaka	06/04-06/14	10.5	250.4	17.6	12.44?	0.04	0.09	0.05	MBA
47786	2000 EQ20	06/15	8.3	246.7	8.2	3.76?	0.09	0.14	0.05	MBA

Table I. Observing circumstances and results. The phase angle is given for the first and last date. L_{PAB} and B_{PAB} are the approximate phase angle bisector longitude and latitude at mid-date range (see Harris et al., 1984). Grp is the asteroid family/group (Warner et al., 2009).

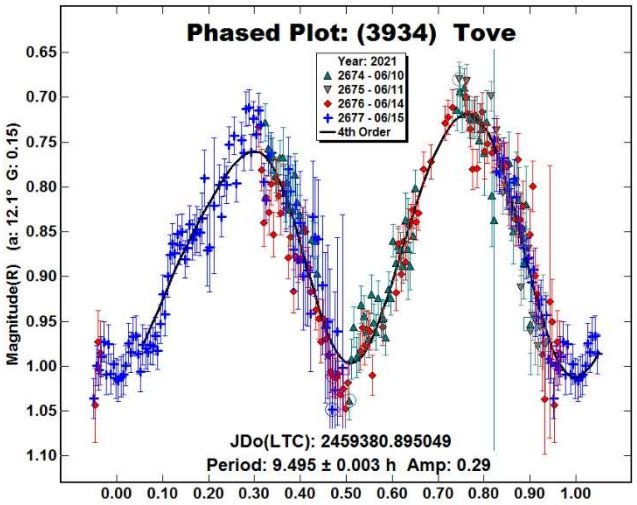

Figure 1: Lightcurve for 3934 Tove.

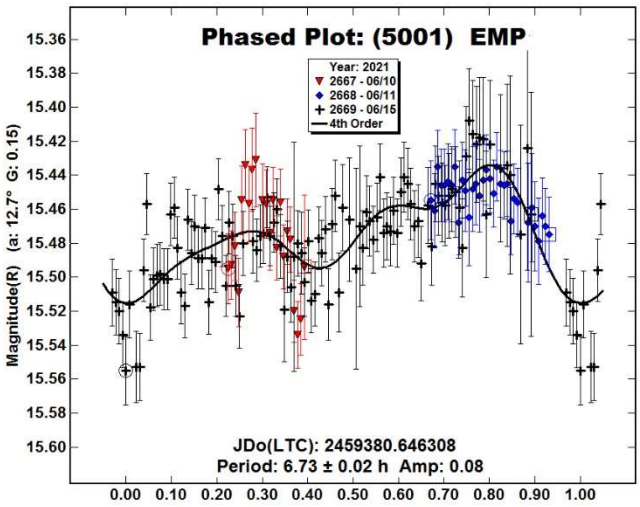

Figure 2: Lightcurve for 5001 EMP.

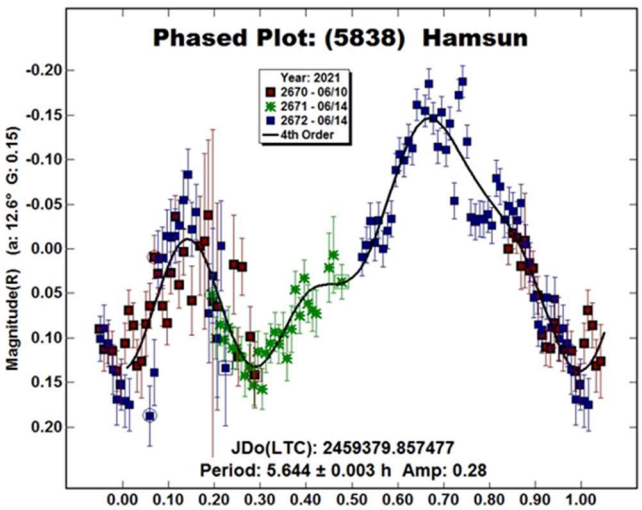

Figure 3: Lightcurve for 5838 Hamsun.

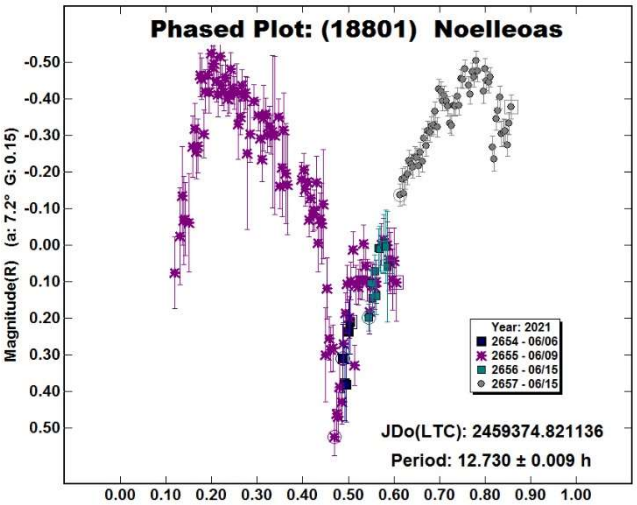

Figure 4: Lightcurve for 18801 Noelleoas.

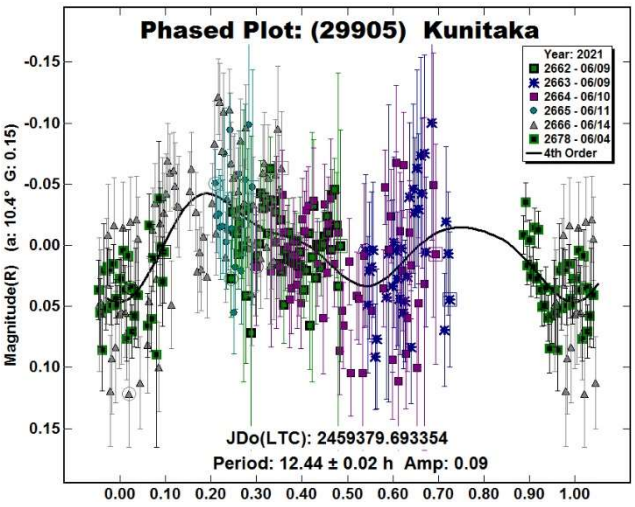

Figure 5: Lightcurve for 29905 Kunitaka.

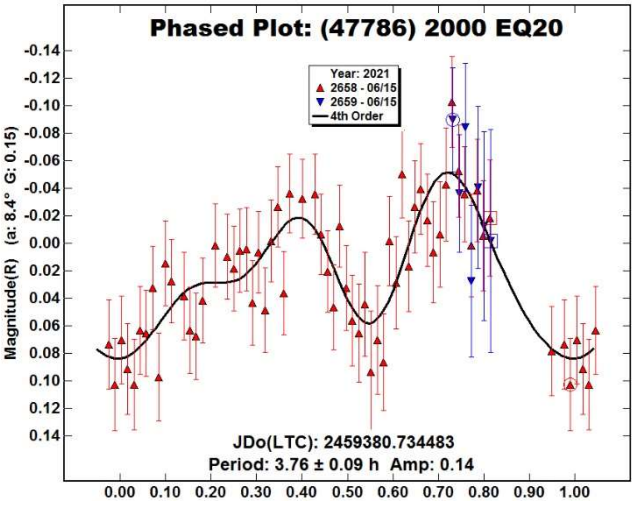

Figure 6: Lightcurve for (47786) 2000 EQ20.

NINE MAIN BELT ASTEROIDS, ONE NEAR EARTH, AND TWO POTENTIALLY HAZARDOUS ASTEROID LIGHTCURVES

Gonzalo Fornas
AVA - CAAT
Centro Astronómico del Alto Turia, SPAIN
gfornas@novaing.com

Alvaro Fornas, Vicente Mas
AVA - CAAT
Centro Astronómico del Alto Turia, SPAIN

(Received: 2022 March 26)

We report on the photometric analysis result of nine main-belt (MBA), one near-Earth (NEA), and two Potentially Hazardous (PHA) asteroids by the Asociación Valenciana de Astronomía (AVA). The work was done from the Astronomical Center Alto Turia (CAAT; MPC J57), located in Aras de los Olmos, Valencia, and operated by members of AVA (*http://www.astroava.org*). This database shows graphic results of the data, mainly lightcurves, with the plot phased to a given period.

We have managed to obtain a number of accurate and complete lightcurves as well as some additional incomplete lightcurves to help analysis at future oppositions.

Observatory	Telescope	CCD
C.A.A.T.	43 cm D-K	SBIG STXL-11002
	106 mm Refractor	ZWO ASI 1600

Table I. List of instruments used for the observations. DK is Dall-Kirkham.

We concentrated on asteroids with no reported period and those where the reported period was poorly established and needed confirmation. All the targets were selected from the Collaborative Asteroid Lightcurve (CALL) website at (*http://www.minorplanet.info/call.html)* and Minor Planet Center (*http://www.minorplanet.net*).

Images were measured using *MPO Canopus* (Bdw Publishing) with a differential photometry technique. The comparison stars were restricted to near solar-color to reduce color dependencies, especially at larger air masses. The lightcurves give the synodic rotation period. The amplitude (peak-to-peak) that is shown is that for the Fourier model curve and not necessarily the true amplitude.

(1537) Transylvania. This outer main-belt asteroid was discovered on 1940 Aug 27 by G. Strommer from the Konkoly Obs, Hung. We made observations on 2022 Feb 3-6. In the ALCDEF database (*https://alcdef.org*), we found data from Polakis (2021). We joined those data to ours to improve the quality of the result. From the data we derive a rotation period of 36.08 ± 0.01h and an amplitude of 0.29 mag. This period doesn't match with the 144.2 h from Polakis (2021) and 141.8 h from Ďurech et al. (2019). We recommend new observing sessions to help find the actual period.

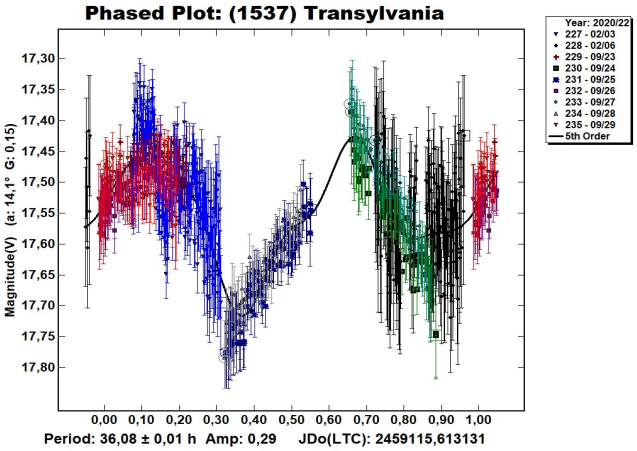

(2197) Shangai. This Themis group asteroid was discovered on 1965 Dec 30 from the Purple Mountain Observatory. We made observations on 2021 Jan 21-22. From our data we derive a rotation period of 5.95 ± 0.005 h and an amplitude of 0.18 mag. Behrend (2011web) found a period of 5.99 h, which is consistent with our observations. Waszczak et al. (2015) found 5.938 h and Ďurech et al. (2020) found 5.94 h.

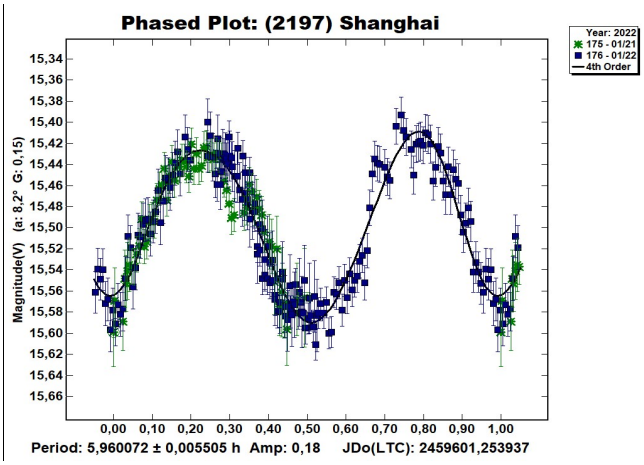

(3822) Segovia. This inner main-belt asteroid was discovered on 1988 Feb 21 by T. Seki at Geisei Observatory in Japan. We made observations on 2022 Feb 20 - March 2.

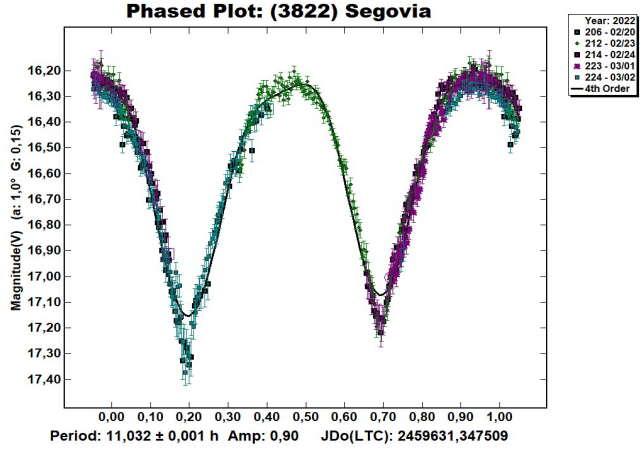

From our data we derive a rotation period of 11.032 ± 0.001 h and an amplitude of 0.90 mag. We assume the lightcurve is bimodal, even with a very symmetrical drawing. Ďurech et al. (2016) found a similar period of 11.03 h.

(4512) Sinuhe. This middle main-belt asteroid was discovered on 1939 Jan 20 by Y. Väisälä at Turku observatory in Finland. We made observations on 2022 Feb 20 - March 2. From our data we derive a rotation period of 21.999 ± 0.001 h and an amplitude of 0.76 mag. We assume it is bimodal, even with a very symmetrical drawing. Behrend (2016web) found a period of 21.5 h and Bennefeld et al. (2009) found 18 h.

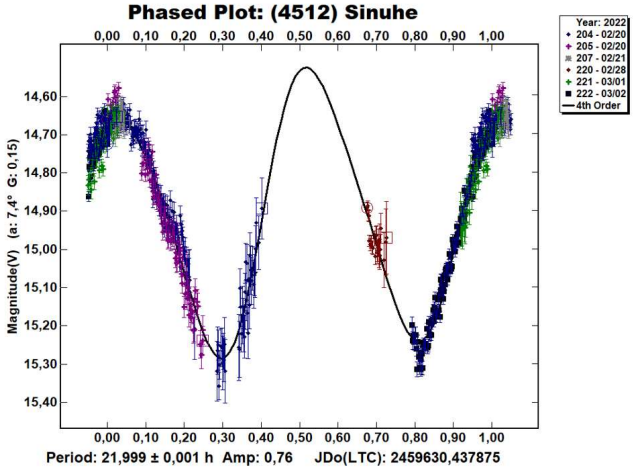

(4588) Wislicenus. This outer main-belt asteroid was discovered in 1931 March 13 by M.F. Wolf at the Heidelberg Observatory, Germany. We made observations on 2022 Feb 20-24. From our data we derive a rotation period of 4.7005 ± 0.0003 h and an amplitude of 0.24 mag. Yeh et al. (2020) found a period of 4.70 h that is rated U = 2 in the LCDB and matches with our results.

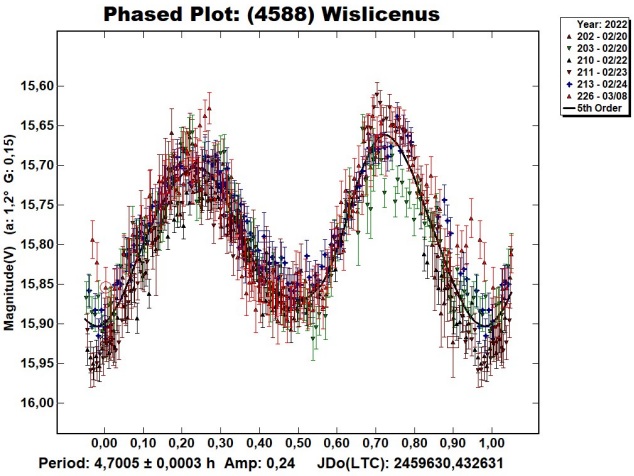

(4706) Dennisreuter. This inner main-belt asteroid was discovered on 1988 Feb 16 by R. Rajamohan at Kavalur Observatory, India. We made observations on 2022 Jan 18-20. From our data we derive a rotation period of 3.69 ± 0.006 h and an amplitude of 0.03 mag. Such a small amplitude pushed the limit the equipment sensitivity. Waszczak et al. (2015) found a period of 2.56 h with incomplete data (U = 1).

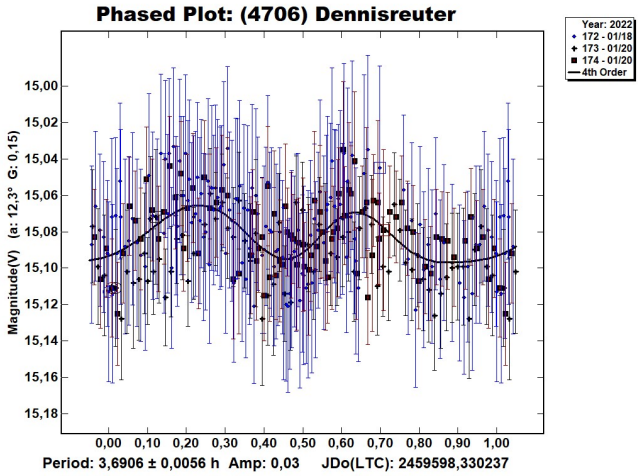

(5506) Artiglio. This member of the Erigone group was discovered on 1987 Sep 24 by H. Debehogne at La Silla, Chile. We made observations on 2022 Feb 24 - March 8. From our data we derive a rotation period of 9.7065 ± 0.0004 h and an amplitude of 1.14 mag. Waszczak et al. (2015) found a period of 9.406 h, Ďurech et al. (2020) found 9.41309 h, and Pál et al. (2020) found 9.409 h. The period we found is not the same, but our data seem to be good.

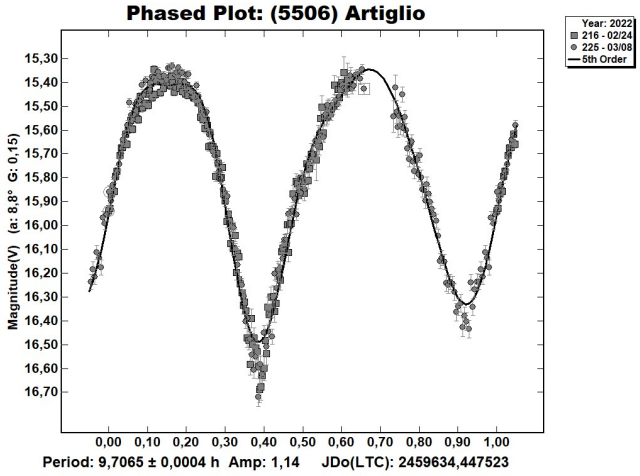

(12685) 1985 VE. This Flora group member was discovered on 1985 Nov 14 by P. Jensen at Brorfelde Observatory, Denmark. We made observations on 2022 Feb 03-06. From our data we derive a rotation period of 8.807 ± 0.01 h and an amplitude of 0.12 mag. The LCDB did not list any previous period results.

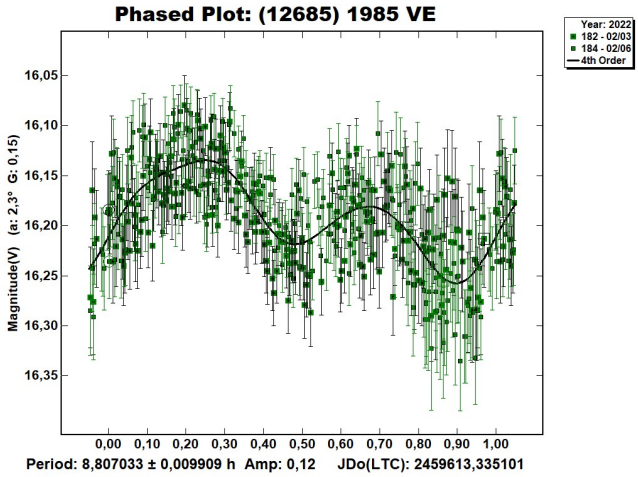

(89958) 2002 LY45. This is a PHA, discovered on 2002 Jun 14 by the project LINEAR at Socorro. We made observations in 2021 June. From our data we derive a rotation period of 3.265 ± 0.001 h and an amplitude of 0.38 mag. The LCDB did not list any previous period results.

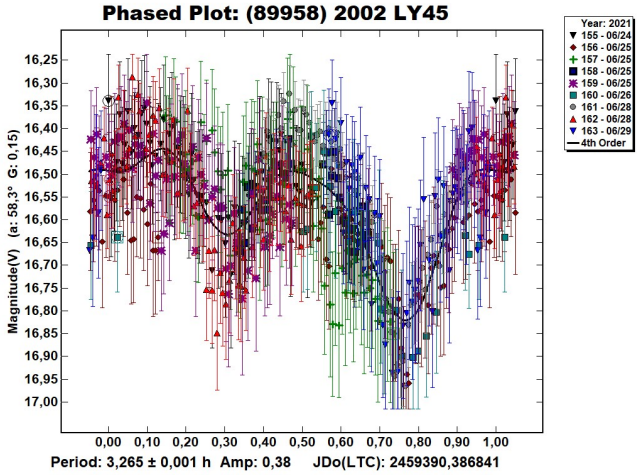

(115916) 2003 WB8. This outer main-belt asteroid, classified as "Unusual" by the Minor Planet Center, was discovered on 2003 Nov 18 by the LINEAR project at Socorro We made observations from 2022 Feb 8-10. In the ALCDEF database we found data from S.C. Percy covering 2022 Jan 18 through 2022 Feb 10. We joined those data to ours to improve the quality of the result. Data analysis found a rotation period of 40.609 ± 0.028 h and an amplitude of 0.15 mag. There are no more previous data on the rotation period of this asteroid.

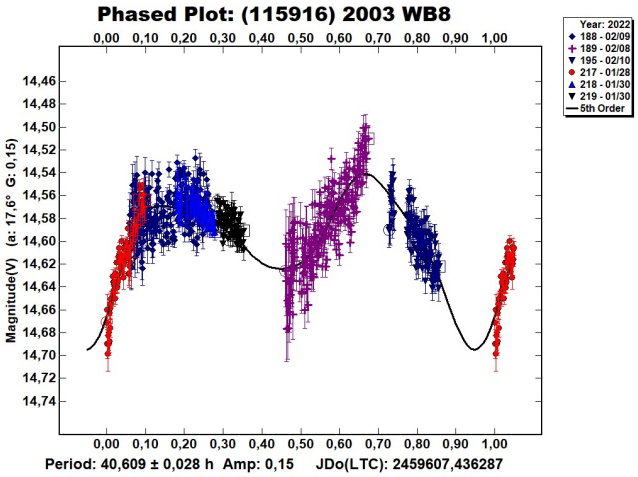

(138971) 2001 CB21. This is a PHA in the Apollo group that was discovered on 2001 Feb 2 Jan 24 by project LINEAR at Socorro.

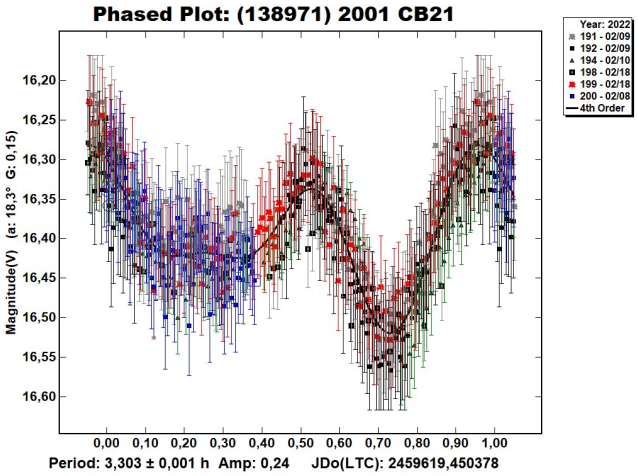

We made observations in 2021 Feb 8-18. From our data, we derive a rotation period of 3.303 ± 0.001 h and an amplitude of 0.24 mag. Galad et al. (2005) found a period of 3.302 h.

(318160) 2004 QZ2. This near-Earth asteroid is in the Amor group. It was discovered on 2004 Aug 20 by the Catalina Sky Survey. We made observations from 2022 Jan 16-28. Data analysis found a rotation period of 7.43 ± 0.01 h and an amplitude of 0.14 mag. The LCDB didn't list any previous period results for this asteroid.

Number	Name	yyyy/mm/dd	Phase	L_{PAB}	B_{PAB}	Period (h)	P.E.	Amp	A.E.	Grp
1537	Transylvania	2022/02/03-02/06	1.8,2.4	132	-5	36.08	0.01	0.29	0.05	MB-O
	(from Polakis)	2020/09/24-09/29	3.7,5.9	357	4					
2197	Shanghai	2022/01/21-22	8.5,9.0	101	2	5.96	0.005	0.18	0.05	MB-O
3822	Segovia	2022/02/20-03/01	0.5,5.03	153	0	11.032	0.001	0.90	0.05	MB-I
4512	Sinuhe	2022/02/20-03/02	7.4,12.04	139	6	21.999	0.001	0.76	0.05	MB-M
4588	Wislicenus	2022/02/20-24	0.74,1.03	153	0	4.7005	0.0003	0.24	0.05	MB-O
4706	Dennisreuter	2022/01/18-20	12.7,13.6	104	-12	3.69	0.006	0.03	0.01	MB-I
5506	Artiglio	2022/02/24-03/03	9.4,15.9	143	5	9.7065	0.0004	1.14	0.05	MB-I
12685	1985 VE	2022/02/3-6	2.46,3.99	132	-4	8.807	0.01	0.12	0.02	MB-I
89958	2002 LY45	2021/06/24-29	58.3,81.9	258	42	3.265	0.001	0.38	0.02	PHA
115916	2003 WB8	2022/02/8-10	17.6,17.7	152	14	40.609	0.028	0.15	0.03	MB-O
	(from Percy)	2022/01/18-02/10	26.5,17.1	149	10					
138971	2001 CB21	2022/02/9-18	39.2,42.7	161	159	3.303	0.001	0.24	0.03	PHA
318160	2004 QZ2	2022/01/16-28	7.3,5.6	132	-2	7.43	0.01	0.14	0.02	NEA

Table II. Observing circumstances and results. Pts is the number of data points. The phase angle values are for the first and last date. L_{PAB} and B_{PAB} are the approximate phase angle bisector longitude and latitude at mid-date range (see Harris et al., 1984). Grp is the asteroid family/group (Warner et al., 2009). ERI: Erigone; EUN: Eunomia; MB-I/O: Main-belt inner/outer; MC: Mars-crosser; NEA: near-Earth; THM: Themis; TRJ: Jupiter Trojan.

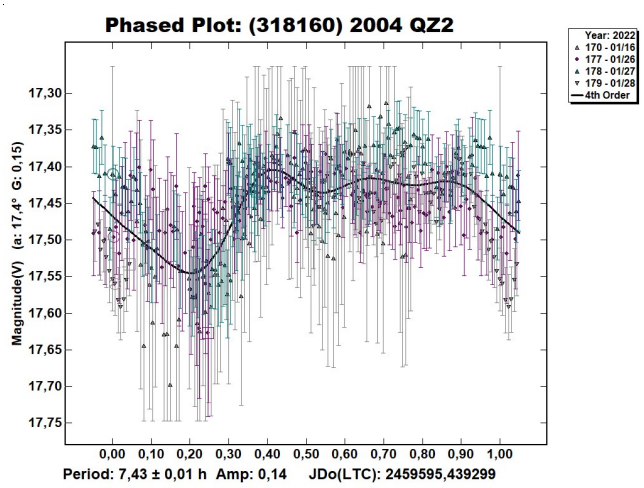

Acknowledgements

We would like to express our gratitude to Brian Warner for supporting the CALL web site and his suggestions made to OBAS group.

References

Behrend, R. (2011web, 2016web) Observatoire de Geneve web site. *http://obswww.unige.ch/~behrend/page_cou.html*

Bennefeld, C.; Cantue, J.; Holly, V.; Jordon, L.; Martin, T.; Soar, E.; Swinney, T. (2009). "Asteroid Lightcurve Analysis at Ricky Observatory." *Minor Planet Bull*. **36**, 45-48.

Ďurech, J.; Hanus, J.; Oszkiewsicz, D.; Vančo, R. (2016). "Asteroid models from the Lowell photometric database." *Astron. Astrophys.* **587**, A48.

Ďurech, J.; Hanuš, J.; Vančo, R. (2019). "Inversion of asteroid photometry from Gaia DR2 and the Lowell Observatory photometric database." *Astron. Astrophys.* **631**, A2.

Ďurech, J.; Tonry, J.; Erasmus, N.; Denneau, L.; Heinze, A.N.; Flewelling, H. (2020). "Asteroid models reconstructed from ATLAS photometry." *Astron. Astrophys.* **643**, A59.

Galad, A.; Pravec, P.; Kusnirak, P.; Gajdos, S.; Kornos, L.; Vilagi, J. (2005). "Joint Lightcurve Observations of 10 Near-Earth Asteroids from Modra and ONDREJOV." *Earth, Moon, and Planets* **97**, 147-163.

Harris, A.W.; Young, J.W.; Scaltriti, F.; Zappala, V. (1984). "Lightcurves and phase relations of the asteroids 82 Alkmene and 444 Gyptis." *Icarus* **57**, 251-258.

Pál, A.; Szakáts, R.; Kiss, C.; Bódi, A.; Bognár, Z.; Kalup, C.; Kiss, L.; Marton, G.; Molnár, L.; Plachy, E.; Sárneczky, K.; Szabó, G.M.; Szabó, R. (2020). "Solar System Objects Observed with TESS – First Data Release: Bright Main-belt and Trojan Asteroids from the Southern Survey." *Ap. J. Suppl Ser*. **247**, id. 26.

Polakis, T. (2021). "Photometric Observations of Seven Minor Planets." *Minor Planet Bull*. **48**, 23-25.

Warner, B.D.; Harris, A.W.; Pravec, P. (2009). "The Asteroid Lightcurve Database." *Icarus* **202**, 134-146. Updated 2022 March. *http://www.minorplanet.info/lightcurvedatabase.html*

Waszczak, A.; Chang, C.-K.; Ofek, E.O.; Laher, R.; Masci, F.; Levitan, D.; Surace, J.; Cheng, Y.-C.; Ip, W.-H.; Kinoshita, D.; Helou, G.; Prince, T.A.; Kulkarni, S. (2015). "Asteroid Light Curves from the Palomar Transient Factory Survey: Rotation Periods and Phase Functions from Sparse Photometry." *Astron. J.* **150**, A75.

Yeh, T.-S.; Li, B.; Chang, C.-K.; Zhao, H.-B.; Ji, J.-H.; Lin, Z.-Y.; Ip, W.-H. (2020). "The Asteroid Rotation Period Survey Using the China Near-Earth Object Survey Telescope (CNEOST)." *Astron. J.* **160**, id. 73.

COLLABORATIVE ASTEROID PHOTOMETRY FROM UAI: 2022 JANUARY-MARCH

Lorenzo Franco
Balzaretto Observatory (A81), Rome, ITALY
lor_franco@libero.it

Alessandro Marchini, Riccardo Papini
Astronomical Observatory, DSFTA - University of Siena (K54)
Via Roma 56, 53100 - Siena, ITALY

Marco Iozzi
HOB Astronomical Observatory (L63), Capraia Fiorentina, ITALY

Giulio Scarfi
Iota Scorpii Observatory (K78), La Spezia, ITALY

Fabio Mortari, Davide Gabellini
Hypatia Observatory (L62), Rimini, ITALY

Paolo Bacci, Martina Maestripieri
GAMP - San Marcello Pistoiese (104), Pistoia, ITALY

Giorgio Baj
M57 Observatory (K38), Saltrio, ITALY

Gianni Galli
GiaGa Observatory (203), Pogliano Milanese, ITALY

Alessandro Coffano, Wladimiro Marinello, Giampaolo Pizzetti
Osservatorio Serafino Zani (130), Lumezzane (BS), ITALY

Pietro Aceti, Massimo Banfi
Seveso Observatory (C24), Seveso, ITALY

Luciano Tinelli
GAV (Gruppo Astrofili Villasanta), Villasanta, ITALY

Nico Montigiani, Massimiliano Mannucci
Osservatorio Astronomico Margherita Hack (A57)
Florence, ITALY

Alfonso Noschese, Maurizio Mollica, Ernesto Guido
Osservatorio Salvatore Di Giacomo (L07)
Agerola (NA), ITALY

Nello Ruocco
Osservatorio Astronomico Nastro Verde (C82), Sorrento, ITALY

Mauro Bachini, Giacomo Succi
BSCR Observatory (K47), Santa Maria a Monte (PI), ITALY

(Received: 2022 Apr 14)

Photometric observations of eleven asteroids were made to acquire lightcurves for shape/spin axis modeling. The synodic period and lightcurve amplitude were found for 49 Pales, 142 Polana, 206 Hersilia, 737 Arequipa, 1071 Brita, 1120 Cannonia, 1166 Sakuntala, 1736 Floirac, 3103 Eger, 4528 Berg and (7482) 1994 PC1. We also found color indices for 49 Pales, 142 Polana, 206 Hersilia, 1071 Brita, 1120 Cannonia, 3103 Eger and 4528 Berg; along with H-G parameters for 49 Pales, 1071 Brita, and 4528 Berg.

Collaborative asteroid photometry was done inside the Italian Amateur Astronomers Union (UAI; 2022) group. The targets were selected mainly in order to acquire lightcurves for shape/spin axis modeling. Table I shows the observing circumstances and results.

The CCD observations of eleven asteroids were made in 2022 January-March using the instrumentation described in the Table II. Lightcurve analysis was performed at the Balzaretto Observatory with *MPO Canopus* (Warner, 2021). All the images were calibrated with dark and flat frames and converted to R magnitudes using solar colored field stars from CMC15 catalogue, distributed with *MPO Canopus*.

For H-G plots, the R magnitudes were converted to V band adding the color index (V-R) and evaluating the half peak to peak magnitude using a Fourier model of the same order of the lightcurve plot (Buchheim, 2010).

For brevity, the following citations to the asteroid lightcurve database (LCDB; Warner et al., 2009) will be summarized only as "LCDB."

49 Pales is a Ch-type (Bus and Binzel, 2002) outer main-belt asteroid. Collaborative observations were made over sixteen nights. Period analysis shows a synodic period of P = 20.704 ± 0.004 h with an amplitude A = 0.15 ± 0.03 mag. The period is close to the previously published results in the LCDB. Multiband photometry was made by P. Aceti on 2022 Jan 30 deriving a color index (V-R) = 0.36 ± 0.03. The wide phase angles covered by the observations allowed us to determine the H-G parameters. We found H = 7.73 ± 0.03 and G = 0. 17 ± 0.04. Both the color index (V-R) and G value are consistent with a low albedo asteroid (Shevchenko and Lupishko, 1998).

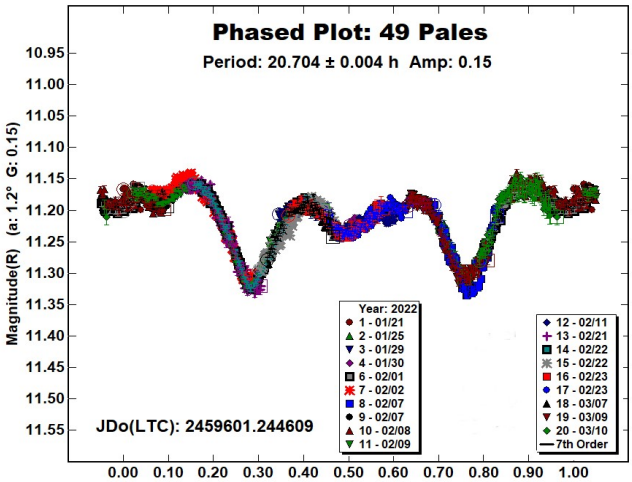

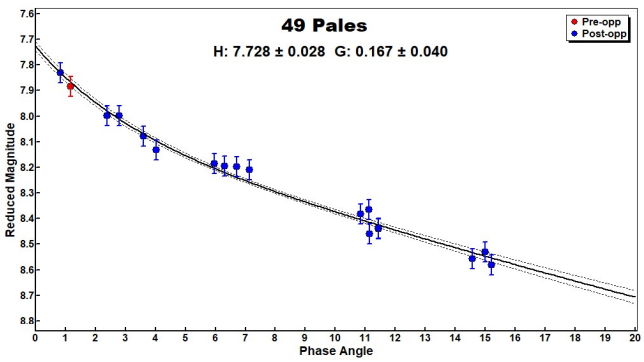

142 Polana is a B-type (Bus and Binzel, 2002) inner main-belt asteroid. Collaborative observations were made over eight nights. The period analysis shows a synodic period of $P = 9.765 \pm 0.002$ h with an amplitude $A = 0.16 \pm 0.02$ mag. The period is close to the previously published results in the LCDB. Multiband photometry was made by P. Bacci and M. Maestripieri on 2022 Mar 14. We found color indices (B-V) = 0.63 ± 0.03; (V-R) = 0.38 ± 0.03, consistent with a low albedo asteroid (Shevchenko and Lupishko, 1998).

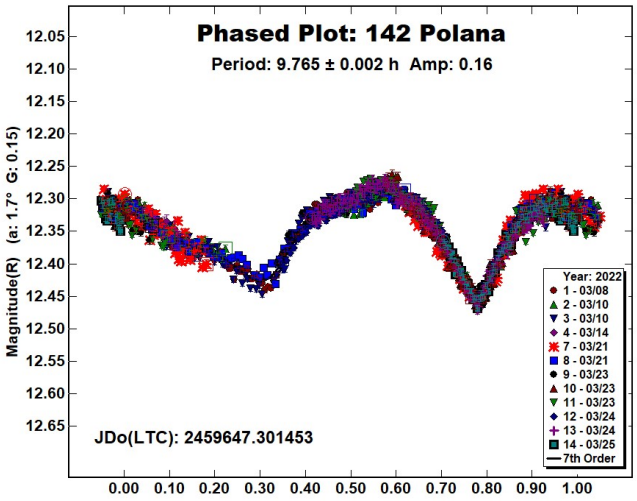

206 Hersilia is a C-type (Bus and Binzel, 2002) middle main-belt asteroid. Collaborative observations were made over ten nights. The period analysis shows a synodic period of $P = 11.112 \pm 0.002$ h with an amplitude $A = 0.16 \pm 0.04$ mag. The period is close to the previously published results in the LCDB. Multiband photometry was made by P. Aceti and M. Banfi on 2022 Feb 27 and by P. Bacci and M. Maestripieri on 2022 Mar 10. We found a color index (V-R) = 0.41 ± 0.03 (average of two independent values), consistent with a low albedo asteroid (Shevchenko and Lupishko, 1998).

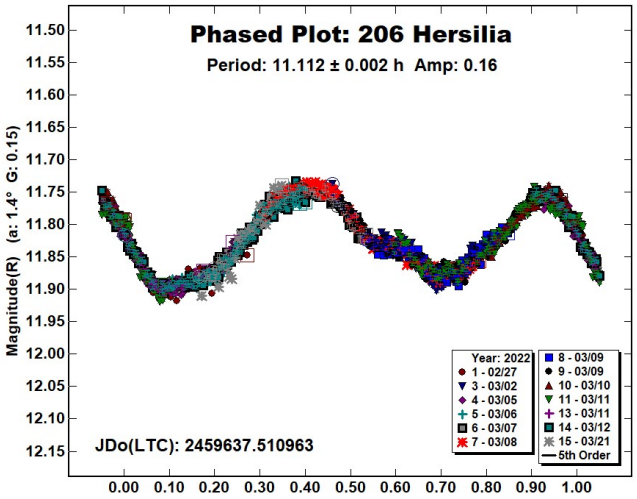

737 Arequipa is an S-type (Bus and Binzel, 2002) middle main-belt asteroid. Collaborative observations were made over seven nights. We found a synodic period of $P = 7.021 \pm 0.001$ h with an amplitude $A = 0.07 \pm 0.03$ mag. The period is close to the previously published results in the LCDB.

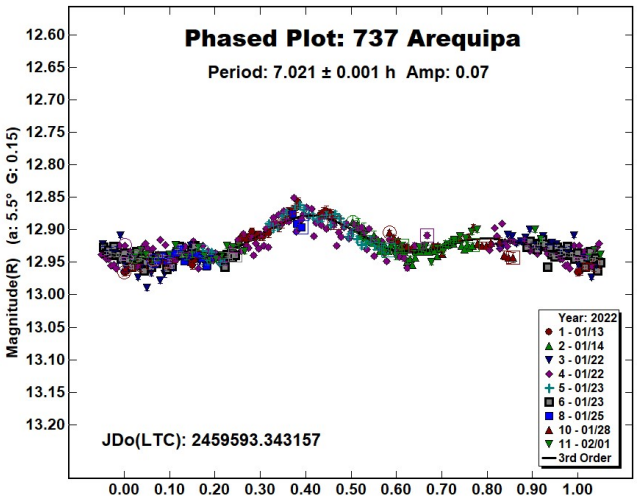

1071 Brita is an Xk-type (Bus and Binzel, 2002) middle main-belt asteroid. Collaborative observations were made over eight nights. We found a synodic period of $P = 5.8166 \pm 0.0002$ h with an amplitude $A = 0.15 \pm 0.03$ mag. The period is close to the previously published results in the LCDB. Multiband photometry was made by P. Aceti on 2022 Jan 31 and by P. Bacci and M. Maestripieri on 2022 Mar 21. We found color indices (B-V) = 0.70 ± 0.04; (V-R) = 0.43 ± 0.04 (average of two independent values). The wide phase angles covered by the observations allowed us to determine the H-G parameters. We found $H = 10.67 \pm 0.04$ and $G = 0.09 \pm 0.05$. Both the color index (V-R) and G value are consistent with a low-medium albedo asteroid (Shevchenko and Lupishko, 1998).

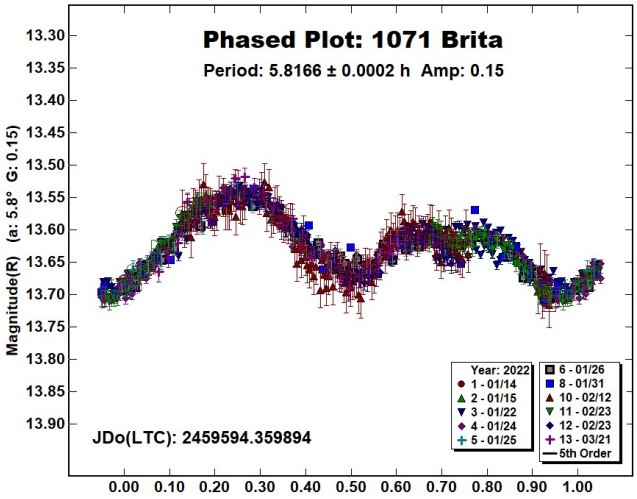

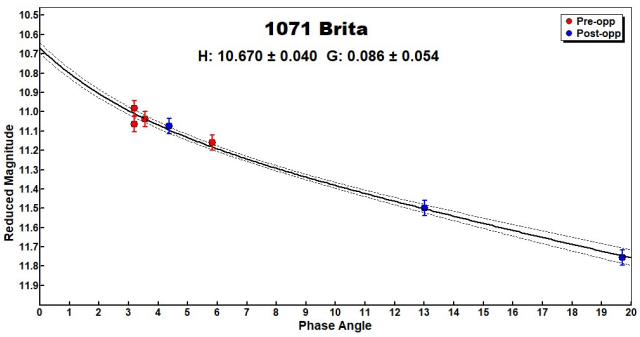

Number	Name	2022 mm/dd	Phase	L_{PAB}	B_{PAB}	Period(h)	P.E.	Amp	A.E.	Grp
49	Pales	01/21-03/10	*1.1,15.2	124	-2	20.704	0.004	0.15	0.03	MB-O
142	Polana	03/08-03/25	*1.6,8.9	169	-3	9.765	0.002	0.16	0.02	MB-I
206	Hersilia	02/27-03/21	*1.1,8.6	161	2	11.112	0.002	0.16	0.04	MB-M
737	Arequipa	01/13-02/01	5.4,9.3	110	-14	7.021	0.001	0.07	0.03	MB-M
1071	Brita	01/14-03/21	*5.8,19.7	126	7	5.8166	0.0002	0.15	0.03	MB-M
1120	Cannonia	01/20-03/09	*5.6,17.6	131	-2	3.8100	0.0001	0.13	0.04	MB-I
1166	Sakuntala	01/29-02/27	*5.3,9.8	137	13	6.291	0.001	0.09	0.02	MB-M
1736	Floirac	03/01-03/21	*2.6,7.9	166	1	6.772	0.001	0.09	0.04	MB-I
3103	Eger	02/07-03/07	*14.4,20.2	149	14	5.7100	0.0005	0.63	0.05	NEA
4528	Berg	02/05-04/04	*14.4,14.2	166	1	3.563	0.001	0.24	0.05	MB-M
7482	1994 PC1	01/20-01/23	105.9,107.2	88	47	2.599	0.001	0.32	0.06	NEA

Table I. Observing circumstances and results. The first line gives the results for the primary of a binary system. The second line gives the orbital period of the satellite and the maximum attenuation. The phase angle is given for the first and last date. If preceded by an asterisk, the phase angle reached an extrema during the period. L_{PAB} and B_{PAB} are the approximate phase angle bisector longitude/latitude at mid-date range (see Harris et al., 1984). Grp is the asteroid family/group (Warner et al., 2009).

1120 Cannonia is an inner main-belt asteroid. Collaborative observations were made over six nights. We found a synodic period of P = 3.8100 ± 0.0001 h with an amplitude A = 0.13 ± 0.04 mag. The period is close to the previously published results in the LCDB. Multiband photometry was made by P. Bacci and M. Maestripieri on 2022 Mar 09. We found color indices (B-V) = 0.88 ± 0.04 and (V-R) = 0.50 ± 0.01, which are consistent with an S-type medium albedo asteroid (Shevchenko and Lupishko, 1998).

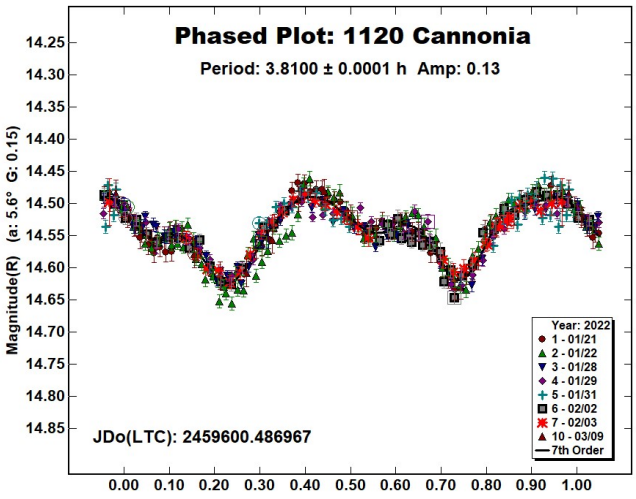

1166 Sakuntala is a medium albedo middle main-belt asteroid. Collaborative observations were made over four nights. We found a synodic period of P = 6.291 ± 0.001 h with an amplitude A = 0.09 ± 0.02 mag. The period is close to the previously published results in the LCDB.

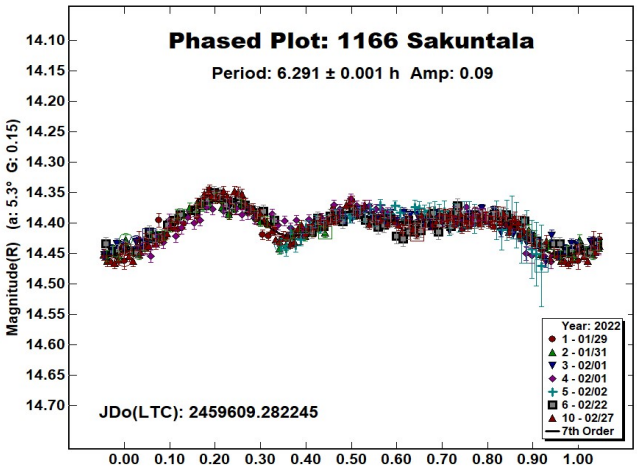

1736 Floirac is a medium albedo inner main-belt asteroid. Collaborative observations were made over four nights. We found a synodic period of P = 6.772 ± 0.001 h with an amplitude A = 0.09 ± 0.04 mag. The period is close to that published by Pravec et al. (2007web).

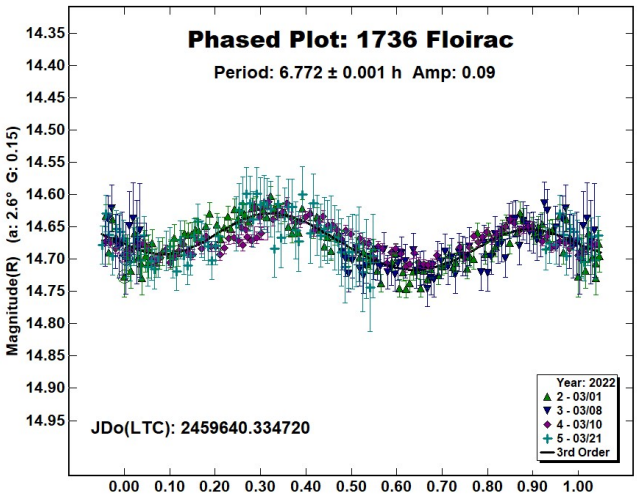

Observatory (MPC code)	Telescope	CCD	Filter	Observed Asteroids (#Sessions)
Astronomical Observatory of the University of Siena(K54)	0.30-m MCT f/5.6	SBIG STL-6303e(bin 2x2)	C,Rc	142(5), 737(1), 1071(2), 1120(2), 1166(2), 3103(3), 4528(2), 7482(4)
HOB Astronomical Observatory (L63)	0.20-m SCT f/6.8	ATIK 383L+	C	49(7), 142(1), 206(5), 737(4)
Iota Scorpii(K78)	0.40-m RCT f/8.0	SBIG STXL-6303e (bin 2x2)	Rc	142(1), 1071(1), 1120(1), 1166(3), 1736(4), 4528(3), 7482(1)
Hypatia Observatory (L62)	0.25-m RCT f/5.3	MORAVIAN G2-8300	C,Rc	49(5), 142(2), 206(3)
GAMP (104)	0.60-m NRT f/4.0	Apogee Alta	C,B, V,Rc	142(1), 206(1), 1071(1), 1120(3), 3103(1), 4528(1)
M57 (K38)	0.35-m RCT f/5.5	SBIG STT1603ME	C,Rc	49(3), 206(2), 1166(1), 4528(1)
GiaGa Observatory (203)	0.36-m SCT f/5.8	Moravian G2-3200	C,Rc	737(1), 1071(2), 7482(2)
Osservatorio Serafino Zani (130)	0.40-m RCT f/8.0	SBIG ST8 XME (bin 2x2)	C	142(2), 1071(1), 4528(2)
Seveso Observatory (C24)	0.30-m SCT f/10	QSI	V,Rc	49(1), 206(1), 1071(1), 4528(1)
GAV	0.20-m SCT f/7.0	SXV-H9	Rc	49(3), 206(1)
Osservatorio Astronomico Margherita Hack (A57)	0.35-m SCT f/8.3	SBIG ST10XME (bin 2x2)	Rc	1736(1), 4528(1)
Osservatorio Salvatore Di Giacomo (L07)	0.50-m RCT f/8.0	FLI Proline	Rc	737(2)
Osservatorio Astronomico Nastro Verde (C82)	0.35-m SCT f/6.3	SBIG ST10XME (bin 2x2)	C	4528(1)
BSCR Observatory (K47)	0.41-m NRT f/3.2	DTA Discovery plus 1600	C	4528(1)
Balzaretto Observatory (A81)	0.20-m SCT f/5.0	SBIG ST7XME	Rc	1071(1)

Table II. Observing Instrumentations. MCT: Maksutov-Cassegrain, NRT: Newtonian Reflector, RCT: Ritchey-Chretien, SCT: Schmidt-Cassegrain.

3103 Eger is an Xe-type (Bus and Binzel, 2002) Apollo Near-Earth asteroid. Collaborative observations were made over four nights. We found a synodic period of P = 5.7100 ± 0.0005 h with an amplitude A = 0.63 ± 0.05 mag. The period is close to the previously published results in the LCDB. Multiband photometry was made by P. Bacci and M. Maestripieri on 2022 Mar 7. We found a color index (V-R) = 0.45 ± 0.09, consistent with a medium albedo asteroid (Shevchenko and Lupishko, 1998).

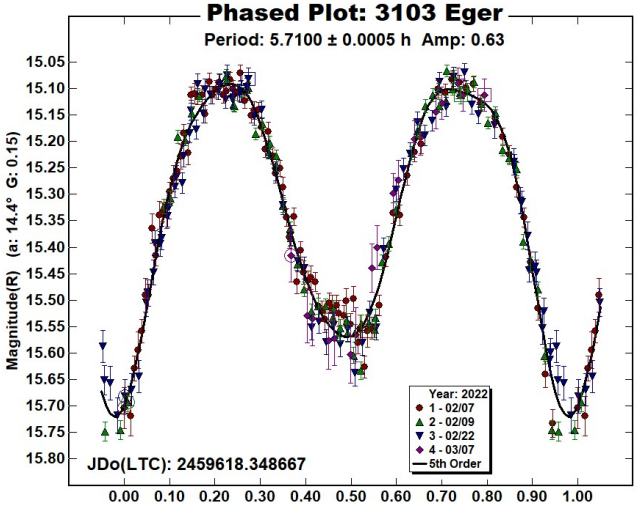

4528 Berg is a middle main-belt asteroid. Collaborative observations were made over nine nights. We found a synodic period of P = 3.563 ± 0.001 h with an amplitude A = 0.24 ± 0.05 mag. The period is close to the previously published results in the LCDB. The lightcurve shows some anomalous attenuations that could possibly be due to a binary nature of this asteroid. Multiband photometry was made by P. Aceti and M. Banfi on 2022 Mar 8. We found a color index (V-R) = 0.46 ± 0.07. The wide phase angle covered by the observations allowed us to determine the H-G parameters. We found H = 12.80 ± 0.05 and G = 0.22 ± 0.08. Both the color index (V-R) and G value are consistent with a medium albedo asteroid (Shevchenko and Lupishko, 1998).

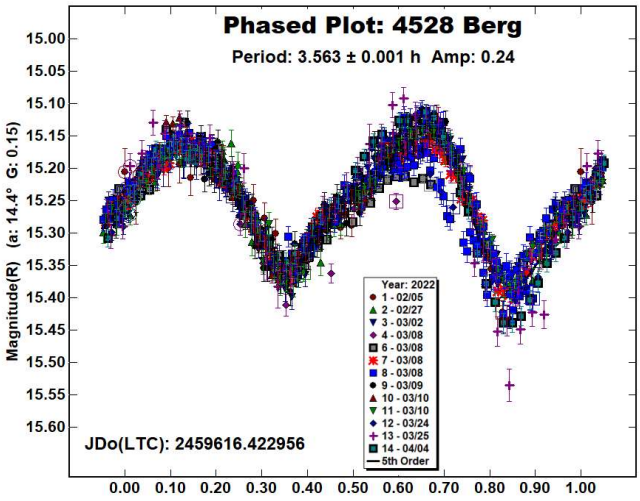

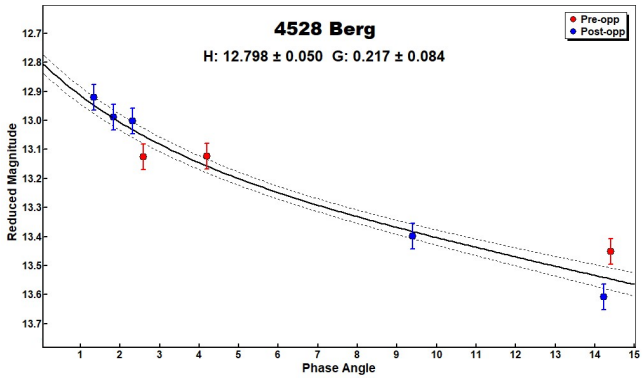

(7482) 1994 PC1 is an S-type (Bus and Binzel, 2002) Apollo Near-Earth asteroid classified as Potentially Hazardous Asteroid (PHA). Collaborative observations were made over four nights. We found a synodic period of P = 2.599 ± 0.001 h with an amplitude A = 0.32 ± 0.06 mag. The period is close to the previously published results in the LCDB.

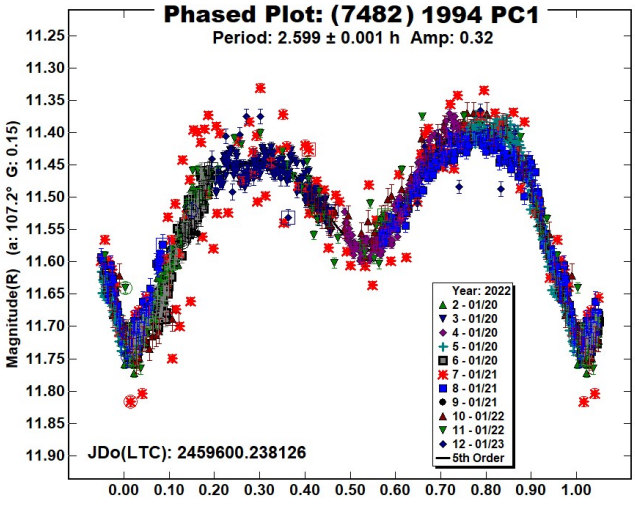

References

Buchheim, R.K. (2010). "Methods and Lessons Learned Determining the H-G Parameters of Asteroid Phase Curves." *Society for Astronomical Sciences Annual Symposium* **29**, 101-115.

Bus, S.J.; Binzel, R.P. (2002). "Phase II of the Small Main-Belt Asteroid Spectroscopic Survey - A Feature-Based Taxonomy." *Icarus* **158**, 146-177.

Harris, A.W.; Young, J.W.; Scaltriti, F.; Zappala, V. (1984). "Lightcurves and phase relations of the asteroids 82 Alkmene and 444 Gyptis." *Icarus* **57**, 251-258.

Pravec, P.; Wolf, M.; Sarounova, L. (2007web). *https://www.asu.cas.cz/~asteroid/binastphotsurvey.htm*

Shevchenko, V.G.; Lupishko, D.F. (1998). "Optical properties of Asteroids from Photometric Data." *Solar System Research* **32**, 220-232.

UAI (2022), "Unione Astrofili Italiani" web site. *https://www.uai.it*

Warner, B.D.; Harris, A.W.; Pravec, P. (2009). "The asteroid lightcurve database." *Icarus* **202**, 134-146. Updated 2022 April 12. *https://minplanobs.org/alcdef/index.php*

Warner, B.D. (2021). MPO Software, *MPO Canopus* v10.8.5.0. Bdw Publishing. *http://minorplanetobserver.com*

MAIN-BELT ASTEROIDS OBSERVED FROM CS3: 2022 JANUARY-MARCH

Robert D. Stephens
Center for Solar System Studies (CS3)
11355 Mount Johnson Ct., Rancho Cucamonga, CA 91737 USA
rstephens@foxandstephens.com

Brian D. Warner
Center for Solar System Studies (CS3)
Eaton, CO

(Received: 2022 April 5)

CCD photometric observations of 21 main-belt asteroids were obtained at the Center for Solar System Studies (CS3) from 2022 January-March.

The Center for Solar System Studies (CS3) has nine telescopes which are normally used in program asteroid family studies. The focus is on near-Earth asteroids, Jovian Trojans and Hildas. When it is not the season to study a family, or when a nearly full moon is too close to the family targets being studied, targets of opportunity amongst the main-belt families were selected.

Table I lists the telescopes and CCD cameras that were used to make the observations. Images were unbinned with no filter and had master flats and darks applied. The exposures depended upon various factors including magnitude of the target, sky motion, and Moon illumination.

Telescope	Camera
0.30-m f/6.3 Schmidt-Cass	SBIG 1001E
0.35-m f/9.1 Schmidt-Cass	FLI Microline 1001E
0.35-m f/9.1 Schmidt-Cass	FLI Microline 1001E
0.35-m f/9.1 Schmidt-Cass	FLI Microline 1001E
0.40-m f/10 Schmidt-Cass	FLI Proline 1001E
0.40-m f/10 Schmidt-Cass	FLI Proline 1001E
0.50-m F8.1 R-C	FLI Proline 1001E

Table I: List of CS3 telescope/CCD camera combinations.

Image processing, measurement, and period analysis were done using *MPO Canopus* (Bdw Publishing), which incorporates the Fourier analysis algorithm (FALC) developed by Harris (Harris et al., 1989). The Comp Star Selector feature in *MPO Canopus* was used to limit the comparison stars to near solar color. Night-to-night calibration was done using field stars from the ATLAS catalog (Tonry et al., 2018), which has Sloan *griz* magnitudes that were derived from the GAIA and Pan-STARR catalogs and are "native" magnitudes of the catalog. Those adjustments are usually ≤ ±0.03 mag. The rare greater corrections may have been related in part to using unfiltered observations, poor centroiding of the reference stars, and not correcting for second-order extinction.

The Y-axis values are ATLAS SR "sky" magnitudes. The two values in the parentheses are the phase angle (a) and the value of *G* used to normalize the data to the comparison stars used in the earliest session. This, in effect, made all the observations seem to be made at a single fixed date/time and phase angle, leaving any variations due only to the asteroid's rotation and/or albedo changes. The X-axis shows rotational phase from -0.05 to 1.05. If the plot includes the amplitude, e.g., "Amp: 0.65", this is the amplitude of the Fourier model curve and *not necessarily the adopted amplitude for the lightcurve*.

For brevity, only some of the previously reported rotational periods may be referenced. A complete list is available at the asteroid lightcurve database (LCDB; Warner et al., 2009).

1405 Sibelius. Rotational periods for this inner main-belt asteroid have been observed several times in the past. Pravec et al. (2007web) and Stephens (2018) both reported periods near 6.05 h. This year's result is in good agreement with those prior findings. Pál et al. (2020), using data from the TESS spacecraft, reported a period of 12.0826 h, a 2:1 alias of the Pravec and Stephens results.

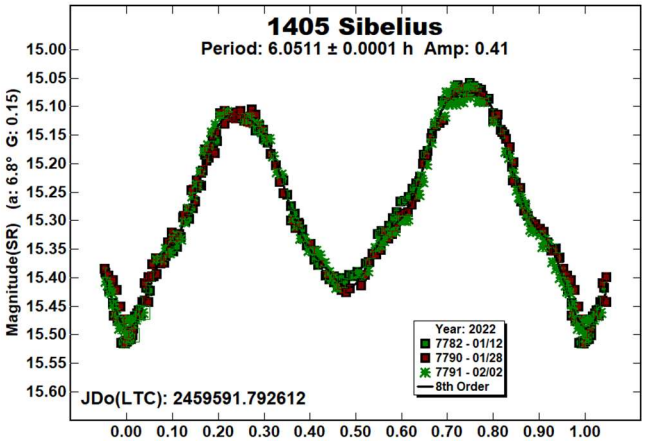

Because of our previous data from 2017, and the availability of the Pál et al. data on the Asteroid Lightcurve Data Exchange Format database (ALCDEF, 2020) web site, we attempted to create a pole/shape model. We added these three dense data sets to additional sparse data from the AstDyS-2 site (AstDyS-2, 2020). We were able to use sparse data from ATLAS, Zwicky Transient Factory, Catalina Sky Survey, USNO, and Lowell Observatory. The following plots show the PAB longitude, latitude and phase angle distributions. Green dots represent the three dense datasets, and red dots represent sparse data from the five surveys.

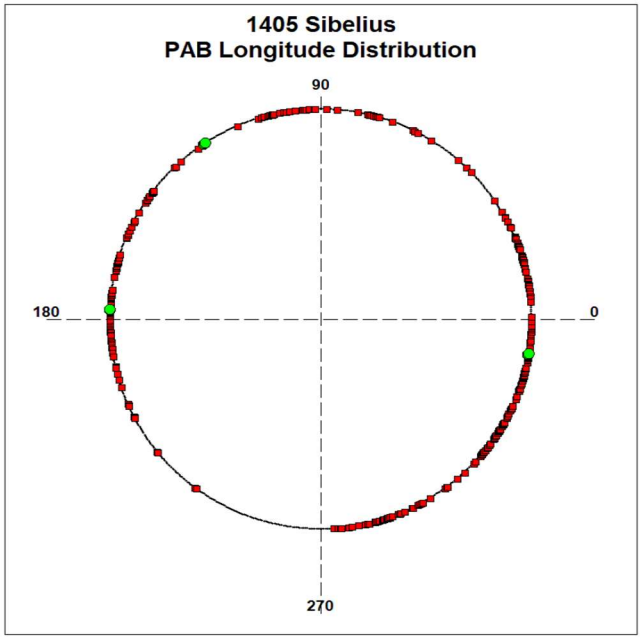

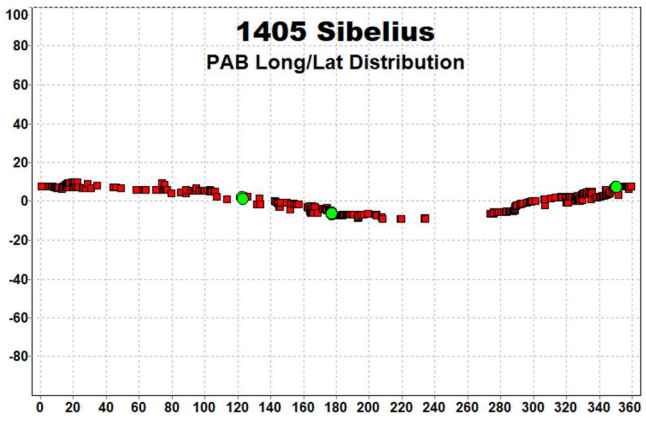

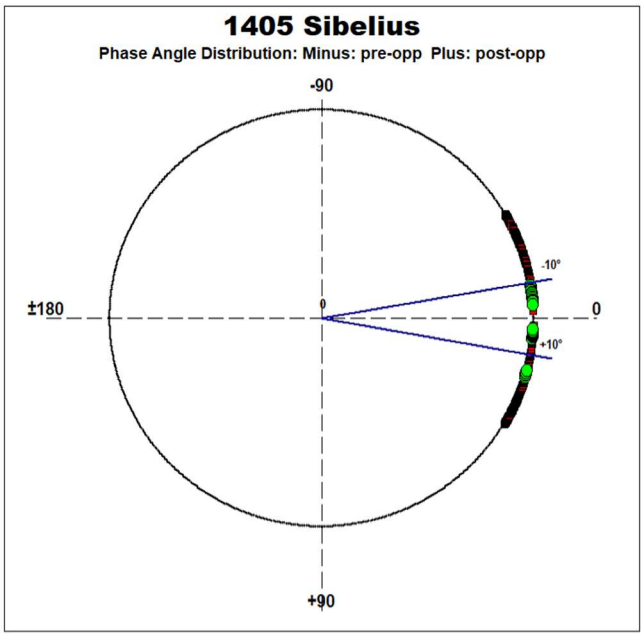

The data were combined using *MPO LCInvert* (Bdw Publishing). This Windows-based program incorporates the algorithms developed by Kaasalainen and Torppa (2001) and Kaasalainen et al. (2001) and converted by Josef Durech from the original FORTRAN to C. A period search was made over a sufficiently wide range to assure finding a global minimum in χ^2 values. The Pál et al. (2020) data was weighted at 50% to the other dense data, and the sparse data weighted between 20% and 40%.

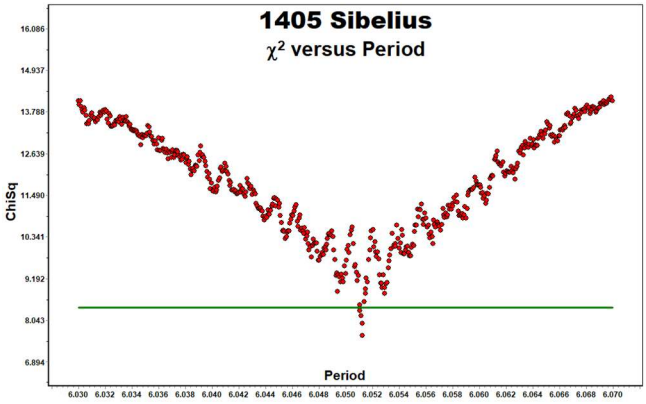

As is often the case, the pole model showed two possible solutions 180° apart; (λ, β, P) = (45°, 30°, 6.05127 h) and (λ, β, P) = (225°, 15°, 6.05127 h). Both solutions have a wide range of possible latitudes. Our preferred solution is the (45°, 30°) pole position.

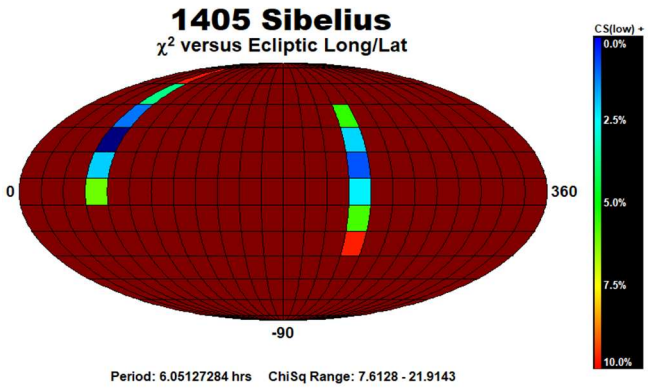

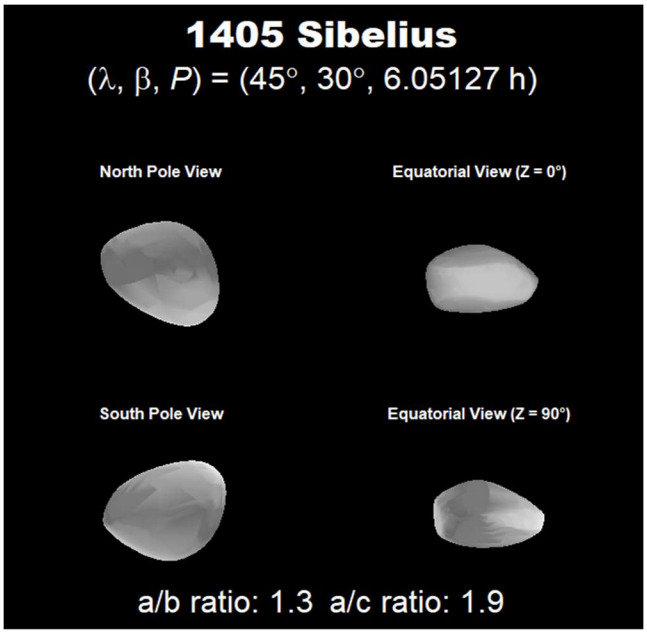

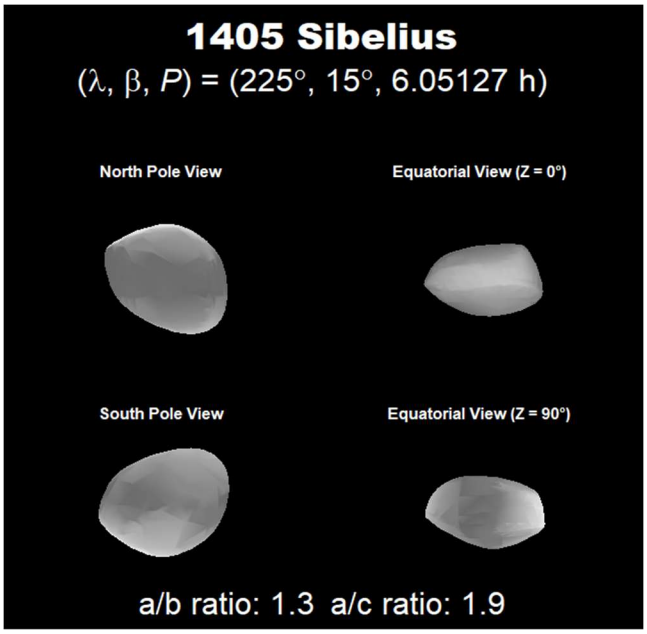

The two pole solutions created similar models, both with a/b ratios of 1.3 and a/c ratios of 1.9.

To test the model, the dense datasets (including the Pál et al. data) were plotted against the predicted lightcurve for each dataset. Each plot resulted in a very good match. Even the Pál et al. data from the TESS spacecraft, which had an expected number of outliers, was a good match to the predicted lightcurve giving high confidence in the pole/shape model result.

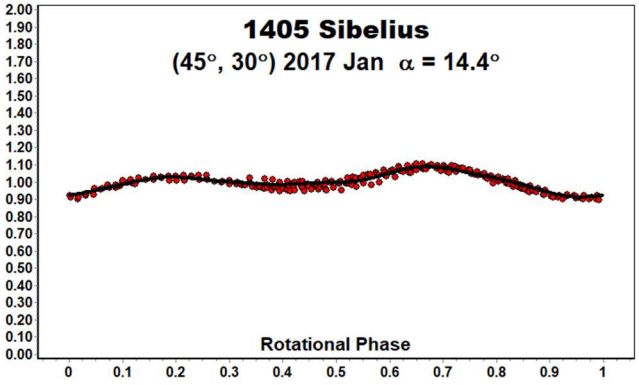

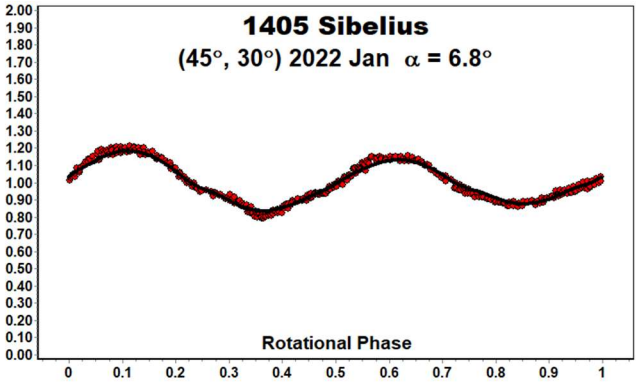

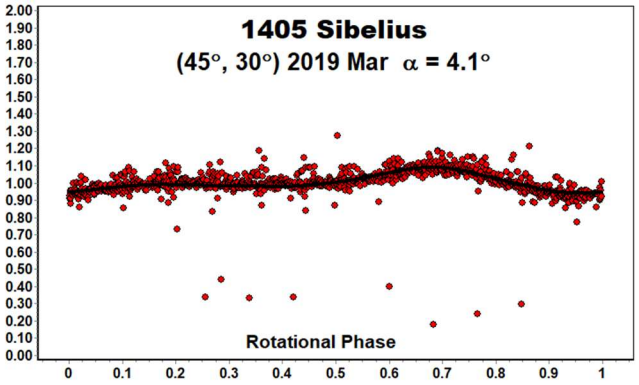

To further refine the model, the next favorable opposition is in 2024 November.

1817 Katanga. Three viable rotational periods were found in the LCDB for this inner main-belt asteroid. Behrend (2001web, 2019web) reported periods of 8.50 h and 8.49602 h. Warner (2008b) reported a period of 8.481 h. In addition, we found unpublished observations from March 2019 coinciding with the Behrend observations. That unpublished 2019 period was 8.501 h. This year's result is in good agreement with those prior findings.

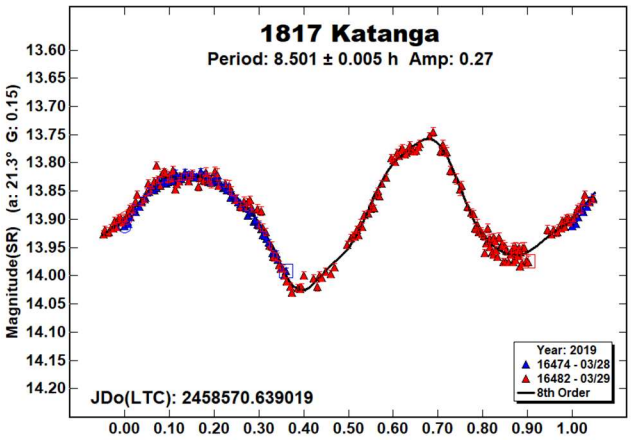

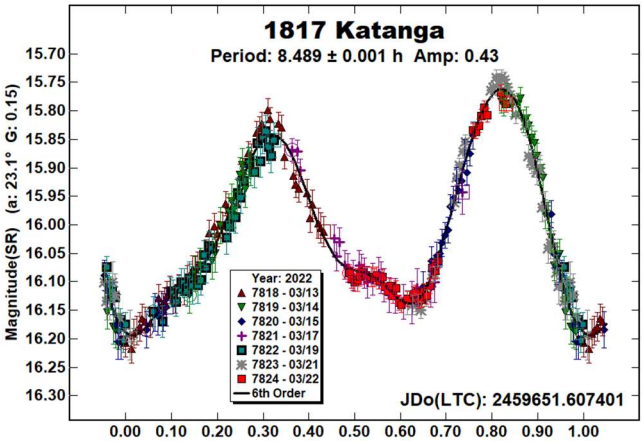

Because of our previous data from 2008 and 2019, we attempted to create a pole/shape model. We added additional sparse data from the AstDyS-2 site (AstDyS-2, 2020). We were able to use sparse data from ATLAS, Zwicky Transient Factory, Catalina Sky Survey, and USNO. The following plots show the PAB longitude, latitude and phase angle distributions. Green dots represent the three dense datasets, and red dots represent sparse data from the four surveys.

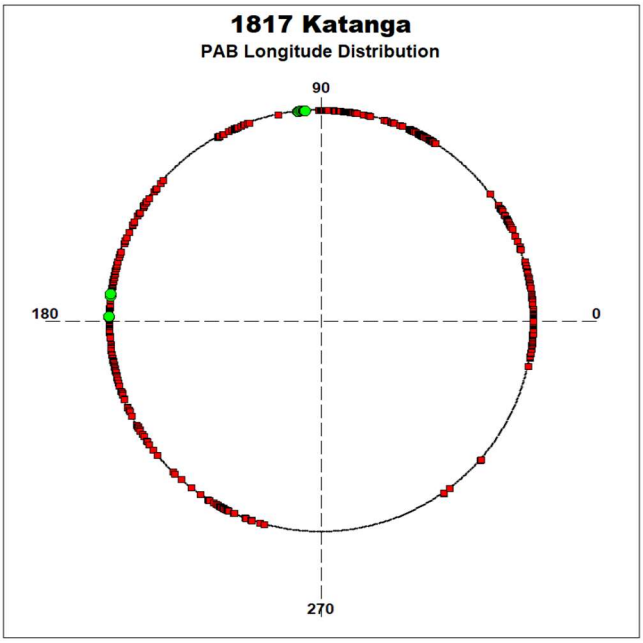

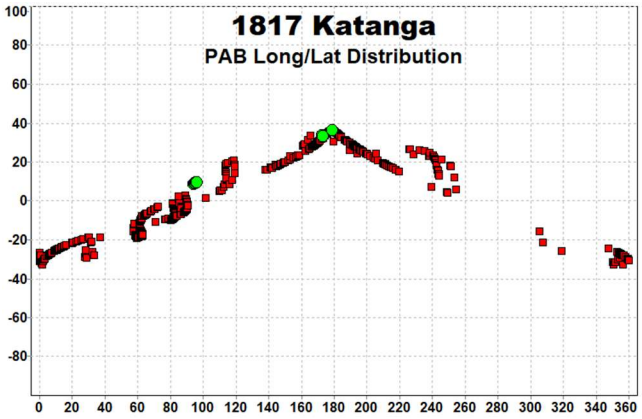

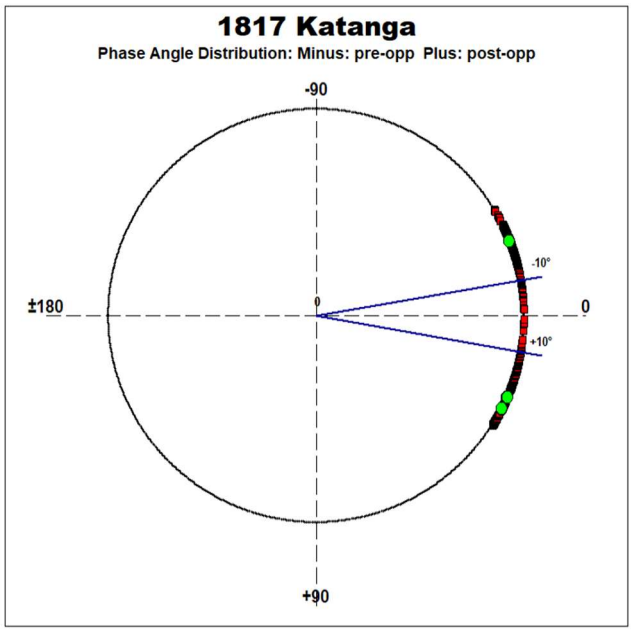

The data were combined using *MPO LCInvert* (Bdw Publishing) described in the 1405 Sibelius section of this article. Only one unique period below the 10% χ^2 line was found.

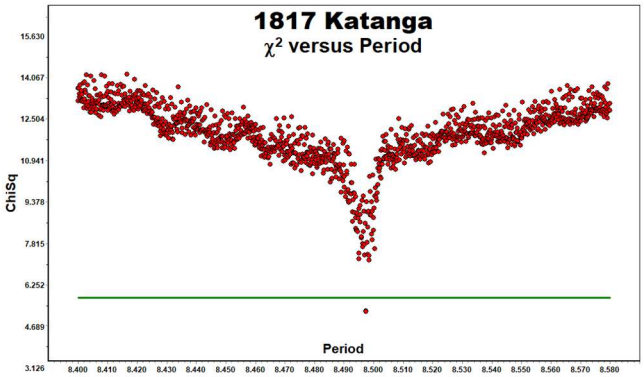

All of the unique solutions were very close to the south ecliptic pole. The best four solutions were all within 10 degrees of the pole indicating the rotation is retrograde. We have adopted (186°, -85°) as our preferred solution, but the longitude is highly ambiguous.

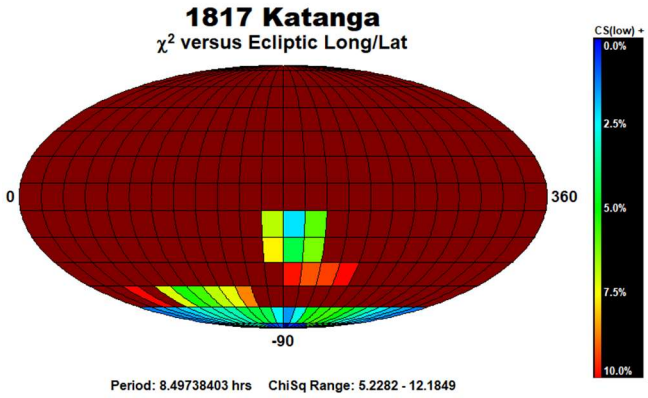

The resulting model, and similar models from other longitudes present a nearly spheroidal body with an a/b ratio of 1.2 and a/c ratio of 1.3. This is expected given that all of the amplitudes reported in the LCDB are 0.33 ± 0.10 mag.

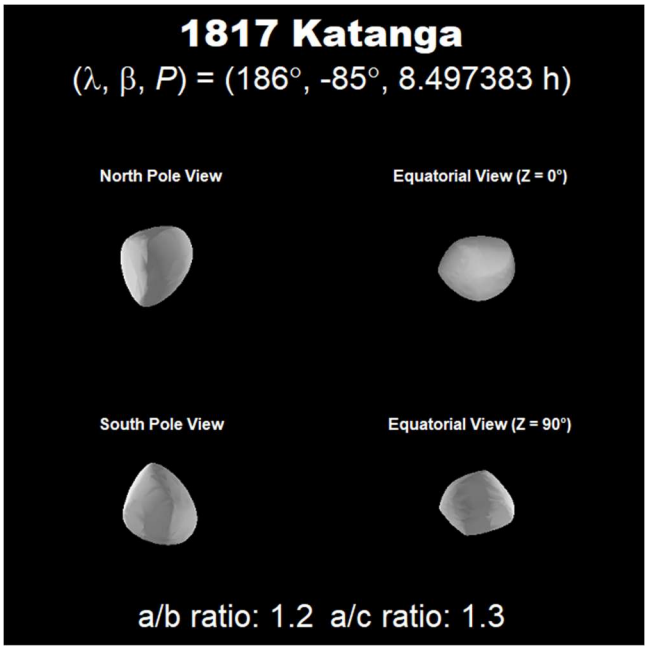

To test the model, these dense datasets were plotted against the predicted lightcurve for each dataset. Each plot for the (186°, -85°) pole position resulted in a good match.

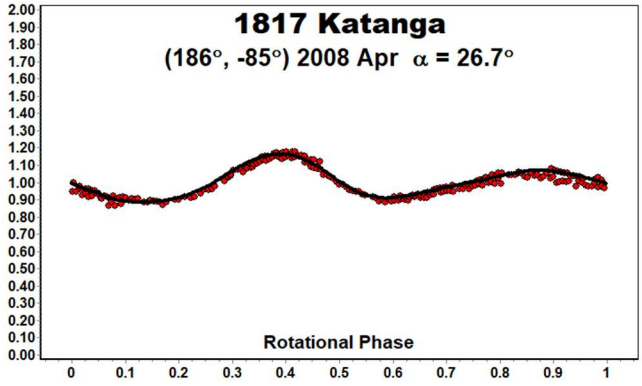

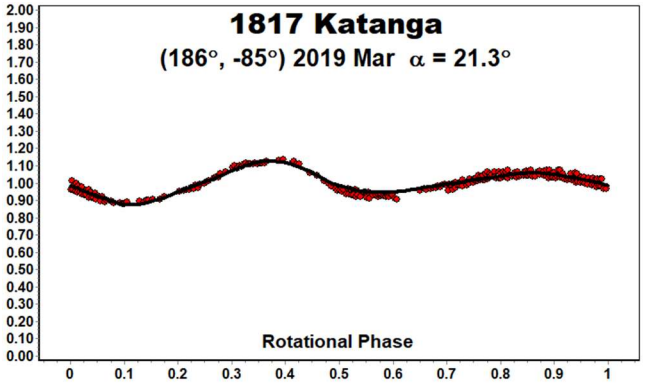

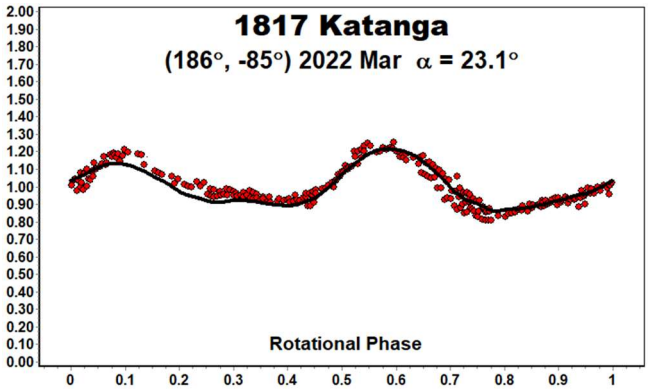

To further refine the model, the next favorable opposition is in 2023 June.

2108 Otto Schmidt. This inner main-belt asteroid had periods reported twice in the past. Behrend (2001web) reported a period of 15.24 h, but the data only spanned half of the plotted lightcurve and the scatter was greater than the reported amplitude. Warner (2017) found a period of 6.90 h. The somewhat sparse dataset did not cover the entire lightcurve and resulted in several possible results in the Period Spectrum, noting that a period of 6.31 h could not be formally excluded.

Our result this year was 6.308 h, confirming the 6.31 h alias found by Warner. We replotted the 2016 data with a period of 6.305 h showing this period to be consistent with the 2022 result.

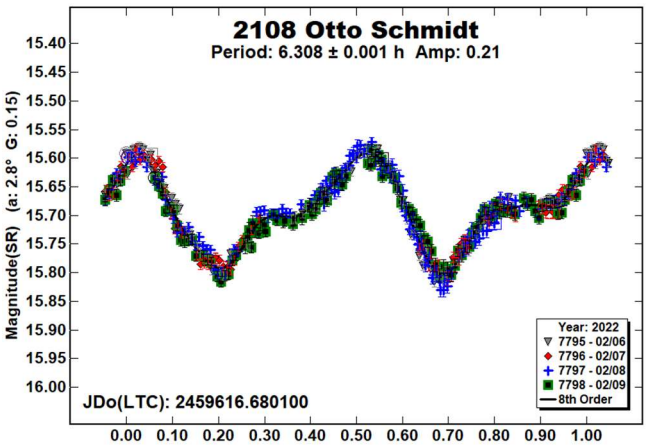

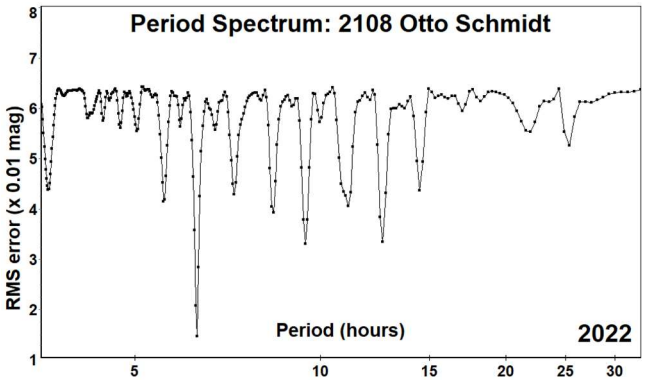

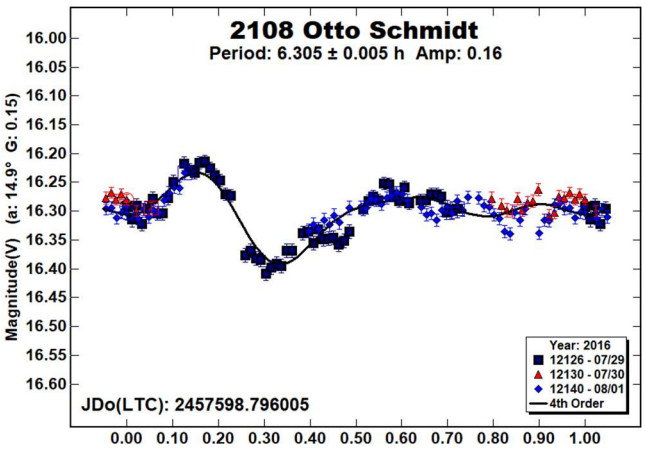

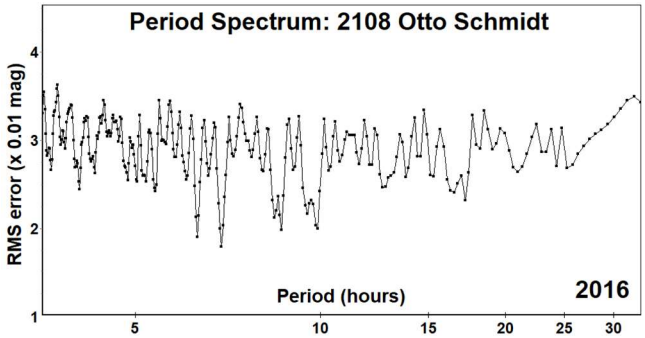

2912 Lapalma. This inner main-belt asteroid has been observed three times in the past. Brinsfield (2008), Pravec et al. (2008web), and Stephens and Warner (2021b) each found a period near 5.71 h. Our results this year is in good agreement with those prior results.

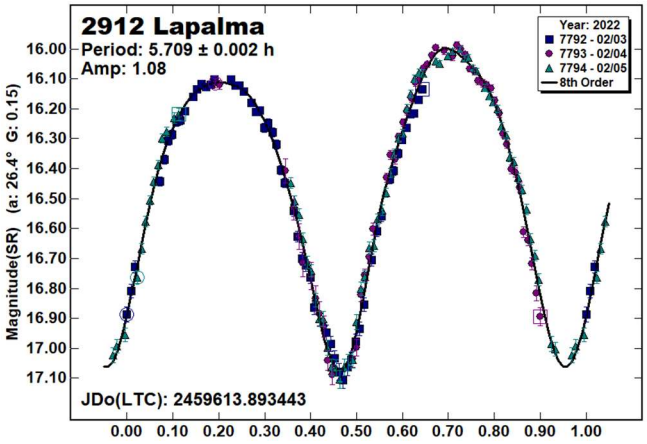

We attempted to model the shape and spin axis. However, the result produced an unlikely shape where the Z-axis (axis of rotation) was longer than X or Y. The corresponding spin axis pole is near -90°. Any solution that is very close to one of the ecliptic poles makes the longitude of the spin axis hard to find with certainty and, as in this case, can lead to physically improbable shapes.

3057 Malaren. The Palomar Transient Factory Survey (Waszczak et al. 2015) previously found this inner main-belt asteroid to have a period of 4.496 h. Our results this year is in good agreement with that prior result.

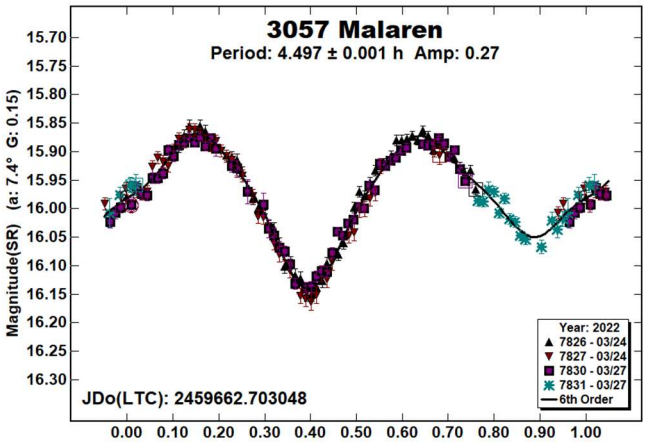

3500 Kobayashi. This member of the Flora dynamical family has been observed three times in the past. Using data from the Palomar Transient Factory, Waszczak (2015) and Chang et al. (2016) found periods near 5.6 h. Later, Pál et al. (2020) using data from the TESS spacecraft, found a period of 5.60643 h. Our results this year were the first dense dataset and are in good agreement with those prior results.

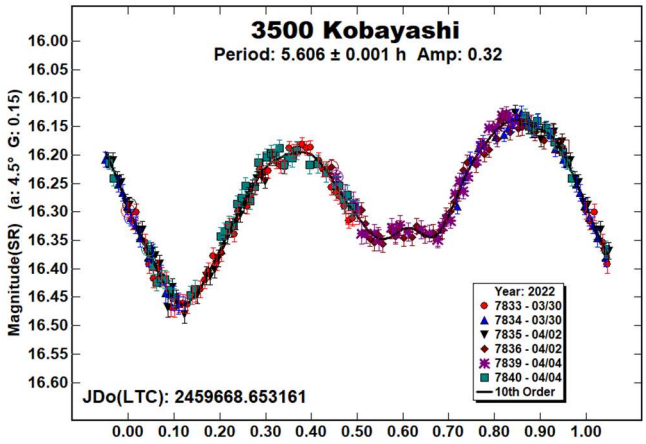

4302 Markeev. We have observed this inner Main-belt asteroid twice in the past (Stephens, 2016; Stephens and Warner, 2020), both times finding a period of 5.13 h. Our result this year is in good agreement with our prior results.

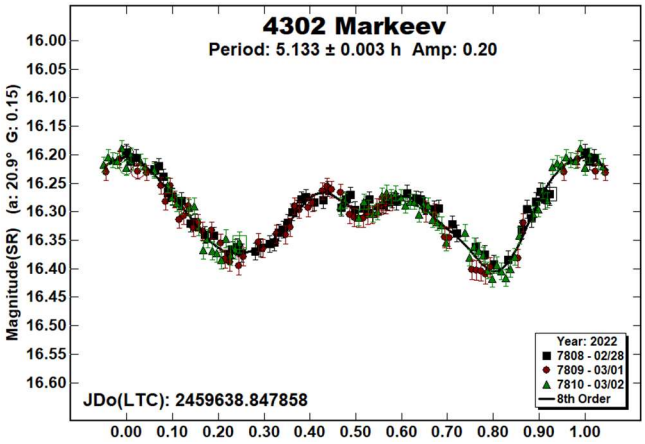

5349 Paulharris. There is only one previously reported result in the LCDB for this Mars-crosser. Benishek (2017) reported a period of 7.890 h and an amplitude of 0.18 mag from observations collected in 2016 September. Our result this year is in good agreement with the Benishek period.

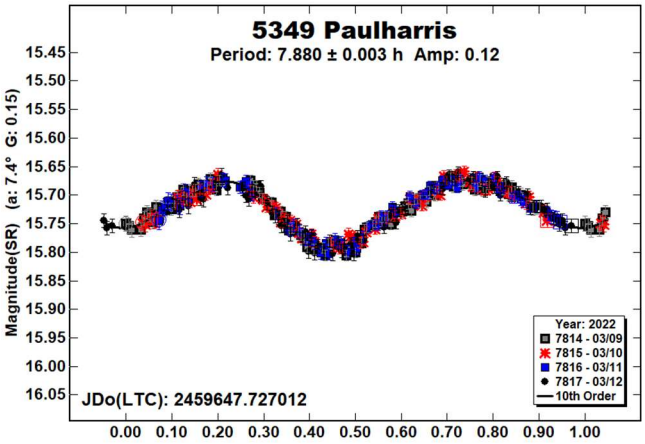

6411 Tamaga. Per the LCDB, this Mars-crosser is estimated to be 7 km in diameter, and has periods reported three times in the past. Higgins et al. (2008), Bembrick et al. (2008), and Waszczak et al. (2015), all reported rotational periods near 8.35 h. Our results this year is in good agreement with those prior results.

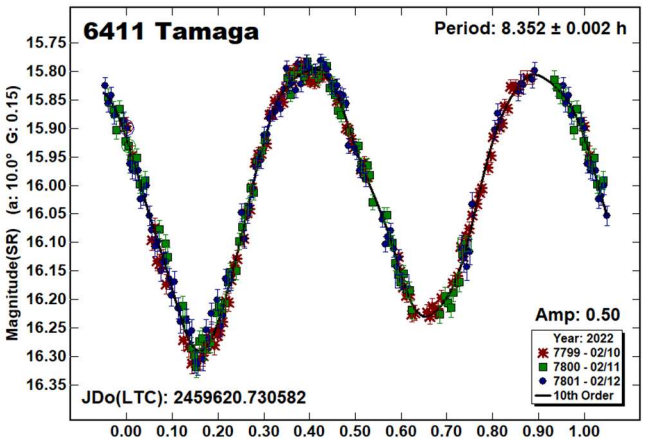

We investigated the possibility of creating a pole/shape model, but found that all of the observations in the ALCDEF database were withing 60° longitude of each other, and there was not sufficient sparse data to compensate for the lack of longitude difference.

6461 Adam. We observed this member of the Hungaria family (Nesvorny et al., 2015; Nesvorny, 2015) twice before. Using 2009 observations, we found a period of 6.17 h (Warner, 2010), but it was rated U = 2–, just barely acceptable for rotation periods analysis. In 2011, new data led to a period of 74 h (Warner et al., 2012), which is rated U = 2, which gave the result higher confidence than before, but it was still not secure.

We obtained new data in 2022 February and March, but they were not as dense as we'd preferred due to a full moon and the asteroid fading. The initial analysis showed that the solution was dominated by a period near 46 hours ("NoSub"), but there were signs of a second period, one that was unlikely due to a satellite.

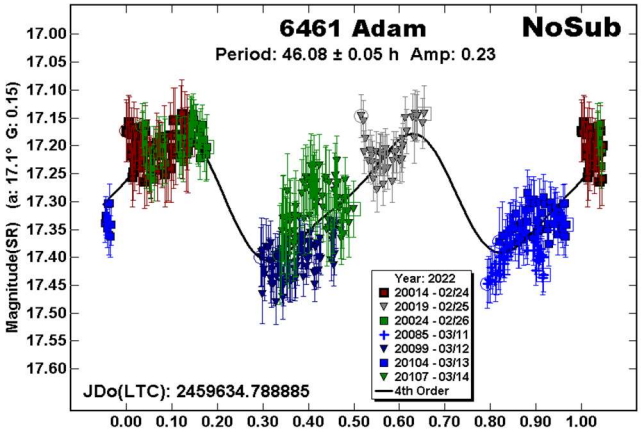

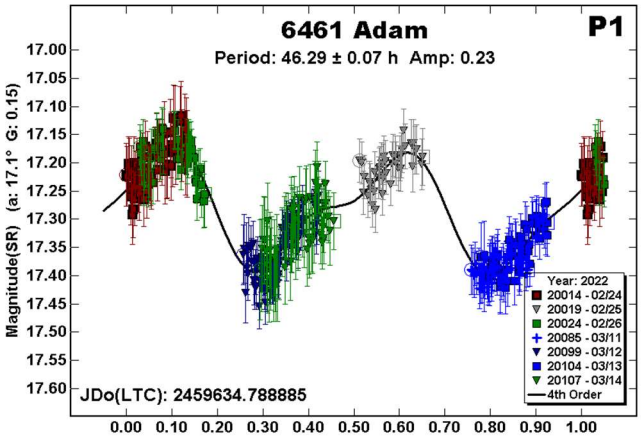

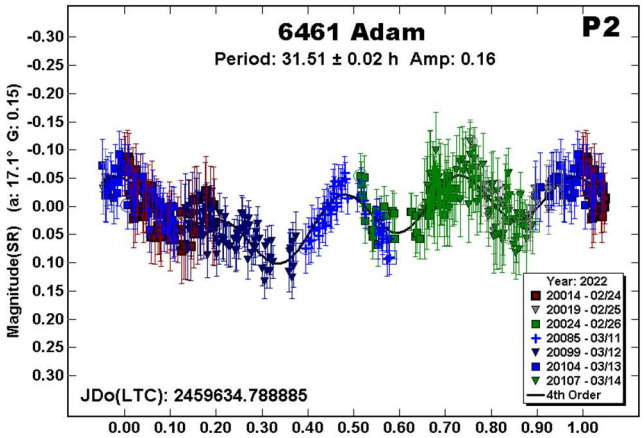

A dual-period search was using in *MPO Canopus*, which is not equipped to work with tumbling asteroids. The dominant period ("P1") from 2022 was also a possible solution in 2011 (47 h; Warner et al., 2012). That 2012 paper has a lengthy discussion regarding tumbling asteroid periods and useful details specific to 6164 Adam.

The 2011 period was near 74 h, which is far removed from the 31.5 h that we found from the 2022 data. We did try to find a second period in the 2022 data near 74 h. There was a very weak solution at about 75.5 h, but applying it did a poor job of subtracting out all deviations, looking more like the "NoSub" plot. The inability for *MPO Canopus* to work accurately with tumbling asteroids could well be the reason for the different secondary periods.

6849 Doloreshuerta. Per the LCDB, this member of the Vesta dynamical family has been observed once in the past. Using data from the ATLAS survey, Erasmus et al. (2020) found a period of 6.256 h. Our results this year is in good agreement with that prior result.

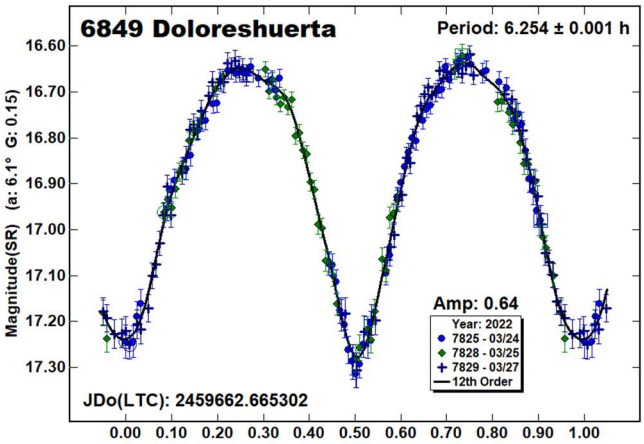

7488 Robertpaul. Two wide-field surveys, Waszczak et al. (2015) and Pál et al. (2020) reported similar periods, 42.922 h and 43.1387 h, respectively. The dominant period of our results is close to those: 42.57 h. However, our data showed very distinctive signs of being in a tumbling state ("NoSub" plot).

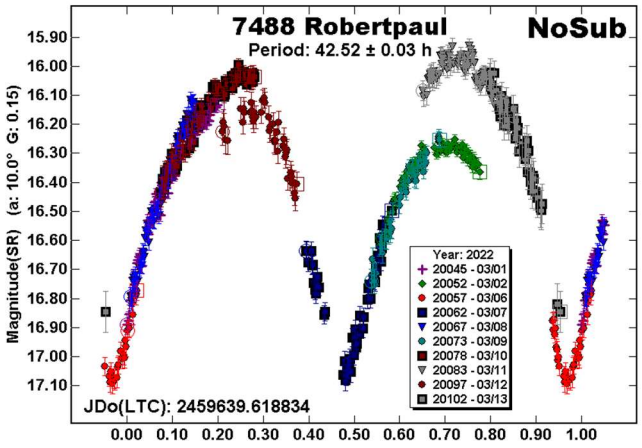

During the dual-period search in *MPO Canopus*, we found a secondary period ("P2" period spectrum) that, when subtracted, left a noisy, flat lightcurve with data from three sessions showing large deviations.

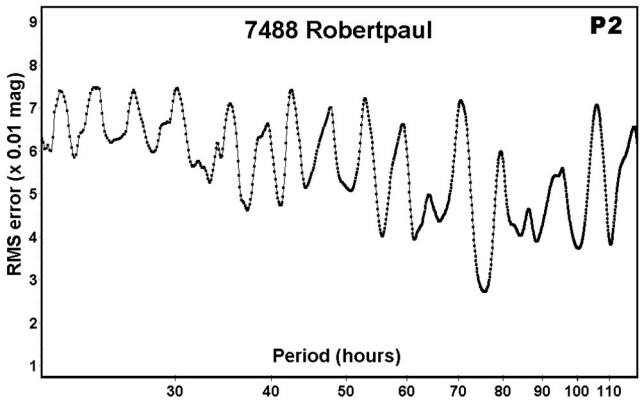

On the presumption that they were "bad," we tried a single period solution that didn't include those three sessions. The result was almost good enough ("P1-3S") and could be made even better by using large zero-point offsets. This seemed to be too much a forced solution and so we stayed with a two-period solution that included the three sessions.

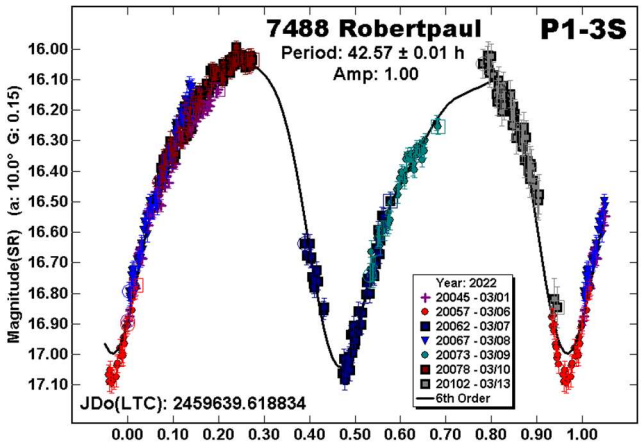

This resulted in a very good fit to a period of 42.57 h ("P1"), close to the single-period solution. It is highly unlikely that the secondary period lightcurve ("P2") has a physical cause, other than the asteroid being a tumbler. It is the best possible solution that *MPO Canopus* could extract after subtracting the dominant period.

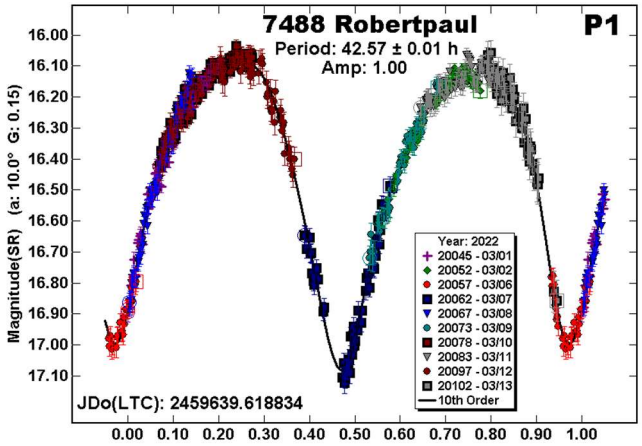

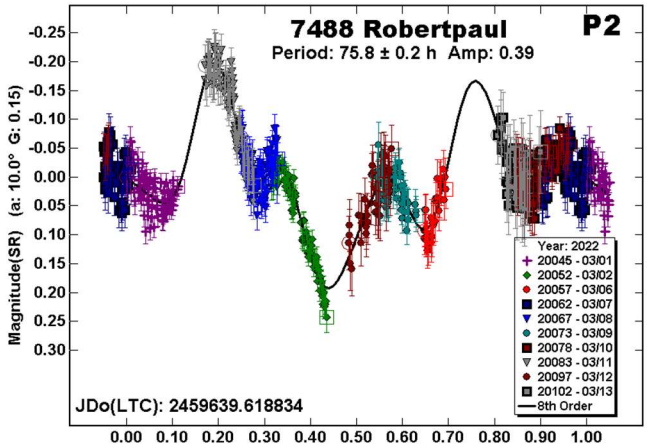

8783 Gopasyuk. Rotational periods for this inner main-belt asteroid have been observed three times in the past. Waszczak et al. (2015) and Stephens (2017) both reported a period of 5.693 h. The Thousand Asteroid Lightcurve Survey (TALC; Masiero et al. 2009) reported a period of 5.6951 h. This year's result is in good agreement with those prior findings.

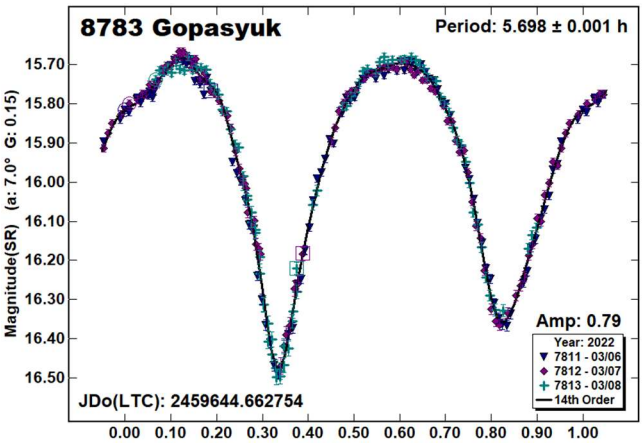

Because of our previous data from 2017, and the availability of the Waszczak et al. data on the Asteroid Lightcurve Data Exchange Format database (ALCDEF, 2020) web site, we attempted to create a pole/shape model. We treated the Waszczak et al. dataset as sparse data, and added additional sparse data from the AstDyS-2 site (AstDyS-2, 2020). We were able to use sparse data from ATLAS, Zwicky Transient Factory, Catalina Sky Survey, and Lowell Observatory. The following plots show the PAB longitude, latitude and phase angle distributions. Green dots represent the three dense datasets, and red dots represent sparse data from the five surveys. The green dots at longitude 19° are the Waszczak et al. dataset which was treated as sparse data in the analysis as they represented 1 - 3 data points per night.

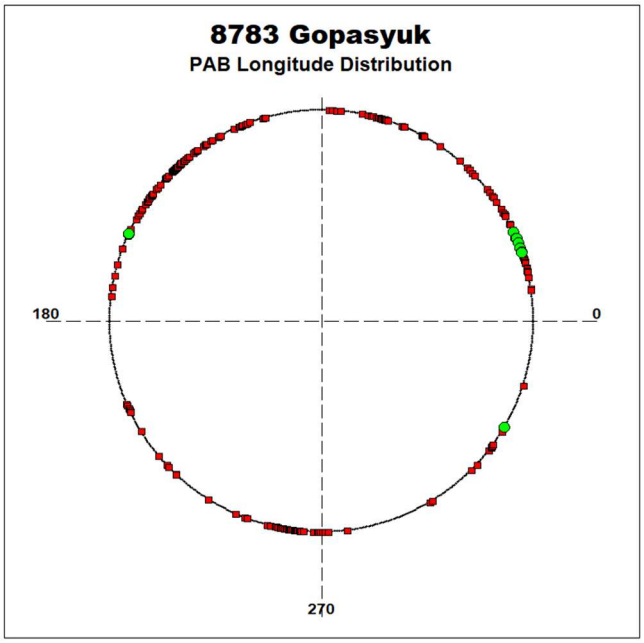

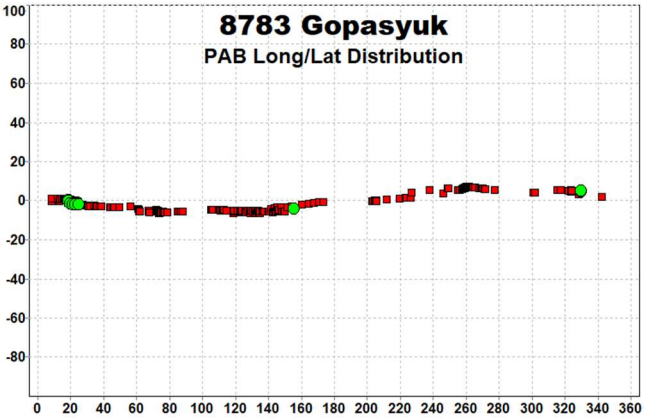

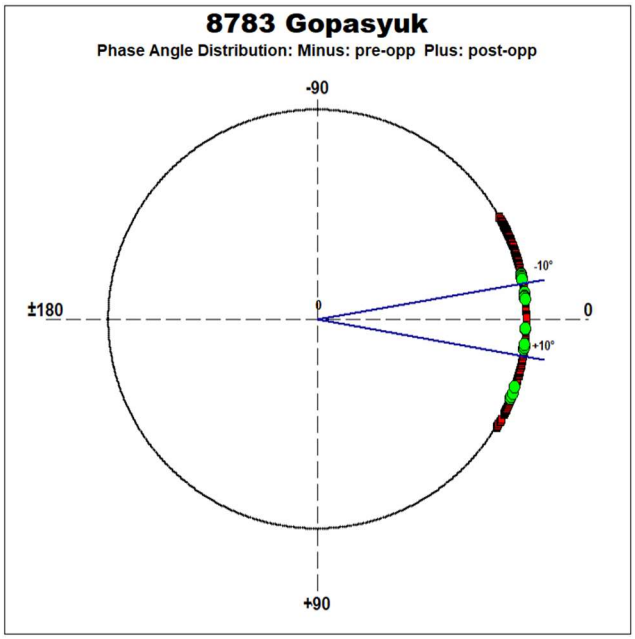

The data were combined using *MPO LCInvert* (Bdw Publishing) described in the 1405 Sibelius section of this article. Only two unique periods below the 10% χ^2 line were found.

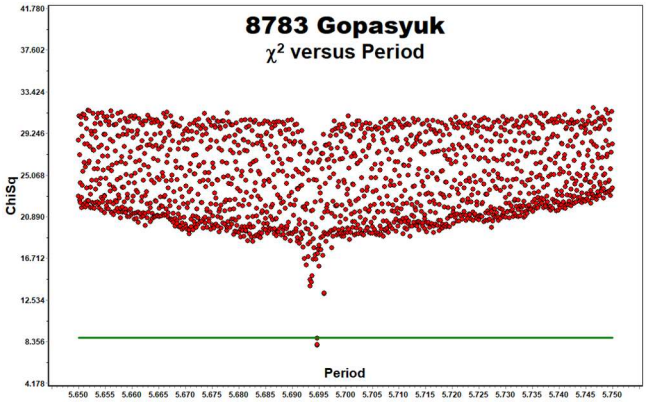

As is often the case, the pole model showed two possible solutions 180° apart; (λ, β, P) = (28°, -82°, 5.69471 h) and (λ, β, P) = (258°, -61°, 5.69471 h). The first solution is very close to one of the ecliptic poles making the longitude of the spin axis hard to find with certainty and, as in this case, can lead to physically improbable shapes. In the first solution, the Z-axis (axis of rotation) was highly flattened like a skipping stone. For this reason, even though the χ^2 is higher, our preferred solution is the (258°, -61°) pole position.

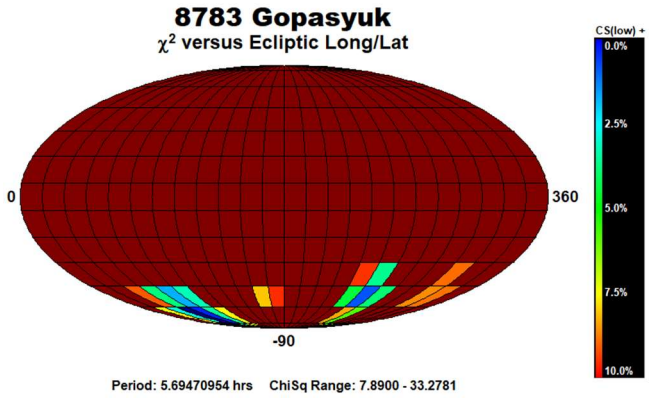

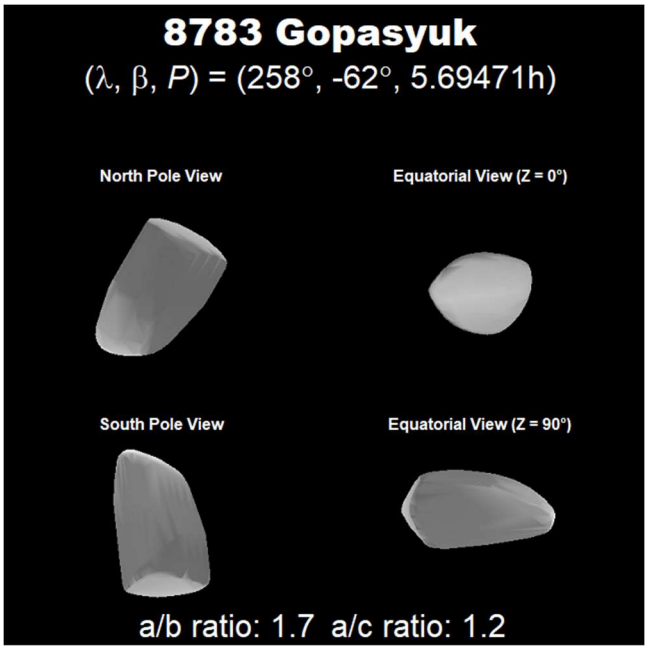

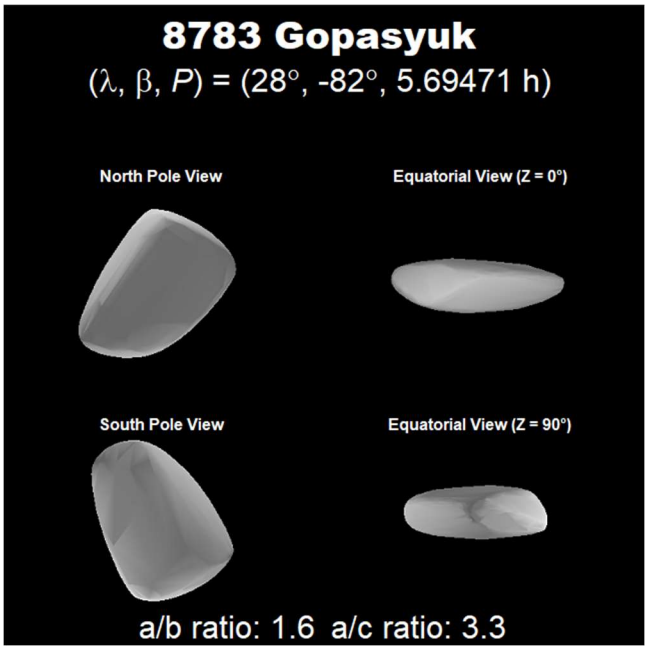

As previously discussed, the two pole solutions created models, with dramatically different a/c ratios.

To test the model, the dense datasets were plotted against the predicted lightcurve for each dataset. Each plot for the (258°, -61°) pole position resulted in a good match.

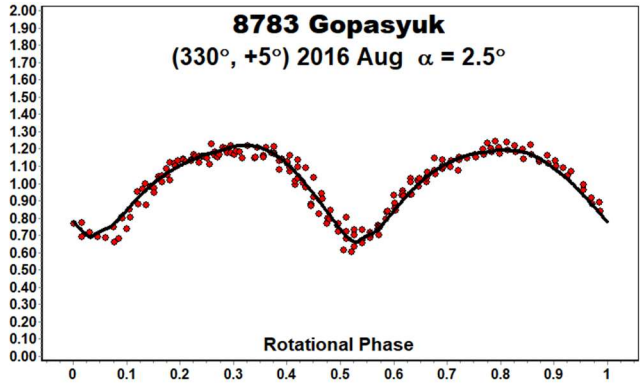

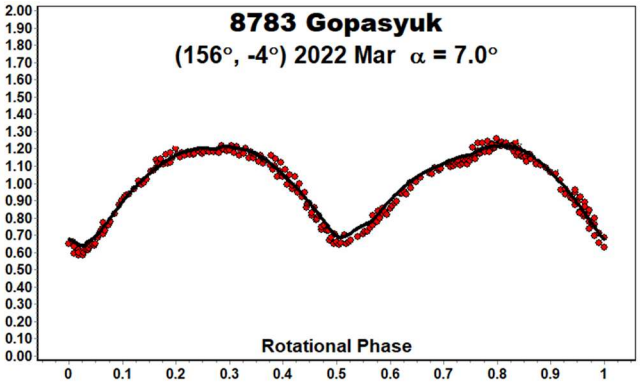

To further refine the model, the next favorable opposition is in 2023 August.

9356 Elineke. This member of the Eunomia dynamical family was a target of opportunity, being in the same field as 7488 Robertpaul for a single night. We observed it once in the past (Warner 2014b) finding a period of 2.750 h. The raw data this year covers almost three cycles and the result is in good agreement with our prior result.

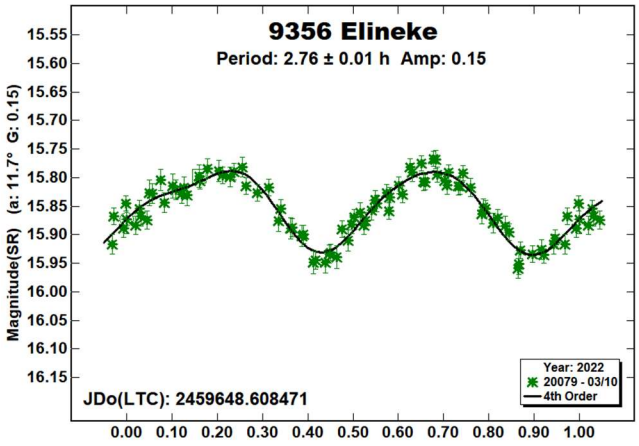

11836 Eileen. The LCDB has an unpublished period for this Mars-crosser by Higgins of 8.810 h. Using data from the Asteroid Terrestrial-impact Last Alert System (ATLAS), Ďurech et al. (2020) created a model with a sidereal period of 8.8116 h and possible pole position of (126º, -72º). Our result this year is in good agreement with those prior results. The Higgins data are available in ALCDEF, but we did not think the two dense datasets sufficient to improve upon the Ďurech et al. model.

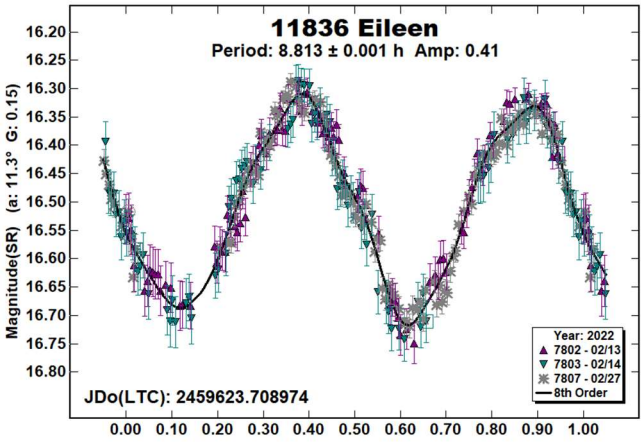

(12494) Doughamilton. We observed this member of the Hungaria collisional family in 2020 (Stephens and Warner 2021a), finding a period of 39.23 h. In addition, using data from the TESS spacecraft, Pál, et al. (2020) found a period of 39.2603 h. Our results this year has a lightcurve with little overlap and differs from those prior results by about 0.3 h.

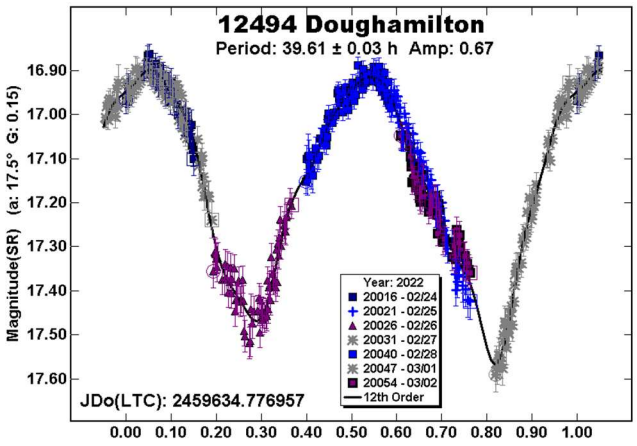

(13186) 1996 UM. We observed this member of the Hungaria collisional family five times in the past (Stephens and Warner 2021a and references therein), each time finding a period near 4.3 h. Our results this year is in good agreement with those prior results.

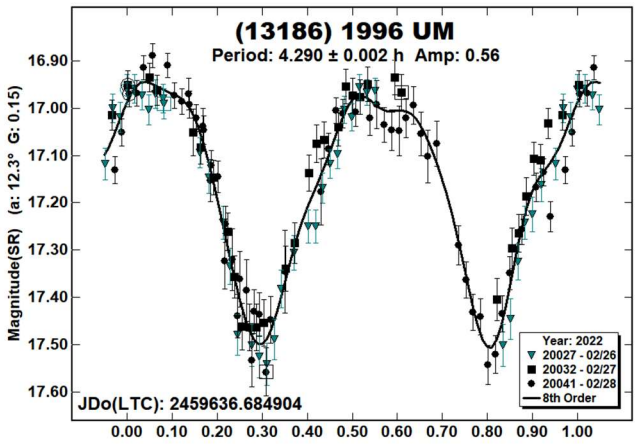

(13578) 1993 MK. We observed this member of the Hungaria collisional family many times in the past (Warner 2014a and references therein), finding periods near 3.96 h. Our result this year is in good agreement with those prior results. In addition, Waszczak et al. (2015), using data from the Palomar Transient Factory Survey, found a period of 3.960 h. Finally, using data from the TESS spacecraft, Pál et al. (2020) found a period of 7.908847 h, a 2:1 alias of the period others found.

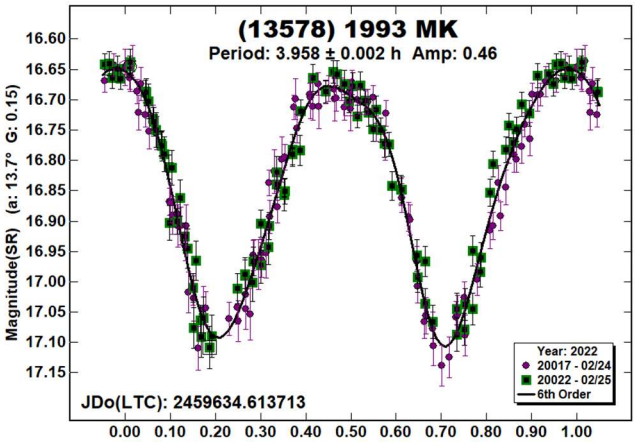

(52314) 1991 XD. We observed this member of the Hungaria collisional family twice before (Warner 2008a and 2014b), finding periods near 7.67 h. Our results this year are in good agreement with those prior results.

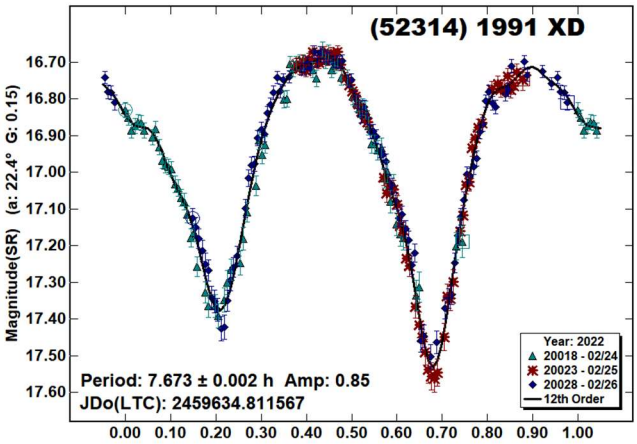

Number	Name	2021/mm/dd	Phase	L_{PAB}	B_{PAB}	Period(h)	P.E.	Amp	A.E.
1405	Sibelius	01/12-02/02	*6.9,5.7	123	1	6.0511	0.0001	0.41	0.02
1817	Katanga	19/03/28-03/29	21.4,21.5	179	36	8.501	0.005	0.27	0.01
1817	Katanga	03/13-03/22	23.1,23.1	95	9	8.489	0.001	0.43	0.02
2108	Otto Schmidt	02/06-02/09	2.8,4.1	133	3	6.308	0.001	0.21	0.02
2912	Lapalma	02/03-02/05	26.4,26.2	194	8	5.709	0.002	1.08	0.02
3057	Malaren	03/24-03/27	7.4,6.5	190	10	4.497	0.001	0.27	0.02
3500	Kobayashi	03/30-04/04	4.6,6.8	181	-4	5.606	0.001	0.32	0.01
4302	Markeev	12/31-12/31	*7.4,6.5	96	-4	5.133	0.003	0.20	0.02
5349	Paulharris	03/09-03/12	7.4,5.7	182	2	7.880	0.003	0.12	0.01
6411	Tamaga	02/10-02/12	10.0,8.8	159	-2	8.352	0.002	0.50	0.02
6461	Adam	02/24-03/14	17.2,10.9	182	13	T46.29	0.07	0.23	0.05
						31.51	0.02	0.16	0.02
6849	Doloreshuerta	03/24-03/27	6.1,7.2	176	-8	6.254	0.001	0.64	0.02
7488	Robertpaul	03/01-03/13	10.0,16.8	151	12	T42.57	0.01	1.00	0.03
						75.8	0.2	0.39	0.03
8783	Gopasyuk	03/06-03/08	7.0,8.1	156	-4	5.698	0.001	0.79	0.02
9356	Elineke	03/10-03/10	11.8	149	13	2.76	0.01	0.15	0.01
11836	Eileen	02/13-02/27	11.3,8.6	159	13	8.813	0.001	0.41	0.02
12494	Doughamilton	02/24-03/02	17.5,16.1	176	20	39.61	0.03	0.67	0.03
13186	1996 UM	02/26-02/28	12.3,12.4	153	-19	4.290	0.002	0.56	0.03
13578	1993 MK	02/24-02/25	13.7,14.0	145	21	3.958	0.002	0.46	0.03
52314	1991 XD	02/24-02/26	22.4,22.0	174	32	7.673	0.002	0.85	0.03
74779	1999 RF241	02/11-02/26	31.0,33.8	112	29	6.191	0.001	0.84	0.03
434307	2004 FT41	03/01-03/01	18.2	175	20	4.88	0.07	0.30	0.04

Table II. Observing circumstances and results. TDominant period for a tumbling asteroid. The phase angle is given for the first and last date. If preceded by an asterisk, the phase angle reached an extremum during the period. L_{PAB} and B_{PAB} are the approximate phase angle bisector longitude/latitude at mid-date range (see Harris et al., 1984).

Number	Name	λ	β	Period	λ	β	Period	a/b ratio	a/c ratio
1405	Sibelius	**45**	**30**	**6.05127**	225	15	6.05127	1.3	1.9
1817	Katanga	**186**	**-85**	**2.679720**	145	-22	8.497383	1.2	1.3
8783	Gopasyuk	**258**	**-61**	**5.69471**	28	-82	5.69471	1.7	1.2

Table III. Results of Pole/Shape modeling. The preferred solution is listed first in bold text. For the ratios, c = 1.0.

(74779) 1999 RF241. Per the LCDB, this member of the Phocaea dynamical family has been observed once before. Skiff et al. (2019) reported a period of 6.1895 h from data acquired in 2010. Our results this year are in good agreement with the Skiff et al. result.

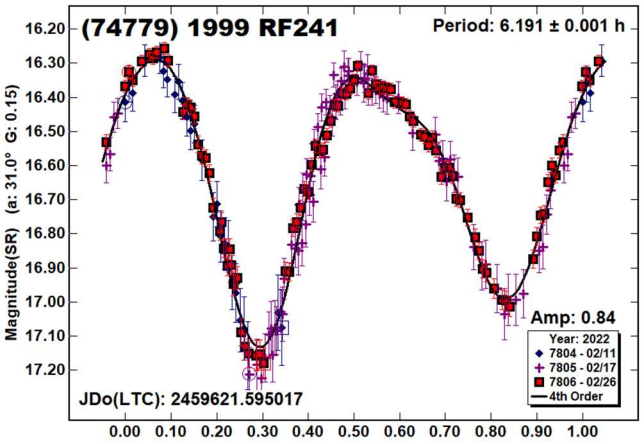

(434307) 2004 FT41. There are no prior entries in the LCDB for this Mars-crosser. It was a target of opportunity, being in the same field as 12494 Doughamilton for a single night. The raw data covers almost two cycles.

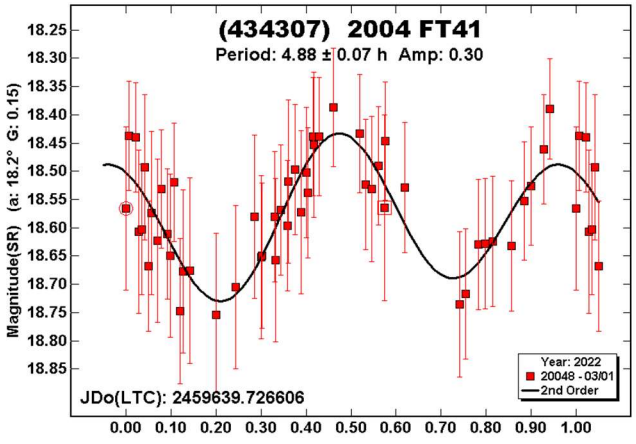

Acknowledgements

This work includes data from the Asteroid Terrestrial-impact Last Alert System (ATLAS) project. ATLAS is primarily funded to search for near earth asteroids through NASA grants NN12AR55G, 80NSSC18K0284, and 80NSSC18K1575; byproducts of the NEO search include images and catalogs from the survey area. The ATLAS science products have been made possible through the contributions of the University of Hawaii Institute for Astronomy, the Queen's University Belfast, the Space Telescope Science Institute, and the South African Astronomical Observatory. The authors gratefully acknowledge Shoemaker NEO Grants from the Planetary Society (2007, 2013). These were used to purchase some of the telescopes and CCD cameras used in this research.

References

ALCDEF (2020). Asteroid Lightcurve Data Exchange Format database. *http://www.alcdef.org/*

AstDys-2 (2020). Asteroids - Dynamic web site. *https://newton.spacedys.com/astdys/*

Behrend, R. (2001web, 2019web) Observatoire de Geneve web site. *http://obswww.unige.ch/~behrend/page_cou.html*

Bembrick, C.; Richards, T.; Allen, B.; Bolt, G. (2008). "Minor Planet 6411 Tamaga." *Minor Planet Bull.* **35**, 138.

Benishek, V. (2017). "Lightcurves and Rotation Periods for Six Asteroids." *Minor Planet Bull.* **44**, 67-69.

Brinsfield, J.W. (2008). "Asteroid Lightcurve Analysis at the Via Capote Observatory: First Quarter 2008." *Minor Planet Bull.* **35**, 119-122.

Chang, C.-K.; Lin, H.-W.; Ip, W.-H.; Prince, T.A.; Kulkarni, S.R.; Levitan, D.; Laher, R.; Surance, J.; (2016). "Large Super-fast Rotator Hunting Using the Intermediate Palomar Transient Factory." *Ap. J. Supp.* **227**, A20.

Ďurech, J.; Sidorin, V.; Kaasalainen, M. (2020). "Asteroid models reconstructed from ATLAS photometry." *Astron. Astrophys*. **643**, A59.

Erasmus, N.; Navarro-Meza, S.; McNeill, A.; Trilling, D.E.; Sickafoose, A.A.; Denneau, L.; Flewelling, H.; Heinze, A.; Tonry, J.L. (2020). "Do Slivan states exist in the Flora family? I. Photometric survey of the Flora region." *Astrophys. J.* **247**, A13.

Harris, A.W.; Young, J.W.; Scaltriti, F.; Zappala, V. (1984). "Lightcurves and phase relations of the asteroids 82 Alkmene and 444 Gyptis." *Icarus* **57**, 251-258.

Harris, A.W.; Young, J.W.; Contreiras, L.; Dockweiler, T.; Belkora, L.; Salo, H.; Harris, W.D.; Bowell, E.; Poutanen, M.; Binzel, R.P.; Tholen, D.J.; Wang, S. (1989). "Phase relations of high albedo asteroids: The unusual opposition brightening of 44 Nysa and 64 Angelina." *Icarus* **81**, 365-374.

Higgins, D.; Pravec, P.; Kusnirak, P.; Hornoch, K.; Brinsfield, J.W.; Allen, B.; Warner, B.D. (2008). "Asteroid Lightcurve Analysis at Hunters Hill Observatory and Collaborating Stations: November 2007 - March 2008." *Minor Planet Bull.* **35**, 123-126.

Kaasalainen, M.; Torppa J. (2001). "Optimization Methods for Asteroid Lightcurve Inversion. I. Shape Determination." *Icarus* **153**, 24-36.

Kaasalainen, M.; Torppa J.; Muinonen, K. (2001). "Optimization Methods for Asteroid Lightcurve Inversion. II. The Complete Inverse Problem." *Icarus* **153**, 37-51.

Masiero, J.; Jedicke, R.; Ďurech, J.; Gwyn, S.; Denneau, L.; Larsen, J. (2009). "The Thousand Asteroid Light Curve Survey." *Icarus* **204**, 145-171.

Nesvorny, D. (2015). "Nesvorny HCM Asteroids Families V3.0." NASA Planetary Data Systems, id. EAR-A-VARGBET-5-NESVORNYFAM-V3.0.

Nesvorny, D.; Broz, M.; Carruba, V. (2015). "Identification and Dynamical Properties of Asteroid Families." In *Asteroids IV* (P. Michel, F. DeMeo, W.F. Bottke, R. Binzel, Eds.). Univ. of Arizona Press, Tucson, also available on astro-ph.

Pál, A.; Szakáts, R.; Kiss, C.; Bódi, A.; Bognár, Z.; Kalup, C.; Kiss, L.L.; Marton, G.; Molnár, L.; Plachy, E.; Sárneczky, K.; Szabó, G.M.; Szabó, R. (2020). "Solar System Objects Observed with TESS - First Data Release: Bright Main-belt and Trojan Asteroids from the Southern Survey." *Ap. J.* **247**, A26.

Pravec, P.; Wolf, M.; Sarounova, L. (2007web, 2008web). *http://www.asu.cas.cz/~ppravec/neo.htm*

Skiff, B.A.; McLelland, K.P.; Sanborn, J.J.; Pravec, P.; Koehn, B.W. (2019). "Lowell Observatory Near-Earth Asteroid Photometric Survey (NEAPS): Paper 4." *Minor Planet Bull.* **46**, 458-503.

Stephens, R.D. (2016). "Asteroids Observed from CS3: 2015 July - September." *Minor Planet Bull.* **43**, 52-56.

Stephens, R.D. (2017). "Asteroids Observed from CS3: 2016 - September." *Minor Planet Bull*. **44**, 49-52.

Stephens, R.D. (2018). "Asteroids Observed from CS3: 2017 October - December." *Minor Planet Bull*. **45**, 135-137.

Stephens, R.D.; Warner, B.D. (2020). "Main-belt Asteroids Observed from CS3: 2020 January to March." *Minor Planet Bull.* **47**, 224-230.

Stephens, R.D.; Warner, B.D. (2021a). "Main-belt Asteroids Observed from CS3: 2020 July to September." *Minor Planet Bull.* **48**, 56-69.

Stephens, R.D.; Warner, B.D. (2021b). "Main-belt Asteroids Observed from CS3: 2020 October to December." *Minor Planet Bull.* **48**, 150-158.

Tonry, J.L.; Denneau, L.; Flewelling, H.; Heinze, A.N.; Onken, C.A.; Smartt, S.J.; Stalder, B.; Weiland, H.J.; Wolf, C. (2018). "The ATLAS All-Sky Stellar Reference Catalog." *Astrophys. J.* **867**, A105.

Warner, B.D. (2008a). "Asteroid Lightcurve Analysis at the Palmer Divide Observatory: September - December 2007." *Minor Planet Bull.* **35**, 67-71.

Warner, B.D. (2008b). "Asteroid Lightcurve Analysis at the Palmer Divide Observatory: February - May 2008." *Minor Planet Bull*. **35**, 163-166.

Warner, B.D. (2010). "Asteroid Lightcurve Analysis at the Palmer Divide Observatory: 2009 June - September. *Minor Planet Bull*. **37**, 24-27.

Warner, B.D. (2014a). "Asteroid Lightcurve Analysis at CS3-Palmer Divide Station: 2014 January - March." *Minor Planet Bull.* **41**, 144-155.

Warner, B.D. (2014b). "Asteroid Lightcurve Analysis at CS3-Palmer Divide Station: 2014 March - June." *Minor Planet Bull.* **41**, 235-241.

Warner, B.D. (2017). "Asteroid Lightcurve Analysis at CS3-Palmer Divide Station: 2016 July - September." *Minor Planet Bull.* **44**, 12-19.

Warner, B.D.; Harris, A.W.; Pravec, P. (2009). "The Asteroid Lightcurve Database." *Icarus* **202**, 134-146. Updated 2021 May. *http://www.minorplanet.info/lightcurvedatabase.html*

Warner, B.D.; Pravec, P.; Kusnirak, P.; Harris, A.W. (2012). "A Trio of Tumbling Hungaria Asteroids." *Minor Planet Bull*. **39**, 89-92.

Waszczak, A.; Chang, C.-K.; Ofek, E.O.; Laher, R.; Masci, F.; Levitan, D.; Surace, J.; Cheng, Y.-C.; Ip, W.-H.; Kinoshita, D.; Helou, G.; Prince, T.A.; Kulkarni, S. (2015). "Asteroid Light Curves from the Palomar Transient Factory Survey: Rotation Periods and Phase Functions from Sparse Photometry." *Astron. J.* **150**, A75.

LIGHTCURVES OF EIGHT ASTEROIDS

Eric V. Dose
3167 San Mateo Blvd NE #329
Albuquerque, NM 87110
mp@ericdose.com

(Received: 2022 April 15)

We present lightcurves, synodic rotation periods, and G value (H-G) estimates for eight asteroids.

We present asteroid lightcurve photometry results, continuing in efforts to measure lightcurves with lower amplitude and generally longer periods. The lightcurves were obtained by following the workflow process described by Dose (2020), with later improvements (Dose, 2021). This workflow applies to each image an ensemble of typically 20-60 nearby ATLAS refcat2 catalog (Tonry et al., 2018) comparison ("comp") stars as a basis for asteroid photometry. Diagnostic plots and the numerous comp stars allow for rapid identification and removal of outlier, variable, and poorly measured comp stars.

Our custom workflow produces a time series of asteroid magnitude estimates on Sloan r' (SR) catalog basis, unreduced and without H-G adjustment. These magnitudes are imported directly into *MPO Canopus* software (Warner, 2021) where they are adjusted for distances and phase-angle dependence, fit by Fourier analysis including identifying and ruling out of aliases, and plotted. Phase-angle dependence is corrected with a H-G model, using the *G* value that minimizes best-fit RMS error across all nights' data.

No nightly zero-point adjustments (DeltaComps in *MPO Canopus* terminology) were made to any session herein, other than by adjusting the G value (H-G phase model). All lightcurve data herein have been submitted to ALCDEF.

Lightcurve Results

Eight asteroids were observed (to February 15) from Deep Sky West observatory (IAU V28) at 2210 meters elevation in northern New Mexico, and (from February 16) from New Mexico Skies observatory at 2310 meters elevation in southern New Mexico. Images were acquired with a 0.35-meter SCT reduced to f/7.7; a SBIG STXL-6303E camera cooled to -35 C and fitted with a Clear filter or Exoplanet/Blue Blocker (BB) filter (Astrodon); and a PlaneWave L-500 mount. The equipment was operated remotely via *ACP software* (DC-3 Dreams, version 8.3), running plan files generated for each night by the author's python scripts (Dose, 2020). Observations usually cycled among 2-4 asteroids. Exposure times targeted 3-4 millimagnitudes uncertainty in asteroid instrumental magnitude, subject to a minimum exposure of 150 seconds to ensure suitable comp-star photometry, and to a maximum of 900 seconds. All exposures were autoguided.

FITS images were plate-solved by *PinPoint* (DC-3 Dreams) or *TheSkyX* (Software Bisque) and were calibrated using temperature-matched, median-averaged dark images and recent flat images of a flux-adjustable flat panel. Every photometric image was visually inspected; the author excluded all images with poor tracking, obvious interference by cloud or moon, or having stars, satellite tracks, cosmic ray artifacts, or other apparent light sources within 10 arcseconds of the target asteroid. Photometry-ready images that pass these screens were submitted to the workflow.

Number	Name	yyyy mm/dd	Phase	L_{PAB}	B_{PAB}	Period(h)	P.E.	Amp	A.E.	Grp
275	Sapientia	2022 04/02-04/09	10.8,7.9	211	6	14.935	0.007	0.10	0.02	MB-O
396	Aeolia	2021-2 12/22-01/30	9.0,17.2	65	0	14.353	0.001	0.34	0.02	MB-M
837	Schwarzschilda	2021-2 11/15-01/25	*10.2,22.4	71	-8	103.432	0.036	0.39	0.05	MB-I
953	Painleva	2021-2 11/16-04/15	*15.4,17.3	107	10	24.884	0.002	0.29	0.04	MB-O
1541	Estonia	2022 02/09-04/04	*13.0,10.5	171	1	6.444	0.001	0.15	0.04	MB-O
2069	Hubble	2021-2 12/02-02/09	*19.2,9.4	122	11	44.765	0.011	0.26	0.05	MB-O
3167	Babcock	2022 02/09-03/09	9.3,16.5	127	18	15.398	0.002	0.36	0.04	MB-I
3835	Korolenko	2021-2 11/26-02/14	*9.9,24.1	74	-16	20.104	0.004	0.15	0.03	EUN

Table I. Observing circumstances and results. The phase angle is given for the first and last date. If preceded by an asterisk, the phase angle reached an extremum during the period. L_{PAB} and B_{PAB} are the approximate phase angle bisector longitude/latitude at mid-date range (see Harris et al., 1984). Grp is the asteroid family/group (Warner et al., 2009).

Early in the work presented here, we adopted an exoplanet/BB filter in place of our previously used Clear filter. The BB filter, a yellow long-wavelength-transmitting filter with relatively sharp cut-off, requires only a modest first-order transform to the standard Sloan r' passband — second-order terms were near zero. By contrast, Clear filters required much larger and second-order transforms coefficients. With the BB filter's smaller and simpler transforms, our night-to-night reproducibility improved, and this advantage has outweighed any loss of signal-to-noise ratio. Indeed, during moonlit nights the BB filter removed so much skyglow that our S/N ratio loss was small or negligible; during moonless nights the loss was perhaps 10-15% relative to images in a Clear filter.

In this work, "period" refers to an asteroid's synodic rotation period unless otherwise noted, "SR" denotes the Sloan r' passband, and "mmag" denotes millimagnitudes (0.001 mag).

275 Sapientia. Previously published synodic rotation periods for this relatively low-amplitude, outer main-belt asteroid, have differed widely (> 20 h, Denchev, 2000; 24.07 h, Behrend, 2006web; 14.766 h, Warner, 2007; 9.5 h, Kaminski, 2009; 14.931 h, Pilcher, 2015; 14.932 h, Pilcher, 2016), which is notable for such a bright and low-numbered asteroid. We closely confirm both results of Pilcher and approximately confirm Warner's result with our new determination of 14.935±0.007 h. Our Fourier fit RMS error is 5 mmag, and our best estimate of G value (H-G) is 0.16.

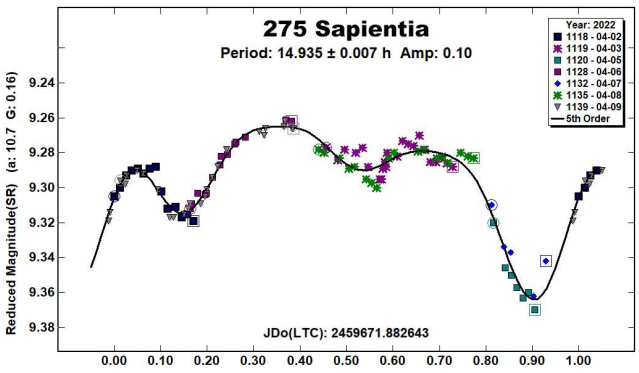

Our period spectrum disfavors previously published period solutions near 9.5 h and 24 h.

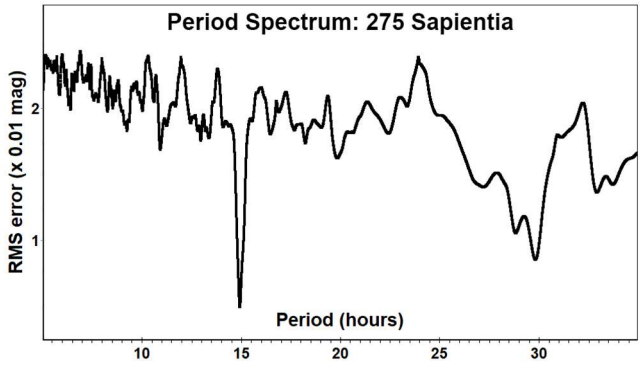

396 Aeolia. This main-belt asteroid, largest member of the Aeolia family of asteroids, is found to have synodic rotation period of 14.353±0.001 h, in agreement with one previous result (14.353 h, Pilcher, 2017) and consistent with another (> 12 h, Lagerkvist, 1978), but at variance with two other results having lower (less certain) LCDB uncertainty scores (21.27 h, Behrend, 2011web; 21.27 h, Behrend, 2020web). Our best G value (H-G) is 0.16; Fourier fit RMS error is 9 mmag.

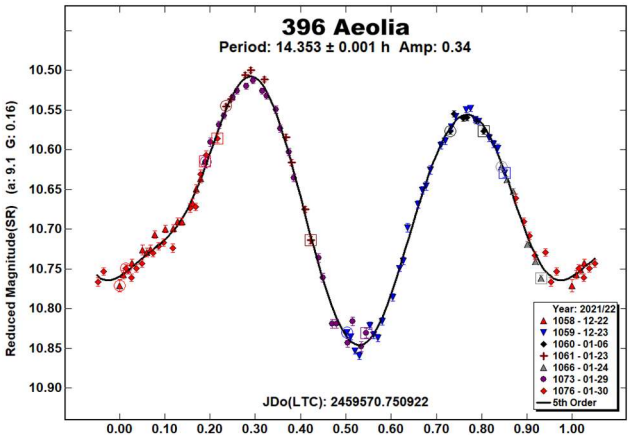

Our period spectrum disfavors the previously published 21.27 h solution, which is close to an alias of our result by ½ period per 24 hours.

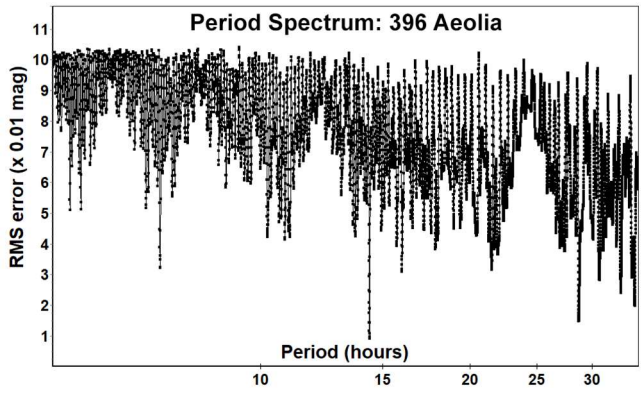

837 Schwarzschilda. This inner main-belt asteroid was found to have rotation period of 103.432±0.036 h, confirming one previously published result (103.595 h, Ďurech, 2019), but differing from two others (24 h, Behrend 2005web; 82.7469 h, Pál, 2020). Our Fourier fit RMS error is 19 mmag; our best estimate of G is 0.49.

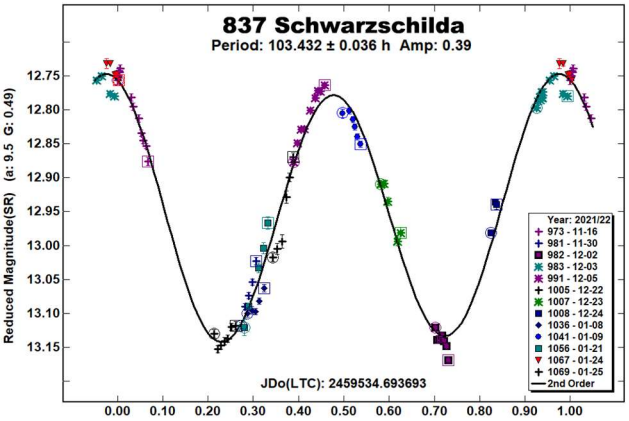

Our period spectrum, built from 13 nights' data, confirms the Ďurech result but strongly disfavors previously published solutions near 24 h and 83 h. A monomodal interpretation of about 51.7 h would be allowed by the lightcurve and period spectrum, but is unlikely given the relatively large amplitude of 0.39 magnitudes.

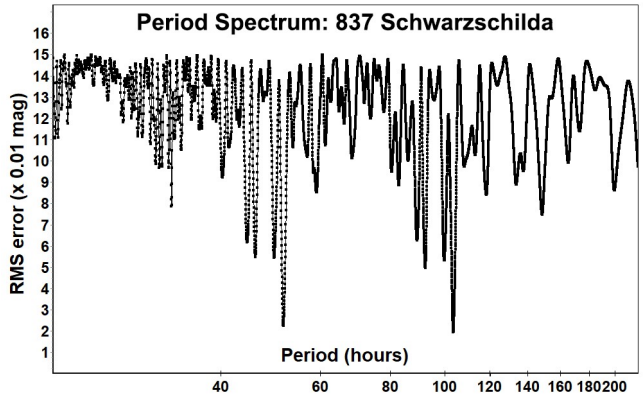

953 Painleva. For this outer main-belt asteroid we find a rotation period of 24.884±0.002 h, in reasonable agreement with two recent survey results (24.8809 h, Ďurech, 2020; 24.9759 h, Pál, 2020), but differing from two other published results (10 h, Behrend, 2006web; 7.389 h, Schmidt, 2015). Our lightcurve construction and Fourier fits benefited from a much higher amplitude of 0.29 magnitude than those previously reported (0.04-0.1 mag). Our lightcurve is clearly bimodal, with Fourier fit RMS error 16 mmag and best G estimate of 0.36.

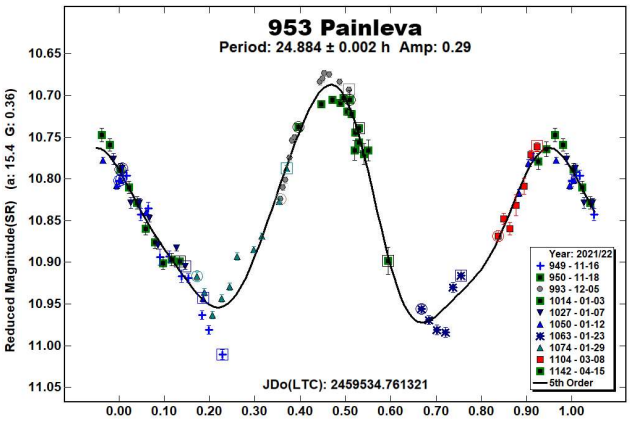

Our period spectrum, built from 10 nights' data over 5 months, disfavors previously published period solutions near 7.4 and 10 h; those periods are not easily explained as synodic, monomodal, or other multiple-based aliases of our result.

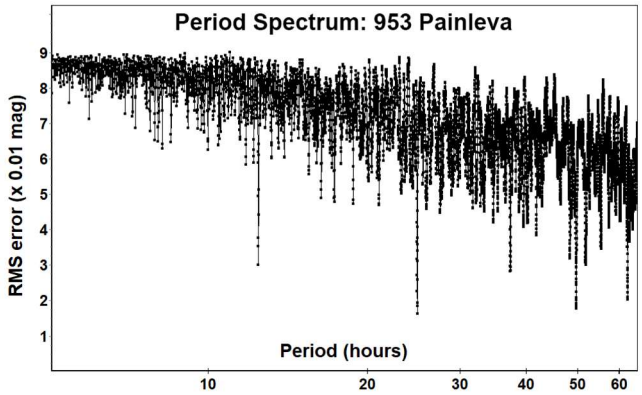

1541 Estonia. For this outer main-belt asteroid we find a synodic rotation period of 6.444±0.001 h, interpreted as a monomodal lightcurve. This differs from one previous result (10.1 h, Behrend, 2015web), but agrees with another (12.86 h, Polakis, 2021) when both lightcurves are interpreted as bimodal. Our Fourier fit RMS error is 12 mmag; our best G estimate is 0.14.

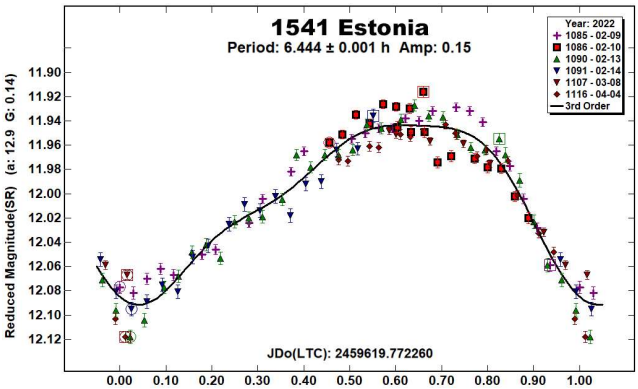

Our period spectrum does not credibly allow for a rotation period near 5 or 10 hours. The previously published 10.1 h solution is close to a ½ period per 24-hour alias of our result interpreted as bimodal.

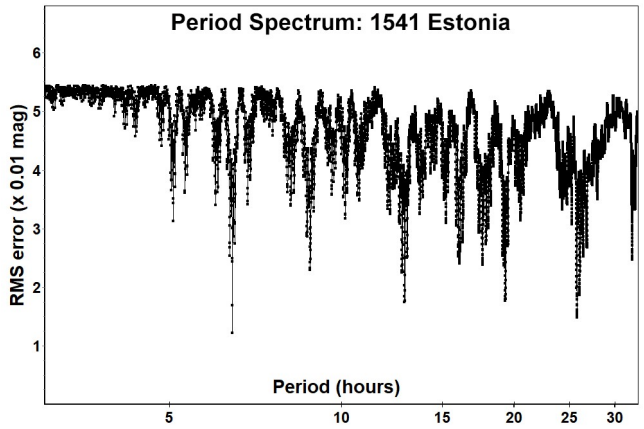

The split-halves phased plot does not strongly support a bimodal interpretation, but it also does not rule out a physical rotation period equal to the bimodal period of 12.889 h.

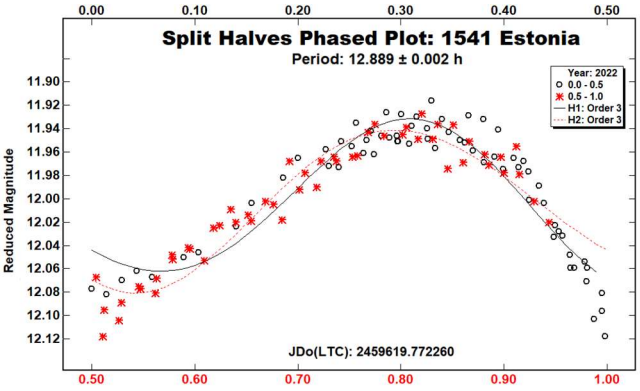

2069 Hubble. For this outer main-belt asteroid, we find a rotation period of 44.765±0.011 h, differing from one known published report (32.52 h, Warner, 2005). Our Fourier fit RMS error is 14 mmag, and our best G value estimate is 0.06. Though our lightcurve suffers from a few gaps in phase, we have 12 nights' observations, including at least two nights' observations at or very near to each minimum and maximum.

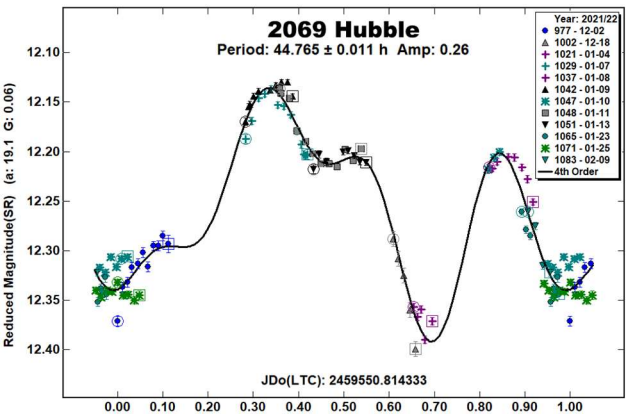

Our period spectrum disfavors solutions near the published 32.62 h result, which we cannot explain as either a synodic-based or multiple-based alias of our result.

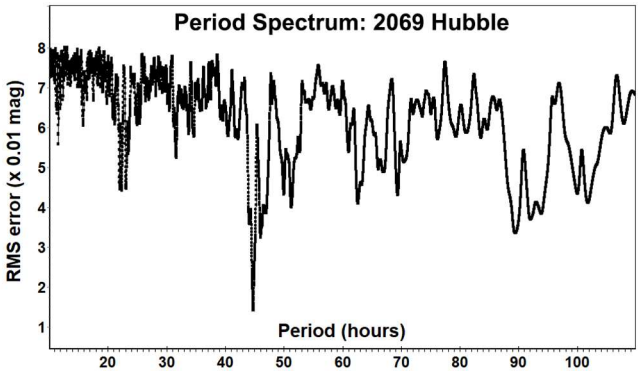

3167 Babcock. For this inner main-belt asteroid, we find a rotation period of 15.398±0.002 h, in agreement with most previously published results (15.45 h, Gross, 2005; 15.4016 h, Ďurech, 2020; 15.4721 h, Pál, 2020), but differing from one other (11.63 h, Behrend, 2006web). Our Fourier fit RMS error is 14 mmag, and our best G estimate is 0.20.

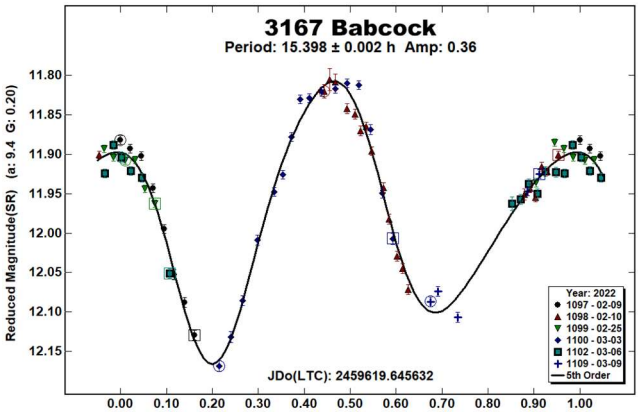

Our period spectrum disfavors rotational periods solutions near 11.6 h, which is almost exactly a ½ period per 24 alias of our proposed rotational period.

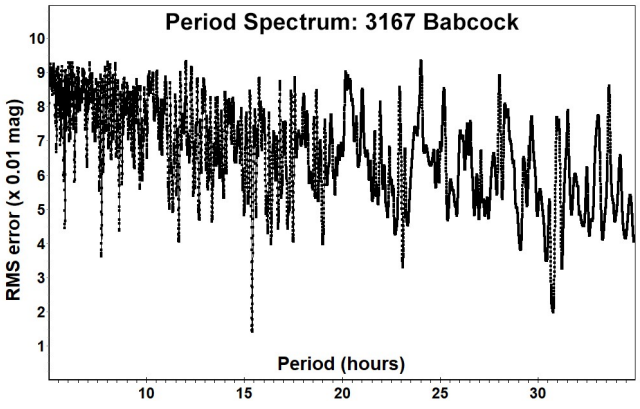

3835 Korolenko. For this Eunomia-family asteroid, we find a rotational period of 20.104±0.004 h. We know of no previously published period determinations. The lightcurve is clearly bimodal. Fourier fit RMS error is 16 mmag, and our best estimate of G is 0.20.

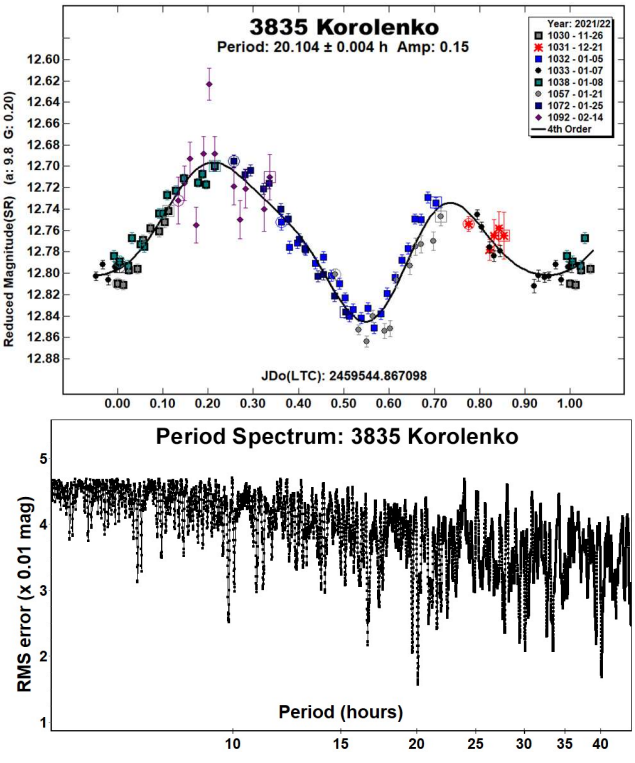

Acknowledgements

The author thanks all authors of the ATLAS paper (Tonry et al, 2018) and its numerous contributors for providing openly and without cost the ATLAS refcat2 catalog release. This project makes extensive use of the python language interpreter and of several supporting packages (notably: astropy, ccdproc, ephem, matplotlib, pandas, photutils, requests, and statsmodels), all made available openly and without cost.

The author thanks Jim Seargeant for his skilful help in relocating the author's observing equipment.

References

Behrend, R. (2005web, 2006web, 2011web, 2015web, 2020web). Observatoire de Genève web site. *http://obswww.unige.ch/~behrend/page_cou.html*

Denchev, P. (2000). "Photometry of 11 asteroids during their 1998 and 1999 apparitions." *Planet. Space Sci.* **48**, 987-992.

Dose, E.V. (2020). "A New Photometric Workflow and Lightcurves of Fifteen Asteroids." *Minor Planet Bull.* **47**, 324-330.

Dose, E.V. (2021). "Lightcurves of Nineteen Asteroids." *Minor Planet Bull.* **48**, 69-76.

Ďurech, J.; Hanuš, J.; Vančo, R. (2019). "Inversion of asteroid photometry from Gaia DR2 and the Lowell Observatory photometry database." *Astron. Astrophys.* **631**, A2.

Ďurech, J.; Tonry, J.; Erasmus, N.; Denneau, L.; Heinze, A.N.; Flewelling, H.; Vančo, R. (2020). "Asteroid models reconstructed from ATLAS photometry." *Astron. Astrophys.* **643**, A59.

Gross, J. (2003). "Sonoran Skies Observatory Lightcurve Results for Asteroids 1054, 1390, 1813, 1838, 2988, 3167, 4448, and 5262." *Minor Planet Bull.* **30**, 44-46.

Harris, A.W.; Young, J.W.; Scaltriti, F.; Zappalà, V. (1984). "Lightcurves and phase relations of the asteroids 82 Alkmene and 444 Gyptis." *Icarus* **57**, 251-258.

Kaminski, L.J.; Leake, M.A.; Berget, D.J (2009). "Differential Photometry and Lightcurve Analysis for Numbered Asteroids 229, 275, 426, 557, 613, 741, 788, 872, 907, and 5010." *J. Southern Assoc. Res. Astron.* **3**, 25-31.

Lagerkvist, C.-I. (1978). "Photographic Photometry of 110 Main-Belt Asteroids." *Astrophys. J. Suppl. Series* **31**, 361-381.

Pál, A.; Szakáts, R.; Kiss, C.; Bódi, A.; Bognár, Z.; Kalup, C.; Kiss, L.L.; Marton, G.; Molnár, L.; Plachy, E.; Sárneczky, K.; Szabó, G.M.; Szabó, R. (2020). "Solar System Objects Observed with TESS - First Data Release: Bright Main-belt and Trojan Asteroids from the Southern Survey." *Astrophys. J. Suppl. Series* **247**, 26.

Pilcher, F. (2015). "Rotation Period Determinations for 275 Sapientia, 309 Fraternitas, and 924 Toni." *Minor Planet Bull.* **42**, 38-39.

Pilcher, F. (2016). "Rotation Period Determinations for 269 Justitia, 275 Sapientia, 331 Etheridgea, and 509 Fulvia." *Minor Planet Bull.* **43**, 135-136.

Pilcher, F. (2017). "Rotation Period Determinations for 396 Aeolia, 398 Admete, 422 Berolina, and 555 Norma." *Minor Planet Bull.* **44**, 112-114.

Polakis, T. (2021). "Period Determinations for Seventeen Minor Planets." *Minor Planet Bull.* **48**, 158-163.

Schmidt, R.E. (2015). "NIR Minor Planet Photometry from Burleith Observatory: 2014 February-June." *Minor Planet Bull.* **42**, 1-3.

Tonry, J.L.; Denneau, L.; Flewelling, H.; Heinze, A.N.; Onken, C.A.; Smartt, S.J.; Stalder, B.; Weiland, H.J.; Wolf, C. (2018). "The ATLAS All-Sky Stellar Reference Catalog." *Astrophys. J.* **867,** A105.

Warner, B.D. (2005). "Asteroid Lightcurve Analysis at the Palmer Divide Observatory - Winter 2004-2005." *Minor Planet Bull.* **32**, 54-58.

Warner, B.D.; Harris, A.W.; Pravec, P. (2009). "The asteroid lightcurve database." *Icarus* **202**, 134-146. Updated 2022 April. *https://minplanobs.org/MPInfo/php/lcdb.php*

Warner, B.D. (2021). *MPO Canopus* Software, version 10.8.4.11. BDW Publishing. *http://www.bdwpublishing.com*

ON CONFIRMED AND SUSPECTED BINARY ASTEROIDS OBSERVED AT THE CENTER FOR SOLAR SYSTEM STUDIES: 2022 FEBRUARY AND MARCH

Brian D. Warner
Center for Solar System Studies
446 Sycamore Ave.
Eaton, CO 80615 USA
brian@MinorPlanetObserver.com

Robert D. Stephens
Center for Solar System Studies
Rancho Cucamonga, CA 91730

(Received: 2022 April 10)

Analysis of CCD photometric observations of three dynamical members of the Hungaria family and one inner main-belt asteroid were made in 2022 February and March at the Center for Solar System Studies.

Observations of three members of the Hungaria dynamical family (Nesvorny, 2015; Nesvorny et al., 2015) and one inner main-belt asteroid were made at the Center for Solar System Studies in 2022 February and March. Either a 0.35-m *f*/9.1 Schmidt-Cassegrain and FLI Microline CCD camera or a 0.5-m *f*/8.1 Ritchey-Chretien and FLI Proline CCD camera was used to acquire images. Both cameras use a KAF-1001E chip, which has a 1024×1024×24m array of pixels. The combination gives a field-of-view of about 26×26 arcminutes and image scale of 1.5 arcsec/pixel for the smaller telescope and 20×20×1.2" for the larger one. The analysis of our data follows.

All lightcurve observations were unfiltered since a clear filter can cause a 0.1-0.3 mag loss. The exposure duration varied depending on the asteroid's brightness and sky motion. Guiding on a field star sometimes resulted in a trailed image for the asteroid.

Measurements were made using *MPO Canopus*. The Comp Star Selector utility in *MPO Canopus* found up to five comparison stars of near solar-color for differential photometry. To reduce the number of adjusted nightly zero points and their amounts, the analysis of the data used the ATLAS catalog r´ (SR) magnitudes (Tonry et al., 2018). The rare zero-point adjustments of ≥ ±0.03 mag may be related in part to using unfiltered observations, poor centroiding of the reference stars, not correcting for second-order extinction, or selecting a star that is an unresolved pair.

The Y-axis values are ATLAS SR "sky" (catalog) magnitudes. The two values in the parentheses are the phase angle (a) and the value of *G* used to normalize the data to the comparison stars used in the earliest session. This, in effect, corrected all the observations to seem to have been made at a single fixed date/time and phase angle, leaving any variations due only to the asteroid's rotation and/or albedo changes. The X-axis shows rotational phase from -0.05 to 1.05. If the plot includes the amplitude, e.g., "Amp: 0.65", this is the amplitude of the Fourier model curve and *not necessarily the adopted amplitude for the lightcurve*.

References to previous works were taken from the asteroid lightcurve database (Warner et al., 2009), known as "LCDB" from here on. Since most listed rotation periods for the primary were very similar, only a few of the LCDB references have been used.

4464 Vulcano. We observed this Hungaria several times in the past. Each time, the period was found to be close to 3.2 h and never with any indication of there being a satellite.

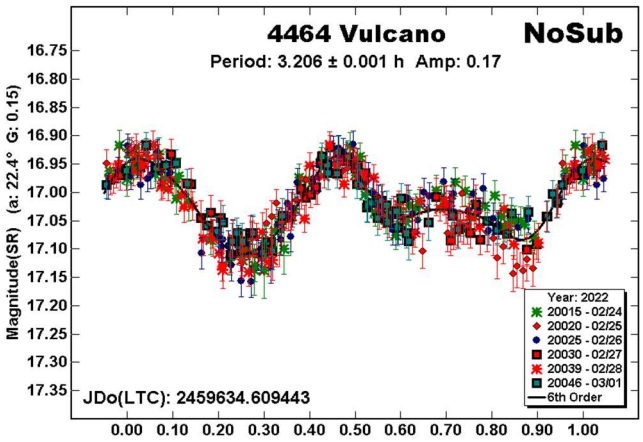

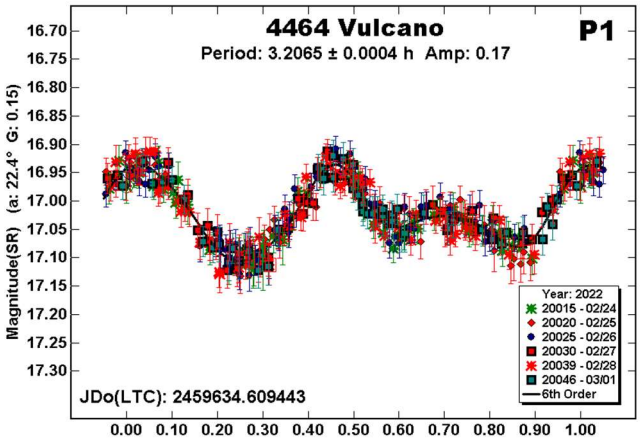

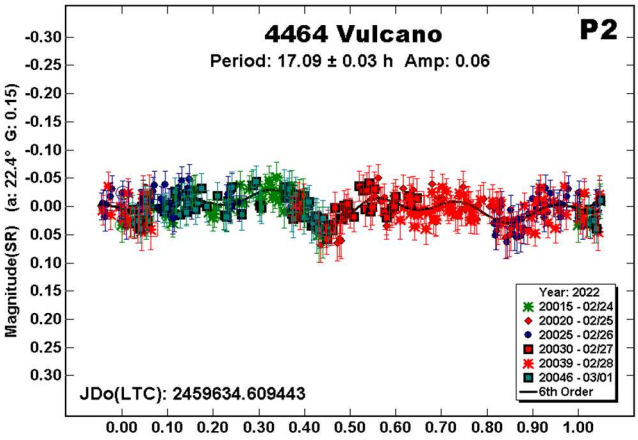

The 2022 data were taken near phase angle bisector longitude (L_{PAB}; Harris et al., 1984) 120°. The past observations were at different longitudes, but some differing by only 20° (of the actual or diametric opposite longitude). Assuming the analysis is correct, that was just enough difference to allow shallow mutual events to be seen. In this case, leading to a satellite-to-primary effective diameter ratio of Ds/Dp ~ 0.14. This is about the limit of detection by lightcurve photometry alone.

The proposed primary and orbital periods are in-line with other small binary asteroids. Future high-precision observations are encouraged.

(16562) 1992 AV1. There are several, disparate results found in the LCDB: Warner (2011, 12.251 h), Warner (2014, 20.18 h), Warner (2017a, 3.219 h), and Warner (2017b, 34.85 h; revised analysis of 2014). It may be surprising, or not, that the results from 2022 have near integral ratio relationships with the earlier results.

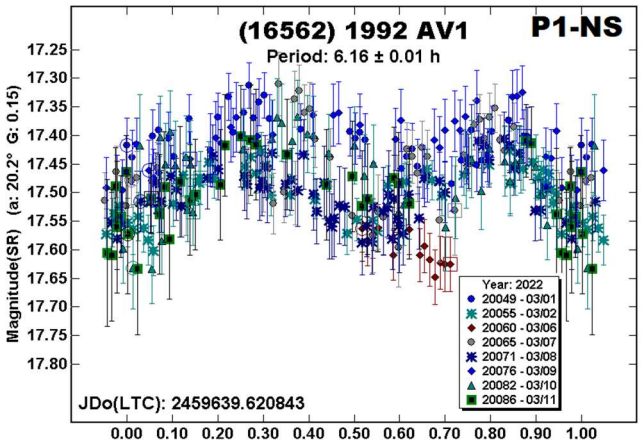

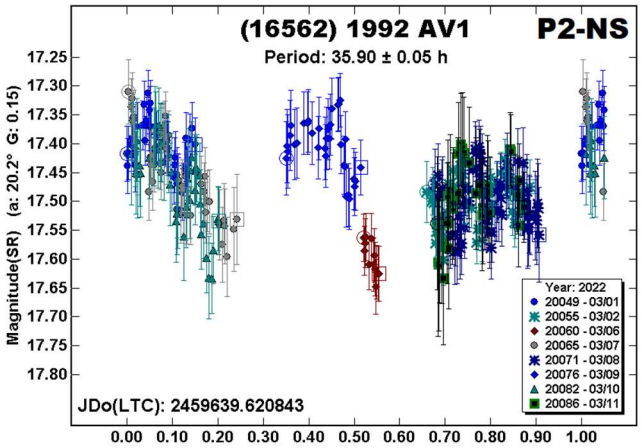

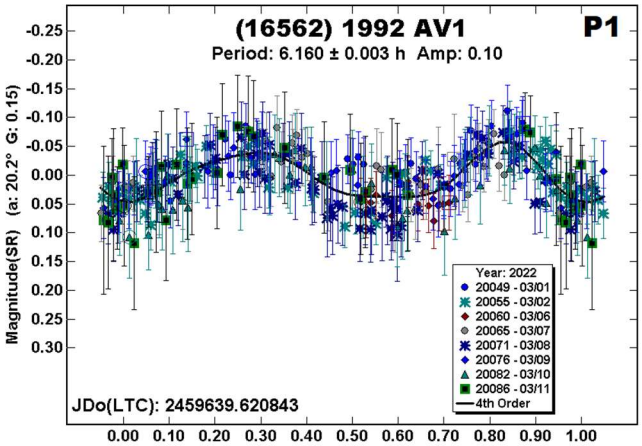

What seems certain is that the 2022 data were the result of two periods. The "NS" (no subtraction of another period) shows the results of searching for two periods independently. The nightly data showed signs of a shorter period while a raw plot of the full data set showed that a longer period might also be possible.

The final dual-period search gave P_1 = 6.160 h and P_2 = 35.90 h. The two periods are related by a close-to integral ratio of 21:11. This may have some dynamical meaning but as far as "simple" aliased periods in Fourier analysis, it doesn't seem significant. The proposed P_2 is close to the one reported in Warner (2017a). Both are hard to establish reliably with data from a single station since they have a nearly 3:2 ratio with an Earth-day. The next two apparitions with V < 17.5 are 2023 August (16.8, –38°) and 2025 April (17.3, +34°).

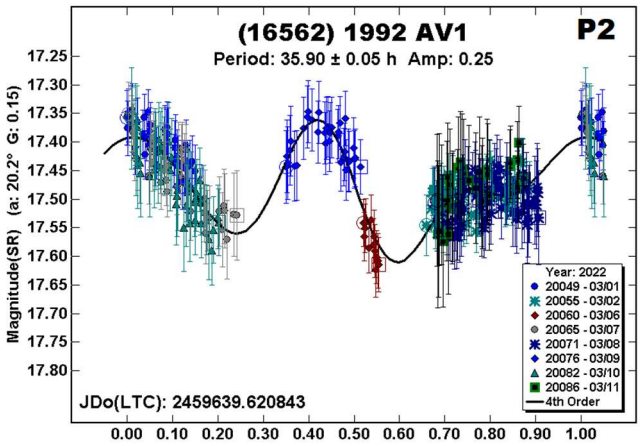

(35783) 1999 JU20. Waszczak et al. (2015) found a period of 40.650 h based on somewhat sparse data from the Palomar Transient Factory. Our result is considerably different.

We initially thought that the period might be < 5 h and so confined the search to that limit. This gave the periods shown in "P1-A" through "P1-C." However, a longer period began to present itself and so the search concentrated on a range of 12-20 h. This led to the "P2" lightcurve, which bears strong resemblance to one produced by a fully-synchronous binary.

Assuming that is so, then the satellite-to-primary effective diameter ratio is Ds/Dp ≥ 0.44 ± 0.04 and what's labeled here as "P2" should really be "P1."

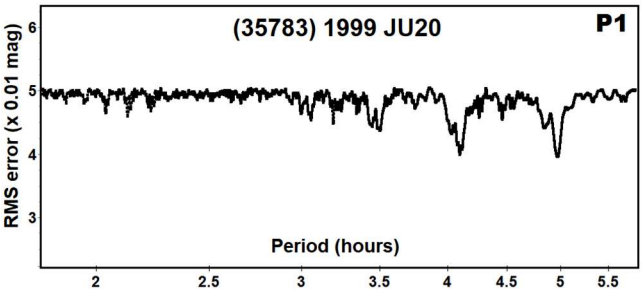

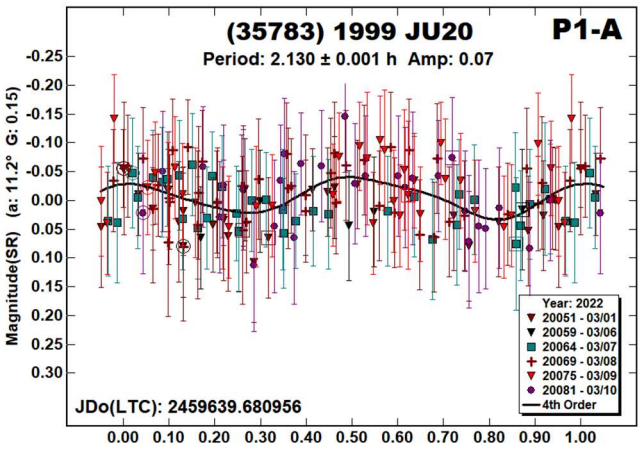

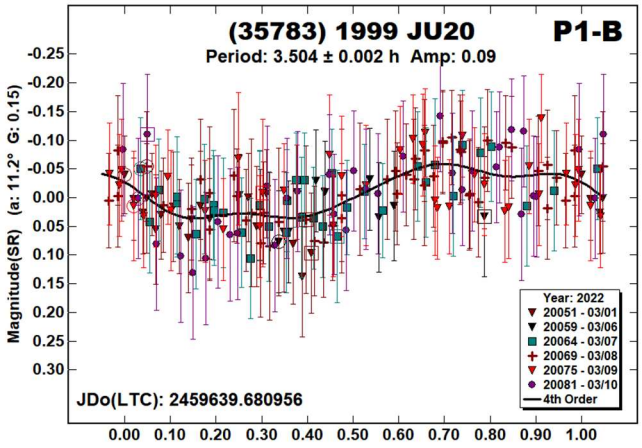

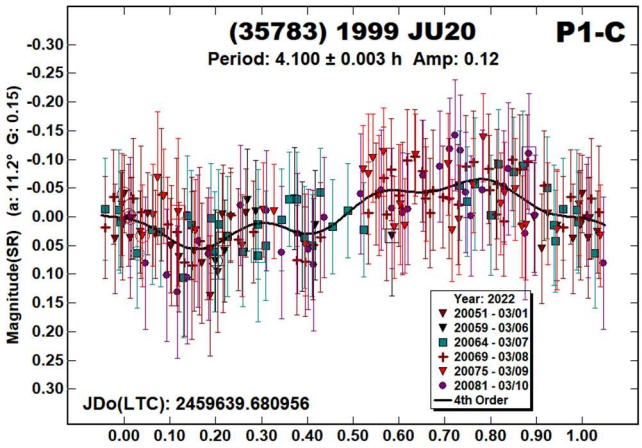

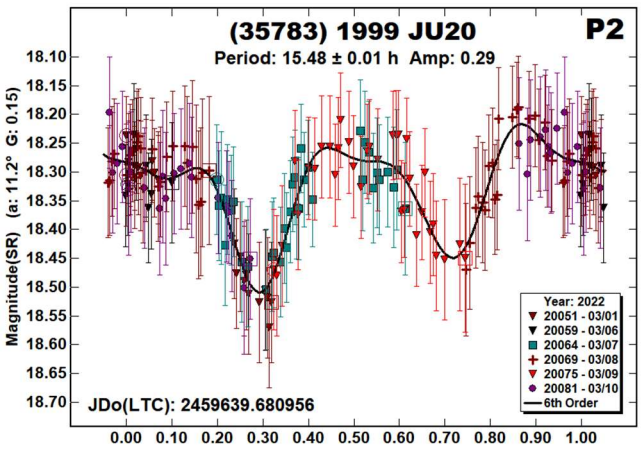

Assuming 15.48 h is the "primary period," the three short-period lightcurves may be nothing more than the Fourier analysis interpreting noise as a real signal with the two longer periods being harmonically related to the shortest one of 2.130 h.

(49669) 1999 RZ30. The only previously reported period is 3.119 h (Warner, 2016) with a substantial amplitude of 0.26 mag. The 2022 data were dominated by a seemingly much longer period near 50 h. Given observing conditions, data from a single station, and the longer period being nearly commensurate with an Earth-day, we were not able to get a complete lightcurve.

As an exercise, we tried a dual-period search in *MPO Canopus*, forcing the search to a range between 3.0-3.5 h. We did find one solution close to the earlier result but the noise was as large as the amplitude, making the solution highly questionable.

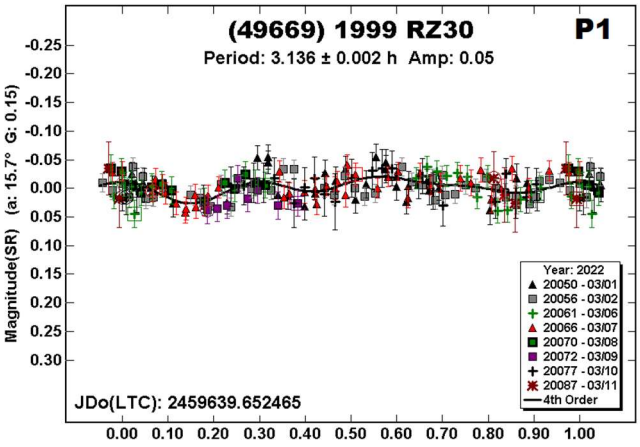

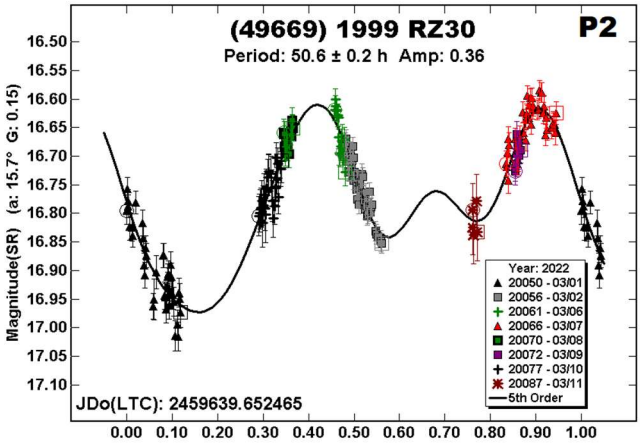

The 2022 data were obtained at L_{PAB} 138° while those in 2015 were at L_{PAB} 10° (190° for the diametric opposite). This is often enough of a difference to reveal *mutual events* or significantly different amplitudes. Looking ahead, the 2023 September (16.9, +22°) and 2025 April (16.6, –43°) apparitions are the next good chances for small-telescope photometry. After that, Northern observers will have to wait until 2030 February for another good opportunity (16.4, +27°).

Number	Name	2022 mm/dd	Phase	L_{PAB}	B_{PAB}	Period(h)	P.E.	Amp	A.E.	Grp/DsDp
4464	Vulcano	02/24-03/01	22.4,23.5	120	23	3.2065	0.0004	0.17	0.02	H (003)
						17.09	0.03	0.06	0.01	≥0.14
16562	1992 AV1	03/01-03/11	20.3,23.8	138	22	6.160	0.003	0.10	0.02	H (003)
						35.90	0.05	0.25	0.02	
35783	1999 JU20	03/01-03/10	11.3,14.5	135	4	15.48	0.01	0.29	0.03	MB-I (9104)
						[A1]2.130	0.001	0.07	0.03	0.44
						[A2]3.504	0.002	0.09	0.03	
						[A3]4.100	0.003	0.12	0.03	
49669	1999 RZ30	03/01-03/11	15.7,20.8	138	3	3.136	0.002	0.05	0.01	H (003)
						50.6	0.2	0.36	0.03	

Table II. Observing circumstances. [A1-A3] Ambiguous periods for the secondary period. The first line gives the primary or dominant period for the system. The additional line(s) give the secondary period(s). The phase angle (α) is given at the start and end of each date range. L_{PAB} and B_{PAB} are, respectively the average phase angle bisector longitude and latitude (see Harris et al.,1984). For the Grp/Dr column, the first line gives the group/family: H: Hungaria; MB-I: inner main-belt. See LCDB readme.pdf in the on-line download version for details on family/group numbers. Numbers above 9000 indicate an orbital group and so unlikely a member of a collisional family.

Acknowledgements

The authors gratefully acknowledge Shoemaker NEO Grants from the Planetary Society (2007, 2013). These were used to purchase some of the telescopes and CCD cameras used in this research. This work includes data from the Asteroid Terrestrial-impact Last Alert System (ATLAS) project. ATLAS is primarily funded to search for near earth asteroids through NASA grants NN12AR55G, 80NSSC18K0284, and 80NSSC18K1575; byproducts of the NEO search include images and catalogs from the survey area. The ATLAS science products have been made possible through the contributions of the University of Hawaii Institute for Astronomy, the Queen's University Belfast, the Space Telescope Science Institute, and the South African Astronomical Observatory. This paper made use of the services provided by the SAO/NASA Astrophysics Data System, which is operated by the Smithsonian Astrophysical Observatory under NASA Cooperative Agreement 80NSSC211M0056.

References

Harris, A.W.; Young, J.W.; Scaltriti, F.; Zappala, V. (1984). "Lightcurves and phase relations of the asteroids 82 Alkmene and 444 Gyptis." *Icarus* **57**, 251-258.

Nesvorny, D. (2015). "Nesvorny HCM Asteroids Families V3.0." NASA Planetary Data Systems, id. EAR-A-VARGBET-5-NESVORNYFAM-V3.0.

Nesvorny, D.; Broz, M.; Carruba, V. (2015). "Identification and Dynamical Properties of Asteroid Families." In *Asteroids IV* (P. Michel, F. DeMeo, W.F. Bottke, R. Binzel, Eds.). Univ. of Arizona Press, Tucson, also available on astro-ph.

Tonry, J.L.; Denneau, L.; Flewelling, H.; Heinze, A.N.; Onken, C.A.; Smartt, S.J.; Stalder, B.; Weiland, H.J.; Wolf, C. (2018). "The ATLAS All-Sky Stellar Reference Catalog." *Ap. J.* **867**, A105.

Warner, B.D. (2011). "Asteroid Lightcurve Analysis at the Palmer Divide Observatory: 2010 December - 2011 March." *Minor Planet Bull*. **38**, 142-149.

Warner, B.D. (2014). "Asteroid Lightcurve Analysis at CS3-Palmer Divide Station: 2014 January - March." *Minor Planet Bull*. **41**, 144-155.

Warner, B.D. (2016). "Asteroid Lightcurve Analysis at CS3-Palmer Divide Station: 2015 October - December" *Minor Planet Bull*. **43**, 137-140. (not listed in ADS).

Warner, B.D. (2017a). "Asteroid Lightcurve Analysis at CS3-Palmer Divide Station: 2017 April thru June." *Minor Planet Bull*. **44**, 289-294.

Warner, B.D. (2017b). "Near-Earth Asteroid Lightcurve at CS3-Palmer Divide Station: 2017 April thru June." *Minor Planet Bull*. **44**, 335-344.

Warner, B.D., Harris, A.W., Pravec, P. (2009). "The Asteroid Lightcurve Database." *Icarus* **202**, 134-146. Updated 2021 May. *http://www.minorplanet.info/lightcurvedatabase.html*

Waszczak, A.; Chang, C.-K.; Ofek, E.O.; Laher, R.; Masci, F.; Levitan, D.; Surace, J.; Cheng, Y.-C.; Ip, W.-H.; Kinoshita, D.; Helou, G.; Prince, T.A.; Kulkarni, S. (2015). "Asteroid Light Curves from the Palomar Transient Factory Survey: Rotation Periods and Phase Functions from Sparse Photometry." *Astron. J.* **150**, A75.

LIGHTCURVE ANALYSIS OF HILDA ASTEROIDS AT THE CENTER FOR SOLAR SYSTEM STUDIES: 2022 JANUARY-MARCH

Brian D. Warner
Center for Solar System Studies (CS3)
446 Sycamore Ave.
Eaton, CO 80615 USA
brian@MinorPlanetObserver.com

Robert D. Stephens
Center for Solar System Studies (CS3)
Rancho Cucamonga, CA

(Received: 2022 April 10)

CCD photometric observations of two Hilda asteroids were made between 2022 January through March. Analysis of the data for 1746 Brouwer produced a period in good agreement with previous results. The period for (7284) 1989 VW was ambiguous with possible solutions at 26.45 and 52.93 h.

CCD photometric observations of two Hilda asteroid were carried out at the Center for Solar System Studies (CS3) from 2021 September through December as part of an ongoing study of the family/group that is located between the outer main-belt and Jupiter Trojans in a 3:2 orbital resonance with Jupiter. The goal is to determine the spin rate statistics of the Hildas and to find pole and shape models when possible. We also look to examine the degree of influence that the YORP (Yarkovsky–O'Keefe–Radzievskii–Paddack) effect (Rubincam, 2000) has on distant objects and to compare the spin rate distribution against the Jupiter Trojans, which can provide evidence that the Hildas are more "comet-like" than main-belt asteroids.

Telescopes	Cameras
0.30-m *f*/6.3 Schmidt-Cass	FLI Microline 1001E
0.35-m *f*/9.1 Schmidt-Cass	FLI Proline 1001E
0.35-m *f*/11 Schmidt-Cass	SBIG STL-1001E
0.40-m f/10 Schmidt-Cass	
0.50-m *f*/8.1 Ritchey-Chrétien	

Table I. List of available telescopes and CCD cameras at CS3. The exact combination for each telescope/camera pair can vary due to maintenance or specific needs.

Table I lists the telescopes and CCD cameras that are combined to make observations. All the cameras use CCD chips from the KAF 1001 blue-enhanced family and so have essentially the same response. The pixel scales ranged from 1.24-1.60 arcsec/pixel. All lightcurve observations were unfiltered since a clear filter can result in a 0.1-0.3 magnitude loss. The exposures varied depending on the asteroid's brightness.

To reduce the number of times and amounts of adjusting nightly zero-points, the ATLAS catalog r´ (SR) magnitudes (Tonry et al., 2018) are used. Those adjustments are usually ≤ ±0.03 mag. The rare greater corrections may have been related in part to using unfiltered observations, poor centroiding of the reference stars, and not correcting for second-order extinction. Another cause may be selecting what appears to be a single star but is actually an unresolved pair.

The Y-axis values are ATLAS SR "sky" (catalog) magnitudes. The two values in the parentheses are the phase angle (a) and the value of *G* used to normalize the data to the comparison stars used in the earliest session. This, in effect, made all the observations seem to be made at a single fixed date/time and phase angle, leaving any variations due only to the asteroid's rotation and/or albedo changes. The X-axis shows rotational phase from -0.05 to 1.05. If the plot includes the amplitude, e.g., "Amp: 0.65", this is the amplitude of the Fourier model curve and *not necessarily the adopted amplitude for the lightcurve*.

For brevity, only some of the previous results are referenced. A more complete listing is in the asteroid lightcurve database (Warner et al, 2009; "LCDB" from here on).

1746 Brouwer. Dahlgren et al. (1998) reported a period of 19.8 h for this 64-km Hilda. Hanuš et al. (2016) determined a shape model with a retrograde spin direction and sidereal period of 19.7255 h, which was later refined by Martikainen et al. (2021). In our previous observations (Warner and Stephens, 2020), we found a period of 19.724 h.

Using the data from 2022, *MPO Canopus* found a synodic period of 19.763 h, which is in good – but not perfect – agreement with those earlier results, and a lightcurve that presented something other than a traditional bimodal shape.

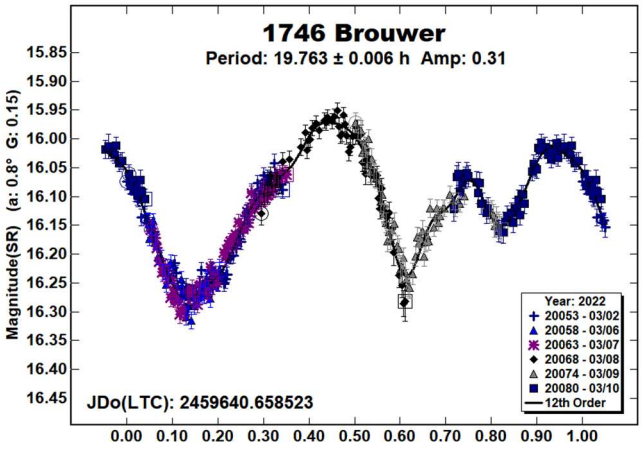

(7284) 1989 VW. Mainzer et al. (2019) used WISE data to find a diameter of 23.4 ± 1.6 km and albedo 0.080 ±0.02 using H = 11.5. The MPCORB orbital elements file (MPC, 2022) gives H = 11.72. Applying the correction outlined in Harris and Harris (1997) leads to D = 23.34 km and p_V = 0.0665 ± 0.0093, which are, effectively, the same as before. If nothing else, the low albedo is expected among the Hilda population.

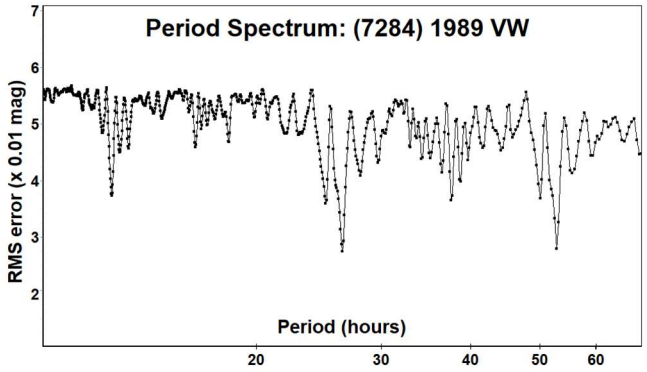

There were no previously-reported rotation periods in the LCDB, so we had little guidance when the analysis found two dominant periods. With low amplitudes and phase angles, assuming a bimodal

Number	Name	2021/mm/dd	Phase	L_{PAB}	B_{PAB}	Period(h)	P.E.	Amp	A.E.
1746	Brouwer	03/02-03/10	0.8,2.3	160	-3	19.763	0.006	0.31	0.02
7284	1989 VW	01/05-01/27	*15.9,15.9	67	2	[A]26.45	0.01	0.15	0.02
						52.93	0.02	0.16	0.02

Table II. Observing circumstances and results. [A]Preferred period of an ambiguous solution. The phase angle (α) is given at the start and end of each date range. The asterisk indicates that the phase angle reached an extremum over the span of the observations. L_{PAB} and B_{PAB} are the average phase angle bisector longitude and latitude (see Harris et al., 1984).

lightcurve is not always safe (Harris et al., 2014). We rejected the longer period of 52.93 h because it was too symmetrical about its two halves and seemed more a *fit by exclusion* (e.g., significant gaps in the lightcurve). The shorter period of 26.45 h is adopted for this work. An even shorter period of about 13.2 h was rejected because of the asymmetry of the lightcurve phased to 26.45 h.

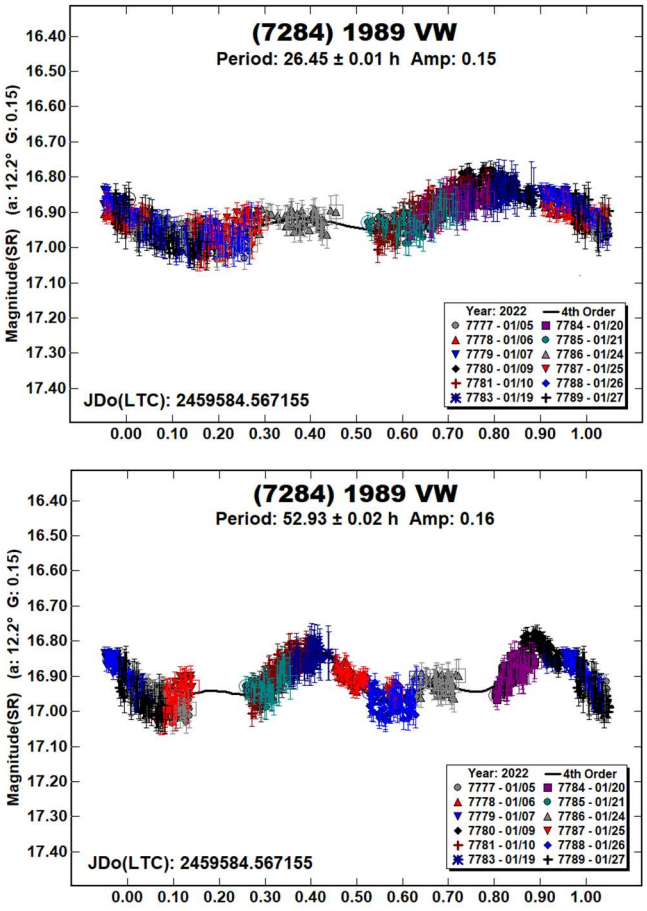

Acknowledgements

This work includes data from the Asteroid Terrestrial-impact Last Alert System (ATLAS) project. ATLAS is primarily funded to search for near earth asteroids through NASA grants NN12AR55G, 80NSSC18K0284, and 80NSSC18K1575; byproducts of the NEO search include images and catalogs from the survey area. The ATLAS science products have been made possible through the contributions of the University of Hawaii Institute for Astronomy, the Queen's University Belfast, the Space Telescope Science Institute, and the South African Astronomical Observatory. The authors gratefully acknowledge Shoemaker NEO Grants from the Planetary Society (2007, 2013). These were used to purchase some of the telescopes and CCD cameras used in this research.

References

Dahlgren, M.; Lahulla, J.F.; Lagerkvist, C.-I.; Lagerros, J.; Mottola, S.; Erikson, A.; Gonano-Beurer, M.; Di Martino, M. (1998). "A Study of Hilda Asteroids. V. Lightcurves of 47 Hilda Asteroids." *Icarus* **133**, 247-285.

Hanuš, J.; Ďurech, J.; Oszkiewicz, D.A.; Behrend, R.; Carry, B.; Delbo, M.; Adam, O.; Afonina, V.; Anquetin, R.; Antonini, P.; and 159 coauthors. (2016). "New and updated convex shape models of asteroids based on optical data from a large collaboration network." *Astron. Astrophys.* **586**, A108.

Harris, A.W.; Harris, A.W. (1997). "On the Revision of Radiometric Albedos and Diameters of Asteroids." *Icarus* **126**, 450-454.

Harris, A.W.; Young, J.W.; Scaltriti, F.; Zappala, V. (1984). "Lightcurves and phase relations of the asteroids 82 Alkmene and 444 Gyptis." *Icarus* **57**, 251-258.

Harris, A.W.; Pravec, P.; Galad, A.; Skiff, B.A.; Warner, B.D.; Vilagi, J.; Gajdos, S.; Carbognani, A.; Hornoch, K.; Kusnirak, P.; Cooney, W.R.; Gross, J.; Terrell, D.; Higgins, D.; Bowell, E.; Koehn, B.W. (2014). "On the maximum amplitude of harmonics on an asteroid lightcurve." *Icarus* **235**, 55-59.

Mainzer, A.; Bauer, J.; Cutri, R.; Grav, T.; Kramer, E.; Masiero, J.; Sonnett, S.; Wright, E., Eds., NEOWISE Diameters and Albedos V2.0. NASA Planetary Data System, 2019. *https://doi.org/10.26033/18S3-2Z54*.

Martikainen, J.; Muinonen, K.; Penttila, A.; Cellino, A.; Wang, X.-B. (2021), "Asteroid absolute magnitudes and phase curve parameters from Gaia photometry." *Astron. Astrophys*. **649**, A98.

MPC (2022). Minor Planet Center MPCORB data file. *https://minorplanetcenter.net/iau/MPCORB.html*

Rubincam, D.P. (2000). "Relative Spin-up and Spin-down of Small Asteroids." *Icarus* **148**, 2-11.

Tonry, J.L.; Denneau, L.; Flewelling, H.; Heinze, A.N.; Onken, C.A.; Smartt, S.J.; Stalder, B.; Weiland, H.J.; Wolf, C. (2018). "The ATLAS All-Sky Stellar Reference Catalog." *Astrophys. J.* **867**, A105.

Warner, B.D.; Stephens, R.D. (2020). "Lightcurve Analysis of Hilda Asteroids at the Center for Solar System Studies: 2019 November." *Minor Planet Bull*. **47**, 123-124.

Warner, B.D.; Harris, A.W.; Pravec, P. (2009). "The Asteroid Lightcurve Database." *Icarus* **202**, 134-146. Updated 2021 June. *http://www.minorplanet.info/lightcurvedatabase.html*

PERIODS DETERMINATIONS FOR SEVENTEEN ASTEORIDS

Rafael González Farfán (Z55)
Observatorio Uraniborg
Écija, Sevilla, SPAIN
uraniborg16@gmail.com

Faustino García de la Cuesta (J38)
La Vara, Valdés,
Asturias, SPAIN

Jesús Delgado Casal (Z73)
Observatorio Nuevos Horizontes
Camas, Sevilla, SPAIN

Esteban Reina Lorenz (232)
Masquefa, Can Parellada
Barcelona, SPAIN

Javier Ruiz Fernández (J96)
Observatorio de Cantabria
Cantabria, SPAIN

Javier De Elías Cantalapiedra (L46)
Observatorio en Majadahonda
Madrid, SPAIN

Ramón Naves Nogues (213)
Observatorio Montcabrer
Cabrils, SPAIN

José M. Fernández. Andújar (Z77)
Observatorio Inmaculada del Molino
Sevilla, SPAIN

Juan-Luis González Carballo (I84)
Observatorio Cerro del Viento
Badajoz, SPAIN

Esteban Fernández Mañanes (Y90)
Observatorio Estelia
Ladines, Asturias, SPAIN

Raúl Martínez Morales
Observatorio de Serón
Serón, Almería, SPAIN

(Received: 2022 Apr 11)

The lightcurves for seventeen asteroids were measured from later months of 2020 to April 2022: 54 Alexandra (7.026 h), 161 Athor (7.213 h), 272 Antonia (3.854 h), 281 Lucretia (4.349 h), 302 Clarissa (14.467 h), 311 Claudia (10.446 h), 441 Bathilde (10.446 h), 554 Peraga (13.721 h), 893 Leopoldina (12.597 h), 915 Cosette (4.467 h), 934 Thuringia (8.165 h), 975 Perseverantia (7.222 h), 1090 Sumida (2.712 h), 1781 Van Biesbroeck (6.385 h), 3103 Eger (5.712 h), 5256 Farquhar (11.536 h), and 6655 Nagahama (5.224 h).

All observations reported here were unfiltered. The images were calibrated in the standard way (bias, darks and flats). Images were measured and periods analysis was done using *FotoDif* (2021) and *Periodos* (2020) packages. All data were light-time corrected. The results are summarized below. Individual lightcurve plots along additional comments as required are also presented.

In all cases we wanted to update the data of these asteroids. Some of them had not been reviewed since 2005-2006, or even older. In some cases, the old data were not sure, so we considered it was necessary to make new observations.

54 Alexandra (A858 RA) is a carbonaceous asteroid from the asteroid belt that was discovered by German-French astronomer Hermann Goldschmidt on 1858 September 10. There are many references about Alexandra in the literature. One of more recent is Behrend (2019web). Our data were taken in 2022 January 25 to February 2. We found $P = 7.026 \pm 0.005$ h and A = 0.13 ± 0.01 mag, which agrees with previous results. There is a model from 2013 on the DAMIT web site. (*https://astro.troja.mff.cuni.cz/projects/damit/*).

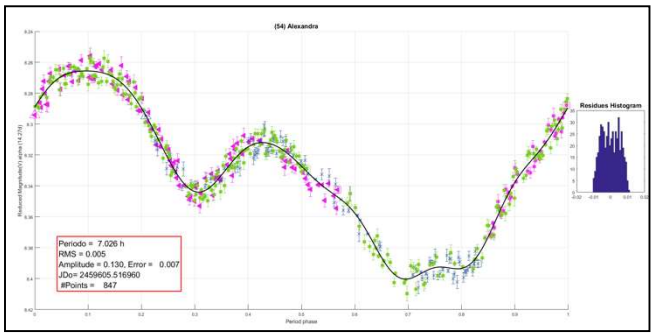

161 Athor (A876 HA) is a stony asteroid that is classified as a near-Earth and potentially hazardous asteroid. It belongs to the Aten group and measures approximately 210 meters in diameter. It was discovered by American astronomer Charles Kowal in 1976 at Palomar Observatory. We studied this asteroid on January 2022 10-20 and found $P = 7.213 \pm 0.008$ h, $A = 0.13 \pm 0.01$ mag. Franco et al. (2012) found a similar result of $P = 7.280$ h.

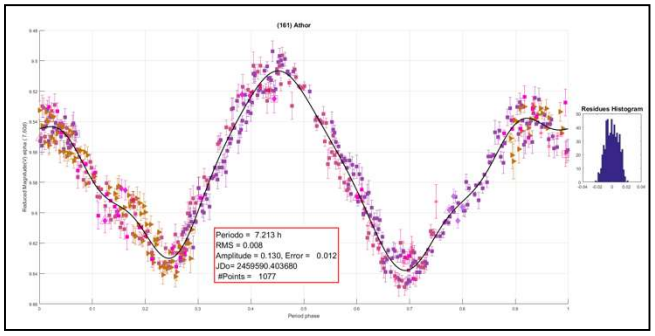

272 Antonia (A888 CA) is an asteroid that is part of the main-belt. It was discovered by Auguste H. Charlois on 1888 February 4 at Niza Observatory. We found few references on this asteroid. One the more recent is Hanuš et. al (2013) and Pilcher (2008) who reported $P = 3.85$ h. Our data were taken in 2022 January 13-28 and lead to a very similar result of $P = 3.854 \pm 0.006$ h, $A = 0.42 \pm 0.01$ mag. There is a model for 272 Antonia in DAMIT database.

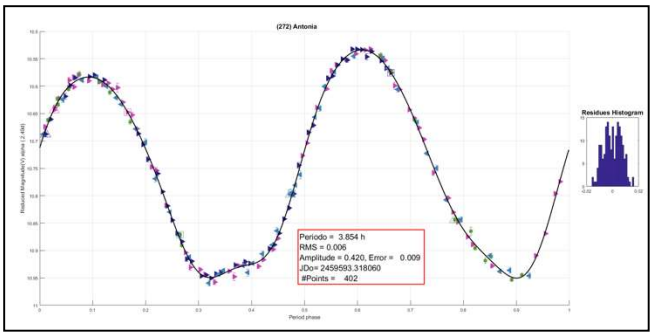

281 Lucretia. (A888 UC) is an asteroid belonging to the Flora family in the main-belt. It was discovered by Johann Palisa on 1888 October 31 in Vienna. We found the first reference on Lucretia to be to Taylor et al. (1976). The latest one is Hanuš et al. (2013), although there is only one set of observations in ALCDEF (2022) by Hopkins. We measured P = 4.349 ± 0.005 h, A = 0.32 ± 0.01 mag using data obtained 2022 January 10-28.

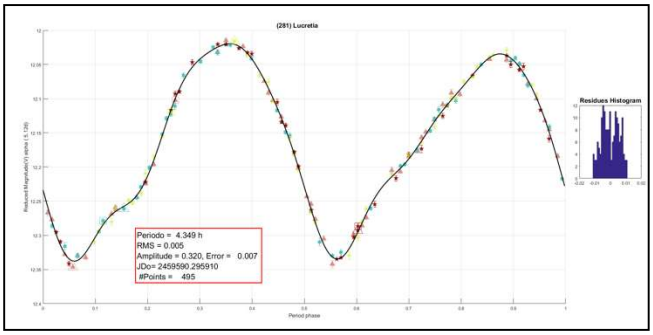

302 Clarissa (A884 MA) was discovered by the French astronomer Auguste Charlois on 1890 November 14 in Nice. At one time, it was considered as a possible fly-by target for the Cassini spacecraft, but was later rejected. Our observations were made in 2021 December 5-30 and we got P = 14.467 ± 0.004 h, A = 0.60 ± 0.01 mag, which agrees with previous results.

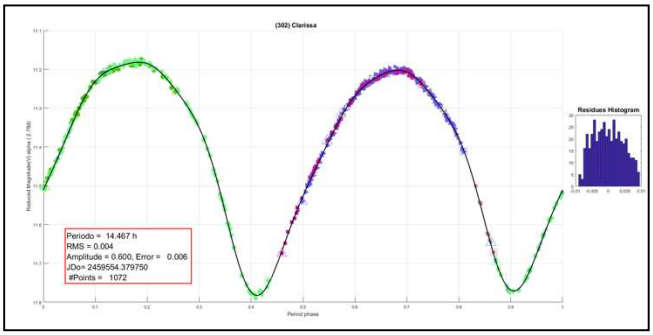

311 Claudia (A891 LA). We observed this main-belt asteroid from 2020 October 31 and November 11. We found P = 5.533 ± 0.011 h, A = 0.58 ± 0.02 mag, which is in good agreement with other periods found in the LCDB.

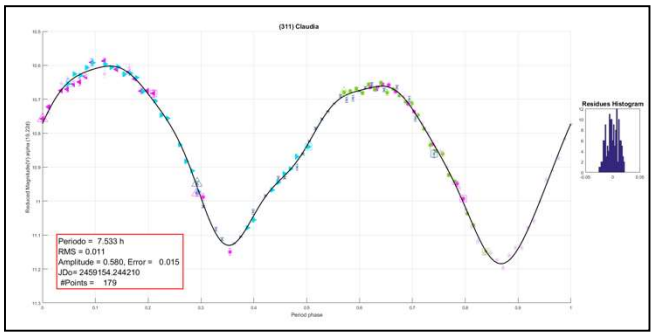

441 Bathilde (A898 XA) is a large main-belt asteroid that was discovered by French astronomer Auguste Charlois on 1898 December 18 in Nice. It is orbiting close to a 5:2 mean motion resonance with Jupiter, which is located at 2.824 AU. In 2006, Behrend (2006web) reported a provisional period P = 10.44 h. The same value we found in the LCDB. Our measurement based on data from 2022 January 8-25, is P = 10.446 ± 0.004 h, A = 0.14 ± 0.01 mag. So, it seems that period has not changed significantly. There is a model in the DAMIT database.

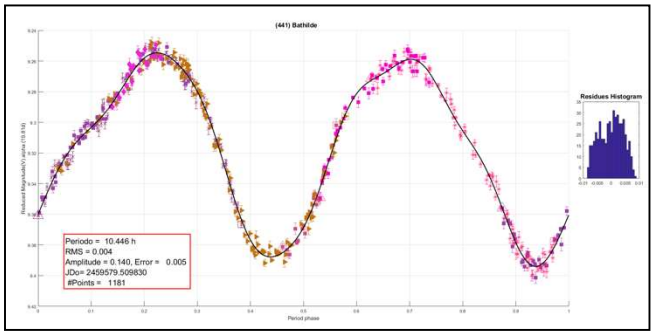

554 Peraga (A905 AE) was discovered by German astronomer Paul Götz on 1905 January 8 from Heidelberg. Radar observations of this asteroid from the Arecibo Observatory between 1980 and 1985 were used to produce a diameter estimate of 101 km. We observed Peraga in 2022 February 6-22. Analysis produced P = 13.721 ± 0.008 h, A = 0.25 ± 0.01 mag, which agrees with previous results (e.g., Higgins et al., 2007).

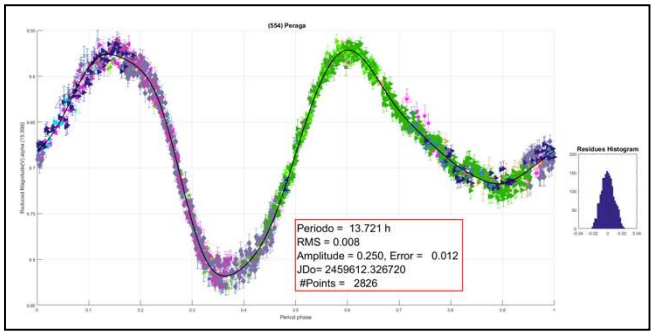

893 Leopoldina (A918 KD). Warner (2005) reported P = 10.51 h for Leopoldina. However, six years later, he found a new measurement of P = 14.115 h. We observed Leopoldina for nine nights, from 2021 October 27 to December 13, and we found P = 12.597 ± 0.005 h, A = 0.32 ± 0.01 mag. The lightcurve fits pretty well to our data.

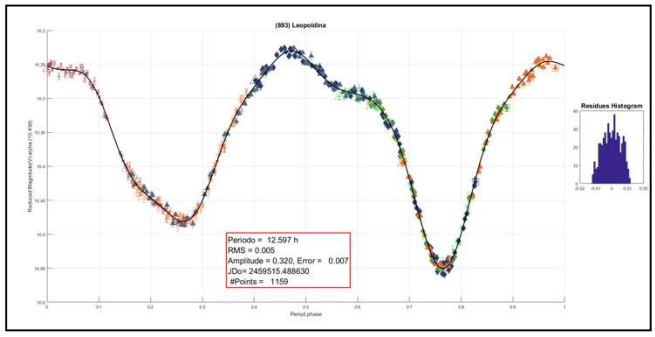

915 Cosette (A918 XB) is an S-type asteroid belonging to the Flora family of main-belt asteroids. We worked Cossete from 2021 December 11-13 at different observatories. We got P = 4.467 ± 0.006 h, A = 0.59 ± 0.01 mag, which is in good accordance with previous results.

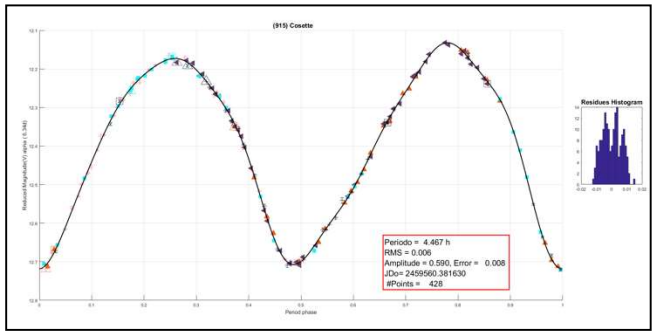

934 Thuringia. (A920 PA). The latest observation on Thuringia we found was by Behrend (2022web), who gives P = 8.165 h. At the same time, from 2021 December 30 to 2022 January 13, we found a similar result of P = 8.165 ± 0.005 h, A = 0.500 ± 0.01 mag. There is a model for Thuringia in DAMIT database.

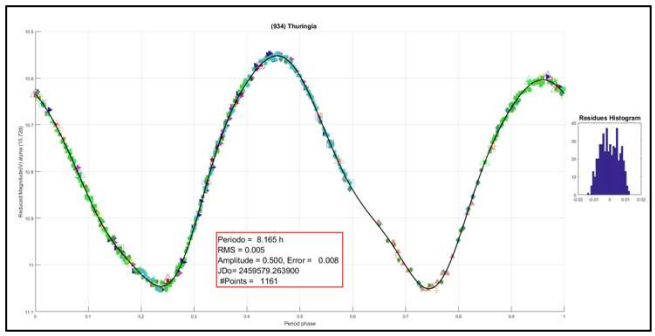

975 Perseverantia (A922 FE) was discovered by Austrian astronomer Johann Palisa on 1922 March 27. This is a member of the Koronis dynamical family of asteroids, meaning that they likely formed as the result of a collisional breakup of a parent body. In 2006, Behrend (2006web) reported P = 7.267 h and a possibility it is a binary asteroid. The LCDB gives the same period. We studied Perseverantia for ten nights from 2022 February 23 to April 6 and found a period of P = 7.222 ± 0.015 h, A = 0.25 ± 0.02 mag.

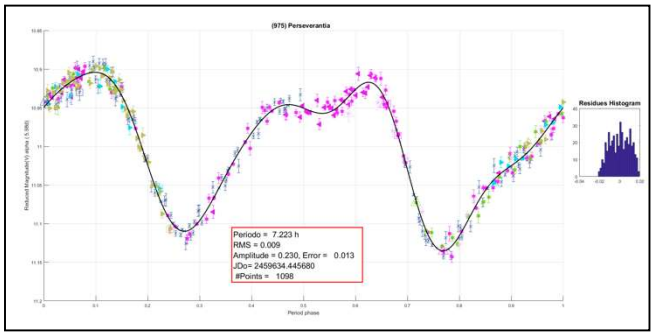

1090 Sumida (1928 DG). We worked on Sumida from 2022 February 14 to 22. We found P = 2.712 ± 0.012 h, A = 0.38 ± 0.04 mag, which is very close to previous results (Blake and Himeno, 2018).

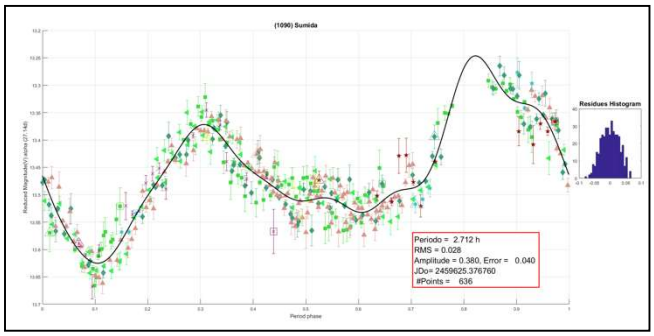

1781 Van Biesbroeck (A906 UB) is a Vesta asteroid that is approximately 8.5 kilometers in diameter. It was discovered on 1906 October 17 by German astronomer A. Kopff at Heidelberg Observatory in southern Germany. There are not many recent observations on this asteroid reported in the literature. We worked on Van Biesbroeck from 2021 November 3-10 at different observatories. We found P = 6.385 ± 0.012 h, A = 0.38 ± 0.02 mag, in good agreement with previous results in the LCDB.

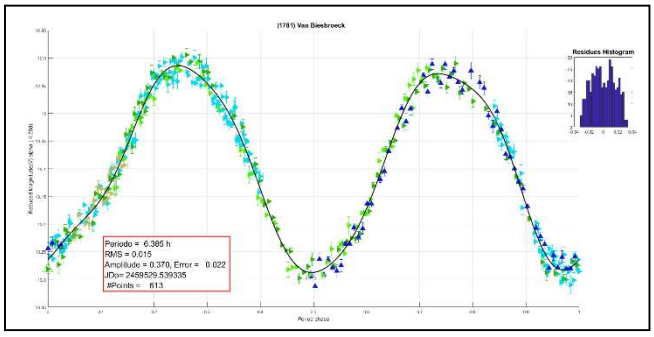

Number	Asteroid	20yy mm/dd	Phase	Period(h)	P.E.	Amp	A.E.
54	Alexandra	22/01/25-22/02/02	14.4-12.7	7.026	0.005	0.130	0.007
161	Athor	22/01/10-22/01/20	7.7-6.5	7.213	0.008	0.130	0.012
272	Antonia	22/01/13-22/01/28	2.5-6.6	3.854	0.006	0.420	0.009
281	Lucretia	22/01/10-22/01/28	5.1-12.7	4.349	0.005	0.320	0.007
302	Clarissa	21/12/05-21/12/30	2.8-5.5	14.467	0.004	0.600	0.006
311	Claudia	20/10/31-20/11/11	19.2-19.8	7.533	0.011	0.580	0.015
441	Bathilde	22/01/08-22/01/25	19.9-13.9	10.446	0.004	0.140	0.005
554	Peraga	22/02/06-22/02/22	15.9-25.2	13.721	0.008	0.250	0.012
893	Leopoldina	21/10/27-21/12/13	10.5-15.4	12.597	0.005	0.320	0.007
915	Cosette	21/12/11-21/12/13	6.2-7.0	4.467	0.006	0.590	0.008
934	Thuringia	21/12/30-22/01/13	10.7-15.3	8.165	0.005	0.500	0.008
975	Perseverantia	22/02/23-22/04/06	5.2-11.9	7.222	0.015	0.250	0.021
1090	Sumida	22/01/14-22/02/22	27.1-31.3	2.712	0.012	0.380	0.004
1781	Van Biesbroeck	21/09/10-21/10/13	4.8-0.7	6.385	0.012	0.380	0.016
3103	Eger	22/01/30-22/02/27	23.4-20.8	5.712	0.032	0.900	0.045
5256	Farquhar	21/11/01-21/12/05	11.2-21.2	11.536	0.008	0.210	0.011
6655	Nagahama	21/12/14-21/12/30	3.5-9.9	5.224	0.009	0.140	0.013

Table I. Observing circumstances and results. Phase is the solar phase angle given at the start and end of the date range. If preceded by an asterisk, the phase angle reached an extrema during the period.

3103 Eger (1982 BB). The most recent data about Eger we have found is Warner (2017; 5.71 h). We studied this asteroid from 2022 January 30 to February 27 at different observatories. Our data analysis, P = 5.712 ± 0.032 h, A = 0.90 ± 0.05 mag, is in good agreement with earlier results.

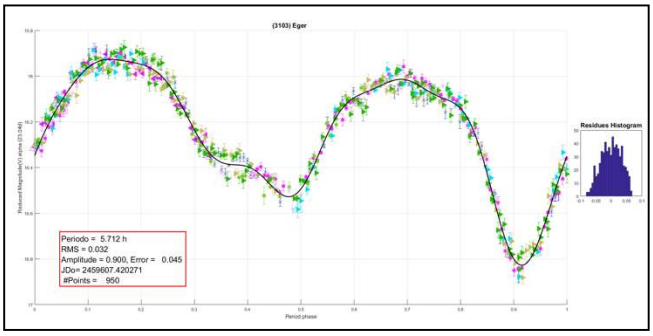

5256 Farquhar (1982 BB). There are contradicting results for Farquhar in the literature, so it was necessary for a deeper study. We worked on Farquhar from 2021 November 1 to December 5 at different observatories. The lightcurve shape could suggest it being a binary asteroid, although there are no mentions of it in any report. We conclude P = 11.536 ± 0.008 h and A = 0.21 ± 0.01 mag.

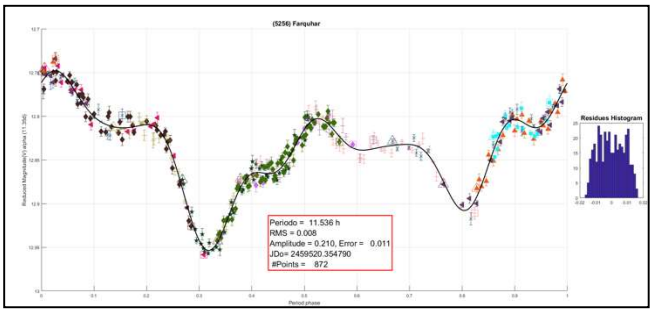

6655 Nagahama (1992 EL1). There is no a sure period of Nagahama among the few previous results. Our data were taken from 2021 December 14-30 and we conclude P = 5.224 ± 0.009 h, A = 0.14 ± 0.01 mag.

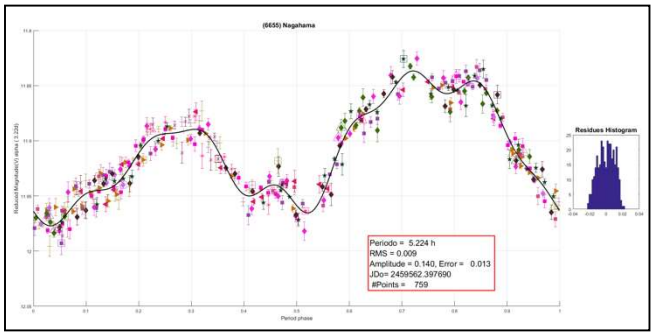

References

ALCDEF (2022). Asteroid Lightcurve Data Exchange Format web site. *https://alcdef.org/*

Behrend, R. (2006web; 2019web; 2022web). Observatoire de Geneve web site. *https://obswww.unige.ch/~behrend/*

Blake, R.M.; Himeno, K. (2018). "A Lightcurve of 1090 Sumida." *Minor Planet Bulletin* **45**, 317.

DAMIT web site. *https://astro.troja.mff.cuni.cz/projects/damit/*

FotoDif (2021) Software. *http://astrosurf.com/orodeno/fotodif/index.htm*

Franco, L.; Pilcher, F.; Higgins, D.; Ďurech, J. (2012). "Shape and Spin Axis Model for 161 Athor." *Minor Planet Bulletin* **39**, 234-236.

Hanuš, J.; Ďurech, J.; Brož, M.; Marciniak, A.; Warner, B.D.; Pilcher, F.; Stephens, R.; Behrend, R.; Carry, B.; and 111 coauthors. (2013). "Asteroids' physical models from combined dense and sparse photometry and scaling of the YORP effect by the observed obliquity distribution." *Astron. Astrophys.* **551**, A67.

Higgins, D.; Warner, B.D.; Dymock, R.; Crow, M. (2007). "Asteroid Lightcurve Analysis of 554 Peraga." *Minor Planet Bulletin* **34**, 30.

Períodos (2020) Software.
http://www.astrosurf.com/salvador/Programas.html

Pilcher, F. (2008). "Period Determinations for 26 Proserpina, 34 Circe 74 Galatea, 143 Adria, 272 Antonia, 419 Aurelia, and 557 Violetta." *Minor Planet Bulletin* **35**, 135-138.

Taylor, R.C.; Gehrels, T.; Capen, R.C. (1976). "Minor planets and related objects. XXI. Photometry of eight asteroids." *Astron. J.* **81**, 778-786.

Warner, B.D. (2005). "Lightcurve analysis for asteroids 242, 893, 921, 1373, 1853, 2120, 2448 3022, 6490, 6517, 7187, 7757, and 18108." *Minor Planet Bulletin* **32,** 4-7.

Warner, B.D. (2017). "Near-Earth Asteroid Lightcurve Analysis at CS3-Palmer Divide Station: 2016 December thru 2017 April." *Minor Planet Bulletin* **44,** 223-237.

GENERAL REPORT OF POSITION OBSERVATIONS BY THE ALPO MINOR PLANETS SECTION FOR THE YEAR 2021

Frederick Pilcher
4438 Organ Mesa Loop
Las Cruces, NM 88011 USA
fpilcher35@gmail.com

(Received: 2022 April 6)

Observations of positions of minor planets by members of the Minor Planets Section in calendar year 2021 are summarized.

During the year 2021 a total of 925 observations of 250 different minor planets were reported by members of the Minor Planets Section.

The summary lists minor planets in numerical order, the observer and telescope aperture (in cm), UT dates of the observations, and the total number of observations in that interval. When a significant departure from the predicted magnitude was noted, it is stated in the next line below the number of positions. The year is 2021 in each case.

Positional observations were contributed by the following observers:

Observer, Instrument	Location	Planets	Positions
Faure, Gérard		38	113
9 cm Celestron	Ré Island (France)		
20 cm Celestron	Vaison la romaine (France)		
20 cm Celestron Fastar	Ré Island (France)		
35 cm Meade LX200	Col de L'Arzelier (France)		
Harvey, G. Roger	Concord, North	214	806
81 cm Newtonian	Carolina, USA		
Pryal, Jim	Ellensburg, WA USA	3	6
20 cm f/10 SCT			

All observations are approximate visual positions.

MINOR PLANET	OBSERVER & APERTURE (cm)	OBSERVING PERIOD (2019)	NO. OBS.
9 Metis	Faure, 20	Apr 15	3
12 Victoria	Faure, 20	Sep 29	2
28 Bellona	Pryal, 20	Apr 18	2
89 Julia	Faure, 9	Oct 7-8	2
97 Klotho	Pryal, 20	Apr 18	2
110 Lydia	Faure, 20	Sep 18	2
511 Davida	Pryal, 20	Apr 18	2
535 Montague	Harvey, 81	Nov 10	6
543 Charlotte	Faure, 20	Jul 18	2
878 Mildred	Faure, 35	Aug 31	4
	Harvey, 81	Aug 30	3
1009 Sirene	Faure, 20	Dec 1	3
1100 Arnica	Faure, 20	Jul 18	2
1335 Demoulina	Faure, 35	Sep 1	2
1455 Mitchella	Faure, 20	May 4	2
1536 Pielinen	Faure, 20	Nov 13	2
1593 Fagnes	Faure, 35	Sep 2	2
1780 Kippes	Faure, 35	Sep 2	2
1956 Artek	Harvey, 81	Nov 1	3
2275 Cuitlahuac	Faure, 35	Aug 31	2
2304 Slavia	Faure, 20	May 4	2
2486 Metsahovi	Faure, 35	Mar 9	2
2515 Gansu	Harvey, 81	Dec 1	3
2638 Gadolin	Faure, 20	Nov 30-Dec 1	2
2691 Sersic	Harvey, 81	Apr 20	3
3142 Kilopi	Harvey, 81	Nov 2	3
3232 Brest	Harvey, 81	Aug 10	3
3409 Abramov	Harvey, 81	Dec 1	3
3525 Paul	Harvey, 81	Mar 8	3
3535 Ditte	Harvey, 81	Dec 3	3

MINOR	PLANET	OBSERVER & APERTURE (cm)	OBSERVING PERIOD (2019)	NO. OBS.
3546	Atanasoff	Harvey, 81	Mar 5	3
3630	Lubomir	Harvey, 81	Sep 28	3
3635	Kreutz	Faure, 35	Jun 13	2
3760	Poutanen	Faure, 20	May 4	2
3922	Heather	Harvey, 81	Oct 11	3
3934	Tove	Faure, 35	May 13-14	3
		Harvey, 81	May 14	3
4071	Rostovdon	Harvey. 81	Sep 29	3
4099	Wiggins	Harvey, 81	Jan 17	3
4154	Rumsey	Harvey, 81	Apr 5	3
4205	David Hughes	Faure, 35	Aug 14	2
4246	Telemann	Harvey, 81	Apr 20	3
4305	Clapton	Harvey, 81	Mar 8	3
4321	Zero	Harvey, 81	Sep 4	3
4468	Pogrebetsku	Harvey, 81	Jan 5	3
4475	Voitkevich	Harvey, 81	Mar 4	3
4555	Josefaperez	Harvey, 81	Sep 29	3
4612	Greenstein	Harvey, 81	Jan 17	6
4660	Nereus	Faure, 20	Nov 30	4
		Harvey, 81	Nov 1	5
4678	Ninian	Harvey, 81	Nov 9	3
4777	Aksenov	Harvey, 81	Oct 11	3
4794	Bogard	Harvey, 81	Mar 9	3
4826	Wilhelms	Faure, 35	Jun 11	2
4899	Candace	Harvey, 81	May 1	3
5001	EMP	Faure, 35	Jun 11	2
5058	Tarrega	Harvey, 81	Sep 27	3
5077	Favaloro	Harvey, 81	Oct 13	3
5095	Escalante	Harvey, 81	Aug 28	3
5189	1990 UQ	Faure, 20	May 4	7
5270	Kakabadze	Harvey, 81	Aug 6	3
5402	Kejosmith	Harvey, 81	Aug 28	3
5403	Takachiho	Harvey, 81	Jan 5	3
5417	Solovaya	Harvey, 81	Jan 17	3
5467	1988 AG	Harvey, 81	Jan 11	3
5535	Annefrank	Harvey, 81	Mar 23	4
5551	Glikson	Harvey, 81	Mar 9	3
5649	Donnashirley	Harvey, 81	Sep 27	3
5667	Nakhimovskaya	Harvey, 81	Sep 28	3
5726	Rubin	Harvey, 81	May 14	3
5823	Oryo	Harvey, 81	Dec 3	3
5879	Almeria	Harvey, 81	Feb 8	6
6052	Junichi	Harvey, 81	Mar 8	3
6058	Carlnielsen	Harvey, 81	Oct 13	3
6083	Janeirabloom	Harvey, 81	Oct 11	3
6117	Brevardastro	Harvey, 81	Mar 9	3
6119	Hjorth	Harvey, 81	Jan 6	3
6141	Durda	Faure, 35	Aug 15	3
6200	Hachinohe	Harvey, 81	Sep 26	3
6232	Zubitskia	Harvey, 81	Mar 22	3
6242	1990 OJ2	Harvey, 81	Nov 24	3
6570	Tomohiro	Harvey, 81	Mar 4	3
6691	Trussoni	Harvey, 81	Jan 6	3
6763	Kochiny	Harvey, 81	Sep 29	3
6764	Kirillavrov	Harvey, 81	May 8	3
6874	1994 JO1	Harvey, 81	Oct 11	3
6914	Becquerel	Harvey, 81	May 14	3
6952	Niccolo	Harvey, 81	Aug 6	3
6975	Hiroaki	Harvey, 81	Jul 31	3
7001	Noether	Harvey, 81	Feb 4	3
7157	Lofgren	Harvey, 81	Aug 6	3
7177	1990 TF	Harvey, 81	Sep 29	3
7192	Cieletespace	Harvey, 81	Sep 6	3
7274	Washioyama	Harvey, 81	Mar 8	3
7309	Shinkawakami	Harvey, 81	May 1	3
7434	Osaka	Harvey, 81	Jan 6	3
7476	Ogilsbie	Faure, 20	Apr 15	2
7479	1994 EC1	Harvey, 81	Jan 10	6
7596	Yumi	Harvey, 81	Oct 27	3
7635	Carolinesmith	Harvey, 81	Nov 25	3
7685	1997 EP17	Harvey, 81	Mar 9	3
7724	Moroso	Harvey, 81	Aug 6	3
7784	Watterson	Faure, 35	Jun 14	2
7822	1991 CS	Faure, 35	Aug 15	2
7854	Laotse	Harvey, 81	Oct 11	3
7916	1981 EN	Harvey, 81	Mar 8	3
8080	Intel	Harvey, 81	Oct 11	3
8084	Dallas	Harvey, 81	Jan 17	3
8167	Ishii	Harvey, 81	Jan 10	3
8424	Toshitsumita	Harvey, 81	Sep 4	3
8464	Polishook	Harvey, 81	Sep 12	3
8747	Asahi	Harvey, 81	Sep 29	3
8762	Hiaticula	Harvey, 81	Mar 4	3
8815	Deanregas	Harvey, 81	Jan 6	3
9044	Karou	Harvey, 81	Apr 20	3
9193	Geoffreycopland	Harvey, 81	Jan 13	3
9209	1994 UK1	Harvey, 81	Sep 4	3
9368	Esashi	Harvey, 81	Jan 17	3
9732	Juchnovski	Harvey, 81	Oct 13	3
9996	ANS	Harvey, 81	Oct 27	3
10027	Perozzi	Harvey, 81	Mar 9	3
10054	Solomin	Harvey, 81	Oct 27	3
10087	1990 SG3	Harvey, 81	Aug 28	3
10389	Robmanning	Harvey, 81	Nov 1	3
10443	van der Pol	Harvey, 81	Oct 27	3
10497	1986 RQ	Harvey, 81	Sep 12	3
10525	1990 TO	Harvey, 81	Nov 2	3
10715	Seine	Harvey, 81	Mar 23	3
10859	1995 GJ7	Harvey, 81	Apr 5	3
11166	Anatolefrance	Harvey, 81	Sep 6	3
11231	1999 JF59	Harvey, 81	Dec 3	3
11310	1993 SB15	Harvey, 81	Jan 13	3
11452	1980 KE	Harvey, 81	Sep 6	3
11569	Virgilsmith	Harvey, 81	Aug 9	3
11705	1998 GN7	Harvey, 81	Oct 27	3
11823	Christen	Harvey, 81	Sep 26-Oct 11	4
12299	1991 PV17	Harvey, 81	Nov 9	3
12352	Jepejacobsen	Harvey, 81	Dec 13	3
12391	Ecoadachi	Harvey, 81	Oct 11	3
12444	Prothoon	Faure, 35	Jun 13	2
12687	de Valory	Harvey, 81	Feb 8	3
12690	Kochimirakagaku	Harvey, 81	Jan 17	3
12923	Zephyr	Harvey, 81	Oct 27	6
13276	1998 QP40	Harvey, 81	Jan 11	3
13521	1991 BK	Harvey, 81	Feb 8	4
13678	Shimada	Harvey, 81	Oct 11	3
13974	1991 YC	Harvey, 81	Jan 10	6
14427	1991 VJ2	Harvey, 81	Aug 9	3
14917	Taco	Harvey, 81	Nov 1	3
15013	1998 QH93	Harvey, 81	Jan 11	3
15304	Wikberg	Harvey, 81	Oct 13	3
15363	Ysaye	Harvey, 81	Sep 26	3
15407	Udakiyoo	Harvey, 81	Sep 28	3
15560	2000 GR24	Harvey, 81	Oct 13	3
15736	Hamanasu	Harvey, 81	Dec 1	3
16126	1999 XQ86	Harvey, 81	Jan 6	3
16635	1993 QO	Harvey, 81	Sep 26	6
16641	Esteban	Harvey, 81	Jul 31	3
17640	Mount Stromlo	Harvey, 81	Dec 3	6
17664	1996 VP30	Harvey, 81	Nov 25	3
17730	1998 AS4	Harvey, 81	Mar 22	3
17764	Schatzman	Harvey, 81	Oct 27	3
17964	1999 JY41	Harvey, 81	Nov 9	3
18226	1182 T-1	Harvey, 81	Oct 11	3
18666	1998 TF53	Harvey, 81	Oct 11	3
18742	1998 XX30	Harvey, 81	Apr 13	3
18863	1999 RC191	Harvey, 81	Aug 6	3
18869	1999 TU222	Harvey, 81	Mar 22	3
19414	1998 FP32	Harvey, 81	Sep 29	3
19519	1998 WB8	Harvey, 81	Apr 5	3
19648	1999 RK104	Harvey, 81	Sep 29	3
19915	Bochkarev	Harvey, 81	Sep 12	3
20802	2000 SR179	Harvey, 81	Nov 1	3
20816	2000 SQ319	Harvey, 81	Sep 27	3
21104	Sveshnikov	Harvey, 81	Nov 24	3
21755	1999 RE190	Harvey, 81	Jan 17	3
22295	1989 SZ9	Harvey, 81	Mar 9	3
22525	1998 FB12	Harvey, 81	Sep 28	3
22978	Nyrola	Harvey, 81	Nov 24	3
23940	1998 UE	Harvey, 81	Feb 8	3
24013	1999 RR113	Harvey, 81	Jan 5	3
26520	2000 CQ75	Harvey, 81	Jan 5	3
27111	1998 VV34	Harvey, 81	Sep 28	3
27225	1999 GB17	Harvey, 81	Apr 13	3
32158	2000 MD2	Harvey, 81	Nov 9	3
32648	3538 P-L	Harvey, 81	Oct 11	3
32906	1994 RH	Harvey, 81	Sep 28	6
33284	1998 HD153	Harvey, 81	Sep 27	3
33916	2000 LF19	Harvey, 81	Sep 6	3
33985	2000 NG25	Harvey, 81	Jan 6	3
35406	1997 YH8	Harvey, 81	Dec 3	3
36360	2000 OH3	Harvey, 81	Jan 6	3
38063	1999 FH	Faure, 35	Aug 7	2
41770	2000 VV37	Harvey, 81	Nov 2	3
42496	1991 XB1	Harvey, 81	Dec 1	3
44553	1999 CH5	Harvey, 81	Dec 1	3
45694	2000 EC150	Harvey, 81	Aug 6	3
46304	2001 OZ62	Harvey, 81	Sep 28	3
46780	1998 HH52	Harvey, 81	Oct 27	3
57108	2001 OS74	Harvey, 81	Nov 2	3

MINOR PLANET	OBSERVER & APERTURE (cm)	OBSERVING PERIOD (2019)	NO. OBS.
58980 1998 RG47	Harvey, 81	Aug 28	3
59490 1999 JD4	Harvey, 81	Jul 17	3
66092 1998 SD	Harvey, 81	Jan 17	3
68063 2000 YJ66	Faure, 20	Aug 7	2
	Harvey, 81	Aug 6	3
68280 2001 FR8	Harvey, 81	Dec 13	3
78754 2002 TA295	Harvey, 81	Sep 6	3
87024 2000 JS66	Harvey, 81	Nov 2	6
87035 2000 KE2	Harvey, 81	Feb 4	3
87309 2000 QP	Harvey, 81	Jul 29	6
89355 2001 VS78	Harvey, 81	Jan 5	6
89958 2002 LY45	Harvey, 81	Jun 17	6
90147 2002 YK14	Harvey, 81	Jan 6	6
95696 2002 JU75	Harvey, 81	Oct 13	6
99942 Apophis	Faure, 35	Mar 9	6
	Harvey, 81	Feb 24-Mar 12	12
106848 2000 YP16	Harvey, 81	Jan 17	3
109603 2001 QD283	Harvey, 81	Jan 10	6
142464 2002 TC9	Harvey, 81	Mar 30	6
143649 2003 QQ47	Faure, 20	Sep 18	8
	Harvey, 81	Sep 19	6
159857 2004 LJ1	Faure, 20	Nov 13	6
	Harvey, 81	Nov 2	6
162149 1998 YQ11	Harvey, 81	Dec 14	6
162186 1999 OP3	Harvey, 81	Feb 4	6
163899 2003 SD220	Faure, 20	Nov 30	3
174050 2002 CC19	Harvey, 81	Feb 3	6
285571 2000 PQ9	Faure, 20	Jul 7 17-18	4
	Harvey, 81	Jul 29	6
326732 2003 HB6	Faure, 20	Aug 7	4
	Harvey, 81	Jul 13	6
332446 2008 AF4	Harvey, 81	Jan 10	6
434431 2005 NC7	Harvey, 81	Sep 12	6
450263 2003 WD158	Harvey, 81	Jun 16	6
495615 2015 PQ291	Harvey, 81	May 4	6
1991 TF3	Harvey, 81	Sep 26	6
1997 GL3	Harvey, 81	Apr 13	6
1999 FJ21	Harvey, 81	Oct 11	6
1999 RM45	Harvey, 81	Feb 20	6
2001 EC	Harvey, 81	Sep 3	6
2003 AF23	Harvey, 81	Jan 5	6
2004 UE	Harvey, 81	Nov 9-10	12
2011 YQ10	Harvey, 81	Sep 3	6
2015 NU13	Harvey, 81	Jan 13	6
2016 CL136	Harvey, 81	Feb 3	6
2016 CO247	Harvey, 81	Jan 10	6
2018 LM4	Harvey, 81	Jul 29	6
2019 XS	Harvey, 81	Nov 10	6
2020 WU5	Harvey, 81	Jan 10	6
2020 XU6	Harvey, 81	Feb 17	6
2021 BC	Harvey, 81	Jan 20	6
2021 CO	Harvey, 81	Feb 10	6
2021 DW1	Harvey, 81	Mar 4	6
2021 FH	Harvey, 81	Mar 23	6
2021 QB3	Harvey, 81	Sep 4	6

LIGHTCURVE PHOTOMETRY OPPORTUNITIES: 2022 JULY-SEPTEMBER

Brian D. Warner
Center for Solar System Studies (CS3)
446 Sycamore Ave.
Eaton, CO 80615 USA
brian@MinorPlanetObserver.com

Alan W. Harris
Center for Solar System Studies (CS3)
La Cañada, CA 91011-3364 USA

Josef Ďurech
Astronomical Institute
Charles University
18000 Prague, CZECH REPUBLIC
durech@sirrah.troja.mff.cuni.cz

Lance A.M. Benner
Jet Propulsion Laboratory
Pasadena, CA 91109-8099 USA
lance.benner@jpl.nasa.gov

We present lists of asteroid photometry opportunities for objects reaching a favorable apparition and have no or poorly-defined lightcurve parameters. Additional data on these objects will help with shape and spin axis modeling using lightcurve inversion. The "Radar-Optical Opportunities" section includes a list of potential radar targets as well as some that might be in critical need of astrometric data. There are two objects of note, one that is also considered a comet and the other being the target of the DART mission.

We present several lists of asteroids that are prime targets for photometry and/or astrometry during the period 2022 July through September. The "Radar-Optical Opportunities" section provides an expanded list of potential NEA targets, many of which are planned for radar observations.

In the first three sets of tables, "Dec" is the declination and "U" is the quality code of the lightcurve. See the latest asteroid lightcurve data base (LCDB from here on; Warner et al., 2009) documentation for an explanation of the U code:

http://www.minorplanet.info/lightcurvedatabase.html

The ephemeris generator on the MinorPlanet.info web site allows creating custom lists for objects reaching V ≤ 18.0 during any month in the current year and up to five years in the future, e.g., limiting the results by magnitude and declination, family, and more.

https://www.minorplanet.info/php/callopplcdbquery.php

We refer you to past articles, e.g., Warner et al. (2021a; 2021b) for more detailed discussions about the individual lists and points of advice regarding observations for objects in each list.

Once you've obtained and analyzed your data, it's important to publish your results. Papers appearing in the *Minor Planet Bulletin* are indexed in the Astrophysical Data System (ADS) and so can be referenced by others in subsequent papers. It's also important to make the data available at least on a personal website or upon request. We urge you to consider submitting your raw data to the ALCDEF database. This can be accessed for uploading and downloading data at

http://www.alcdef.org

The database contains more than 3.9 million observations for 15,000+ objects, making it one of the more useful sources for raw data of dense time-series asteroid photometry.

Lightcurve/Photometry Opportunities

Objects with U = 3– or 3 are excluded from this list since they will likely appear in the list for shape and spin axis modeling. Those asteroids rated U = 1 should be given higher priority over those rated U = 2 or 2+, but not necessarily over those with no period. On the other hand, do not overlook asteroids with U = 2/2+ on the assumption that the period is sufficiently established. Regardless, do not let the existing period influence your analysis since even highly-rated result have been proven wrong at times. Note that the lightcurve amplitude in the tables could be more or less than what's given. Use the listing only as a guide.

An entry in bold italics is a near-Earth asteroid (NEA).

		Brightest			LCDB Data		
Number	Name	Date	Mag	Dec	Period	Amp	U
2035	Stearns	07 02.5	13.9	-55	93	0.14-0.7	2+
2316	Jo-Ann	07 03.8	14.8	-20	33	0.33	2-
7559	Kirstinemeyer	07 04.0	14.6	-29	5.475	0.05	2
6027	1993 SS2	07 04.3	14.0	-22	46.927		2-
2122	Pyatiletka	07 07.1	14.7	-22	8.899	0.10	1
10283	Cromer	07 09.9	15.3	-27	9.772		2-
5387	Casleo	07 16.7	15.3	-19	4.051		2
13236	1998 HF96	07 20.8	15.3	-14	7.201		2
4090	Risehvezd	07 21.4	14.5	-19	4.55	0.32-0.41	2
19763	Klimesh	07 23.3	15.0	-8	101	0.67	2
6263	Druckmuller	07 25.3	15.4	-17	3.464	0.05	1
2481	Burgi	07 26.5	15.2	-24	30.086	0.20	2
3403	Tammy	07 27.2	14.7	-10	11.85	0.10-0.12	1
19337	1997 AT	08 01.0	15.5	-24	12.041	0.20	2
1476	Cox	08 04.1	14.2	-22	7.699	0.08-0.13	2
3805	Goldreich	08 04.1	15.4	-18	4.841	0.75	2
2717	Tellervo	08 04.5	13.1	-13	4.213	0.40	2+
13918	Tsukinada	08 06.2	14.7	-16	7.5	0.29	1+
4087	Part	08 08.2	15.1	-25	16.47	0.59	2
5216	Cannizzo	08 09.7	14.2	-15	32.206	0.31-0.46	2
1543	Bourgeois	08 10.3	13.3	-2	2.48	0.03	1
4384	Henrybuhl	08 11.6	14.7	-14	7.92	0.38	2+
1428	Mombasa	08 11.9	13.6	-26	16.67	0.15-0.25	2+
1683	Castafiore	08 12.2	14.1	-18	13.931	0.66	2+
4768	Hartley	08 13.2	14.2	-15	22.08	0.11	2
5038	Overbeek	08 13.3	15.3	-35	4.038	0.39	2
10141	Gotenba	08 14.9	15.3	-37	30.957	0.11	2
3893	DeLaeter	08 16.7	15.4	+23	9.61	0.13-0.20	2
5512	1988 VD7	08 17.7	14.8	-26	3.036	0.12	2
3631	Sigyn	08 19.0	14.9	-11	41	0.1	1
19230	Sugazi	08 24.2	15.4	-12	13.14	0.27	2
6238	Septimaclark	08 27.6	15.2	-22	10.833	0.60-0.73	2
3000	Leonardo	08 28.0	15.5	-6	7.524	0.26	2
2915	Moskvina	08 28.7	15.3	-18	2.177	0.47	2
3479	Malaparte	08 29.3	15.5	+3	16.3	0.42	2
11023	1986 QZ	08 30.2	15.2	-14	22.176		2-
6425	1994 WZ3	08 31.4	14.7	+12	103.9	0.92	2
1458	Mineura	09 01.4	14.1	+0	36	0.04	1
15302	1992 TJ1	09 02.4	15.4	-12	27.556	0.10	2
6624	1980 SG	09 03.3	15.5	-16	8.696	0.18	2
7996	Vedernikov	09 04.8	14.9	-3	5.828	0.09-0.14	2
12523	1998 HH100	09 05.3	15.1	-18	2.122	0.11-0.14	2
14471	1993 SG1	09 06.3	15.0	-1	77.623	0.56	2
2945	Zanstra	09 06.8	15.3	-10	10.05	0.14	1
5321	Jagras	09 08.1	14.9	+11	2.638	0.06	2
960	Birgit	09 09.7	13.9	+1	8.85	0.28	2+
10449	Takuma	09 14.4	14.8	-4	7.33	0.46	2
16698	1995 CX	09 16.1	15.5	-20	52.8	0.20	2
3560	Chenqian	09 17.2	14.6	+4	12.454	0.17-0.26	2
2237	Melnikov	09 18.2	15.2	-5	31.725		2
3438	Inarradas	09 20.4	14.7	-4	24.82	0.38	2
3108	Lyubov	09 22.0	15.2	-2	4.83	0.18-0.21	2
4135	Svetlanov	09 22.0	14.7	+4	10.559	0.10-0.15	2
12127	Mamiya	09 22.8	15.5	-3	7.867	0.17	2
1986	Plaut	09 23.0	15.1	-2	18.773		2-
4308	Magarach	09 24.8	15.4	+16	33.8	0.07	1
7449	Dollen	09 24.8	15.4	+7	10	0.10	2-
1731	Smuts	09 25.0	14.3	-3	12.5	0.08	2
2907	Nekrasov	09 26.4	15.3	-1	25.149	0.43	2
7189	Kuniko	09 28.9	15.1	+0	2.922	0.15	2
2161	Grissom	09 30.7	15.1	-7	5.063	0.27	2+

Low Phase Angle Opportunities

The Low Phase Angle list includes asteroids that reach very low phase angles ($\alpha < 1°$). The "α" column is the minimum solar phase angle for the asteroid. Getting accurate, calibrated measurements (usually V band) at or very near the day of opposition can provide important information for those studying the "opposition effect." Use the on-line query form for the LCDB to get more details about a specific asteroid.

https://www.minorplanet.info/php/callopplcdbquery.php

The best chance of success comes with covering at least half a cycle a night, meaning periods generally < 16 h, when working objects with low amplitude. Objects with large amplitudes and/or long periods are much more difficult for phase angle studies since, for proper analysis, the data must be reduced to the average magnitude of the asteroid for each night. Refer to Harris et al. (1989) for the details of the analysis procedure.

As an aside, it is arguably better for physical interpretation (e.g., *G* value versus albedo) to use the maximum light rather than mean level to find the phase slope parameter (*G*). This models better the behavior of a spherical object of the same albedo, but it can produce significantly different values for both *H* and *G* versus using average light, which is the method used for values listed by the Minor Planet Center. Using and reporting the results of both methods can provide additional insights into the physical properties of an asteroid.

The International Astronomical Union (IAU) has adopted a new system, H-G_{12}, introduced by Muinonen et al. (2010). It will be some years before H-G_{12} becomes widely used, and hopefully not until a discontinuity flaw in the G_{12} function has been fixed. This discontinuity results in false "clusters" or "holes" in the solution density and makes it impossible to draw accurate conclusions.

We strongly encourage obtaining data as close to 0° as possible, then every 1-2° out to 7°, below which the curve tends to be non-linear due to the opposition effect. From 7° out to about 30°, observations at 3-6° intervals should be sufficient. Coverage beyond 50° or so is not generally helpful since the H-G system is best defined with data from 0-30°.

It's important to emphasize that all observations should (must) be made using high-quality catalogs to set the comparison star magnitudes. These include ATLAS, Pan-STARRS, SkyMapper, and Gaia2/3. Catalogs such as CMC-15, APASS, or the MPOSC from *MPO Canopus* have too high of significant systematic errors.

Also important is that that there are sufficient data from each observing run such that their location can be found on a combined, phased lightcurve derived from two or more nights obtained *near the same phase angle.* If necessary, the magnitudes for a given run should be adjusted so that they correspond to mid-light of the combined lightcurve. This goes back to the H-G system being based on average, not maximum or minimum light.

The asteroid magnitudes are brighter than in others lists because higher precision is required and the asteroid may be a full magnitude or fainter when it reaches phase angles out to 20-30°.

Num	Name	Date	α	V	Dec	Period	Amp	U
639	Latona	07 01.9	0.06	12.0	-23	6.193	0.07-0.35	3
6027	1993 SS2	07 04.3	0.55	13.9	-22			
465	Alekto	07 05.7	0.85	13.2	-25	10.936	0.12-0.18	3
23606	1996 AS1	07 19.7	0.73	13.4	-20		1.67	
559	Nanon	07 20.1	0.53	12.7	-22	10.059	0.09-0.26	3
113	Amalthea	08 01.1	0.33	11.2	-19	9.950	0.19-0.22	3
1638	Ruanda	08 02.4	0.28	13.9	-17	4.2397	0.10-0.10	3

Num	Name	Date	α	V	Dec	Period	Amp	U
334	Chicago	08 05.0	0.06	12.9	-17	7.361	0.20-0.67	3
506	Marion	08 08.0	0.29	13.5	-15	13.546	0.17-0.35	3
122	Gerda	08 11.4	0.46	12.2	-14	10.685	0.10-0.26	3
271	Penthesilea	08 18.5	0.36	13.6	-14	18.787	0.23-0.33	3
184	Dejopeja	08 21.5	0.13	12.9	-12	6.4416	0.22-0.3	3
987	Wallia	08 23.1	0.81	12.2	-10	10.0813	0.11-0.36	3
2199	Klet	08 25.2	0.84	14.0	-12	12.857	0.10-0.13	3
174	Phaedra	08 28.0	0.86	11.8	-08	5.744	0.10-0.58	3
809	Lundia	09 01.1	0.59	13.2	-09	15.4142	0.16-1.12	3
300	Geraldina	09 03.4	0.34	13.8	-08	6.8423	0.04-0.32	3
569	Misa	09 05.5	0.52	13.5	-06	11.595	0.09-0.25	3
3	Juno	09 07.9	0.90	7.8	-04	7.210	0.13-0.22	3
24	Themis	09 13.4	0.24	11.9	-04	8.374	0.09-0.14	3
664	Judith	09 15.2	0.14	13.6	-03	13.764	0.15-0.4	2+
799	Gudula	09 22.8	0.90	13.3	-02	14.814	0.27-0.30	3
48	Doris	09 26.0	0.06	11.1	+01	11.89	0.17-0.36	3
125	Liberatrix	09 26.0	0.65	12.2	-01	3.968	0.20-0.71	3
65	Cybele	09 29.9	0.73	11.8	+00	6.0814	0.02-0.12	3

Shape/Spin Modeling Opportunities

Those doing work for modeling should contact Josef Ďurech at the email address above. If looking to add lightcurves for objects with existing models, visit the Database of Asteroid Models from Inversion Techniques (DAMIT) web site

https://astro.troja.mff.cuni.cz/projects/damit/

Additional lightcurves could lead to the asteroid being added to or improving one in DAMIT, thus increasing the total number of asteroids with spin axis and shape models.

Included in the list below are objects that:

1. Are rated U = 3– or 3 in the LCDB.
2. Do not have reported pole in the LCDB Summary table.
3. Have at least three entries in the Details table of the LCDB where the lightcurve is rated U ≥ 2.

The caveat for condition #3 is that no check was made to see if the lightcurves are from the same apparition or if the phase angle bisector longitudes differ significantly from the upcoming apparition. The last check is often not possible because the LCDB does not list the approximate date of observations for all details records. Including that information is an on-going project.

Favorable apparitions are in bold text. NEAs are in italics.

		Brightest			LCDB Data		
Num	Name	Date	Mag	Dec	Period	Amp	U
465	Alekto	07 05.6	13.2	-25	10.936	0.12-0.18	3
2000	Herschel	07 06.8	14.9	-28	133.6	0.17-1.16	3
4263	**Abashiri**	**07 08.6**	**14.4**	**-25**	**4.882**	**0.11-0.42**	**3**
2375	Radek	07 13.7	14.4	-22	16.875	0.17-0.35	3
339	Dorothea	07 15.8	13.4	-8	5.974	0.06-0.10	3
481	Emita	07 17.4	12.9	-32	14.412	0.13-0.30	3
1152	Pawona	07 17.5	14.2	-26	3.415	0.16-0.26	3
307	Nike	07 19.0	14.4	-23	11.857	0.15-0.23	3
559	**Nanon**	**07 20.1**	**12.8**	**-22**	**10.059**	**0.07-0.26**	**3**
363	Padua	07 22.4	12.6	-28	8.401	0.08-0.3	3
1086	Nata	07 23.3	14.2	-23	18.061	0.17-0.18	3-
346	Hermentaria	07 24.9	10.9	-27	28.523	0.07-0.20	3
1131	**Porzia**	**07 25.9**	**13.6**	**-23**	**4.658**	**0.15-0.23**	**3**
1060	**Magnolia**	**07 26.4**	**14.0**	**-6**	**2.911**	**0.05-0.32**	**3**
909	Ulla	07 31.9	13.7	-10	8.716	0.08-0.24	3
3317	**Paris**	**08 01.8**	**14.8**	**-14**	**7.081**	**0.08-0.14**	**3**
1254	Erfordia	08 04.3	15.0	-13	12.287	0.33-0.47	3
198	**Ampella**	**08 06.6**	**10.5**	**-4**	**10.379**	**0.11-0.22**	**3**
412	Elisabetha	08 06.9	13.1	-26	19.635	0.08-0.20	3
541	Deborah	08 08.8	13.8	-9	29.368	0.07-0.10	3
2019	van Albada	08 13.4	14.1	-7	2.729	0.14-0.22	3
195	Eurykleia	08 17.7	13.3	-20	16.521	0.10-0.24	3
2402	Satpaev	08 20.6	14.8	-14	8.113	0.07-0.38	3
895	Helio	08 21.0	13.6	+18	9.347	0.10-0.23	3
987	**Wallia**	**08 23.2**	**12.3**	**-10**	**10.081**	**0.11-0.36**	**3**
815	Coppelia	08 23.8	15.0	-31	4.421	0.13-0.24	3
1385	Gelria	08 26.2	14.1	-17	4.624	0.08-0.23	3
1308	Halleria	08 26.3	14.8	-13	6.028	0.14-0.17	3
2152	Hannibal	08 27.5	14.8	+9	5.978	0.06-0.32	3
6084	**Bascom**	**08 28.1**	**14.8**	**-16**	**2.745**	**0.14-0.23**	**3**
3433	Fehrenbach	08 31.4	14.8	-9	3.916	0.24-0.34	3
527	**Euryanthe**	**09 02.6**	**13.3**	**-18**	**42.75**	**0.11-0.20**	**3**
300	**Geraldina**	**09 03.4**	**13.8**	**-8**	**6.842**	**0.04-0.32**	**3**
2768	Gorky	09 03.4	14.1	-20	4.507	0.15-0.51	3
1718	**Namibia**	**09 03.9**	**14.8**	**+4**	**8.603**	**0.13-0.25**	**3**
569	Misa	09 05.6	13.5	-6	11.595	0.09-0.25	3
1806	Derice	09 11.0	14.8	+1	3.224	0.07-0.19	3
2343	**Siding Spring**	**09 12.1**	**14.3**	**-2**	**2.107**	**0.15-0.19**	**3**
78	Diana	09 16.2	12.3	+1	7.299	0.02-0.30	3
964	Subamara	09 20.8	14.5	-8	6.868	0.11-0.25	3
799	**Gudula**	**09 22.8**	**13.3**	**-2**	**14.814**	**0.27-0.30**	**3**
3223	Forsius	09 24.6	14.7	-3	2.343	0.20-0.28	3
469	Argentina	09 29.0	14.0	+10	17.573	0.11-0.15	3
491	**Carina**	**09 30.5**	**13.2**	**-3**	**14.836**	**0.08-0.13**	**3**

Radar-Optical Opportunities

Table I below gives a list of near-Earth asteroids reaching maximum brightness for the current quarter-year based on calculations by Warner. We switched to this presentation in lieu of ephemerides for reasons outlined in the 2021 October-December opportunities paper (Warner et al., 2021b), which centered on the potential problems with ephemerides generated several months before publication.

The initial list of targets started using the planning tool at

https://www.minorplanet.info/php/callopplcdbquery.php

where the search was limited to near-Earth asteroids only that were V ≤ 18 for at least part of the quarter.

The list was then filtered to include objects that might be targets for the Goldstone radar facility or, if it were still operational, the Arecibo radar. This was based on the calculated radar SNR using

http://www.naic.edu/~eriverav/scripts/index.php

and assuming a rotation period of 4 hours (2 hours if $D \leq 200$ m) if a period was not given in the asteroid lightcurve database (LCDB; Warner et al., 2009). The SNR values are estimates only and assume that the radar is fully functional.

If an asteroid was on the list but failed the SNR test, we checked if it might be a suitable target for radar and/or photometry sometime through 2050. If so, it was kept on the list to encourage physical and astrometric observations during the current apparition. In most of those cases, the SNR values in the "A" and "G" columns are not for the current quarter but the year given in the Notes column. If a better apparition is forthcoming through 2050, the Notes column in Table I contains SNR values for that time.

The final step was to cross-reference our list with that found on the Goldstone planned targets schedule at

http://echo.jpl.nasa.gov/asteroids/goldstone_asteroid_schedule.html

It's important to note that the final list in Table I is based on *known* targets and orbital elements when it was prepared. It is common for newly discovered objects to move in or out of the list. We recommend that you keep up with the latest discoveries by using the Minor Planet Center observing tools.

In particular, monitor NEAs and be flexible with your observing program. In some cases, you may have only 1-3 days when the asteroid is within reach of your equipment. Be sure to keep in touch with the radar team (through Benner's email or their Facebook or Twitter accounts) if you get data. The team may not always be observing the target but your initial results may change their plans. In all cases, your efforts are greatly appreciated.

For observation planning, use these two sites

MPC: *http://www.minorplanetcenter.net/iau/MPEph/MPEph.html*
JPL: *http://ssd.jpl.nasa.gov/?horizons*

Cross-check the ephemerides from the two sites just in case there is discrepancy that might have you imaging an empty sky.

About YORP Acceleration

Near-Earth asteroids are particularly sensitive to YORP acceleration. YORP (Yarkovsky–O'Keefe–Radzievskii–Paddack; Rubincam, 2000) is the asymmetric thermal re-radiation of sunlight that can cause an asteroid's rotation period to increase or decrease. High precision lightcurves at multiple apparitions can be used to model the asteroid's *sidereal* rotation period and see if it's changing.

It usually takes four apparitions to have sufficient data to determine if the asteroid rotation rate is changing under the influence of YORP. This is why observing an asteroid that already has a well-known period remains a valuable use of telescope time. It is even more so when considering the BYORP (binary-YORP) effect among binary asteroids that has stabilized the spin so that acceleration of the primary body is not the same as if it would be if there were no satellite.

The Quarterly Target List Table

The Table I columns are

Num	Asteroid number, if any.
Name	Name assigned by the MPC.
H	Absolute magnitude from MPCOrb.
Dkm	Diameter (km) assuming $p_V = 0.2$.
Date	Date (mm dd.d) of brightest magnitude.
V	Approximate V magnitude at brightest.
Dec	Approximate declination at brightest.
Period	Synodic rotation period from summary line in the LCDB summary table.
Amp	Amplitude range (or single value) of reported lightcurves.
U	LCDB U (solution quality) from 1 (probably wrong) to 3 (secure).
A	Approximate SNR for Arecibo (if operational and at full power).
G	Approximate SNR for Goldstone radar at full power.
Notes	Comments about the object.

"PHA" is a potentially hazardous asteroid. For good measure, consider that astrometry and photometry have been requested to support Goldstone observations. The sources for the rotation period are given in the Notes column. If none are qualified with a specific period, then the periods from multiple sources were in general agreement. Higher priority should be given to those where the current apparition is the last one V ≤ 18 through 2050 or several years to come.

4015 Wilson-Harrington is also known as 107P/Wilson-Harrington since it has been shown to being more a comet – if the definition of which includes a coma and/or tail. This opens the debate about what makes asteroid an asteroid but not a comet? Are some asteroids actually inactive comets?

The other asteroid of particular interest is the binary 65803 Didymos, a binary asteroid that is the target of the Double Asteroid Redirection Test (DART) mission. In addition to the many web sites, a good overview of the science under consideration can be found in Rivkin et al. (2021), which is a free, open-access paper.

High-quality lightcurves obtained before and after the test to be run between 2022 September 25 and October 2, will be of particular use.

References

Harris, A.W.; Young, J.W.; Contreiras, L.; Dockweiler, T.; Belkora, L.; Salo, H.; Harris, W.D.; Bowell, E.; Poutanen, M.; Binzel, R.P.; Tholen, D.J.; Wang, S. (1989). "Phase relations of high albedo asteroids: The unusual opposition brightening of 44 Nysa and 64 Angelina." *Icarus* **81**, 365-374.

Muinonen, K.; Belskaya, I.N.; Cellino, A.; Delbò, M.; Levasseur-Regourd, A.-C.; Penttilä, A.; Tedesco, E.F. (2010). "A three-parameter magnitude phase function for asteroids." *Icarus* **209**, 542-555.

Ostro, S.J.; Harris, A.W.; Campbell, D.B.; Shapiro, I.I.; Young, J. (1984). "Radar and photoelectric observations of asteroid 2100 Ra-Shalom." *Icarus* **60**, 391-403.

Pravec, P.; Hahn, G. (1997). "Two-Period Lightcurve of 1994 AW1: Indication of a Binary Asteroid?" *Icarus* **127**, 431-440.

Pravec, P.; Wolf, M.; Sarounova, L. (2003web). *http://www.asu.cas.cz/~ppravec/neo.htm*

Pravec, P.; Benner, L.A.M.; Nolan, M.C.; Kusnirak, P.; Pray, D.; Giorgini, J.D.; Jurgens, R.F.; Ostroy S.J.; Margot, J.-L.; Magri, C.; Grauer, A.; Larson, S. (2003). "(65803) 1996 GT." *IAUC* **8244**.

Pravec, P.; Harris, A.W.; Scheirich, P.; Kušnirák, P.; Šarounová, L.; Hergenrother, C.W.; Mottola, S.; Hicks, M.D.; Masi, G.; Krugly, Yu.N.; Shevchenko, V.G.; Nolan, M.C.; Howell, E.S.; Kaasalainen, M.; Galád, A.; Brown, P.; Degraff, D.R.; Lambert, J.V.; Cooney, W.R.; Foglia, S. (2005). "Tumbling asteroids." *Icarus* **173**, 108-131.

Rivkin, A.S.; Chabot, N.L.; Stickle, A.M.; Thomas, C.A.; Richardson, D.C.; Barnouin, O.; Fahnestock, E.G.; Ernst, C.M.; Cheng, A.F.; Chesley, S.; Naidu, S.; Statler, T.S.; Barbee, B., Agrusa, H.; Moskovitz, N.; Terik Daly, R.; Pravec, P.; Scheirich, P.; Dotto, E.; Corte, V.D.; Michel, P.; Kuppers, M.; Atchison, J.; Hirabayashi, M. (2021). "The Double Asteroid Redirection Test (DART): Planetary Defense Investigations and Requirements." *Planet. Sci. J.* **2**, 173.

Rubincam, D.P. (2000). "Radiative Spin-up and Spin-down of Small Asteroids." *Icarus* **148**, 2-11.

Urakawa, S.; Okumura, S.-I.; Nishiyama, K.; Sakamoto, T.; et al. (2011). "Photometric observations of 107P/Wilson-Harrington." *Icarus* **215**, 17-26.

Warner, B.D. (2013). "Asteroid Lightcurve Analysis at the Palmer Divide Observatory: 2013 January - March." *Minor Planet Bull*. **40**, 137-145.

Warner, B.D.; Harris, A.W.; Pravec, P. (2009). "The asteroid lightcurve database." *Icarus* **202**, 134-146.

Num	Name	H	D	Date	V	Dec	Period	Amp	U	A	G	Notes
0	2013 BC18	18.88	0.498	07 01.9	16.0	-60				20	-	
152637	1997 NC1	18.05	0.729	07 05.9	15.7	-33				25	-	
385186	**1994 AW1**	**17.56**	**0.914**	**07 08.5**	**15.6**	**13**	**2.5193**	**0.12 0.17**	**3**	**30**	**10**	Binary Pravec and Hahn (1997)
4015	Wilson-Harrington	16.02	1.860	07 13.3	16.6	11	3.5736	0.1	2			Also considered to be a comet. Urakawa et al. (2011)
23606	1996 AS1	18.31	0.647	07 19.7	13.4	-20				30	10	
349068	**2006 YT13**	**18.30**	**0.650**	**07 23.4**	**15.7**	**-48**	**2.433**		**3**	**950**	**270**	PHA Warner (2013)
531944	**2013 CU83**	**21.40**	**0.156**	**07 29.2**	**16.1**	**-19**				**70**	**20**	PHA
3102	Krok	16.15	1.750	08 26.2	16.0	-6	149.4	1.3 1.6	3	10	-	Pravec et al. (2005)
0	2012 PG6	20.30	0.259	08 30.0	16.5	53				115	30	
161989	**Cacus**	**17.15**	**1.100**	**09 03.3**	**13.4**	**1**	**3.7538**	**0.8 1.1**	**3**	**770**	**220**	PHA Pravec et al. (2003web)
2100	**Ra-Shalom**	**16.24**	**1.680**	**09 03.9**	**13.9**	**8**	**19.797**	**0.3 0.55**	**3**	**30**	**-**	PHA Ostro et al. (1984) Many others.
162825	2001 BO61	18.04	0.733	09 15.0	15.4	-36				100	25	
65803	**Didymos**	**18.07**	**0.723**	**09 26.3**	**14.4**	**-34**	**2.2593**		**3**	**135**	**35**	Binary / DART Pravec et al. (2003) Rivkin et al. (2021)

Table I. A list of near-Earth asteroids reaching brightest in the third quarter of 2022. PHA: potentially hazardous asteroid. Diameters are based on p_V = 0.20. The Date, V, and Dec columns are the mm/dd.d, approximate magnitude, and declination when at brightest. Amp is the single or range of amplitudes. The A and G columns are the approximate SNRs for an assumed full-power Arecibo (not operational) and Goldstone radars. The references in the Notes column are those for the reported periods and amplitudes.

Warner, B.D.; Harris, A.W.; Durech, J.; Benner, L.A.M. (2021a). "Lightcurve Photometry Opportunities" 2021 January - March." *Minor Planet Bull.* **48**, 89-97.

Warner, B.D.; Harris, A.W.; Durech, J.; Benner, L.A.M. (2021b). "Lightcurve Photometry Opportunities" 2021 October - December." *Minor Planet Bull.* **48**, 406-410.

IN THIS ISSUE

This list gives those asteroids in this issue for which physical observations (excluding astrometric only) were made. This includes lightcurves, color index, and H-G determinations, etc. In some cases, no specific results are reported due to a lack of or poor-quality data. The page number is for the first page of the paper mentioning the asteroid. EP is the "go to page" value in the electronic version.

Number	Name	EP	Page
748	Simeisa	6	164
837	Schwarzschilda	60	218
866	Fatme	21	179
877	Walkure	31	189
893	Leopoldina	71	229
915	Cosette	71	229
923	Herluga	21	179
934	Thuringia	71	229
953	Painleva	60	218
975	Perseverantia	71	229
995	Sternberga	31	189
1030	Vitja	21	179
1071	Brita	42	200
1090	Sumida	71	229
1120	Cannonia	42	200
1122	Neith	21	179
1166	Sakuntala	42	200
1261	Legia	27	185
1351	Uzbekistania	21	179
1405	Sibelius	47	205
1450	Raimonda	21	179
1537	Transylvania	38	196
1541	Estonia	27	185
1541	Estonia	60	218
1637	Swings	1	159
1657	Roemera	21	179
1736	Floirac	42	200
1746	Brouwer	69	227
1781	Van Biesbroeck	71	229
1815	Beethoven	21	179
1817	Katanga	47	205
1903	Adzhimushkaj	2	160
2068	Dangreen	21	179
2069	Hubble	21	179
2069	Hubble	60	218
2108	Otto Schmidt	47	205
2197	Shanghai	38	196
2282	Andres Bello	8	166
2912	Lapalma	47	205
3057	Malaren	47	205
3103	Eger	18	176
3103	Eger	42	200
3103	Eger	71	229
3167	Babcock	60	218
3500	Kobayashi	47	205
3822	Segovia	38	196
3835	Korolenko	60	218
3934	Tove	36	194
4302	Markeev	47	205
4464	Vulcano	65	223
4512	Sinuhe	21	179
4512	Sinuhe	38	196
4528	Berg	42	200
4588	Wislicenus	38	196
4706	Dennisreuter	38	196
5001	EMP	36	194
5256	Farquhar	71	229
5332	Davidaguilar	18	176
5349	Paulharris	47	205
5392	Parker	21	179
5506	Artiglio	38	196
5838	Hamsun	36	194
6371	Heinlein	27	185
6411	Tamaga	47	205
6461	Adam	47	205
6655	Nagahama	71	229
6849	Doloreshuerta	47	205
7284	1989 VW	69	227
7482	1994 PC1	42	200
7488	Robertpaul	47	205
8783	Gopasyuk	47	205
9356	Elineke	47	205
9659	1996 EJ	9	167
11836	Eileen	47	205
12494	Doughamilton	47	205
12685	1985 VE	38	196
13186	1996 UM	47	205
13249	Marcallen	21	179
13578	1993 MK	47	205
16562	1992 AV1	65	223
18801	Noelleoas	36	194
19469	1998 HV45	34	192
22099	2000 EX106	18	176
29905	Kunitaka	36	194
35783	1999 JU20	65	223
47786	2000 EQ20	36	194
49669	1999 RZ30	65	223
51442	2001 FZ25	34	192
52314	1991 XD	47	205
74779	1999 RF241	47	205
89958	2002 LY45	38	196
115916	2003 WB8	38	196
138971	2001 CB21	18	176
138971	2001 CB21	38	196
170891	2004 TY16	18	176
318160	2004 QZ2	38	196
434307	2004 FT41	47	205
	2010 VG1	18	176
	2022 AO6	11	169
	2022 CO6	11	169
	2022 CV5	11	169
	2022 DA	11	169
	2022 ER5	11	169
	2022 FB2	11	169
	2022 FC	11	169
	2022 FD	11	169
	2022 FL4	11	169

THE MINOR PLANET BULLETIN (ISSN 1052-8091) is the quarterly journal of the Minor Planets Section of the Association of Lunar and Planetary Observers (ALPO, http://www.alpo-astronomy.org). Current and most recent issues of the *MPB* are available on line, free of charge from:

https://mpbulletin.org/

The Minor Planets Section is directed by its Coordinator, Prof. Frederick Pilcher, 4438 Organ Mesa Loop, Las Cruces, NM 88011 USA (fpilcher35@gmail.com). Robert Stephens (rstephens@foxandstephens.com) serves as Associate Coordinator. Dr. Alan W. Harris (MoreData! Inc.; harrisaw@colorado.edu), and Dr. Petr Pravec (Ondrejov Observatory; ppravec@asu.cas.cz) serve as Scientific Advisors. The Asteroid Photometry Coordinator is Brian D. Warner (Center for Solar System Studies), Palmer Divide Observatory, 446 Sycamore Ave., Eaton, CO 80615 USA (brian@MinorPlanetObserver.com).

The Minor Planet Bulletin is edited by Professor Richard P. Binzel, MIT 54-410, 77 Massachusetts Ave, Cambridge, MA 02139 USA (rpb@mit.edu). Brian D. Warner (address above) is Associate Editor, and Dr. David Polishook, Department of Earth and Planetary Sciences, Weizmann Institute of Science (david.polishook@weizmann.ac.il) is Assistant Editor. The *MPB* is produced by Dr. Pedro A. Valdés Sada (psada2@ix.netcom.com). The MPB is distributed by Dr. Melissa Hayes-Gehrke. Direct all subscriptions, contributions, address changes, etc. to:

Dr. Melissa Hayes-Gehrke
UMD Astronomy Department
1113 PSC Bldg 415
College Park, MD 20742 USA
(mhayesge@umd.edu)

Effective with Volume 38, the *Minor Planet Bulletin* is a limited print journal, where print subscriptions are available only to libraries and major institutions for long-term archival purposes. Effective with Volume 50, January 1, 2023 and beyond, printed issues of the *Minor Planet Bulletin* will no longer be distributed. In addition to the free electronic download of the *MPB* noted above, electronic retrieval of all *Minor Planet Bulletin* articles (back to Volume 1, Issue Number 1) is available through the Astrophysical Data System:

http://www.adsabs.harvard.edu/

Authors should submit their manuscripts by electronic mail (rpb@mit.edu). Author instructions and a Microsoft Word template document are available at the web page given above. All materials must arrive by the deadline for each issue. Visual photometry observations, positional observations, any type of observation not covered above, and general information requests should be sent to the Coordinator.

* * * * *

The deadline for the next issue (49-4) is July 15, 2022. The deadline for issue 50-1 is October 15, 2022.